

Regulation of cell to cell adhesion and differentiation of spermatogonial stem cells by 14-3-3 γ

By

Vishal Sonali Shrinivas Meena

(LIFE09201104010)

Tata Memorial Centre, Mumbai

A thesis submitted to the

Board of Studies in Life Sciences

In partial fulfillment of requirements

for the Degree of

DOCTOR OF PHILOSOPHY

of

HOMI BHABHA NATIONAL INSTITUTE


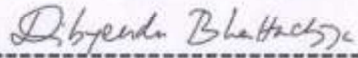


August, 2018

Homi Bhabha National Institute

Recommendations of the Viva Voce Committee

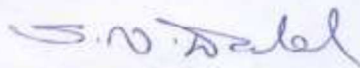
As members of the Viva Voce Committee, we certify that we have read the dissertation prepared by Ms. Vishal Sonali Shrinivas Meena entitled "Regulation of cell to cell adhesion and differentiation of spermatogonial stem cells by 14-3-3 γ " and recommend that it may be accepted as fulfilling the thesis requirement for the award of Degree of Doctor of Philosophy.

	21/8/18
Chairperson – Prof. S. V. Chiplunkar	Date:
	20/8/18
Guide/Convener – Dr. S. N. Dalal	Date:
	20-8-18
External Examiner – Dr. Colin Jamora	Date:
	20/8/18
Member – Dr. M.M. Vaidya	Date:
	20.8.18
Member - Dr. D. Bhattacharyya	Date:

Final approval and acceptance of this thesis is contingent upon the candidate's submission of the final copies of the thesis to HBNI.

I hereby certify that I have read this thesis prepared under my direction and recommend that it may be accepted as fulfilling the thesis requirement.

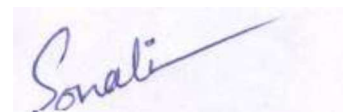
Date: 20/8/18
Place: Navi Mumbai


Dr. S. N. Dalal
Guide

STATEMENT BY AUTHOR

This dissertation has been submitted in partial fulfillment of requirements for an advanced degree at Homi Bhabha National Institute (HBNI) and is deposited in the library to be made available to borrowers under rules of the HBNI.

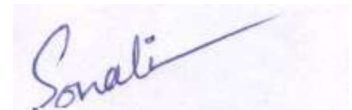
Brief quotations from this dissertation are allowable without special permission, provided that accurate acknowledgement of source is made. Requests for permission for extended quotation from or reproduction of this manuscript in whole or in part may be granted by the Competent Authority of HBNI when in his or her judgment, the proposed use of the material is in the interests of scholarship. In all the other instances, however, permission must be obtained from the author.

A handwritten signature in blue ink, reading "Sonali", with a long horizontal stroke extending to the right.

Vishal Sonali Shrinivas Meena

DECLARATION

I, hereby declare that the investigation presented in the thesis has been carried out by me. The work is original and has not been submitted earlier as a whole or in part for a degree/diploma at this or any other Institution or University.

A handwritten signature in blue ink, reading "Sonali", with a long horizontal stroke extending to the right.

Vishal Sonali Shrinivas Meena

List of Publications arising from the thesis

Journal:

1. **“Plakoglobin localization to the cell border restores desmosome function in cells lacking 14-3-3 γ .”** Vishal SS, Tilwani S, Dalal SN. *Biochemical and Biophysical Research Communications*, **2018**, 495, 1998-2003.
2. **“Generation of mice with tissue specific transgene expression using sperm mediated gene transfer.”** Vishal SS, Tilwani S, Thorat R, Dalal SN. *International Journal of Pharma and Bio Sciences*, **2017**, Apr; 8(2): (B) 324-329.
3. **“14-3-3 γ -Mediated transport of plakoglobin to the cell border is required for the initiation of desmosome assembly *in vitro* and *in vivo*.”** Sehgal L, Mukhopadhyay A, Rajan A*, Khapare N*, Sawant M*, Vishal SS, Bhatt K, Ambatipudi S, Antao N, Alam H, Gurjar M, Basu S, Mathur R, Borde L, Hosing AS, Vaidya MM, Thorat R, Samaniego F, Kolthur-Seetharam U, Dalal SN, *Journal of Cell Science*, **2014**, 127(Pt 10):2174-2188. (* All the authors contributed equally to the work).
4. **“Transgenesis: Embryo modification to sperm mediated gene transfer.”** Vishal SS, Dalal SN. *Indian Journal of Biotechnology*. **2016**, Oct; 15:459-466 (Review).

Conferences:

1. Poster entitled “Regulation of cell-cell adhesion and differentiation of spermatogonial stem cells by 14-3-3 γ ” was presented at the “Stem Cells to Organogenesis symposium”, held at inStem, NCBS, Bangalore, India, from 10th to 12th 2013.

2. Poster entitled “Plakoglobin localization to the cell border rescues desmosome assembly in cells lacking 14-3-3 γ ” was presented at the XXXIX All India Cell Biology Conference (AICBC), held at Thiruvananthapuram, India, from 6th to 8th December 2015.

(Received Prof. B.R. Seshachar Memorial prize for the best paper presentation by young scientist in poster session)

3. Poster entitled “Plakoglobin localization to the cell border rescues desmosome assembly in cells lacking 14-3-3 γ ” was presented at the Gordon Research Seminar and the Gordon Research Conference on Protein transport across cell membranes: Mechanism, Structure and Regulation, held at Galveston, USA, from 5th to 11th March 2016.

Workshops:

1. “inStem Mouse Embryology Workshop: Stem Cells to Organogenesis” held at inStem, NCBS, Bangalore, India, from 13th March to 23rd March 2013.

Others:

1. Part of organizing committee of “**10th National Research Scholars Meet (NRSM) conference**”, ACTREC, Navi Mumbai, 2014.
2. Part of organizing committee of “**International Conference on Radiation Biology (ICRB) conference**” conducted on the occasion of the 11th Biennial meeting of the Indian Society for Radiation Biology (ISRB), held at ACTREC, Navi Mumbai, 2012.

This Thesis is dedicated to

My beloved family

and

All my friends who supported and inspired me

throughout my educational journey.

ACKNOWLEDGEMENTS

I was happiest when I got selected in ACTREC because I wanted to join ACTREC since I was in first year of B.Sc. and I will always remember the time I have spent in ACTREC.

I want to thank Sorab for selecting me to work on this project. The first time I spoke to him he said he is difficult to work with and after spending such a long time in his lab I would like to say he is easy to work with. The six years, 11 months and 26 days of my PhD. journey would have been very difficult without Sorab's guidance and support. He taught me lot of things from designing proper experiments to writing thesis. He taught me to be logical whenever my experiments failed and always cheered me up whenever I was sad. I could not thank him enough for his support and understanding. He is a very good teacher and a very good human being.

I would like to thank Dr. Shubhada Chiplunkar (Director, ACTREC), Dr. Rajiv Sarin (ex-Director, ACTREC), Dr. Sudeep Gupta (Dy. Director, CRC, ACTREC), Dr. HKV Narayan (Dy. Director, ACTREC) and Dr. Surekha Zingde (ex-Dy. Director, ACTREC), for providing good infrastructure, academic and technical support. I thank Dr. Shubhada Chiplunkar (DC Chairperson), Dr. Milind M. Vaidya and Dr. Dibyendu Bhattacharyya (my DC members) for giving their valuable suggestions and technical inputs during my PhD work.

I would like to thank ACTREC for providing me PhD fellowship. I would like to thank Sorab to provide me fellowship for the last 22 months. I thank DBT for funding this project and fellowship.

The project involved extensive mice work and it would have been difficult to handle all of it without the help from Sarika and Neha who did most of the mouse genotyping and standardized different PCR programs. I thank them for all their work. I would like to thank Sarika for generating the pLentiCRISPR K14 14-3-3 γ gRNA vector and its packaging. I would like to thank Dr. Arvind Ingle and Dr. Rahul Thorat for helping with the suggestions in the mouse project. Also, Dr. Rahul Thorat performed some of the mice surgeries and taught me how to perform the mice surgery. Maintenance, numbering and supply of so many animals would have been impossible without the help from the animal house staff Mr. Abhijeet, Mr. Sandeep, Mr. Sadanand, Mr. Makrand, Mr. Mahesh, Mr. Surendra, Mr. Shashi, Mr. Manish, Mr. Ravi, Mr. R. M. Pawar and Mr. Lokare. I would also like to thank trainees Prafful, Nikita, Keerthana, Shivangi and Ashlin, who helped me to look after the mice and change doxycycline water.

I would like to thank Mr. Shashi Ahire for his help with standardizing the genomic DNA extraction from tissue. I would like to thank Mr. Prakash Chavan, Mrs. Aarti, Mr. Vasudev Sakpal and Mr. Dinesh for cryosectioning and hematoxylin and eosin staining.

The microscopy related work described in this project was possible because of the help from the imaging facility Mrs. Vaishali Kailaje, Mrs. Tanuja and Mr. Jayraj. I would also like to thank them for teaching me how to use confocal and inverted microscopes.

I would like to thank all the members from Common instrument facility, Flow Cytometry facility, DNA sequencing facility, IT facility (Anand Sir), Library (Mrs. Mugdha, Mrs. Swati), Scope Cell (Dr. Nalini Hasgekar, Dr. Aparna Bagwe, and Mrs. Ojaswini Upasini), Administration (Mrs. Chitra, Mrs. Sharvari, Mrs. Alka and Mr. Anil), Accounts and Program

office (Mrs. Maya Dolas) for their help. I would like to thank Dr. Neelam Mamnia for motivating me and guiding me on how to deal with stress.

I would like to thank Dr. Subeer Majumdar and his laboratory for the electroporation experiments. I would like to thank Lalit and Dr. Felipe Samaniego for the *in vitro* kinase assay. I would like to thank Manoj and Dr. Prasanna's laboratory for their help with site directed mutagenesis and GST protein purification. I would like to thank Dr. Francesca Miselli to provide pCCLK14 GFP construct to Dr. Vaidya's laboratory. I would like to thank Richa from Dr. Vaidya's laboratory for sharing this construct with us and also for sharing site directed mutagenesis protocol. I would like to thank Shalaka and Dr. Shirsat's laboratory for sharing pLentiCRISPR Cas V1 vector and help with shRNA cloning. I would like to thank Mrs. Siddhi and Dr. Vinita for providing glutaraldehyde for hanging drop experiments.

I would like to thank the lab members Srikanta, Arunabha, Sarika, Neha, Kumar, Mansa, Neelima, Lalit, Amitabh and Mugdha. They are the ones who taught me how to do experiments. I want to thank them for their scientific discussions and suggestions. I would like to thank Pawar Kaka, Vishal and Arun for all the help with administrative work and reagents.

It became easy to beat the stress and to keep up with Sorab's yelling because of the following people in the lab: Srikanta, Arunabha, Sarika, Neha, Kumar, Mansa, Neelima, Lalit, Amitabh, Mugdha Nazia, Rahul Akash, Amol, Monika, Neha, Poonam, Rajan, Suruchi, Pawar, Arun, Vishal, Keerthana, Prafful, Nikita, Shivangi, Ashlin, Anushree Gulvady, Khyati, Dipika, Anandi, Jervis, Snehal, Apurva, Sarita, Simone, Carol, Asma, Noelle, Trupti, Roseline, Jazeel, Aakanksha, Aparajitha, Samadritta, Anushree Sawant, Rabiya, Ria, Paloma, Shraddha, Oindrila, Kruthi, Tejashree, Rohan, Shreya, Debolina, Shweta, Harshini, Sufiya, Shreshtha, Simona,

Simran, Jincy, Rohit and Sumaiya. I want to specially thank Srikanta and Arunabha for listening to my problems and making me laugh when I really thought that it was just impossible for me to laugh.

I want to thank Priyanka, Manish, Usha and Mayuri from Dr. Mahimkar's laboratory and Asmita and Ram from Dr. Gupta's laboratory for being good friends and allowing me to use instruments and reagents from their laboratories. I would like to thank my batchmates, Moquitul, Sajad, Prasanna, Qadir, Rahul, Rasika, Divya, Ekjot, Pratik, Pawan, Vijay, Subhoshree, Debolina, Amit, Mugdha and Priyanka Sathe, for bearing with me through all the lectures and presentations.

I would like to thank my childhood friend Sonal, my college friends Sagar, Pooja, Kalpana, Sumeet, Sandhya, Akshay, Vaishali, Shonti, Ajay, Ganesh, Rashmi, Ridhi, Arvind, Gayatri, Shazia, Shailaja, Nidhi, Rajeshwary, Ashlesha, Shalaka, Pooja Singh, Shilpa, Sana and Aarti for their love and support. I would like to thank Krupa, Zuzer and Tejeshwar for their help with preparations for ACTREC entrance.

I would like to thank Sameera Kaku (Pooja's Mom), Late Radha Aaji (my jogging friend), Mau (my previous neighbor) and Miss Mahalakshmi (my Bharatnatyam teacher) who really inspired me in different ways and made me happy.

I would like to thank my school teachers and college teachers who taught me and inspired me to continue my education. I would like to thank my grandparents, aunts, uncles and cousins. I am thankful to my parents and my sisters Bobby and Mani for their support, understanding and unconditional love and care. These six years made me realize the importance of my family in my life. I would like to thank God for giving me: i) courage to go through the failures and not give up and ii) for everything.

INDEX

Section	Contents	Page No.
i.	Synopsis	05
ii.	List of Tables	21
iii.	List of Figures	24
1.	Chapter1: Introduction	29
1.1	Transgenesis	30
1.1.1	Structure of the testis	31
1.1.2	Spermatogenesis	33
1.1.3	Sperm mediated gene transfer	37
1.1.4	Site specific recombination and targeted knockouts	45
1.2	14-3-3 proteins	47
1.2.1	Structure	47
1.2.2	Ligand binding	48
1.3	14-3-3 γ	50
1.3.1	Functions of 14-3-3 γ	50
1.3.2	Mouse models of 14-3-3 γ loss	63
1.4	Cell adhesion junctions	64
1.4.1	Cell-cell adhesion junctions found in testis	65
1.4.2	BTB and its function	67
1.4.3	Adherens junctions	68
1.4.4	Desmosomes	71
1.4.5	Regulation of desmosome formation by 14-3-3 γ	74

2.	Chapter 2: Aims and Objectives	76
3.	Chapter 3: Materials and methods	78
3.1	Plasmids and constructs	79
3.2	Cell lines, transfections and transductions	100
3.3	Animal experiments	105
3.4	Antibodies and Western blotting	114
3.5	Immunofluorescence and confocal microscopy	120
3.6	Calcium switch assay	121
3.7	Hanging drop assay	121
3.8	GST protein preparation	121
3.9	RNA isolation and reverse transcriptase PCR	124
4.	Chapter 4: Results and discussions: Generate inducible and epidermis specific knockdown mice for 14-3-3 γ	126
4.1	Generation of tetracycline inducible 14-3-3 γ knockdown mice	127
4.1.1	Validation of pLKO Tet Puro 14-3-3 γ shRNA vector	128
4.1.2	Generation of pLKO Tet Puro 14-3-3 γ shRNA positive transgenic mice	129
4.1.3	Stable inheritance of transgene from one generation to next generation	133
4.1.4	Doxycycline treatment for pre-founder mice and transgenic pups	136
4.1.5	Effect of 14-3-3 γ knockdown on spermatogenesis in pre-founder mice	138
4.1.6	Effect of 14-3-3 γ knockdown on the physiology of transgene	147

	positive mice ¹	
4.2	Generation of epidermis specific 14-3-3 γ knockdown mice	150
4.2.1	Validation of pCCLK14 Turbo RFP 14-3-3 γ shRNAmir vector	152
4.2.2	Generation of pCCLK14 Turbo RFP 14-3-3 γ shRNAmir positive transgenic mice	153
4.2.3	PCR amplification of the 14-3-3 γ shRNAmir from pre-founder mice	160
4.2.4	Stable inheritance of transgene from one generation to next generation	174
4.2.5	Stable expression of Turbo RFP in the epidermis of the transgenic mice	175
4.2.6	Generation of epidermis specific 14-3-3 γ knockdown mice using electroporation	177
4.2.7	Generation of epidermis specific 14-3-3 γ knockout mice	180
4.3	Discussion	191
5.	Chapter 5: Results and discussions: Determine the mechanisms by which 14-3-3 γ loss leads to defect in the desmosome formation	195
5.1	Results	196
5.1.1	PKC μ phosphorylates PG	196
5.1.2	Mutation of PG serine 236 to alanine and its effect on PG localization	199
5.1.3	Effect of PKC μ loss on desmosome formation	200
5.1.4	Sertoli cell isolation to study desmosomes	202

5.1.5	Generation of HA tagged PG deletion constructs	203
5.1.6	Validation of pLentiCRISPR PG gRNA constructs	206
5.1.7	Validation of PG-EGFP and PG-EGFP-f constructs	207
5.1.8	PG-EGFP-f recruits desmosomal proteins to the cell border in the absence of 14-3-3 γ	208
5.1.9	PG-EGFP-f increased DPI/II protein levels in 14-3-3 γ knockdown cells	214
5.1.10	PG-EGFP-f stabilizes DSG2 at the cell border in the absence of 14-3-3 γ	216
5.1.11	PG-EGFP-f restores desmosome formation in the 14-3-3 γ knockdown cells	219
5.1.12	PG-EGFP-f/PG-EGFP restores desmosome formation in PG knockdown cells	221
5.1.13	PG-EGFP-f requires PKP3 to restore desmosome formation	224
5.1.14	PG-EGFP-f requires KIF5B to restore DSG2 to the cell border	228
5.1.15	PG-EGFP-f does not alter the localization or levels of adherens junction proteins	234
5.2	Discussions	237
6.	Chapter 6: Conclusions	246
7.	Chapter 7: Bibliography	250

Synopsis



Homi Bhabha National Institute

SYNOPSIS OF Ph. D. THESIS

1. **Name of the Student:** Vishal Sonali Shrinivas Meena
2. **Name of the Constituent Institution:** Tata Memorial Centre, Advanced Centre for Treatment, Research and Education in Cancer
3. **Enrolment No. :** LIFE09201104010
4. **Title of the Thesis:** Regulation of cell to cell adhesion and differentiation of spermatogonial stem cells by 14-3-3 γ .
5. **Board of Studies:** Life Sciences

SYNOPSIS

Introduction:

14-3-3 proteins belong to a family of acidic proteins with a molecular weight of 25-32 kDa. [1, 2]. This protein family binds to phosphorylated proteins containing a serine residue in one of two consensus motifs [3, 4]. There are seven 14-3-3 isoforms i.e. β , γ , ϵ , ζ , η , τ and σ [5, 6]. Two 14-3-3 proteins, 14-3-3 ϵ and 14-3-3 γ , are required to inhibit cell cycle progression in response to DNA damage and incomplete S phase [7, 8]. Therefore, we wished to determine the role of 14-3-3 γ in growth and development. However, knockout mice for 14-3-3 γ were viable and did not show any growth defects or developmental abnormalities [9]. These results suggested that other family members could possibly compensate for the loss of 14-3-3 γ during the process of development. Therefore, it was hypothesized that the generation of a hypomorphic mutant for 14-3-3 γ could reveal 14-3-3 γ functions that were required for cell growth and differentiation.

To address the role of 14-3-3 γ in growth and development, lentiviral particles generated using pLKO EGFP-f 14-3-3 γ shRNA were injected into the testes of prepubescent CRL:CFW (Swiss) mice such that lentiviruses infect spermatogonial stem cells and the viral genome gets integrated into the genome of the infected cells and is passed on to the developing spermatocytes and spermatozoa to generate transgenic animals. This technique is known as sperm mediated gene transfer (SMGT) [10]. Knockdown of 14-3-3 γ in the testes led to defects in cell-cell adhesion, and cell matrix adhesion leading to collapse of the blood testes barrier (BTB) and defects in spermatogonial stem cell differentiation and spermatocyte development and maturation[11]. Loss of cell-cell adhesion between Sertoli cells in the testes and between Sertoli cells and germ cells leads to sterility (reviewed in [12-15]) because spermatocyte development requires an intact Blood Testes Barrier (BTB), which is formed by tight junction proteins and also has adherens like junctions and desmosome like junctions (reviewed in [12, 15-18]). Other important cell-cell adhesion junctions in the seminiferous epithelium that are required for BTB formation and spermatogenesis are adherens junctions, desmosome like junctions, tight junctions, gap junctions and ectoplasmic specializations (specialized actin based junctions) [19]. Cadmium chloride treatment results in the collapse of the BTB and disruption of junctions between sertoli cells and developing spermatocytes due to a depletion of junctional components at the cell border resulting in a loss of cell-cell adhesion and sterility [19].

Desmosomes are adherens like cell-cell adhesion junctions present in all epithelial tissues [20]. Desmosomes are made up of three types of proteins, the desmosomal cadherins, desmogleins (DSGs) and desmocollins (DSCs), the armadillo (ARM) repeat containing proteins, plakoglobin (PG) and plakophilins (PKPs) and plakin family proteins such as desmoplakin (DP). The desmosomal cadherins of two neighboring cells interact with each other in a homophilic or heterophilic manner to form cell-cell contacts. The cytoplasmic domains of these

cadherins interacts with PG and the PKP proteins (PKP1-3) to form an electron dense structure known as the desmosomal plaque. In the plaque, the ARM proteins are connected to intermediate filaments via DP thus forming a tissue wide intermediate filament network that provides strength and stability to tissues [21]. The importance of desmosome is illustrated by experiments in mice demonstrating that the deletion of desmosomal protein showed embryonic lethality e.g. PG knockout mice die at embryonic day 10.5 due to severe heart defects [22], DP knockout mice die at embryonic day 6.5 with perturbed keratin network and defect in egg cylinder elongation [23], DSG2 knockout embryos die shortly after implantation [24] and PKP2 knockout mice die at embryonic day 10.5 due to defects in the atrial wall and leakage of blood into pericardium and peritoneal cavity [25].

To identify which of the junctions in the seminiferous epithelium were affected by loss of 14-3-3 γ , cell extracts of HCT116 cells (colon cancer cell line) were used to perform GST pulldown assays using GST or GST 14-3-3 γ . GST14-3-3 γ binds to the desmosomal proteins PG, PKP3 and DP [11]. To determine if 14-3-3 γ loss led to defects in desmosome formation, cell-cell adhesion was measured in HCT116 derived 14-3-3 γ knockdown cells. Cell-cell adhesion was decreased in the 14-3-3 γ knockdown cells as compared to the vector control cells. In addition, the levels of the desmosomal proteins at the cell border were decreased upon loss of 14-3-3 γ and this was due to the inability of the desmosomal plaque protein plakoglobin (PG) to localize to the cell border in the absence of 14-3-3 γ [11]. These observations suggest that 14-3-3 γ loss might lead to global changes in cell-cell adhesion in multiple tissue types.

Objectives:

1. Generate inducible and epidermis specific knockdown mice for 14-3-3 γ .

2. Determine the mechanisms by which 14-3-3 γ loss leads to defects in the desmosome formation.

Results and discussion.

1. Generate inducible and epidermis specific knockdown mice for 14-3-3 γ :

Inducible 14-3-3 γ knockdown mice Loss of 14-3-3 γ affects cell cycle progression in response to DNA damage and S-phase arrest [7] and desmosome formation [11]. Constitutive 14-3-3 γ shRNA production in pre-founder mice leads to sterility by affecting spermatogenesis [11], and therefore transgenic pups could not be obtained from such mice. To overcome this problem, 14-3-3 γ shRNA was cloned downstream of H1/Tet inducible promoter. This promoter is negatively regulated by Tet repressor protein in the absence of tetracycline. Administration of tetracycline or doxycycline will result into release of tet repressor from H1/Tet promoter allowing RNA polymerase to bind to this promoter and induce shRNA production. Lentiviral particles generated using either pLKO Tet Puromycin (Addgene) [26] or pLKO Tet Puromycin 14-3-3 γ shRNA were surgically injected into the testes of pre-pubescent male BALB/c mice. Five weeks post injection these mice were mated with wild type female mice to obtain pups. Pups obtained were screened for the presence of puromycin resistance gene by using genomic DNA isolated from tail tips of pups as a template to amplify the Puromycin resistance gene. All the pups were found to be positive for puromycin resistance gene and genomic DNA from WT mouse was used as a negative control. The transgene positive vector control and 14-3-3 γ shRNA mice were given doxycycline but no phenotypic changes were observed. An analysis of 14-3-3 γ levels suggested that there was no loss of 14-3-3 γ upon addition of doxycycline.

To identify the stage in the spermatogenesis cycle that is affected by loss of 14-3-3 γ , lentiviral particles generated using either pLKO Tet Puromycin or pLKO Tet Puromycin 14-3-3 γ shRNA were surgically injected into the testes of pre-pubescent male CRL:CFW (Swiss) mice.

Immediately after surgery, one set (three mice) of pLKO Tet Puromycin or pLKO Tet Puromycin 14-3-3 γ shRNA pre-founder mice were given doxycycline in the drinking water and the other set of pLKO Tet Puromycin or pLKO Tet Puromycin 14-3-3 γ shRNA pre-founder mice did not receive doxycycline and served as a control. Five weeks post-surgery, both sets were mated with the wild type female mice. Doxycycline was given throughout the breeding experiments and the pups obtained from these crosses were also administered doxycycline. Control mice and pups derived from these crosses were not provided with doxycycline. Pups were screened for the presence of puromycin resistance transgene and it was observed that all the pups of all the sets were transgene positive. Transgene positive mice were inbred to check their fertility. Out of the three doxycycline administered pLKO Tet Puromycin positive breeding pairs of F1 generation, only one pair gave birth to pups and in the un-induced control set, two breeding pairs gave birth to pups. None of the doxycycline administered pLKO Tet Puromycin 14-3-3 γ shRNA positive breeding pairs of F1 generation gave birth to pups and in un-induced control set, only one pair gave birth to pups. The testes of all the male mice used in the above mating experiments were collected and IHC and RT-PCR for 14-3-3 γ will be performed to analyze if the spermatogenesis was disrupted in the inducible and un-inducible transgene positive pups.

Epidermis specific 14-3-3 γ knockdown mice As desmosome assembly is affected by 14-3-3 γ loss, we asked whether epidermal tissue specific ablation of 14-3-3 γ will affect barrier function of skin, as has been demonstrated in desmosome knockout models of DSC1 and DSG3 [27, 28]. To address this question we tried to generate tissue specific 14-3-3 γ knockdown mice by introducing RFP and 14-3-3 γ shRNA_{mir} downstream of Keratin14 (K14) promoter in pCCLK14 lentivector (a kind gift from Dr. F. Miselli) [29]. Keratin 14 promoter activity is highly regulated and K14 is expressed only in the basal layers of epidermis and tongue palate

[29]. To make epidermis specific transgenic mice, lentiviral particles generated using either pCCLK14 RFP or pCCLK14 RFP 14-3-3 γ shRNAmir were injected into the testes of pre-pubescent male mice [CrI:CFW(SW)]. Five weeks post-injection, these mice were mated with wild type female mice. The pups obtained from pre-founder mice were screened for turbo RFP gene by using genomic DNA isolated from tail tips to PCR amplify the turbo RFP transgene or the turbo RFP 14-3-3 γ shRNAmir transgene. Genomic DNA from wild type mouse was used as a negative control. All the pups were found to be positive for turbo RFP transgene. Control mice expressed the turbo RFP transgene in the epidermis and hair follicle, but not in the dermis, suggesting that this vector system was capable of driving transgene production [30]. In contrast, the PCR fragment, obtained from the pups of pre-founder mice injected with the shRNAmir viruses, did not contain the 14-3-3 γ shRNAmir sequence. This suggests that all the pups were negative for 14-3-3 γ shRNAmir sequence. To check whether the 14-3-3 γ shRNAmir sequence was present in the pre-founder mice, RFP 14-3-3 γ shRNAmir was PCR amplified and cloned into TA vector (Thermo Scientific) and sequenced. The sequence matched with RFP 14-3-3 γ shRNAmir suggesting during embryo formation lentiviral recombination might have led to the deletion of shRNAmir sequence. Multiple attempts at generating pups positive for pCCLK14 RFP 14-3-3 γ shRNAmir, resulted in the generation of only transgene negative pups.

The experimental strategy described above was dependent on shRNA mediated degradation of the 14-3-3 γ mRNA in epidermis. An alternative strategy would be to delete the 14-3-3 γ gene specifically in the epidermis. As generating a conventional tissue specific knockout is cumbersome and floxed 14-3-3 γ mice are not available, we chose the CRISPR Cas system, which induces small deletions in the targeted gene leading to a loss of gene expression [31]. The CRISPR cas system is composed of a guide RNA and a nuclease Cas9. The guide RNA binds to one of the exons of the targeted gene and Cas 9 nuclease creates a double strand break in the

genomic DNA where the guide RNA is bound, leading to the activation of DNA repair pathways, which results in frame shift mutations due to inaccurate DNA repair [32]. The guide RNA targeting exon 1 of 14-3-3 γ was cloned into the Lenticrispr cas v1 plasmid (Addgene) downstream of U6 promoter and the EFS promoter driving Cas 9 nuclease expression was replaced with K14 promoter to target 14-3-3 γ gene only in epidermis. The Lenticrispr cas v1, Lenticrispr cas v1 14-3-3 γ gRNA viruses (for generating constitutive knockout), K14 Lenticrispr cas v1 and the K14 Lenticrispr cas v1 14-3-3 γ gRNA viruses (for generating epithelium specific knockout) were tested *in vitro* and used for virus mediated transgenesis. Pups were obtained from these pre-founder mice. Pups obtained were screened for presence of puromycin resistance gene by using genomic DNA isolated from tail tips as a template to amplify the Puromycin resistance gene. Epidermis section of transgene positive pups will be screened for the mutations in exon 1 region of 14-3-3 γ using T7 endonuclease assay to identify epidermis specific 14-3-3 γ knockdown/knockout animals.

2. Determine the mechanisms by which 14-3-3 γ loss leads to defects in the desmosome formation:

Plakoglobin (PG) interacts with 14-3-3 γ but the binding site was not known. Using scansite software, phosphorylated S236 residue was predicted as binding site of 14-3-3 γ on PG. Using site directed mutagenesis, Myc tagged S236A PG mutants were generated and using GST pulldown assays, it was shown that Myc S236A PG failed to bind 14-3-3 γ whereas binding of Myc PG (wild type) to 14-3-3 γ was unaltered [11]. Immunofluorescence experiments using Myc antibody showed that Myc S236A PG had pan-cellular localization whereas Myc PG (wild type) was largely localized to the cell border. Scansite software also predicted that residue S236 was phosphorylated by PKC μ . To determine whether PKC μ was required for the cell border localization of PG, localization of PG and other desmosomal proteins was checked in HCT116

derived PKC μ knockdown cells and it was observed that PG, DP and PKP3 showed cytoplasmic localization. Moreover, levels of PG and DP were also reduced in HCT116 derived PKC μ knockdown cells as compared to the vector control cells. PKC μ could phosphorylate PG *in vitro*, probably at S236 residue, and this phosphorylated residue served as a binding site for 14-3-3 γ . 14-3-3 γ might load PG on to the motor protein Kif5B to transport PG to the cell border [11].

It was previously shown in the lab that in PKP3 knockdown cells, none of the desmosomal proteins were present at the cell border, with PG being a notable exception [33]. In 14-3-3 γ knockdown cells none of the desmosomal proteins localize to the cell border therefore, we wished to observe whether in the absence of 14-3-3 γ , PG localized to the cell border can rescue the phenotype observed in the 14-3-3 γ knockdown cells by recruiting the other desmosomal proteins to the cell border and stimulating desmosome formation. To address this query, we cloned PG cDNA into pEGFP-f vector, adding a farnesyl moiety to the protein resulting in the modified protein localizing to the cell membrane [34]. We observed that an increase in the levels of the desmosomal proteins at the cell border in HCT116 derived 14-3-3 γ knockdown cells transfected with farnesylated PG (PG-EGFP-f) as compared to the cells transfected with either farnesylated EGFP (EGFP-f) or PG fused to an unfarnesylated GFP protein (PG-EGFP). PG-EGFP was unable to localize to the border suggesting that the defect in the 14-3-3 γ knockdown cells was due to a defect in the localization of PG to the cell border. 14-3-3 γ knockdown cells transfected with PG-EGFP-f also had increased levels of desmosomal protein when compared to the EGFP-f transfected cells. These results indicate farnesylated PG is capable of stabilizing and recruiting desmosomal proteins DP and DSG2 to the cell border in the 14-3-3 γ knockdown cells. Moreover, hanging drop assay showed increase in cell-cell adhesion in cells expressing PG-EGFP-f when compared to the EGFP-f expressing cells

suggesting that desmosomal proteins not only localized to the cell border but also formed functional desmosomes. This result is in accordance with the literature suggesting PG along with one desmosomal cadherin and DP can form functional desmosomes [35].

The PG 14-3-3 γ complex is transported to the cell border by the kinesin motor protein Kif5B and therefore in the absence of Kif5B, PG is not localized to the cell border resulting in a decrease in the levels of the desmosomal proteins at the border and a disruption of cell-cell adhesion. Expression of PG-EGFP-f in the Kif5B knockdown cells lead to an increase in the levels of DP at the cell border, however the levels of the other desmosomal proteins at the border were not altered and therefore no increase in desmosome formation and function was observed. This data suggests PG-EGFP-f cannot completely rescue desmosomal protein localization in the absence of Kif5B [11]. To determine whether the altered localization of DP in HCT116 derived 14-3-3 γ knockdown cells expressing PG-EGFP-f was not because of the PG overexpression, PG-EGFP or EGFP was expressed in HCT116 derived 14-3-3 γ knockdown cells and stained for DP. It was observed that PG-EGFP had largely cytoplasmic localization and the endogenous DP was also cytoplasmic suggesting 14-3-3 γ is required for the transport of both overexpressed and endogenous PG [11]. Moreover, expression of PG-EGFP in HCT116 derived Kif5B knockdown cells could not rescue DP localization suggesting Kif5B is required for transport of PG. Kif5B has been reported to be required for the transport of desmosomal cadherins to the cell border [36] and thus Kif5B might be required for the transport of other desmosomal proteins to the cell border resulting in defects in desmosome formation. This is consistent with our data that the inhibition of Kif5B expression in the testis leads to a more severe phenotype than loss of 14-3-3 γ [11].

14-3-3 γ and Kif5B are required for the transport of PG to the cell border and therefore in the absence of 14-3-3 γ or Kif5B, none of the desmosomal proteins are transported to the

cell border. In the absence of 14-3-3 γ , when PG is artificially localized to the cell border, PG signals the transport of DSG2, DP and PKP3 at the cell border thus stimulating desmosome formation. This suggests presence of PG at the cell border is either required for transport of DSG2, PKP3 and DP or for stabilizing these proteins at the cell border. The inability of PG-EGFP-f to recruit DSC2/3 to the cell border might be due to the incomplete recruitment of PKP3 to the cell border as while an increase in PKP3 levels is observed at the cell border in 14-3-3 γ knockdown cells expressing PG-EGFP-f, a complete restoration of PKP3 levels at the cell border is not observed in these cells suggesting 14-3-3 γ might be required for PKP3 transport or stabilization of PKP3 at the cell border. These data also suggest that the transport of DP and DSG2 is not dependent on 14-3-3 γ . In the absence of Kif5B, the artificial localization of PG to the cell border stimulated the localization of DP to the border but not of PKP3 and DSG2. Desmosome formation cannot be rescued in the absence of Kif5B by rescuing PG and DP transport because at least one desmosomal cadherin is required for initiation of desmosome formation. This suggests Kif5B is required not only for the transport of PG but also for the transport of DSG2 and PKP3.

To conclude, our results suggest that one major role of the 14-3-3 γ /KIF5B complex is to mediate the transport of PG to the cell border. The presence of PG at the cell border results in the increased recruitment of DP, DSG2 and PKP3 to the cell border in cells lacking 14-3-3 γ , however, the level of PKP3 and DSG2 at the cell border is attenuated in cells lacking KIF5B suggesting that Kif5B play a role in the transport of PKP3 and DSG2 to the cell border.

References:

1. Ichimura T, Isobe T, Okuyama T, Takahashi N, Araki K, Kuwano R, Takahashi Y: **Molecular cloning of cDNA coding for brain-specific 14-3-3 protein, a protein kinase-**

- dependent activator of tyrosine and tryptophan hydroxylases. *Proc Natl Acad Sci U S A* 1988, **85**(19):7084-7088.
2. Comparot S, Lingiah G, Martin T: **Function and specificity of 14-3-3 proteins in the regulation of carbohydrate and nitrogen metabolism.** *J Exp Bot* 2003, **54**(382):595-604.
 3. Yaffe MB, Rittinger K, Volinia S, Caron PR, Aitken A, Leffers H, Gambelin SJ, Smerdon SJ, Cantley LC: **The structural basis for 14-3-3 phosphopeptide binding specificity.** *Cell* 1998, **91**:961-971.
 4. Muslin AJ, Tanner JW, Allen PM, Shaw AS: **Interaction of 14-3-3 with signaling proteins is mediated by the recognition of phosphoserine.** *Cell* 1996, **84**(6):889-897.
 5. De S, Marcinkiewicz JL, Vijayaraghavan S, Kline D: **Expression of 14-3-3 protein isoforms in mouse oocytes, eggs and ovarian follicular development.** *BMC Res Notes* 2012, **5**:57.
 6. Benzinger A, Popowicz GM, Joy JK, Majumdar S, Holak TA, Hermeking H: **The crystal structure of the non-liganded 14-3-3sigma protein: insights into determinants of isoform specific ligand binding and dimerization.** *Cell Res* 2005, **15**(4):219-227.
 7. Hosing AS, Kundu ST, Dalal SN: **14-3-3 Gamma is required to enforce both the incomplete S phase and G2 DNA damage checkpoints.** *Cell Cycle* 2008, **7**(20):3171-3179.
 8. Telles E, Hosing AS, Kundu ST, Venkatraman P, Dalal SN: **A novel pocket in 14-3-3epsilon is required to mediate specific complex formation with cdc25C and to inhibit cell cycle progression upon activation of checkpoint pathways.** *Exp Cell Res* 2009, **315**(8):1448-1457.
 9. Steinacker P, Schwarz P, Reim K, Brechlin P, Jahn O, Kratzin H, Aitken A, Wiltfang J, Aguzzi A, Bahn E *et al*: **Unchanged survival rates of 14-3-3gamma knockout mice after inoculation with pathological prion protein.** *Mol Cell Biol* 2005, **25**(4):1339-1346.
 10. Sehgal L, Thorat R, Khapare N, Mukhopadhyaya A, Sawant M, Dalal SN: **Lentiviral mediated transgenesis by in vivo manipulation of spermatogonial stem cells.** *PLoS One* 2011, **6**(7):e21975.
 11. Sehgal L, Mukhopadhyay A, Rajan A, Khapare N, Sawant M, Vishal SS, Bhatt K, Ambatipudi S, Antao N, Alam H *et al*: **14-3-3gamma-Mediated transport of plakoglobin to the cell border is required for the initiation of desmosome assembly in vitro and in vivo.** *J Cell Sci* 2014, **127**(Pt 10):2174-2188.
 12. Cheng CY, Mruk DD: **Cell junction dynamics in the testis: Sertoli-germ cell interactions and male contraceptive development.** *Physiol Rev* 2002, **82**(4):825-874.

13. Mruk DD, Cheng CY: **Cell-cell interactions at the ectoplasmic specialization in the testis.** *Trends Endocrinol Metab* 2004, **15**(9):439-447.
14. Mruk DD, Cheng CY: **Sertoli-Sertoli and Sertoli-germ cell interactions and their significance in germ cell movement in the seminiferous epithelium during spermatogenesis.** *Endocr Rev* 2004, **25**(5):747-806.
15. Mruk DD, Cheng CY: **Tight junctions in the testis: new perspectives.** *Philos Trans R Soc Lond B Biol Sci* 2010, **365**(1546):1621-1635.
16. Mruk DD, Cheng CY: **Desmosomes in the testis: Moving into an uncharted territory.** *Spermatogenesis* 2011, **1**(1):47-51.
17. Mruk DD, Wong CH, Silvestrini B, Cheng CY: **A male contraceptive targeting germ cell adhesion.** *Nat Med* 2006, **12**(11):1323-1328.
18. Wong EW, Mruk DD, Lee WM, Cheng CY: **Par3/Par6 polarity complex coordinates apical ectoplasmic specialization and blood-testis barrier restructuring during spermatogenesis.** *Proc Natl Acad Sci U S A* 2008, **105**(28):9657-9662.
19. Wong CH, Mruk DD, Lui WY, Cheng CY: **Regulation of blood-testis barrier dynamics: an in vivo study.** *J Cell Sci* 2004, **117**(Pt 5):783-798.
20. Troyanovsky SM: **Mechanism of cell-cell adhesion complex assembly.** *Curr Opin Cell Biol* 1999, **11**(5):561-566.
21. Green KJ, Simpson CL: **Desmosomes: new perspectives on a classic.** *J Invest Dermatol* 2007, **127**(11):2499-2515.
22. Bierkamp C, McLaughlin KJ, Schwarz H, Huber O, Kemler R: **Embryonic heart and skin defects in mice lacking plakoglobin.** *Dev Biol* 1996, **180**(2):780-785.
23. Gallicano GI, Kouklis P, Bauer C, Yin M, Vasioukhin V, Degenstein L, Fuchs E: **Desmoplakin is required early in development for assembly of desmosomes and cytoskeletal linkage.** *J Cell Biol* 1998, **143**(7):2009-2022.
24. Eshkind L, Tian Q, Schmidt A, Franke WW, Windoffer R, Leube RE: **Loss of desmoglein 2 suggests essential functions for early embryonic development and proliferation of embryonal stem cells.** *Eur J Cell Biol* 2002, **81**(11):592-598.
25. Grossmann KS, Grund C, Huelsken J, Behrend M, Erdmann B, Franke WW, Birchmeier W: **Requirement of plakophilin 2 for heart morphogenesis and cardiac junction formation.** *J Cell Biol* 2004, **167**(1):149-160.
26. Wiederschain D, Wee S, Chen L, Loo A, Yang G, Huang A, Chen Y, Caponigro G, Yao YM, Lengauer C *et al*: **Single-vector inducible lentiviral RNAi system for oncology target validation.** *Cell Cycle* 2009, **8**(3):498-504.

27. Chidgey M, Brakebusch C, Gustafsson E, Cruchley A, Hail C, Kirk S, Merritt A, North A, Tselepis C, Hewitt J *et al*: **Mice lacking desmocollin 1 show epidermal fragility accompanied by barrier defects and abnormal differentiation.** *J Cell Biol* 2001, **155**(5):821-832.
28. Koch PJ, Mahoney MG, Ishikawa H, Pulkkinen L, Uitto J, Shultz L, Murphy GF, Whitaker-Menezes D, Stanley JR: **Targeted disruption of the pemphigus vulgaris antigen (desmoglein 3) gene in mice causes loss of keratinocyte cell adhesion with a phenotype similar to pemphigus vulgaris.** *J Cell Biol* 1997, **137**(5):1091-1102.
29. Di Nunzio F, Maruggi G, Ferrari S, Di Iorio E, Poletti V, Garcia M, Del Rio M, De Luca M, Larcher F, Pellegrini G *et al*: **Correction of laminin-5 deficiency in human epidermal stem cells by transcriptionally targeted lentiviral vectors.** *Mol Ther* 2008, **16**(12):1977-1985.
30. Vishal S S, Tilwani S, Thorat R, Dalal S N: **Generation of mice with tissue specific transgene expression using sperm mediated gene transfer.** *International Journal of Pharma and Bio Sciences* 2017 (Article in press).
31. Li D, Qiu Z, Shao Y, Chen Y, Guan Y, Liu M, Li Y, Gao N, Wang L, Lu X *et al*: **Heritable gene targeting in the mouse and rat using a CRISPR-Cas system.** *Nat Biotechnol* 2013, **31**(8):681-683.
32. Sato T, Sakuma T, Yokonishi T, Katagiri K, Kamimura S, Ogonuki N, Ogura A, Yamamoto T, Ogawa T: **Genome Editing in Mouse Spermatogonial Stem Cell Lines Using TALEN and Double-Nicking CRISPR/Cas9.** *Stem Cell Reports* 2015.
33. Gosavi P, Kundu ST, Khapare N, Sehgal L, Karkhanis MS, Dalal SN: **E-cadherin and plakoglobin recruit plakophilin3 to the cell border to initiate desmosome assembly.** *Cell Mol Life Sci* 2011, **68**(8):1439-1454.
34. Kalinowski A, Qin Z, Coffey K, Kodali R, Buehler MJ, Losche M, Dahl KN: **Calcium causes a conformational change in lamin A tail domain that promotes farnesyl-mediated membrane association.** *Biophys J* 2013, **104**(10):2246-2253.
35. Kowalczyk AP, Bornslaeger EA, Borgwardt JE, Palka HL, Dhaliwal AS, Corcoran CM, Denning MF, Green KJ: **The amino-terminal domain of desmoplakin binds to plakoglobin and clusters desmosomal cadherin-plakoglobin complexes.** *J Cell Biol* 1997, **139**(3):773-784.
36. Nekrasova OE, Amargo EV, Smith WO, Chen J, Kreitzer GE, Green KJ: **Desmosomal cadherins utilize distinct kinesins for assembly into desmosomes.** *J Cell Biol* 2011, **195**(7):1185-1203.

Publications in Refereed Journal:

a. Published

1. Sehgal L, Mukhopadhyay A, Rajan A, Khapare N, Sawant M, **Vishal SS**, Bhatt K, Ambatipudi S, Antao N, Alam H et al: 14-3-3gamma-Mediated transport of plakoglobin to the cell border is required for the initiation of desmosome assembly in vitro and in vivo. Journal of Cell Science.2014, 127(Pt 10):2174-2188. DOI: 10.1038/srep26580
2. **Vishal SS**, Dalal SN. Transgenesis: Embryo modification to sperm mediated gene transfer. Indian Journal of Biotechnology. 2016 Oct;15:459-466. URI: <http://nopr.niscair.res.in/handle/123456789/41038>
3. **Vishal SS**, Tilwani S, Thorat R, Dalal SN. Generation of mice with tissue specific transgene expression using sperm mediated gene transfer. International Journal of Pharma and Bio Sciences. 2017 Apr; 8(2): (B) 324-329. DOI: <http://dx.doi.org/10.22376/ijpbs.2017.8.2.b324-329>

b. Accepted:

Vishal SS, Tilwani S, and Dalal SN. Plakoglobin localization to the cell border restores desmosome function in cells lacking 14-3-3 γ . Biochemical and Biophysical Research Communications. 2017. DOI: <https://doi.org/10.1016/j.bbrc.2017.12.080>

c. Communicated:

d. Other Publications:

1. Award for the poster / oral presentation if any:

Prof. B.R. Seshachar Memorial prize for the best paper presentation by young scientist in poster session for poster titled “Plakoglobin localization to the cell border rescues desmosome assembly in cells lacking 14-3-3 γ ” at the **XXXIX All India Cell Biology Conference (AICBC)**, held at Thiruvananthapuram, India, 2015.

2. Workshops attended:

“instem Mouse Embryology Workshop: Stem Cells to Organogenesis” held at inStem, NCBS, Bangalore, India, 2013.

3. Poster presented at following conferences:

- i) Presented poster titled "Regulation of cell-cell adhesion and differentiation of spermatogonial stem cells by 14-3-3 γ " at "Stem Cells to Organogenesis symposium", held at inStem, NCBS, Bangalore, India, 2013.
- ii) Presented poster titled "Plakoglobin localization to the cell border rescues desmosome assembly in cells lacking 14-3-3 γ " at the XXXIX All India Cell Biology Conference (AICBC), held at Thiruvananthapuram, India, 2015.
- iii) Presented poster titled "Plakoglobin localization to the cell border rescues desmosome assembly in cells lacking 14-3-3 γ " at the Gordon Research Seminar and the Gordon Research Conference on Protein transport across cell membranes: Mechanism, Structure and Regulation, held at Galveston, USA, 2016.

Signature of Student:

Date: 18 December 17

Doctoral Committee:

S. No.	Name	Designation	Signature	Date
1.	Dr. S. V. Chiplunkar	Chairperson	<i>[Signature]</i>	18/12/17
2.	Dr. S. N. Dalal	Guide/ Convener	<i>[Signature]</i>	18/12/17
3.	Dr. M. M. Vaidya	Member	<i>[Signature]</i>	18/Dec/17
4.	Dr. D. Bhattacharyya	Member	<i>[Signature]</i>	

Forwarded Through:

[Signature]
26/12/17

Dr. S.V. Chiplunkar

Director, ACTREC &

Chairperson, Academic & Training Program, ACTREC.

Dr. S. V. Chiplunkar
Director

Advanced Centre for Treatment, Research & Education in Cancer (ACTREC)
Tata Memorial Centre
Kharghar, Navi Mumbai - 410 210.

[Signature] 18/12/17
[Signature]
Prof. K. Sharma

Director, Academics

T.M.C.

Prof. K. S. Sharma
DIRECTOR - ACADEMICS, TMC
Mumbai - 400 012.

LIST OF TABLES

Table No.	Title of Table	Page No.
3.1	List of oligonucleotides used for cloning shRNA, cDNA cloning and site directed mutagenesis (SDM).	81
3.2	List of components used in making sited directed mutagenesis (SDM) PCR mix.	94
3.3	A table describing different components used for making calcium phosphate DNA transfection mix.	100
3.4	A table describing the different components used in making DNA:Lipofectamine LTX transfection mix.	101
3.5	A table describing different components used for making DNA:PEI transfection mix.	102
3.6	Transfection mix for lentiviral packaging using ViraPower.	103
3.7	List of components used in genotyping PCR mix.	108
3.8	List of oligonucleotides used for genotyping.	110
3.9	List of components used in 14-3-3 γ exon 1PCR mix.	112
3.10	Composition of 1X Sample buffer.	115
3.11	List of the primary antibodies used for Western blotting experiments.	116
3.12	Composition of TBST.	116
3.13	Composition of Total lysis buffer.	118
3.14	Composition of Cytoskeletal buffer.	119
3.15	Composition of sample buffer used for extraction of insoluble fraction.	119
3.16	List of the primary antibodies used for immunofluorescence assay in this	120

	study.	
3.17	Composition of NET-N buffer.	123
3.18	Composition of elution buffer.	123
3.19	PCR components for mRNA to cDNA conversion.	124
3.20	List of oligonucleotides used for GAPDH reverse transcriptase PCR.	125
4.1	Pups obtained from pLKO Tet Puro pre-founder mice (F1 generation) [Strain: BALB/c].	131
4.2	Pups obtained from pLKO Tet Puro14-3-3 γ shRNA pre-founder mice (F1 generation) [Strain: BALB/c].	132
4.3	Pups obtained from inbreeding of pLKO Tet Puro14-3-3 γ shRNA positive mice (Inbreeding of F1 generation) [Strain: BALB/c].	135
4.4	Pups obtained from inbreeding of pLKO Tet Puro14-3-3 γ shRNA positive mice (Inbreeding of F2 generation) [Strain: BALB/c].	136
4.5	Pups obtained from pLKO Tet Puro pre-founder mice (F1 generation) [Strain: Crl:CFW (SW)].	142
4.6	Pups obtained from pLKO Tet Puro 14-3-3 γ shRNA pre-founder mice (F1 generation) [Strain: Crl:CFW (SW)].	146
4.7	Pups obtained from the inbreeding of the control pLKO Tet Puro positive mice and control pLKO Tet Puro 14-3-3 γ shRNA positive mice [Strain: Crl:CFW (SW)].	148
4.8	Pups obtained from the inbreeding of the doxycycline untreated pLKO Tet Puro positive mice and doxycycline treated pLKO Tet Puro 14-3-3 γ shRNA positive mice [Strain: Crl:CFW (SW)].	149

4.9	Pups obtained from pCCLK14 Turbo RFP vector pre-founder mice (F1 generation) [Strain: Crl:CFW(SW)].	157
4.10	Pups obtained from pCCLK14 Turbo RFP 14-3-3 γ shRNAmir pre-founder mice (F1 generation) [Strain: Crl:CFW(SW)].	160
4.11	Pups obtained from pCCLK14 Turbo RFP pre-founder mice (F1 generation) [Strain: Crl:CFW(SW)].	169
4.12	Pups obtained from pCCLK14 Turbo RFP 14-3-3 γ shRNAmir pre-founder mice (F1 generation) [Strain: Crl:CFW(SW)].	172
4.13	Pups obtained from inbreeding of Turbo RFP positive mice (Inbreeding of F1 generation) [Strain: Crl:CFW(SW)].	175
4.14	Pups obtained from the K14 Turbo RFP14-3-3 γ shRNAmir pro-founder mouse [Strain: FVB].	180
4.15	Pups obtained from the pLentiCRISPR K14 Cas9 pre-founder mice [Strain: Crl:CFW(SW)].	186
4.16	Pups obtained from the pLentiCRISPR K14 Cas914-3-3 γ gRNA pre-founder mice [Strain: Crl:CFW(SW)].	187
5.1	A table showing different types of HA tagged PG deletion constructs with the expected molecular weight.	204

LIST OF FIGURES

Figure No.	Figure Title	Page No.
1.1	The schematic representation of structure of testis	32
1.2	Different stages of spermatogenesis and different SMGT techniques used at these stages.	36
1.3	Different types of cell-cell adhesion junctions seen in seminiferous tubules	66
1.4	Structure of adherens junction.	70
1.4	Structure of desmosomes.	74
3.1	Design of pLKO Tet Puro vector	81
3.2	Vector map of pLKO Tet Puro vector and pLKO Tet Puro 14-3-3 γ shRNA vector.	83
3.3	Vector map of pTRIPz vector and pTRIPz 14-3-3 γ shRNAmir vector.	86
3.4	Vector map of pCCLK14 Turbo RFP vector and pCCLK14 Turbo RFP 14-3-3 γ shRNAmir vector.	88
3.5	Vector map of pLentiCRISPR Cas V1 vector and pLentiCRISPR Cas V1 14-3-3 γ gRNA vector.	91
3.6	Vector map of pLentiCRISPR K14 Cas9 vector and pLentiCRISPR K14 Cas9 14-3-3 γ gRNA vector.	93
3.7	Sequence analysis of PG cDNA (NCBI), Myc PG WT and Myc PG S236A.	96
3.8	A cartoon representing the structure of the PG deletion mutants.	99
3.9	The schematic representation of the principle of T7 endonuclease assay	113

4.1	Validation of pLKO Tet Puro 14-3-3 γ shRNA construct.	128
4.2	Pedigree analysis of the pLKO Tet Puro vector pre-founder mice and pLKO Tet Puro 14-3-3 γ shRNA pre-founder mice [Strain: BALB/c].	130
4.3	Cloning and sequencing of the puromycin resistance cDNA PCR product.	133
4.4	Pedigree analysis of F2 and F3 generation obtained from inbreeding of pLKO Tet Puro 14-3-3 γ shRNA positive F1 generation mice [Strain: BALB/c].	134
4.5	Effect of doxycycline treatment on 14-3-3 γ levels in pLKO Tet Puro 14-3-3 γ shRNA positive mice.	137
4.6	Pedigree analysis of the pLKO Tet Puro pre-founder mice and pLKO Tet Puro 14-3-3 γ shRNA pre-founder mice [Strain: CrI:CFW(SW)].	139
4.7	The effect of doxycycline treatment on 14-3-3 γ levels in the doxycycline treated and untreated pLKO Tet Puro pre-founder mice and pLKO Tet Puro 14-3-3 γ shRNA pre-founder mice.	147
4.8	Structure of Epidermis	151
4.9	Validation of pCCLK14 Turbo RFP 14-3-3 γ shRNAmir construct.	152
4.10	Pedigree analysis of the pCCLK14 Turbo RFP vector pre-founder mice and pCCLK14 Turbo RFP 14-3-3 γ shRNAmir pre-founder mice [Strain: CrI:CFW(SW)].	154
4.11	PCR amplification of Turbo RFP from transgenic mice and its sequencing.	161
4.12	PCR amplification of Turbo RFP 14-3-3 γ shRNAmir from transgenic	163

	mice and its sequencing.	
4.13	PCR amplification of Turbo RFP 14-3-3 γ shRNAmir from the testis of pre-founder mice and its sequencing.	165
4.14	PCR amplification of Turbo RFP 14-3-3 γ shRNAmir from the testis of D/1537 and its sequencing.	173
4.15	Pedigree analysis of F2 generation obtained from inbreeding of Turbo RFP positive F1 generation mice [Strain: Crl:CFW(SW)].	174
4.16	Turbo RFP expression in the epidermis of Turbo RFP positive mice.	176
4.17	Pedigree analysis of pups obtained from the K14 Turbo RFP 14-3-3 γ shRNAmir pro-founder mouse [Strain: FVB].	178
4.18	Validation of 14-3-3 γ gRNA.	182
4.19	Pedigree analysis of the pLentiCRISPR K14 Cas9 and pLentiCRISPR K14 Cas9 14-3-3 γ gRNA pre-founder mice [Strain: Crl:CFW(SW)].	184
4.20	Levels of 14-3-3 γ in the epidermis of pLentiCRISPR K14 Cas9 14-3-3 γ gRNA positive mice.	188
4.21	PCR amplification of 14-3-3 γ exon 1 sequence from the pLentiCRISPR K14 Cas9 14-3-3 γ gRNA positive pups.	190
5.1	PKC μ phosphorylates PG.	198
5.2	Cytoplasmic localization of S236A PG.	200
5.3	The loss of PKC μ affects desmosome assembly and the levels of desmosomal proteins.	201
5.4	Sertoli cell isolation and culture.	203
5.5	Expression of HA tagged PG deletion constructs.	205

5.6	The validation of PG gRNA clones in HCT116 cells.	206
5.7	Expression of PG-EGFP-f and PG-EGFP in HCT116 cells.	208
5.8	Cell border localization of PG is altered upon loss of 14-3-3 γ .	209
5.9	PG-EGFP-f rescues cell border localization of DSG2, DP and PKP3 upon 14-3-3 γ loss.	211
5.10	PG-EGFP-f expression in 14-3-3 γ knockdown cells led to the increase in the cell border localization of DP and DSG2.	212
5.11	PG-EGFP does not restore DP to the cell border upon 14-3-3 γ loss.	213
5.12	The expression of PG-EGFP-f in 14-3-3 γ knockdown cells led to the increase in the DPI/II protein levels.	215
5.13	PG-EGFP-f stabilizes the DSG2 at the cell border and stimulates DSG2 transport.	218
5.14	HCT116 derived 14-3-3 γ knockdown cells expressing PG-EGFP-f have increased cell-cell adhesion.	220
5.15	PG-EGFP-f does not require endogenous PG to restore desmosomal protein localization.	223
5.16	PG-EGFP-f requires PKP3 to restore desmosomal protein to the cell border.	227
5.17	PG-EGFP-f requires KIF5B to restore desmosomal cadherins to the cell border.	233
5.18	PG-EGFP-f does not affect adherens junction protein localization	236
5.19	Model illustrating the role of PG and 14-3-3 γ in regulating desmosome assembly.	240

5.20	Model illustrating the role of PG and KIF5B in regulating desmosome assembly.	243
------	---	-----

1. Introduction

1. Introduction

1.1 Transgenesis

The study of human disease cannot be restricted by observations made in affected individuals and *in vitro* studies. To understand the cause of the disease and different genetic, physiological and environmental factors affecting disease outcome, animal models of diseases are required. These animal models are generated by introducing changes in their genome that are inherited by the progeny. The process of introducing genetic changes into the genome of an animal by using foreign DNA is termed as transgenesis.

To stably modify the genome of an organism, it is necessary that the changes are made at the early stages of embryogenesis such that the transgene is integrated into the germline. Dr. Ralph Brinster developed a technique that permitted the isolation and culture of ova and embryos [1]. After a decade of this technical advancement, the initial experiments of embryo manipulation were successfully performed by multiple groups. Briefly, cultured embryos were aggregated with teratoma cells resulting into generation of progeny expressing teratoma specific genes [2, 3].

Gordon *et al.*, showed that the foreign DNA can be directly injected into male pro-nucleus of the 0.5 dpc (day post coitus) embryo. The injected embryo was then transplanted into the pseudo-pregnant mother for further development. The pups obtained from the pseudo-pregnant mother were transgene positive [4]. This technique is known as DNA microinjection. Using this technique, Brinster developed transgenic mice expressing Herpes Simplex Virus (HSV) thymidine kinase [5]. Instead of injecting DNA, some groups infected the embryos with retroviruses to obtain transgenic animals [6, 7]. Isolation, culture and modification of embryonic

stem cells led to the development of generation of transgenic animals by injecting modified embryonic stem cells into the blastocoel cavity of embryo [8].

All the above mentioned methods involved modification of fertilized ovum and the efficiency of transgenesis using these techniques is very low. Other difficulties in using these methods of transgenesis includes: difficulties in culturing embryos, ovum and embryonic stem cells; maintenance of the pluripotency of embryonic stem cells, disruption of the embryos during microinjection, difficulty in implantation of embryos into pseudo-pregnant mothers, poor integration of the transgene [9] and physiological stress to animals. Apart from these factors, these methods are laborious, time consuming and expensive.

Another way to generate transgenic animals is to modify gametes. The female gametes or ova cannot be used to generate transgenic animals because the number of female gametes available for modification are limited and it was observed that ova do not bind to DNA [10]. In contrast, the male gametes (spermatozoa) are present in large numbers and bind to DNA [11]. Therefore, different groups started modifying spermatozoa in an attempt to generate transgenic animals. A brief description of the process of spermatogenesis and testis morphology is required to understand the principle behind the methods that use spermatozoa as a vehicle for transgene delivery.

1.1.1 Structure of the Testis

Testes are the oval-shaped organs of the male reproductive system which produce male gametes. Each testis is covered by connective tissue sheath known as tunica albuginea (Figure 1.1). The tunica albuginea extends inwards forming testicular septa and divides testis into different lobules known as testicular lobules. There are around 250 lobules and each lobule contains around 4-5

seminiferous tubules. The seminiferous tubules from all the lobules converge to form rete testis and rete testis further extend to form a mass of tightly coiled tubes known as epididymis. Epididymis is divided into three parts: head, body and tail. The tail of epididymis is connected to vas deferens also known as efferent ductules or ductus deferens. Epididymis stores the sperm and promotes maturation of sperms until they pass through the vas deferens. The testis can be divided into two compartments an interstitial compartment (region between the testicular lobules), made up of macrophages and Leydig cells (involved in hormone production), and tubular compartment (made up of testicular lobles), made up of seminiferous tubules (involved in spermatogenesis) [12]. Seminiferous tubules in pre-pubescent animals are made up of Sertoli cells and spermatogonial stem cells (SSC). SSCs are the progenitor cells which give rise to spermatocytes by the process of spermatogenesis. SSC arises from primordial germ cells after a series of division and Sertoli cells arise from mesenchymal cells [13].

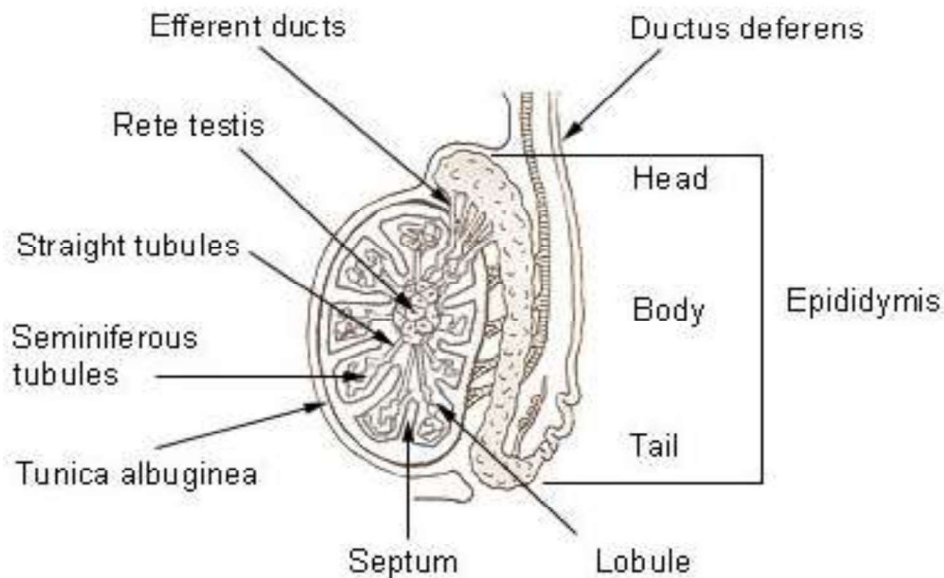


Figure 1.1: The schematic representation of structure of testis. The schematic drawing showing anatomy of a testis highlighting different parts of testis [14].

1.1.2 Spermatogenesis

Spermatogenesis is the process by which SSC divides and differentiates to give rise to mature sperm (Figure. 1.1). The process of spermatogenesis is divided into three steps, i.e., spermatogonial renewal, meiosis and spermiogenesis [13]. In spermatogonial renewal, also called as spermatogoniogenesis, a type A spermatogonium(also called as A_s) undergoes a series of mitotic division (A_s to A_{pr} to A_{al} to A_{1-4} to Intermediate spermatogonium) to give rise to a type B spermatogonium [15]. Expression of Stem Cell Factor (SCF) by Sertoli cells and expression of cKit, the receptor for SCF, by the spermatogonial cells is important for the mitotic division of spermatogonial cells. In spermatogonial renewal, a balance is maintained between the pluripotent SSC population and the pool of SSCs committed to differentiation. This balance is maintained with the help of proteins like Nanos homolog 2 (NANOS2), Inhibitor of DNA binding 4 (ID4) and Zinc finger and BTB domain containing 16 (ZBTB16). NANOS2 suppresses expression of Stimulated by Retinoic Acid gene 8 (STRA8) which is required for pre-meiotic DNA replication [16, 17]. Glial cell line derived neurotrophic factor (GDNF), secreted by Sertoli cells and peritubular myoid cells, binds to GRNF-family receptor $\alpha 1$ (GFR $\alpha 1$) present on SSCs and catalyzes activation of c-RET receptor leading to the activation of PI3K/AKT, MEK and Src kinases. GDNF also induces expression of ID4. ZBTB16 represses cKit which is required for SSC differentiation. Spermatogenesis and oogenesis specific helix-loop-helix proteins (SOHLH) SOHLH1 and SOHLH2 are important for repressing the genes responsible for stem cell self-renewal [17].

Type B spermatogonia differentiate into primary spermatocytes, which enter the meiotic program. Primary spermatocytes undergo meiosis I to give rise to secondary spermatocytes, which undergo meiosis II and differentiate into round spermatids with a haploid DNA content.

Initiation of meiosis requires expression of Deleted in Azoospermia-like protein (Dazl), which induces expression of Stra8 which is required for meiosis [16]. Prophase of meiosis I is divided into four steps, viz., leptotene, zygotene, pachytene and diplotene. DNA replication occurs in the pre-leptotene phase of meiosis I [18] and at leptotene stage of prophase I, double stranded DNA breaks (DSB) are introduced by SPO11 and the proteins involved in DNA repair pathways e.g. γ H2AX, ATM (Ataxia Telangiectasia Mutated), ATR (Ataxia Telangiectasia and Rad-3 related) and DMC1 (DNA meiotic recombinase1) are recruited to the DSB sites [17]. In the leptotene stage, synaptonemal complex protein 2 (SYCP2), SYCP3 and cohesin start forming axial elements of synaptonemal complex along the homologous chromosomes. In the zygotene stage, axial elements are called as lateral elements and they are joined by SYCP1 leading to formation of synaptonemal complex thus initiating synapsis (pairing of homologous chromosomes) and meiotic recombination. At pachytene stage complete synapsis is observed, the DSB are repaired and meiotic recombination are completed. In diplotene stage, synaptonemal complex is degraded, crossover of sister chromatids or chiasmata is observed [17]. The sister chromatids are held together by cohesins. The cells then progress to diakinesis where meiotic spindle formation begins. The primary spermatocytes then undergo anaphase I, followed by metaphase I and telophase I. After the end of telophase I, cells undergo second meiotic division, known as meiosis II. In meiosis II, DNA replication does not occur. The chiasmata are resolved at metaphase II/anaphase II stage of meiosis II and sister chromatids are separated by removal of cohesins thus giving rise to haploid cells [17, 18].

During the process of spermiogenesis, haploid round spermatids undergo a series of changes, such as flagella formation, manchette formation, the removal of a large portion of cytoplasm resulting in the formation of elongated spermatids, acrosome formation and nuclear

condensation [13]. Flagellum is required for the motility and flagellum formation starts at the centriole and is composed of a microtubule based structure called the axoneme. Axoneme formation is controlled by proteins like Hsp70-Hsp90 organizing protein (HOP) and Sperm associated antigen 6 (SPAG6) [17]. The manchette is a microtubular structure attached to the nucleus and it helps in the elongation of sperm nucleus. Removal of cytoplasm is important for the development of sperms as it contributes to the elongated slender shape. A major part of the cytoplasm is removed by tubulobulbar complex and the remaining cytoplasm is removed by the residual body and cytoplasmic droplet. Acrosome biogenesis starts with the fusion of pro-acrosomic vesicles above the sperm nucleus. Acrosome contains the hydrolytic enzymes required to penetrate the zona pelucida of the ovum. Nuclear condensation leads to the cessation of transcription. A defect in any of these steps leads to sterility [17]. After nuclear condensation, the disassembly of apical ectoplasmic specialization junctions, present between Sertoli cells and elongated spermatids, takes place thus allowing the elongated spermatids to leave the seminiferous tubules and migrate to the epididymis, where they mature to give rise to spermatozoa (Figure. 1.2). Therefore, each SSC gives rise to multiple spermatozoa and spermatozoa are regularly produced as opposed to ova. Hence, it is easier to generate larger numbers of transgenic animals by modifying spermatozoa and using them as a vehicle for the delivery of the transgene.

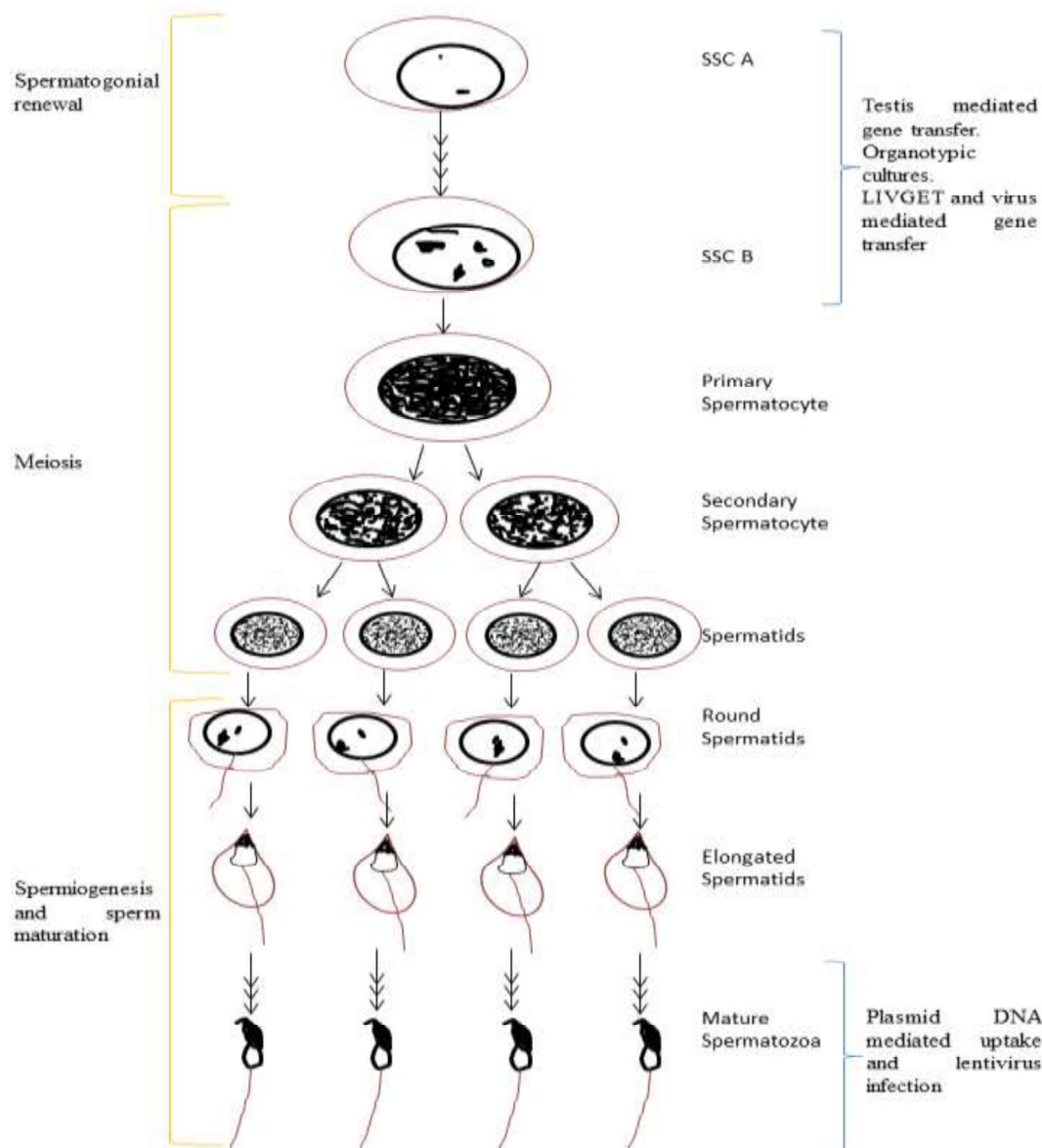


Figure 1.2: Different stages of spermatogenesis and different SMGT techniques used at these stages. The process of spermatogenesis is divided into three steps: Spermatogonial renewal, meiosis and spermiogenesis and sperm maturation. The figure also indicates which cell types are modified using the different SMGT techniques [19].

1.1.3 Sperm Mediated Gene Transfer

Different techniques have been developed to generate transgenic mice by modifying spermatozoa or SSCs (as indicated in Figure. 1.1) and these have been broadly grouped under the term "Sperm Mediated Gene Transfer" (SMGT). The different techniques by which SMGT is achieved are listed below.

i) Gene transfer mediated by Spermatozoa

As mentioned earlier, it was observed that spermatozoa can bind to DNA [10] and therefore, spermatozoa incubated with transgenic DNA can be used for generating transgenic animals. The binding of DNA to spermatozoa is not random and is dependent on a receptor present on the spermatozoa and this receptor can be blocked by Inhibition factor 1 (IF1) present in seminal fluid [20]. Binding of DNA to its receptor led to the internalization of the DNA bound receptor followed by the release of DNA into sperm nuclei. In addition to DNA receptor, MHC II and CD4 molecules played an important role in DNA uptake and internalization by spermatozoa [21]. Moreover, blocking CD4 receptors also prevented DNA internalization in spermatozoa [21].

Lavitrano *et al.*, [11] generated a transgenic mouse by incubating a suspension of spermatozoa (washed spermatozoa to remove IF1) with circular plasmid DNA encoding bacterial chloramphenicol acetyltransferase (CAT) and using this suspension for *in vitro* fertilization. The transgenic mice thus obtained, did not express the CAT gene due to the rearrangement of the transgene [11]. This method of transgenesis is not very promising as several groups who have tried this technique failed to obtain transgenic animals (reviewed in [22]). The major problems with this technique were: DNA uptake efficiency was highly variable [23], the transgene did not

integrate into the host genome and a high occurrence of rearrangement of the transgene upon integration. Intra-Cytoplasmic Sperm Injection (ICSI) (the injection of sperm into an ovum) is used to improve the efficiency of obtaining transgenic animals using this method [24].

In an attempt to obtain mice that express the transgene, Lavitrano *et al.*, [11] incubated spermatozoa with a linear DNA fragment of a plasmid expressing CAT and used these spermatozoa for *in vitro* fertilization. They found that transgenic animals, obtained from this method, expressed the CAT gene and the efficiency of obtaining transgenic progeny with this protocol was higher compared to that observed with circular plasmid DNA. Using this technology, the Lavitrano laboratory had successfully generated transgenic pigs expressing human decay accelerating factor with an efficiency of 57% [25] and transgenic pigs expressing multiple transgenes, *i.e.*, enhanced blue fluorescent protein, enhanced green fluorescent protein and DsRed2 [26]. Kroll *et al.*, [27] further modified the above-described protocol by incubating purified *Xenopus* sperm nuclei for a short period of time (10 min) with restriction enzymes in the presence of linearized plasmid DNA containing cDNA sequence of GFP. As a result, an improvement was observed in the efficiency of integration of linearized plasmid DNA into the genome and this method was named Restriction Enzyme Mediated Insertion (REMI) SMGT. This modified sperm nuclei were injected into the unfertilized ovum to generate transgenic embryos [27]. Another method used to improve the efficiency of DNA uptake by spermatozoa was to disrupt the cell membrane of spermatozoa by freeze-thaw cycles and inject the membrane-disrupted spermatozoa along with a plasmid DNA fragment containing a GFP expression cassette into oocytes [28]. This change in protocol resulted in an increase in the efficiency of generating transgenic animals by 20%. The most critical factors associated with this

method were the choice of enzyme, which is used to linearize the plasmid DNA and the processing of sperm nuclei.

Since DNA uptake by spermatozoa has not been very efficient, some groups tried using transfection reagent lipofectamine to introduce exogenous DNA into spermatozoa [29-32]. Lipofectamine complexed with linearized DNA (lipofection combined with REMI) gave efficient transgenesis compared to lipofectamine complexed with circularized DNA [30, 32]. Some groups have also used nanoparticles, like magnetic nanoparticles, mesoporous silica nanoparticles, and halloysite clay nanotubes, to deliver exogenous DNA to sperm [33-36]. Briefly, magnetic nanoparticles mixed with linearized DNA fragments were incubated with sperm and subjected to the magnetic field for 90 min. Unbound DNA magnetic nanoparticle complex was removed and oocytes were fertilized with magnetofacted sperm to obtain GFP positive embryos [33]. Using mesoporous silica nanoparticles only binding with sperm was studied to show that the binding of the nanoparticle does not affect sperm but it was not used for making transgenic embryos [35]. Campos *et al.*, showed that the sperm could be transfected with plasmid (circularized and linearized in the ratio of 1:1) using halloysite clay nanotubes or nanopolymer, transfected sperm was washed to remove the excess of transfection mixture, transfected sperm was then used for *in vitro* fertilization. It was observed that the more transgenic embryos were obtained with sperm transfected using nanopolymer or halloysite clay nanotubes when compared with sperm transfected using lipofectamine [34]. The use of nanoparticles for SMGT was termed as NanoSMGT [36].

ii) Transplantation of Modified Spermatogonial Stem Cells into Testis

Spermatogonial stem cells (SSCs) are progenitor cells, which undergo meiosis followed by differentiation to form spermatozoa, as described above. These cells are mostly quiescent; however, they can be cultured and easily modified *in vitro*. Brinster *et al.*, [37] demonstrated that transplanting SSCs from a fertile animal to an infertile animal resulted in the restoration of male fertility and suggested that modified SSCs could be used to generate transgenic animals. This technique did not involve *in vitro* fertilization or ICSI. It was also shown that SSC transplantation in a fertile mouse resulted in the generation of some pups derived from spermatozoa from the donor and some from spermatozoa derived from the recipient [38]. Though Brinster *et al.*, did not use modified SSCs, the Brinster laboratory showed that SSCs can be isolated, cultured and transfected with a plasmid DNA or infected with retroviruses. These stably transfected SSCs were then transplanted into recipient testis where modified SSCs form colonies and these colonies were positive for transgene *lacZ* [39, 40]. However, they did not use these mice to generate transgenic animals. Alternatively, SSCs can be transduced *in vivo* using retroviruses to obtain transgene positive spermatozoa [39]. Ivics *et al.*, standardized the protocol to modify SSCs *in vitro* by transposons [41]. None of these articles used the transgene positive spermatozoa for fertilization of ovum but these experiments demonstrated that even a few transgenic SSCs upon transplantation can be used for the generation of transgene positive spermatozoa and hence can be used to generate transgenic animals. The principle behind this technique formed the basis for the evolution of SMGT techniques used today.

An organotypic culture technique, for the culture of testicular cells of the neonatal mouse, to obtain fertile spermatozoa *in vitro* has also been developed. In this technique, fragments of neonatal testis were cultured using gas-liquid interphase method in KSR medium and it was

observed that the SSCs differentiated to form haploid spermatocytes, round and elongated spermatids. Both round and elongated spermatids were found to be fertile when used for fertilizing ova using round spermatid injection (ROSI) and ICSI technique respectively. Fertilized ova were transplanted, and some of the pups were found to be transgene positive [42]. Though establishing organotypic cultures is not easy, the cultures once established can generate spermatozoa for a period of up to two months. It is tempting to speculate that recombinant spermatozoa generated *in vitro* in these organotypic cultures could result in the generation of compound transgenic animals carrying and expressing multiple transgenes in a single step rather than the multiple rounds of transgenesis and mating that is the current norm.

iii) Electroporation of Transgenic DNA into Testis

DNA can be introduced directly into target organs either in adult animals or pups and embryos using a number of procedures that are covered by the term LIVGET (localized *in vivo* gene transfer technique). LIVGET achieves the integration of plasmid DNA into the target organs by three distinct methods. The DNA is encapsulated either in a microparticle or a lipid particle that is injected into the target organ, or DNA is injected into the target organ followed by an electrical pulse across the organ. All these procedures resulted in the incorporation of the DNA construct into the cells of the target organ. DNA injection into the seminiferous tubules or testis is termed as TMGT (testicular mediated gene transfer). Sato *et al.*, for the first time suggested that DNA can be directly injected into the testis and showed that DNA calcium phosphate complex when injected into the testis is taken up by the cells of the testis as shown by southern blotting but with the passage of time there was loss of transgene and the injected mice could not sire transgene positive pups [43]. Muramatsu *et al.*, [44] then compared the efficiency of microparticle

bombardment and electroporation for testis specific expression of the CAT gene. This was the first report in which cells in the testis were modified successfully *in vivo*. They showed that, upon intra-testicular DNA injection and electroporation, testicular cells showed CAT expression. Further, they also injected a plasmid expressing lacZ into the testes followed by the application of an electric current across the testis. Post 48 hours of electroporation, sections of electroporated testis were stained with X-gal, hematoxylin and eosin, and they observed lac Z expression in spermatogonium like cells, spermatocyte like cells and spermatid like cells. But they did not determine whether the plasmid DNA had integrated into the genome of these cells [45]. Yamazaki *et al.*, [45] demonstrated that injection of linearized plasmid DNA into seminiferous tubules, followed by the application of an electric current to the testis, resulted in long term expression of the lac-Z transgene and also in the modification of spermatogonial stem cells. The above mentioned reports did not use transgene positive sperms, obtained using electroporation, for generating transgenic animals. Huang *et al.*, generated transgenic mice expressing YFP by electroporation. Briefly, DNA/HBS complex was injected into the testis of 14 day old mice followed by electroporation, transgene expression was detected using fluorescent microscopy, the tubules expressing YFP were collected to obtain transgenic spermatozoa for fertilizing ovum using ICSI and embryos were transplanted into pseudo-pregnant female mice to obtain transgenic pups [46]. The Majumdar laboratory has recently reported a method for DNA electroporation in which the *in vitro* fertilization and embryo transplantation steps are bypassed and the electroporated mouse is directly mated with female mice to obtain pups. In this method linearized plasmid DNA was injected at multiple locations on one of the mouse testicle followed by electroporation and the other testicle was castrated, 35 days post injection, this pre-founder mouse was mated with wild type female mice to obtain pups and pups were screened for the

presence of the transgene [47]. Later on this technique was modified and both the testicles were injected and electroporated. The efficiency of this method was around 57-62% because different vector constructs used in this study had different efficiency of integration [48]. However, the pulse intensity and pulse interval will have to be standardized for different species such that the testicular cells will not be affected by electroporation leading to their cell death.

iv) Virus Mediated Transgenesis

As mentioned earlier, Nagano *et al.*, demonstrated that spermatogonial cells could be infected with retroviruses *in vitro* and these cells upon reintroduction into the recipient testis differentiated into transgene containing spermatozoa [39]. These recipient male mice were able to sire transgenic pups (expressing lac Z) when mated with wild type female mice. The transgene positive pups obtained from the recipient male mouse were inbred and it was determined that the lac Z transgene was stably integrated as the pups obtained from inbreeding of transgene positive animals were also positive for lac Z expression [49]. The same group suggested that the use of lentiviruses would increase the efficiency of transgenesis due to their ability to infect quiescent germ cells [40]. Pfeifer *et al.*, [50] independently demonstrated that lentiviruses could infect embryonic stem (ES) cells. They also showed that morula stage embryos could be infected with lentiviruses *in vitro* and the infected morula could be implanted into the surrogate mother to obtain transgene positive animals. Hamra *et al.*, [51] demonstrated that purified SSCs isolated from rat testis could be infected with lentiviruses *in vitro*. And these modified SSC's could give rise to transgenic progeny when implanted in the rat testis. While the techniques mentioned above resulted in the generation of transgenic animals, these were cumbersome for the following reasons. SSCs need to be isolated and cultured *in vitro* and care has to be taken to prevent the

differentiation of SSCs. Further, the transduced SSCs need to be propagated in culture, which is not a trivial protocol though it has become easier over time. In addition, spermatocytes need to be depleted from the recipient male mice and often the transplantation of the recombinant SSCs into recipient mice failed, probably due to immune reactions against the modified SSCs. This protocol is also difficult to use in larger animals where spermatocyte depletion and surgery might pose unforeseen problems. In 2004, Kanatsu-Shinohara *et al.*, [52] suggested that all the difficulties in obtaining and culturing SSCs can be bypassed by *in vivo* retroviral transduction of SSCs. By injecting retroviruses into the testis of sexually immature mice, they obtained transgenic pups but the efficiency of obtaining transgenic pups (22%) was little less compared to the *in vitro* transduction technique (33-38%).

In 2011, Sehgal *et al.*, [53] reported that, upon *in vivo* lentiviral transduction of pre-pubescent male mice, the EGFP-f transgene could integrate into the DNA of the SSCs and the transgene was expressed in all the cells in the testis. More than 60% of the pups generated by mating these pre-founder mice with wild type female mice were positive for the transgene. The transgene integration sites were mapped in the transgene positive pups and demonstrated that the transgene was stably inherited to next generation and that most of the animals contained one or two integrant [53]. This method is cost effective, simple and highly efficient for generation of transgenic animals as compared to the methods described above. But the site where integration is going to occur cannot be predicted and the transgene will be expressed by all the testicular cells, which are infected by lentiviruses. Few groups have also tried using adenoviruses for generating transgenic animals but adenoviral infection did not lead to the integration of virus genome into the host cell. Hence, adenoviruses when used to generate transgenic animal by injection into seminiferous tubules did not show integration into the genome of the progeny but some of the

pups expressed the transgene [54]. Recently, using GFP expressing pseudotyped lentivirus infected spermatozoa, GFP positive transgenic mice were obtained [55]. Briefly, cauda epididymis and the distal end of vas deferens were placed in a dish, punctured with a needle and incubated with concentrated virus soup for 30 min to 2 hours. Then the spermatozoa were washed with buffer and used for IVF to generate transgenic mouse. The efficiency of obtaining transgenic animal using this technique was found greater than 42% [55]. The critical factor, which affected the efficiency of fertilization in this technique, was the time interval for which viruses were incubated with spermatozoa.

1.1.4 Site Specific Recombination and Targeted Knockouts

Until recently, the ability to generate knockout and knock-in mice was limited to technology requiring the modification of embryonic stem cells *in vitro*, followed by embryo aggregation or blastocyst injection. These methods are difficult to develop and require facilities not available in most laboratories. Kanatsu-Shinohara *et al.*, tried to generate knockout mice by infecting cultured SSCs with retroviruses containing neomycin resistant cassette [56]. SSC colonies resistant to neomycin were sequenced to identify the genes flanking the retroviral genome and to find out if the neomycin resistant cassette became the part of the open reading frame (ORF) of the flanking gene sequences, suggesting disruption of that gene. Using this random mutagenesis approach, they found that one of the disrupted genes was *occludin*. The SSC colony with a disrupted *occludin* allele was transferred to the recipient testis to generate occludin knockout mice; though the efficiency to generate knockout mice with this method was very low (1.7%) [56]. However, the advent of the SMGT technologies allows the exploitation of the nucleases like TALENS (Transcription Activator-Like Effector Nucleases) and CRISPR-Cas system

(Clustered Regularly Interspaced Short Palindromic Repeats; Cas-CRISPR associated protein) to achieve targeted insertions or deletions or modifications with higher efficiency.

While using TALENS, the DNA or RNA sequences (transgene) can be injected into the oocytes or embryos. Once inside the nucleus, TALENS bind to specific DNA sequences and introduce a double stranded break, which causes activation of the Non Homologous End Joining (NHEJ) pathway. During NHEJ, the exogenously provided template DNA or RNA is used to insert or delete a few bases at the site of strand breakage. Recently, knock-in and knockout mice, and mice with a site-specific mutation were generated using TALENS [57-59]. Elimination of germline mitochondrial DNA mutations was achieved with the help of TALENS [60]. Instead of the embryo injections, the TALENS can be encoded in a lentiviral vector and used to infect cultured SSCs. Recently, TALENS complexed with lipofectamine were used to transfect SSCs to generate or correct mutations, even electroporation of SSCs has also been done to deliver TALENS without affecting the cell viability or proliferation of SSCs [61, 62].

In the CRISPR-Cas system, a single guide RNA (sgRNA) (20 nucleotides) directs the Cas9 nuclease to its target. Once activated, Cas generates double stranded breaks, activates NHEJ and NHEJ activation leads to insertion or deletion of specific nucleotides. To generate transgenic mice using CRISPR-Cas system, Cas mRNA, sgRNA and a linearized vector coding for the transgene were injected into the pronucleus or into the cytoplasm of a two/four cell embryo [63]. Transgenic mice containing a conditional allele for *Mecp2* were generated by injecting mouse embryos with a mixture of Cas9 mRNA, sgRNA and loxP oligonucleotides [63]. These mice with conditional alleles can be mated with mice expressing tissue specific CRE recombinase to generate mice with a tissue specific knockout of *Mecp2* gene. A conditional allele can also be generated by using a pair of Cas9 nucleases and a single DNA expressing guide RNA flanked by

loxP sites [64]. Recently, using a single plasmid system for expressing sgRNA targeting the gene of interest and Cas9 nuclease, a tyrosinase knockout rabbit was generated [65]. CRISPR-Cas had been used in SSCs for genome correction with 100% efficiency, as in the case of mice carrying the mutant Crygc gene (responsible for causing cataract), resulting into the generation of healthy progeny [66]. To make the activity of Cas highly specific and reduce off-target effects, multiple sgRNA or a pair of sgRNAs can be used [67].

1.2 14-3-3 Proteins

14-3-3 proteins belong to a family of acidic proteins with a molecular weight of 25-32 kDa [68, 69]. Moore and Perez first isolated these proteins from bovine brain homogenate. They were named '14-3-3' because of their elution position in 2-dimensional DEAE cellulose chromatography and migration pattern on starch gel electrophoresis [70]. In mammals there are seven isoforms of 14-3-3, namely, β , γ , ϵ , η , σ , τ and ζ . The phosphorylated forms of 14-3-3 β and 14-3-3 ζ are known as 14-3-3 α and 14-3-3 δ respectively [71]. 14-3-3 proteins bind to proteins involved in different pathways. 14-3-3 proteins regulate multiple cellular pathways including cell cycle progression, centrosome duplication, DNA damage repair, transcription, cell growth, survival, apoptosis, protein trafficking and mitochondrial protein import and tumor suppression [72-76].

1.2.1 Structure

14-3-3 proteins form dimers. Each 14-3-3 monomer in the dimer contains a channel for ligand binding. The structure resembles the shape of a horseshoe. Each monomer is made up of nine

anti-parallel α helices (α A- α I) [72, 77]. Helices α A and α B of one isomer interact with the helices α C' and α D' of the other monomer [72, 77]. Helices α A, α B, α C and α D form the base of the inner channel [72]. Helices α E- α H forms remaining part of the channel. The amino acids which are present at the interior face of this channel are conserved across the different isoforms but the amino acids present at the exterior face of this channel are variable and is probably responsible for the isoform specific ligand interaction [72, 78]. Helices α C, α E, α G and α I are involved in ligand binding [79]. Tyrosine, lysine and arginine residues present in these helices binds to the phosphate groups present on the ligand [79, 80]. All 14-3-3 isoforms form both homodimers and heterodimers with the exception of 14-3-3 σ , which only forms homodimers whereas 14-3-3 ϵ preferentially forms heterodimers [77, 79].

1.2.2 Ligand binding

14-3-3 proteins bind to phosphorylated ligands containing phosphorylated Ser/Thr residues in one of the two consensus motifs RSXpS/pTXP and RXY/FXpSXP [80, 81]. Muslin *et al.*, in 1996, identified RSXpSXP as a mode I binding site after scanning the Raf-1 protein sequence as Raf-1 was known to bind to 14-3-3 ζ . They generated a short Raf peptide, Raf 259, containing phosphorylated Serine at 259 position, and showed that when the phosphorylation of Ser259 is inhibited it cannot bind to 14-3-3 proteins. They also showed that the phosphorylation of Ser257 alone or phosphorylation of both Ser257 and Ser259 abrogated 14-3-3 binding. Similarly, presence of Arginine, Serine and Proline with respect to pSer is important and critical for 14-3-3 binding as the peptides which had these residues mutated or the degenerate peptides (containing Proline or Serine or Arginine at different positions with respect to pSer) could not bind to 14-3-3

proteins at all or the binding was very weak [81]. The 14-3-3 binding motif RSXpSXP is present in other 14-3-3 ligands such as cdc25C, Bad, Mos, PLC γ , etc.[81]. Yaffe *et al.*, in 1997, screened pSer oriented degenerate peptide libraries to identify peptides which showed strong binding to 14-3-3 proteins. They identified RXY/FXpSXP as a mode two consensus motif. The 14-3-3 binding proteins containing mode two consensus motif are cdc25A, keratin 8, PKC γ , etc. [80]. Some proteins bind to 14-3-3 via their C terminus and the deletion of the C terminus abrogates 14-3-3 binding. The proteins which bind to 14-3-3 via their C terminus are glycoprotein complex Ib-IX-V, plant H⁺-ATPase, interleukin 9 receptor α , potassium channels KCNK3, KCNK9, ovine arylalkylamin N-acetyl-transferase (oAANAT), etc. Coblitz *et al.*, identified a mode three 14-3-3 binding site for such proteins, pSX1-2-COOH, after analyzing the 14-3-3 binding sites in oAANAT and H⁺-ATPase [82, 83].

Yaffe *et al.*, also described the structure of 14-3-3 protein bound to phosphorylated ligands by using 14-3-3 ζ bound to phospho-peptide, containing mode 1 consensus sequence similar to that of Polyomavirus middle T antigen. The bound phospho-peptide initially has an extended chain conformation and then its phospho-serine residue forms salt bridges with Arg, Lys and Tyr residues present in the central channel [80]. Yang *et al.*, had hypothesized that two types of interactions take place between the phosphorylated target protein and 14-3-3 proteins. The phosphorylated serine interacts with the inner channel of 14-3-3 and salt bridges are formed between the phosphate group and the Arg, Arg and Tyr triad; this interaction is known as primary interaction. The secondary interaction is the interaction of the target protein with the outer surface of 14-3-3 proteins to form a strong complex [79].

1.3 14-3-3 γ

14-3-3 γ was first identified by Ichimura *et al.*, in 1988 from bovine brain homogenate using reverse phase chromatography in an attempt to resolve the heterogeneous 14-3-3 protein complex [68]. In humans 14-3-3 γ gene also known as YWHAG is located on chromosome 7q11.23 [84]. 14-3-3 γ is ubiquitously expressed but is abundantly expressed in the brain [85].

1.3.1 Functions of 14-3-3 γ

14-3-3 γ interacts with various proteins to regulate different pathways. Some of the important functions of 14-3-3 γ are described below.

1.3.1.1 Regulation of cell cycle checkpoint control by 14-3-3 γ

14-3-3 proteins bind to cdc25C [86]. cdc25C is a dual specificity phosphatase which activates mitotic complex, cyclinB/cdk1, leading to the initiation of mitosis [87]. During interphase, cell cycle arrest and DNA damage, cdc25C is phosphorylated at a Serine residue at position 216 (S216) which leads to the generation of a 14-3-3 binding site. 14-3-3 bound cdc25C is sequestered in the cytoplasm during interphase and in response to checkpoint activation, thereby preventing premature activation of the mitotic complex, cyclinB/cdk1 [87]. Of the different isoforms of 14-3-3, only 14-3-3 γ and 14-3-3 ϵ were found to interact with cdc25C *in vitro* and *in vivo* [88]. To understand the significance of cdc25C binding to 14-3-3 γ , 14-3-3 γ -cdc25C complex formation was disrupted by expressing S216A cdc25C mutant which failed to bind 14-3-3 γ and the cells expressing S216A cdc25C mutant showed premature chromatin condensation (PCC) [88]. PCC is seen in S phase cells in which mitosis is induced [88] by overriding of incomplete S phase and G2 checkpoint pathways. In HCT116 cells, disruption of endogenous 14-3-3 γ -cdc25C complex by loss of 14-3-3 γ also resulted in premature activation of

cyclinB/cdk1 complex by cdc25C and increased PCC [89]. These observations highlight the importance of regulation of cdc25C function by 14-3-3 γ in maintenance of checkpoint pathways and prevention of PCC.

14-3-3 isoforms are known to regulate different functions of checkpoint kinase 1 (chk1). chk1 is activated upon DNA damage by ATR kinase. Activation of chk1 prevents cell cycle progression and causes G2/M arrest by phosphorylating cdc25c at S216 position [90, 91] and as described above S216 phosphorylated cdc25C cannot mediate activation of cyclinB/cdk1 [87]. chk1 is phosphorylated at S345, which upon phosphorylation serves as 14-3-3 β and 14-3-3 ζ binding site to promote the nuclear retention of chk1 by masking the nuclear export signal of chk1 [92]. Recently, 14-3-3 γ is reported to bind chk1 at S296 position. chk1 auto-phosphorylated itself at S296 position upon activation by the ATR kinase. Phosphorylation of S296 residue generated 14-3-3 binding site. Out of different 14-3-3 isoforms, only 14-3-3 γ binds to chk1 at S296 position [93]. Binding of chk1 to 14-3-3 γ promotes interaction of chk1 with cdc25A and thus promoting phosphorylation of cdc25A at S76 by chk1 and the degradation of cdc25A [93, 94]. cdc25A activates cyclin E/cdk2 and cyclin A/cdk2 complexes and is required for G1/S transition [95].

14-3-3 γ also regulates G2/M transition by interacting with Cdt2 (cell division cycle protein 2). Cdt2 is an adaptor of CRL4 (member of cullin-RING E3 ligases). CRL4^{Cdt2} complex is composed of cullin4a or cullin4b (acts as scaffold), Rbx1/2 (RING box protein 1/2) which binds to E2 enzyme (ubiquitin donor), DDB1 (damage-specific DNA binding protein 1) and Cdt2 which recognize substrates bound to PCNA (proliferating cell nuclear antigen). The C terminus of cullin4a/b is bound to Rbx1/2 at the C terminus and the N terminus of cullin4a/b interacts with DDB1 which is in turn bound to Cdt2 [96, 97]. CRL4^{Cdt2} is considered as the master

regulator of cell cycle. CRL4^{Cdt2} is required for the degradation of Set8, p21, Cdt1(necessary for DNA replication) and cdc6. CRL4^{Cdt2} activity is required for cell cycle progression, PCNA mediated DNA damage repair, preventing genomic instability and abnormal relicensing of origin which leads to re-replication [96, 97]. Similarly, Cdt2 loss is associated with the re-replication and G2 arrest. Cdt2 is phosphorylated by cyclinA/cdk2 and cyclinB/cdk1 complex at T464 position, phosphorylated Cdt2 binds 14-3-3 γ and 14-3-3 γ prevents FbxO11 (F-box only protein 11) mediated Cdt2 polyubiquitination and degradation. Loss of 14-3-3 γ leads to decrease in the levels of Cdt2 and an increase in the substrates of CRL4^{Cdt2} [97]. Therefore, 14-3-3 regulates cell cycle progression by regulating functions of cdc25A, cdc25C and stability of CRL4^{Cdt2}.

1.3.1.2 Regulation of centrosome duplication by 14-3-3 γ

First report which suggested role of 14-3-3 γ in centrosome formation came in 1996 when Pietromonaco *et al.*, showed that 14-3-3 γ is present in centrosomal fractions of mouse 3T3 cells [75]. After two decades, it was shown that loss of 14-3-3 γ in HCT116 cells led to increase in the number of centrosomes [98]. The increase in centrosome number in the absence of 14-3-3 γ was due to centriole over duplication. The centriole over duplication resulted from uninhibited function of cdc25C which led to premature activation of cdk1 [98]. Activated cdk1 phosphorylates Nucleophosmin (NPM1), an inter centriolar linker protein which links two centrioles. NPM1 upon phosphorylation by cdk1 at T199 position is detached from centriolar linker thereby increasing distance between two centrioles and providing signals for procentriole biogenesis [98]. Therefore, 14-3-3 γ not only regulates cell cycle but it also regulates centrosome duplication by regulating cdc25C function.

1.3.1.3 Regulation of adeno-associated virus type 2 replication by 14-3-3 γ

Adeno-associated virus type 2 is a non-pathogenic human parvovirus which requires a helper virus for efficient DNA replication. The virus encodes for four rep proteins i.e. Rep78, Rep68, Rep52 and Rep40 from one *rep* gene. The major function of rep proteins is to replicate DNA and site specific integration. It was found that Rep 68 upon phosphorylation at S535 position binds to 14-3-3 γ -14-3-3 ϵ heterodimer to form a ternary complex. S535A Rep 68 mutant which failed to bind 14-3-3 proteins had increased affinity for DNA binding and was more efficient in viral DNA replication compared to the wild type Rep68. The mechanism by which 14-3-3 regulates process of viral DNA replication by Rep68 is not known [99].

1.3.1.4 Regulation of p53 activity by 14-3-3 γ and suppression of 14-3-3 γ expression by p53.

p53 is a tumor suppressor protein known to be activated in response to ionizing radiation (IR). p53 is a transcription factor and is known to regulate genes responsible for cell cycle arrest, DNA repair and apoptosis. In non-irradiated cells, S376 and S378 residues of p53 are phosphorylated. In response to IR, ATM dephosphorylates S376 residue of p53 and exposes pS378 residue which serves as a 14-3-3 binding site [100]. Different 14-3-3 isoforms were screened for their ability to bind p53 and it was observed that 14-3-3 γ binds to p53 in both GST pulldown assay and co-immunoprecipitation experiments [101]. The p53 mutants who failed to bind 14-3-3 were unable to induce cell cycle arrest in response to IR suggesting that the p53 binding to 14-3-3 was important for p53 function [101]. 14-3-3 γ helps in oligomerization of p53 and the 14-3-3 γ -p53 complex had higher affinity to bind DNA when compared to p53 alone [100, 102, 103]. Recently, it was shown that in non-small cell lung cancers mutation of p53 was

directly correlated with the increase in the levels of 14-3-3 γ . Using chromatin immunoprecipitation assay (CHIP) and luciferase assay it was shown that p53 binds to the 14-3-3 γ promoter and suppresses 14-3-3 γ expression in response to IR [104]. p53 regulates level of 14-3-3 γ just not at the level of transcription but also at the level of proteasomal degradation by enhancing ubiquitination of 14-3-3 γ [105].

1.3.1.5 Regulation of transcription of synaptic genes by 14-3-3 γ

The muscle-specific receptor tyrosine kinase (MuSK) is present at post synaptic sites and is responsible for aggregation of synaptic proteins including acetylcholine receptors leading to differentiation of neuromuscular junction. In an attempt to identify interacting partners of MuSK in post synaptic membranes of *Torpedo* electrocytes using mass spectrometry, Strohlic *et al.*, identified 14-3-3 γ . 14-3-3 γ formed a complex with MuSK in muscle cells also. In muscle cells expression of 14-3-3 γ was found to localize at neuromuscular junction and expression 14-3-3 γ in C2C12 myotubes led to the inhibition of the transcription of synaptic genes and alteration in the morphology of neuromuscular junction [106]. It was speculated that the binding of MuSK to 14-3-3 γ led to the inactivation of Raf1, an effector of avian erythroblastosis oncogene B (ErbB)/Neuregulin-1 (NGU) pathway, thereby preventing transcription of Erk responsive genes [107].

1.3.1.6 Regulation of mRNA stability by 14-3-3 γ

Most of the 14-3-3 γ functions are dependent on protein-protein interactions but a decade ago, 14-3-3 γ was found to interact with mRNA. 14-3-3 β , 14-3-3 γ , 14-3-3 η , 14-3-3 ζ and 14-3-3 τ were found to bind 3' UTR of low molecular weight Neurofilament (NFL) mRNA. Neurofilament protein belongs to the family of intermediate filament proteins. The binding of 14-3-3 isoforms to 3'UTR of NFL mRNA is dependent on the presence of a couple of hexanucleotide sequence and the mutation the of these sequences abolished 14-3-3 binding and increased the stability of the 3'UTR of NFL mRNA [108]. The mechanism by which 14-3-3 proteins regulate stability of NFL mRNA is unclear [108].

14-3-3 proteins were also found to bind mRNA of human surfactant protein SP-A. SP-A is expressed in lungs and is important for innate immunity. SP-A is encoded by two genes SP-A1 and SP-A2. The 5'UTR splice variants of SP-A2 which contains exon B are ABD and ABD'. These splice variants are efficiently translated and have a lower decay rate when compared to the splice variants which lack exon B. Exon B is an enhancer of transcription and translation [109]. 14-3-3 γ , 14-3-3 ϵ , 14-3-3 η , 14-3-3 σ and 14-3-3 τ binds to exon B and the levels of SP-A2 decrease in cells with loss of these 14-3-3 isoforms. These findings suggest that 14-3-3 isoforms play an important role in SP-A2 translation but the exact function of 14-3-3 binding to exon B is not clear [110].

1.3.1.7 Role of 14-3-3 γ in Parkinson's disease

14-3-3 γ levels are often deregulated in different neurodegenerative disorders. Parkinson's disease is a neurodegenerative disease which affects motor functions. The exact cause of this

disease is unknown. It has been reported that the aggregates of α -synuclein protein are seen in the neurons in this disease. Mutations in α -synuclein are the cause of aggregate formation. 14-3-3 proteins share structural homology with α -synuclein and are seen in α -syn inclusion bodies. Over-expression of α -synuclein in mouse model was studied and it was found that 14-3-3 expression was deregulated with a significant reduction in the levels of 14-3-3 γ and reduction in 14-3-3 θ and 14-3-3 ϵ . The over-expression of 14-3-3 γ , 14-3-3 ϵ and 14-3-3 θ in the neuroglioma cells led to the reduction of the α -synuclein aggregates. The mechanism by which 14-3-3 isoforms regulate α -synuclein aggregation is not clear. Exposure of rotenone and 1-Methyl-4-phenyl pyridinium in animals causes Parkinsonian like syndrome. Dopaminergic cells which over-expressed 14-3-3 γ , 14-3-3 ϵ and 14-3-3 θ isoforms were resistant to the toxicity caused by rotenone and 1-Methyl-4-phenyl pyridinium. The β , σ and ζ isoforms of 14-3-3 did not give any protection against the cytotoxicity caused by rotenone and 1-Methyl-4-phenyl pyridinium. Thus 14-3-3 γ provides protective function against Parkinson's disease [111].

Leucine rich repeat kinase-2 (LRRK2) is a multidomain protein and is mutated in familial Parkinson's disease. LRRK2 is phosphorylated by protein kinase A at multiple sites. LRRK2 phosphorylated at S1444 residue serves as binding site for 14-3-3 γ . The kinase activity of LRRK2 is attenuated by binding to 14-3-3 γ . In Parkinson's disease R1441C, R1441G and R1441H mutations of LRRK2 are reported and all these mutants lack 14-3-3 γ binding site and have more kinase activity compared to the wild type LRRK2 [112]. Different mutations in LRRK2 have different effects on neurons. Expression of R1441C mutant in mouse led to the reduction in substantia nigra dopaminergic neurons and led to the increase in transcription of genes responsible for cell death and decrease in the transcription of genes responsible for neuroprotection [113]. Expression of G2019S mutant affected lysosome morphology, autophagy

efflux resulting into the formation of aggregates of detergent insoluble α -synuclein and release of α -synuclein in neurons [114].

1.3.1.8 Regulation of class switching in B cells by 14-3-3 γ

14-3-3 proteins are known to bind DNA [115]. 14-3-3 γ binds to supercoiled DNA as well as cruciform DNA [116]. 14-3-3 proteins bind to the AGCT sequence. Multiple AGCT repeats are present in intronic switch region of immunoglobulin heavy chain. Class switch DNA recombination (CSR) happens in this intronic switch region. 14-3-3 expression increases in B cells undergoing CSR *in vitro* [117]. 14-3-3 γ binds to the AGCT repeats and helps in recruitment or stabilization of activation-induced cytidine deaminase (AID), protein kinase A (PKA) and uracil DNA glycosylase by binding to these proteins as shown by bimolecular fluorescence complementation and GST pulldown assays. Moreover, binding of 14-3-3 γ , 14-3-3 σ and 14-3-3 ζ enhances activity of AID and inhibition of recruitment of 14-3-3 γ and AID led to the inhibition of class switch DNA recombination [118].

1.3.1.9 Regulation of ion channel activation by 14-3-3 γ

14-3-3 γ is reported to bind various ion channel transporters namely, Uncoupling proteins 2 and 3 (UCP2 and UCP3), TWIK-related spinal cord K channel (TREK), large-conductance Ca^{2+} -activated K^{+} (BK) channel, Cystic fibrosis transmembrane conductance regulator (CFTR), TWIK-related acid-sensitive potassium channel (TASK), Urea transporter (UT-A1), Bestrophin 1 (Best1) and Transient receptor potential melastatin 4b (TRPM4b) [119-126]. UCPs

belong to the family of mitochondrial anion carrier proteins (MATP). UCPs are present in the inner mitochondrial membrane and the UCP2 is expressed by all the cells whereas UCP3 is expressed only in skeletal muscles. 14-3-3 γ , 14-3-3 θ , 14-3-3 β and 14-3-3 ζ were found to interact with UCP2 and UCP3 using yeast two hybrid assay and it was speculated that it helps in the translocation of UCP3 [119].

TRESK is a two-pore domain K⁺ channel is a type of a leak channel to allow movement of free K⁺ ions from high gradient to low gradient. TRESK is activated by calcium via calcineurin. Calcineurin binds to nuclear factor of activated T cells like (NFAT) domain present in the intracellular loop of TRESK and dephosphorylates TRESK thus activating TRESK. TRESK is phosphorylated at intracellular loop by protein kinase A (PKA), this phosphorylation generates binding site for proteins and binding with 14-3-3 proteins prevents the activation and prolongs the recovery of TRESK. 14-3-3 γ and 14-3-3 η were found to interact with TRESK by GST pulldown assays [120].

Another K⁺ channel BK, is also activated by calcium and found to interact with 14-3-3 γ by mass spectrometry and co-immunoprecipitation assay. The loss of 14-3-3 γ leads to increase in expression of BK but the mechanism behind the regulation of BK by 14-3-3 γ is not clear [121]. TASK is an acid sensitive K⁺ channel expressed in neurons, T cells and B cells. TASK is important for proliferation of T cells and cytokine production by regulating Ca²⁺ influx. 14-3-3 γ , 14-3-3 ϵ and 14-3-3 ζ were found to bind TASK by co-immunoprecipitation assay followed by mass spectrometry. The 14-3-3 proteins bind to C terminus region of TASK and facilitate the transport of TASK to the cell border. Inhibition of 14-3-3 binding to TASK inhibited T cell effector functions [123].

CFTR is responsible for anion secretion activity is dependent on cAMP and PKA phosphorylation for its activation. CFTR is phosphorylated by PKA at regulatory region; this phosphorylation causes conformational change which allows ATP binding and ATP hydrolysis to drive channel gating. CFTR transcription is dependent on levels of cAMP. 14-3-3 β , 14-3-3 γ and 14-3-3 ϵ were found to interact with CFTR in co-immunoprecipitation assay. The expression of 14-3-3 β and 14-3-3 ϵ correlated with CFTR levels. Binding of 14-3-3 proteins led to the stabilization of CFTR by preventing its association with COPI thereby preventing retrograde transport of CFTR to the endoplasmic reticulum. The importance of 14-3-3 γ binding to CFTR is not clear as 14-3-3 γ levels did not affect CFTR levels [122].

UT-A1 helps in concentrating urine thus maintaining water balance. UT-A1 functions are regulated by vasopressin. Vasopressin binds to its receptor V₂, causes phosphorylation of UT-A1 by PKA leading to accumulation of UT-A1 in the cell membrane. UT-A1 was found to interact specifically with 14-3-3 γ . 14-3-3 γ also interacts with mouse double minute 2 (MDM2), an E3 ubiquitin ligase which is known to mediate ubiquitination of UT-A1. 14-3-3 γ therefore binds to UT-A1 and recruits MDM2 to facilitate ubiquitination and degradation of UT-A1 [124].

Best1 is a calcium dependent anion channel expressed by non-neural tissues and peripheral neurons. In an attempt to identify the binding partners of Best1 by yeast two hybrid assay was done 14-3-3 γ was found to interact with Best1. The interaction of Best1 and 14-3-3 γ was confirmed by co-immunoprecipitation assay. Best1 did not interact with other 14-3-3 isoforms. C terminus region of Best1 bound to 14-3-3 γ . Loss of 14-3-3 γ led to the reduced membrane expression of Best1 in astrocytes and reduced the activity of Best1 [125].

TRPM4b is also a calcium dependent non-selective cation channel. TRPM4b, full length protein localized to plasma membrane whereas 1-174 amino acids truncated TRPM4a is cytoplasmic.

TRPM4b interacted with 14-3-3 γ specifically and S88 of TRPM4b is critical for interaction with 14-3-3 γ . Loss of 14-3-3 γ led to the reduced surface expression of TRPM4b and increased the glutamate-induced cell death in neurons [126].

The above section highlighted the role of 14-3-3 γ in the transport of ion channels to the cell membrane. The ligand bound 14-3-3 γ has high affinity for membranes when compared to the other 14-3-3 isoforms. Histidine residues present at 158 and 195 position of 14-3-3 γ , unique to 14-3-3 γ , contributed to the interaction of ligand bound 14-3-3 γ with membrane. This ability of 14-3-3 γ to bind to membranes might contribute in transporting ligands to the membrane [127].

1.3.1.10 Regulation of mitochondrial functions by 14-3-3 γ

Mitochondrial damage leads to autophagy and sometimes instead of autophagy mitochondrial repair system MALM (Mieap induced accumulation of lysosome like organelles within mitochondria) is activated to decrease ROS levels (reactive oxygen species) and increase ATP synthesis [128]. Inhibition of MALM leads to the formation of MIV (Mieap induced vacuole like structures) which fuses with lysosome and degrades unhealthy mitochondria. Mieap is a p53 induced protein involved in mitochondrial repair pathways MALM and MIV [129]. Mieap interacts with 14-3-3 γ upon induction of MALM and is localized to the mitochondria. Loss of 14-3-3 γ does not inhibit MALM but it inhibited the degradation of oxidized mitochondrial proteins [130]. The mechanism by which 14-3-3 γ regulates degradation of mitochondrial proteins is not clear yet but this report shows 14-3-3 γ is required for mitochondrial functions and mitochondrial quality control.

1.3.1.11 Regulation of P-body formation by 14-3-3 γ

When level of ribosome free mRNA increases in the cytoplasm due to environmental stress these ribosome free mRNAs associate with ribonuclear proteins and form a cytoplasmic membraneless organelles known as stress granules and P bodies (processing bodies) [131, 132]. The mRNAs stored in P bodies are degraded by decay machinery but the mRNAs present in stress granules are utilized for translation after recovery from stress [132]. It is observed that upon UV radiation of U2OS cells, chk1/chk2 phosphorylate LATS2 (Large tumor suppressor homolog2, a downstream effector of Hippo pathway) at S408. Phosphorylated LATS2 interacts with 14-3-3 γ and phosphorylate 14-3-3 γ on S9 position. Upon phosphorylation, 14-3-3 γ translocated to P body and moreover, 14-3-3 γ is required for P body formation as loss of 14-3-3 γ inhibited P body formation. The loss of LATS2 did not affect the P body formation [133]. This was the first report which showed importance of 14-3-3 γ in P body formation.

1.3.1.12 Role of 14-3-3 γ in cancer progression

The role of 14-3-3 γ in cancer progression is controversial. Loss of 14-3-3 γ expression is associated with the increased proliferation in uterine leiomyoma [134] whereas increased expression of 14-3-3 γ is associated with poor prognosis and survival in breast cancer, hepatocellular cancer and non small cell lung cancer (NSCLC) [135-137]. Stimulation of immortalized NIH3T3 by IL3 leads to an increase in 14-3-3 γ , which further activates cell proliferation and survival by activation of PI3K-Akt and MAPK signaling [138]. The over-expression of 14-3-3 γ alone in NIH3T3 cells leads to transformation by activation of PI3K-Akt and MAPK signaling pathway [139]. The transformation of NIH3T3 and activation of PI3K and

MAPK signaling pathway by 14-3-3 γ is mediated by the variable region I and II (VRI and VRII) of 14-3-3 γ because when the VRI and VRII of 14-3-3 γ is introduced in 14-3-3 σ , the resultant chimeric protein is capable of transforming NIH3T3 cells and activating PI3K and MAPK signaling pathway [140].

In NSCLC, the expression of mir-509-5p is often lost and 14-3-3 γ is the direct target of this micro RNA as loss of mir-509-5p is correlated with the increased 14-3-3 γ protein levels [141]. Expression of mir-509-5p in NSCLC resulted into the decreased proliferation and migration by preventing 14-3-3 mediated Akt activation. Similarly, loss of 14-3-3 γ in NSCLC reduces proliferation and migration [141, 142]. 14-3-3 γ and 14-3-3 β forms complex with the transcription factor snail and inhibit the transcription of epithelial genes, such as E-cadherin, by binding to the promoter of epithelial genes [143]. Taken together, 14-3-3 γ promotes tumour progression by activation of PI3K-Akt and MAPK signaling pathways.

1.3.1.13 Regulation of neuronal differentiation by 14-3-3 γ

Copine1 (CPNE1) belongs to the family of calcium dependent membrane binding protein. CPNE1 is known to promote the neuronal differentiation in the hippocampal progenitor cells by activation of Akt pathway [144]. It was recently found that, CPNE1 interacts with 14-3-3 γ using yeast two hybrid assay and the CPNE1-14-3-3 γ interaction is important for the activation of Akt pathway and neuronal differentiation. 14-3-3 γ binds to the phosphorylated S54 of CPNE1 and mutation of this residue decreased levels of pAkt and inhibited neuronal differentiation of hippocampal progenitor cells [145]. This report highlighted role of 14-3-3 γ in neuronal differentiation.

1.3.2 Mouse models of 14-3-3 γ loss

14-3-3 γ gene in mouse is located on chromosome 5 and it has only two exons (www.ncbi.nlm.nih.gov/gene/22628). In order to study the role of 14-3-3 γ *in vivo*, Steinacker *et al.*, developed 14-3-3 γ knockout mice by introducing neomycin resistance cassette in exon2 of the 14-3-3 γ coding sequence in embryonic stem cells [85]. The modified embryonic stem cells were then used to generate chimeras. Inbreeding of the chimeric mouse resulted in the generation of 14-3-3 γ knockout animals. These mice did not have any physiological or developmental abnormalities. Since the level of 14-3-3 γ increases in the cerebrospinal fluid of Creutzfeldt-Jakob disease, a fatal neurodegenerative disease caused by prions, 14-3-3 γ knockout mice were injected with prions to study if the loss of 14-3-3 γ affects Creutzfeldt-Jakob disease progression. No change in the disease progression was observed in wild type mice, heterozygous mice and knockout mice [85]. To address the question whether the absence of phenotype in 14-3-3 γ knockout mice was due to the increase in the levels of other 14-3-3 isoforms, western blots using isoform specific 14-3-3 antibodies were done but no change was observed in the levels of other 14-3-3 isoforms (ϵ , β , η , ζ) in the 14-3-3 γ knockout mice. In this study the levels of 14-3-3 σ and 14-3-3 τ were not reported [85].

The expression of 14-3-3 γ starts at the E11.5 (E is embryonic day) and is at its peak from E11.5 to E17.5 suggesting that 14-3-3 γ plays an important role in the embryonic development. The 14-3-3 γ expressed in cortex, preplate, intermediate zone and marginal zone. 14-3-3 γ shRNA was injected into the lateral ventricle of the brains of the embryo followed by electroporation. The knockdown of 14-3-3 γ in embryo led to the delayed neuronal migration due to the abnormal morphology of neurons and the decreased migration velocity of neurons. These neurons had thicker stem and highly branched processes [146]. Similarly, the over-expression of 14-3-3 γ in

electroporated embryos also led to the delay in neuronal migration [147]. Mutations in 14-3-3 γ in gene leads to epilepsy and one of the major causes of epilepsy is defective neuronal migration [148]. These mouse models of 14-3-3 γ support the fact that 14-3-3 γ is responsible for neuronal migration.

To study gene function *in vivo*, complete loss of a gene function or gene knockout may not mimic the phenotype observed *in vitro*. Moreover, genes which are involved in multiple pathways may show no phenotype in knockout animals [149]. In such cases, studying phenotype of animals with partial loss of gene function becomes important. The mutations or modifications which lead to partial loss of gene function are called hypomorphic mutations [149]. The partial loss of the gene function may have severe defects than the complete loss of gene function.

In order to generate hypomorphic mutant of 14-3-3 γ , lentiviruses expressing 14-3-3 γ shRNA were injected into the testes of pre-pubescent male mice. These pre-founder male mice had become sterile and the testis section of these mice showed loss of cell-cell adhesion, and cell-matrix adhesion leading to collapse of the blood-testis barrier (BTB) and defects in spermatogonial stem cell differentiation and spermatocyte development and maturation [150]. This suggested 14-3-3 γ plays an important role in mediating cell-cell adhesion and cell-cell adhesion is an important determinant of tissue structure and function.

1.4 Cell adhesion Junctions

Cell adhesion junctions are multi-protein complexes which connect cells to each other or extracellular matrix. These cell-cell adhesion junctions are important for structure and function of tissues [151]. Cell adhesion junctions are formed by following types of proteins, a

transmembrane protein which will interact with the other transmembrane proteins present on neighboring cells, a linker protein which connects these transmembrane proteins to cytoskeletal proteins to provide stability and strength to the cells [151]. Epithelial cells have following types of cell-cell adhesion junctions: adherens junction, desmosomes and tight junctions [152]. Cells are connected to basement membrane or extracellular matrix by hemidesmosomes and focal adhesions [152].

1.4.1 Cell-cell adhesion junctions found in testis

The seminiferous epithelium of testis has following types of cell-cell adhesion junctions, tight junctions, adherens junctions, desmosome like junctions, gap junctions, ectoplasmic specialization and tubulobulbar complex (Figure 1.2) [153, 154]. Adherens junctions, ectoplasmic specialization and tubulobulbar complexes are actin based junctions. Desmosomes like junctions are intermediate filament based junctions [153, 154].

Seminiferous tubules are divided into luminal and adluminal compartments by blood testis barrier (BTB). BTB is formed between adjacent Sertoli cells and is made up of tight junctions, gap junctions, basal ectoplasmic localizations, adherens junctions and desmosome like junctions. BTB does not allow immunological cells to enter testis. Proteins present on developing spermatocytes are recognized as antigens by immunological cells as these proteins were not present in the embryonic stage when immune system was developing. Thus, BTB prevents autoimmune response against spermatocytes and provides an “immune privileged niche” [155]. During the process of spermatogenesis, BTB undergoes restructuring to allow the pre-leptotene spermatocytes to enter luminal compartment for further development [155].

During spermatogenesis, developing spermatocytes are attached to Sertoli cells via different cell-cell adhesion junctions. Desmosome like junctions, gap junctions and adherens junctions are associated with initial stages of spermatocyte development and can be seen both in the luminal and adluminal compartments. Ectoplasmic specialization and tubulobulbar complexes are associated with elongating spermatids and are seen in adluminal compartments [153, 154]. These cell-cell adhesion junctions are important for the development of spermatocytes as the developing spermatocytes require nourishment and support which are provided by Sertoli cells via these junctions.

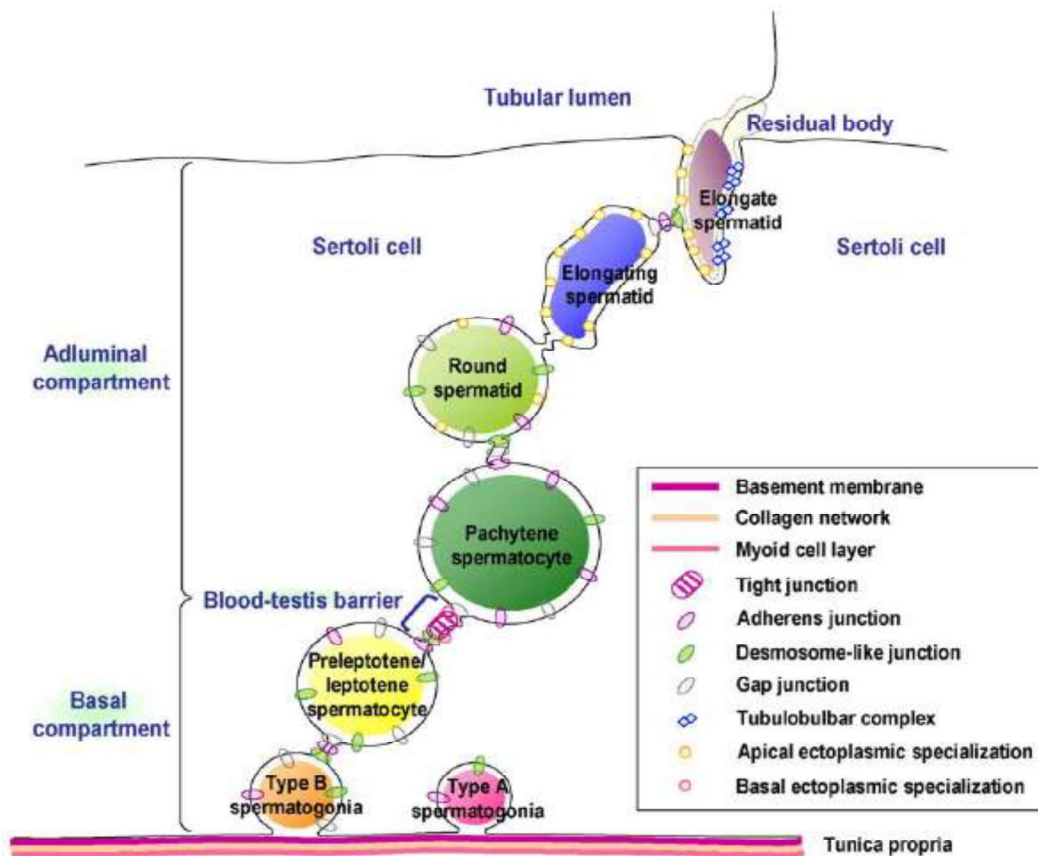


Figure 1.3: Different types of cell-cell adhesion junctions seen in seminiferous tubules [153].

1.4.2 BTB and its function

BTB is formed between adjacent Sertoli cells and it acts as an immunological barrier. As seminiferous epithelium lacks blood vessels, BTB controls the transport of electrolytes, hormones, etc. and maintains cell polarity [155, 156]. The cell adhesion complexes that are involved in BTB formation are tight junctions, gap junctions, ectoplasmic specialization and desmosome like junctions [153, 154]. Developing spermatocytes present at the luminal compartment have to pass through BTB by restructuring BTB to reach adluminal compartment for further development [154]. Inhibition of BTB affects spermatogenesis for e.g., treatment of neonatal rats with diethylstilbestrol (non-steroidal estrogen) led to inhibition of BTB formation leading to disruption of spermatogenesis due to the exfoliation of spermatocytes at initial stages of development [157].

It was also reported that loss of cell-cell adhesion in testis led to the disruption of BTB and spermatogenesis for e.g., intraperitoneal administration of cadmium chloride in rat led to sterility due to the disruption of BTB. This disruption was associated with the decrease in the levels of tight junction and adherens junction proteins accompanied by the decrease in the levels of cytoskeletal proteins [158]. Other compounds which affect cell-cell adhesion in testis are perfluorooctanesulfonate and bisphenol A [159]. Perfluorooctanesulfonate perturbed F-actin organization thereby affecting actin mediated cell adhesion junctions [159]. Bisphenol A disrupted BTB in immature rats by affecting tight junction protein levels and levels of gap junction proteins and basal ectoplasmic junction proteins were also slightly affected [160]. These reports highlight importance of cell adhesion junctions in spermatogenesis.

To understand how 14-3-3 γ affected cell-cell adhesion, BTB and spermatogenesis, the interaction of 14-3-3 γ with different cell adhesion junction protein was studied *in vitro*. Briefly, cell extracts of HCT116 cells (colon cancer cell line) were used to perform GST pulldown assays using GST or GST 14-3-3 γ . GST14-3-3 γ binds to the desmosomal proteins plakoglobin, plakophilin3 and desmoplakinI/II [150]. It did not interact with other cell adhesion junction proteins suggesting 14-3-3 γ might regulate desmosome or desmosome like junctions in testis.

1.4.3 Adherens Junction

Adherens junction is an actin based cell-cell adhesion junction. This junction is present in multiple cell types. In polarized epithelial tissues, adherens junction is also called as zonula adherens. Adherens junction is calcium dependent cell-cell adhesion junction [161].

The adherens junctions are made up of two types of complexes i.e. cadherin/catenin complex and nectin/afadin complex, as shown in Figure 1.3.

1.4.3.1 Cadherin/Catenin Complex

Cadherins are named according to the type of tissue on which cadherins are expressed for e.g., E-cadherin for cadherins found on epithelial tissues, N-cadherin for cadherins expressed on neural tissues, P-cadherin is expressed on placental tissues [161]. Cadherins are calcium dependent transmembrane proteins which interact with each other in homophilic manner in presence of calcium. Cadherins have an extracellular membrane, a transmembrane region and a cytoplasmic tail. The cytoplasmic tail of cadherins interacts with β -catenin or γ -catenin (Plakoglobin) or

p120catenin. β -catenin or γ -catenin in turn, interacts with α -catenin and α -catenin connects this cadherin/catenin complex to actin filaments. Just like cadherins, α -catenin is named as α -E-catenin α -N-catenin and α -P-catenin. p120catenin stabilizes adherens junction by cadherin clustering and regulate actin dynamics by inhibiting Rho GTPases [162].

Adherens junction are important for embryonic development as most of the mouse models of adherens junction proteins are embryonic lethal. Mice embryos lacking E-cadherin could not form blastocyst cavity and died suggesting E cadherin plays an important role in formation of epithelium [163]. Loss of N-cadherin in mouse led to embryonic lethality at 10dpc as heart failed to develop normally. Also, loss of N-cadherin affected neuroepithelium and somites [164]. P-cadherin null mice had normal lifespan but the female mice with loss of P-cadherin had unregulated growth of mammary glands suggesting P-cadherin negatively regulates growth of mammary glands [165]. β -catenin null embryos died at 7dpc and the ectoderm formation was affected in these embryos [166]. Mouse embryos lacking γ -catenin died at 10dpc [167]. Expression of loss of function mutant of α -E-catenin in mouse also led to the embryonic lethality by disruption of trophoblast ectoderm thus affecting blastocyst development [168]. Mouse model of p120 knockout in endothelium is also embryonic lethal as the vascular endothelial cells of these mice had proliferation defects [169].

1.4.3.2 Nectin/Afadin Complex

Nectin belongs to the IgG superfamily of proteins. There are four types of nectin nectin1-nectin4 and five nectin like proteins Necl1-Necl5. Interaction of nectin with other nectins or nectin like proteins is not dependent on calcium. Nectin has an extracellular domain which participates in hemophilic or heterophilic interaction with other nectins, a transmembrane region and a cytoplasmic domain which interacts with actin binding protein, afadin. Afadin interacts with Ras/Rap family of GTPases and with α -catenin [162]. Loss of afadin leads to embryonic lethality due to defect in ectoderm and mesoderm formation [170].

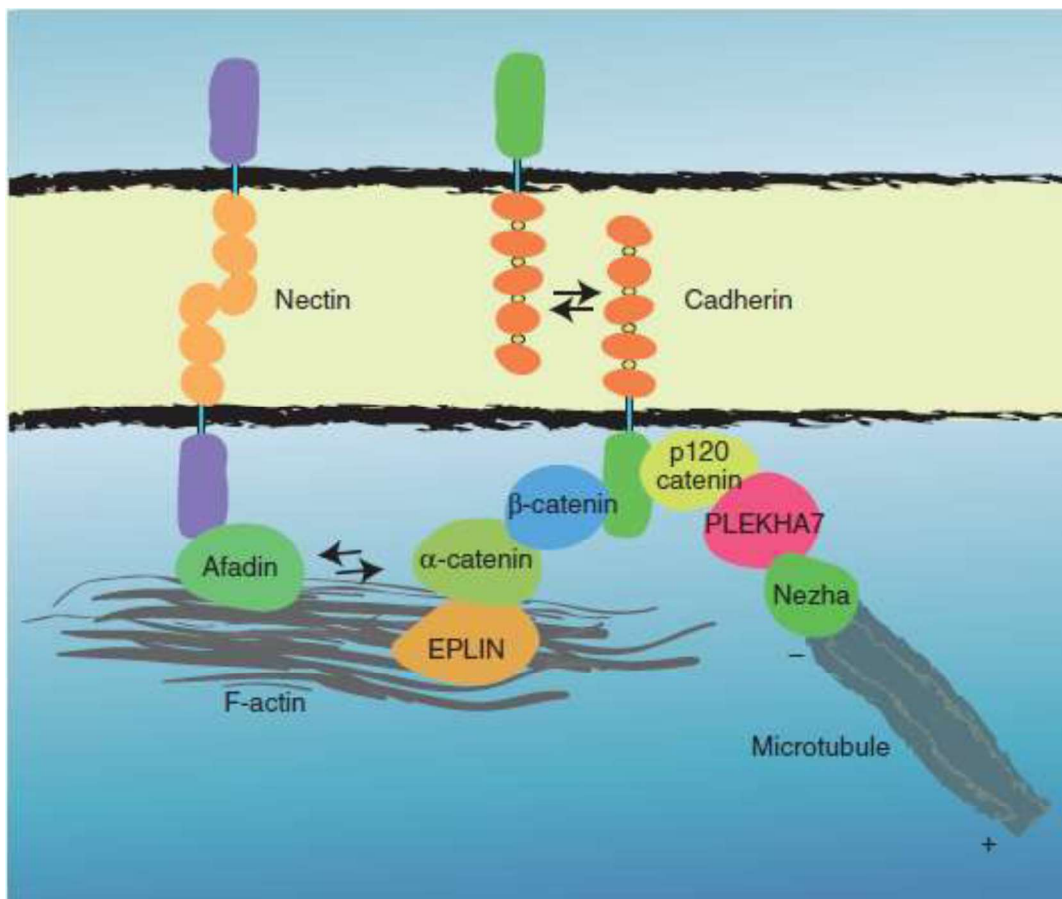


Figure 1.4: Structure of adherens junction. A cartoon depicting the molecular structure of adherens junction [161].

1.4.4 Desmosomes

Desmosomes are one of the important cell-cell adhesion junctions present in seminiferous epithelium. Desmosomes are present at BTB and between Sertoli cells and round spermatocytes in both adluminal and luminal compartment (Figure 1.2). Desmosomes are calcium dependent adherens like cell-cell adhesion junctions present in all epithelial tissues [171]. Desmosomes are made up of three types of proteins, the desmosomal cadherins, armadillo repeat containing proteins and plakin family of proteins. The desmosomal cadherins of two neighboring cells interact with each other in a homophilic or heterophilic manner to form cell-cell contacts. These contacts can be seen as dense midline in an electron micrograph (Figure 1.4). This dense midline is absent in desmosome like junctions present in seminiferous epithelium [172]. The cytoplasmic domain of the cadherins interacts with armadillo repeat containing proteins to form an electron dense structure known as the desmosomal plaque. In the plaque, armadillo repeat containing proteins are connected to intermediate filaments by plakin family of proteins thus forming a tissue wide intermediate filament network that provides strength and stability to tissues (Figure 1.4)[173]. A disruption in desmosome function in humans, leads to skin and heart disorders such as epidermolysis bullosa, ectodermal dysplasia, keratosis, keratoderma, woolly hair, and arrhythmogenic right ventricular cardiomyopathy [174-180].

The structure and the function of the desmosomal proteins are described below:

1.4.4.1 Desmosomal Cadherins

There are two types of desmosomal cadherins namely desmogleins and desmocollins. Desmosomal cadherins have extracellular domain, a transmembrane region and a short cytoplasmic tail. The extracellular domain is involved in homophilic and heterophilic interactions

with the desmosomal cadherins present on the adjacent cells and cytoplasmic tails are used for binding armadillo proteins. Desmocollins are of three types, DSC1-3. There are two splice variants of DSCs namely DSCa and DSCb, and the b form has shorter cytoplasmic domain which cannot bind plakoglobin[181]. There are four DSG isoforms DSG1-4. The DSG2 and DSC2 are expressed in simple epithelium, basal layers of stratified epithelium, cardiomyocytes and meningotheia [182]. Expression of DSG1, DSG4 and DSC1 is seen in the upper layers of stratified epithelium and expression of DSC3 and DSG3 is seen in the lower layers of stratified epithelium [182].

The function of desmosomal proteins were first determined by the use of animal models, for e.g., loss of DSG2 in mouse led to embryonic lethality as embryos died shortly after implantation due to the defect in the proliferation of embryonic stem cells, suggesting role of DSG2 in regulating embryonic stem cells [183]. Similarly, DSC3 knockout embryos died before implantation but role of DSC3 in blastocyst is not clear [184]. Loss of DSC1 in mouse led to epidermal flaking and loss of barrier function [185]. Loss of DSG3 led to runting, epidermal acantholysis, oral lesions and hair loss [186]. All these reports suggest that desmosomal cadherins are required for embryonic development, growth, barrier function and hair cycle.

1.4.4.2 Armadillo Repeat Containing proteins

This family of proteins got their name from the *Drosophila* protein armadillo involved in segment polarity. Armadillo is the homolog of β -catenin and γ -catenin (also called as plakoglobin). Proteins belonging to this family have repeats of 42 amino acid long sequence, known as arm repeats. Plakoglobin (PG), β -catenin, p120catenin and plakophilins (1-4) are the members of armadillo repeat containing proteins. Plakoglobin and plakophilins bind to

cytoplasmic tails of cadherins and connect them to plakin family of proteins[187]. PG has 12 arm repeats and binds to E-cadherin and desmosomal cadherins. PG binds to desmosomal cadherins with higher affinity than E-cadherin[187]. PKPs have 9 arm repeats. PKP1 and PKP2 are expressed as 'a' and 'b' isoforms and 'b' isoform is larger than 'a' isoform. PKP1 is expressed in suprabasal layer of epithelium whereas PKP2 is expressed in simple epithelium, stratified epithelium, cardiomyocytes and lymph nodes [187]. PKP3 is expressed in all the epithelial cells with an exception of hepatocytes [188]. PKP4 also known as p0071 is less studied isoform of PKP and its function in desmosome formation is not clear.

Arm repeat containing proteins are important for embryonic development as both PG knockout mice and PKP2 knockout mice die at embryonic day 10.5 due to severe heart defects [189, 190]. PKP3 knockout mice had a normal lifespan. PKP3 knockout mice showed hair loss accompanied by reduced hair follicles and are prone to skin inflammation [191]. PKP1 knockout mice were normal at birth but died within 24 hours of birth [192]. PKP1 loss led to the fragile skin, loss of tight junction barrier and reduced desmosomes [192].

1.4.4.3 Plakin family of proteins

The members of plakin family are Desmoplakin (DP), envoplakin, periplakin and plectin. The function of this family is to connect the cytoskeleton proteins to the cell membrane. There are three domains of DP, N terminal domain binds PG or PKP, a central rod domain for oligomerization and C terminal domain binds to intermediate filaments[181]. There are two splice variants of DP, DPI and DPII [193]. DP knockout mice die at embryonic day 6.5 with perturbed keratin network and defect in egg cylinder elongation [194].

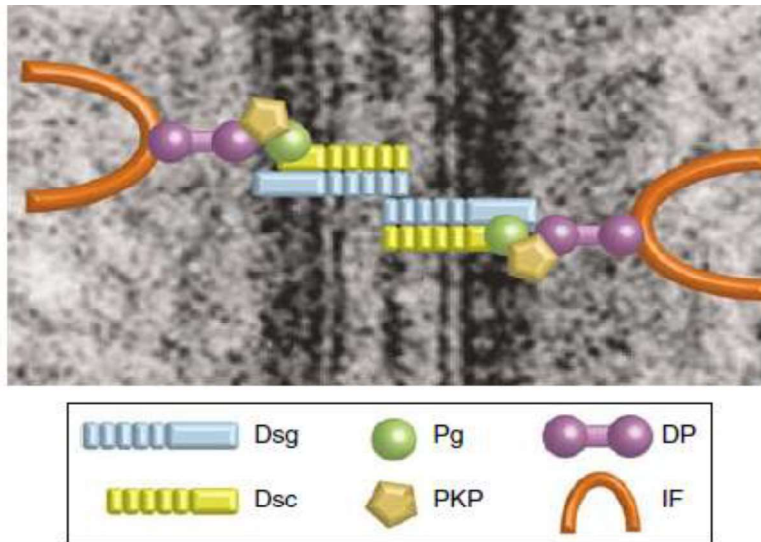


Figure 1.5: Structure of desmosomes. An electron micrograph of desmosome is shown, over which cartoon depicting the molecular model of desmosome is superimposed. The image is taken from [173].

1.4.5 Regulation of Desmosome formation by 14-3-3 γ .

As mentioned earlier, 14-3-3 forms complex with desmosomal proteins. To determine the function of this complex, desmosomal protein localization was observed in 14-3-3 γ knockdown testis and vector control testis. It was observed that 14-3-3 γ knockdown testis had decreased cell border localization of desmosomal protein compared to wild type testis [150]. Even though plakoglobin or γ -catenin is a part of both desmosomes and adherens junction, loss of 14-3-3 γ did not affect localization of other adherens junction proteins.

The cell-cell adhesion was also studied in HCT116 derived vector control and 14-3-3 γ knockdown cells. Decreased cell-cell adhesion was observed in the 14-3-3 γ knockdown cells as compared to the vector control cells. In addition, the levels of the desmosomal proteins at the cell

border were decreased upon loss of 14-3-3 γ in HCT116 cells [150]. On the basis of these results, it was concluded that 14-3-3 γ forms complex with desmosomal protein for transporting desmosomal proteins from cytoplasm to the cell border to initiate desmosome formation.

14-3-3 γ also forms a complex with kinesin motor protein, KIF5B [150]. Loss of KIF5B in the testes led to sterility due to the defect in desmosome formation. Also, HCT116 derived KIF5B knockdown cells have decreased cell-cell adhesion and disrupted desmosome formation [150]. Therefore, desmosome assembly is dependent on both 14-3-3 γ and KIF5B and their loss affects cell-cell adhesion both *in vitro* and *in vivo* [150]. We hypothesized that desmosomal proteins are transported from cytoplasm to the cell border in the following steps: 14-3-3 γ and desmosomal protein forms a complex, 14-3-3 γ then loads desmosomal protein cargo on to KIF5B motor proteins to transport desmosmal proteins from cytoplasm to the border [150]. However, due to the fact that loss of 14-3-3 γ in the testis resulted in sterility, the role of 14-3-3 γ in regulating desmosome formation in other tissues was still un-resolved.

2. Aims and objectives

2. Aims and objectives

1. Generate inducible and epidermis specific knockdown mice for 14-3-3 γ .
2. Determine the mechanisms by which 14-3-3 γ loss leads to defect in the desmosome formation.

3. Materials and methods

3. Materials and methods

3.1 Plasmids and constructs

All the primers used in generating following vector constructs are given in Table 3.1. All the DNA constructs, described in this section, were sequenced before using for expression and other studies. All the vector maps were created using SnapGene Viewer software.

Name of the oligonucleotide	Sequence of the oligonucleotides
14-3-3 γ shRNA Forward	CCGGACTATTACCGTTACCTGGCCTCGAGGCCAGGTAA CGGTAATAGTTTTT
14-3-3 γ shRNA Reverse	AATTAAAAAACTATTACCGTTACCTGGCCTCGAGGCCA GGTAACGGTAATAGT
14-3-3 γ shRNAmir Forward	AACTCGAGAAGGTATATTGCTGTTGACAGTGAGCGG ACTATTACCGTTACCTGGCTAGTGAAGCCACAGATG TA
14-3-3 γ shRNAmir Reverse	CCGAATTCCGAGGCAGTAGGCAGACTATTACCGTTA CCTGGCTACATCTGTGGCTTCACTAGCCAGGTAACG G
Turbo RFP AgeI Forward	GGACCGGTCGCCACCATGAGC
shRNAmir Sall Reverse	GGGTCGACTGGCCGGCCGCATTAGTCT
14-3-3 γ gRNA Forward	CACCGGCGCTACGACGATATGGCCG
14-3-3 γ gRNA Reverse	AAACCGGCCATATCGTCGTAGCGCC
K14 promoter XhoI Forward	GGCTCGAGGGGCTCCGGAGCTTCTATT
K14 promoter BamHI Reverse	GGGGATCCTCTCGGGTAAATTGCAAAGG

PKC μ shRNA Forward	CCGGCCATTGATCTTATCAATAACTCGAGTTATTGAT AAGATCAATGGTTTTTG
PKC μ shRNA Reverse	AATTCAAAAACCATTGATCTTATCAATAACTCGAGTT ATTGATAAGATCAATGG
PG S236A Forward	GTCCGCATGCTCGCTAGCCCTGTGGAGTCG
PG S235A Reverse	CGACTCCACAGGGCTAGCGAGCATGCGGAC
PG Q591R Forward	CCCCTGTTTGTGCAATTGCTGTACTCGTCG
PG Q591R Reverse	CGACGAGTACAGCAATTGCACAAACAGGGG
PG 300 Bam HI Forward (PG N term forward)	AAGGATCCATGGAGGTGATGAACCTGATGGAG
PG 300 XhoI Reverse	AACTCGAGCTGGTTGCCGTAGGCCAG
PG NheI Forward	GGCGCTAGCATGGAGGTGATGAA
PG AgeI Reverse	GCACCGGTCGGGCCAGCATGTGGT
shRNA6 Res PG Forward	TGCTCTGGACCACCTCGCGAGTGCTCAAGGTGCT
shRNA6 Res PG Reverse	AGCACCTTGAGCACTCGCGAGGTGGTCCAGAGCA
PG Arm 1 Forward	AAGGATCCATGAACTACCAGGACGATGCCGAGC
PG Arm 12 Reverse	CTCGAGCTAGTCCTCGGAGATGCGGAAC
PG N term Reverse	CTCGAGCTAATGAGATGCACAATGGCCGA
PG Arm 9 Reverse	CTCGAGCTACAGGGCCAGATTCTTGATCAA
PG Arm 10 Forward	AAGGATCCATGCCAGCCAACCATGCCCC
PG C term Forward	AAGGATCCATGAAGAACCCAGACTACCGGAAGCG
PG C term Reverse	CTCGAGCTAGGCCAGCATGTGGTCTGCA
PG gRNA exon 1 Forward	CACCGGCAGACATACACCTACGACTCGG

PG gRNA exon1 Reverse	AAACCCGAGTCGTAGGTGTATGTCTGC
PG gRNA exon2 Forward	CACCGAACGGGTGCGGGAGGCCATG
PG gRNA exon2 Reverse	AAACCATGGCCTCCCGCACCCGTT

Table 3.1: List of oligonucleotides used for cloning shRNA, cDNA cloning and site directed mutagenesis (SDM).

3.1.1 Cloning of 14-3-3 γ shRNA downstream of inducible promoter

To achieve inducible expression of 14-3-3 γ shRNA, pLKO Tet Puro vector (Addgene) was used to clone 14-3-3 γ shRNA. This vector has modified H1 promoter, containing tetracycline responsive elements (TRE), which in the absence of doxycycline is bound by Tetracycline repressor protein, TetR, preventing transcription of shRNA, as shown in Figure. 3.1. In the presence of doxycycline, TetR does not bind to TRE allowing transcription of shRNA [195].

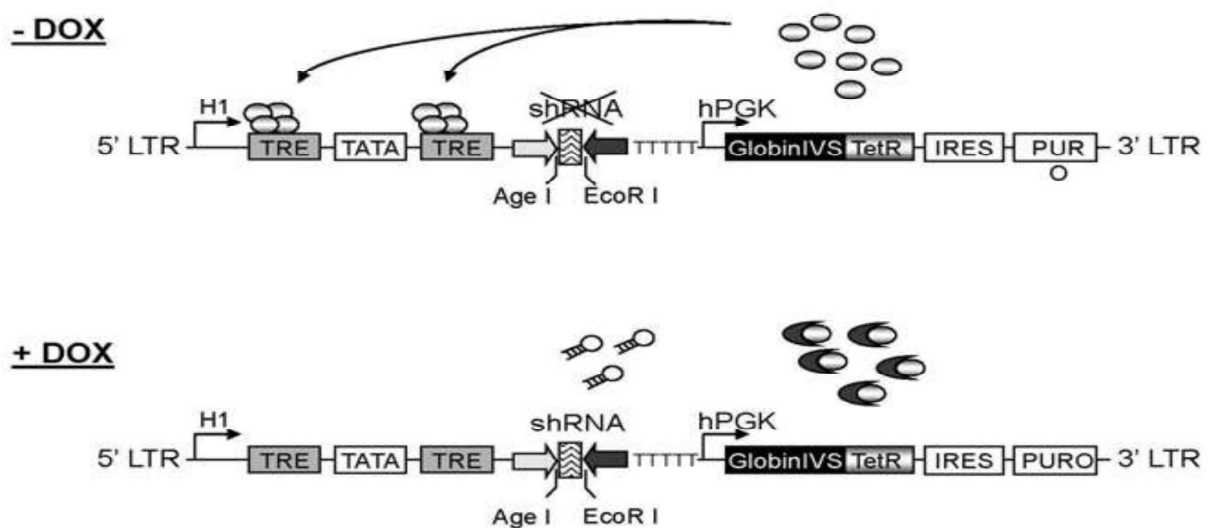


Figure 3.1: Design of pLKO Tet Puro vector [195].

pLKO Tet Puro vector was digested with restriction enzymes AgeI and EcoRI (NEB) at 37°C for 4 hours to remove the stuffer sequence present downstream of H1 Tet promoter. After restriction digestion, vector was resolved on 1% agarose gel. The vector backbone was eluted from the gel using Qiagen kit.

The shRNA sequence was designed using pLKO manual and was previously validated [196]. 20 pmols of shRNA forward and reverse oligonucleotides were mixed with NEB buffer 2 and incubated at 95°C for 4 minutes followed by incubation at 70°C for 10 minutes and the reaction gradually cooled to room temperature. 2µl of annealed oligonucleotides were phosphorylated by T4 Polynucleotide Kinase (T4 PNK) enzyme at 37°C. After phosphorylation, T4 PNK enzyme was inactivated by incubating the reaction mixture at 70°C for 10 minutes. After heat inactivation, shRNA was ligated to the AgeI and EcoRI digested vector using T4 DNA ligase (NEB) at 16°C for 16 hours. The ligation mixture was incubated at 65°C for 10 minutes to heat inactivate T4 DNA ligase and then used for transforming DH5α competent cells. All the lentiviral vector transformants were grown at 30°C to avoid recombination. The pLKO Tet Puro shRNA clones obtained were screened using AgeI and EcoRI restriction enzymes. The vector map for pLKO Tet Puro and pLKO Tet Puro 14-3-3γ shRNA is given in Figure 3.2.

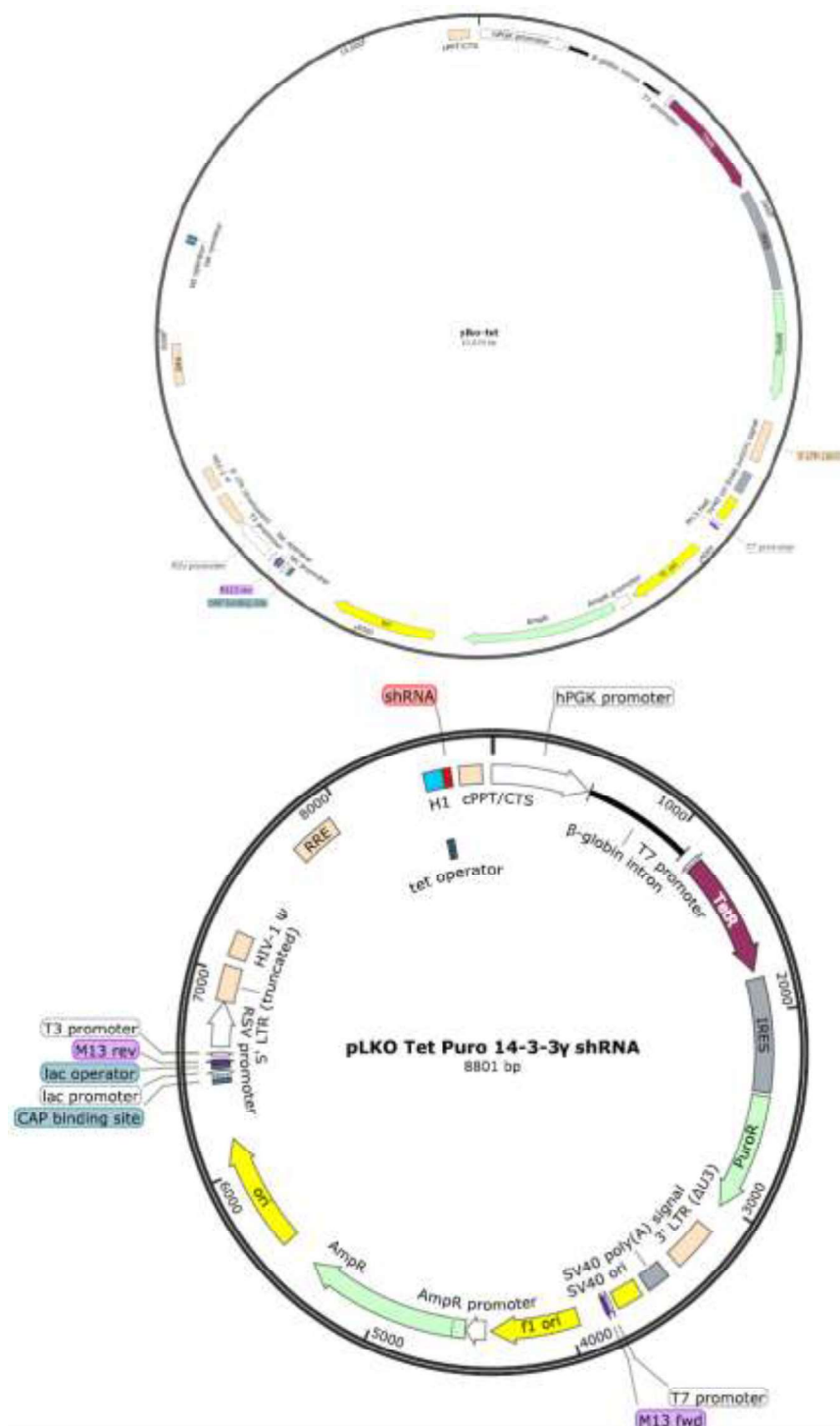


Figure 3.2: Vector map of pLKO Tet Puro vector and pLKO Tet Puro 14-3-3 γ shRNA vector. The unique restriction sites are same in both the vectors except for Age I, EcoRI, BstBI and SmaI. These sites are lost when shRNA is cloned.

3.1.2 Cloning Turbo RFP and Turbo RFP with 14-3-3 γ shRNAmir into pCCLK14 GFP vector for epidermis specific expression of 14-3-3 γ shRNAmir.

To generate mice that express the transgene only in the epidermis, we selected the Keratin 14 (K14) promoter because K14 and Keratin 5 (K5) are expressed in the basal layers of epidermis [197], are specific markers of the basal epithelium and the K14 promoter has been widely used to generate epidermis specific transgenic animals [198-200]. The K14 promoter is a RNA pol II based promoter and cannot be used for driving expression of shRNA therefore, 14-3-3 γ shRNA had to be cloned in the form of microRNA as 14-3-3 γ shRNAmir.

14-3-3 γ shRNA sequence was utilized for generating 14-3-3 γ shRNAmir. Overlapping oligonucleotides (Table 3.1) were ordered and full length shRNAmir was obtained by annealing and extension of oligonucleotides by using *Taq* polymerase (NEB). Following PCR program was used to generate full length shRNAmir using a mixture containing shRNAmir forward and reverse oligonucleotides, standard *Taq* buffer, 10mM dNTPs, DMSO and *Taq* polymerase.

- 1) Initial denaturation at 94°C for 3minutes.
- 2) Denaturation at 94°C for 1 minute.
- 3) Annealing at 55°C for 2 minutes.
- 4) Extension at 72°C for 1 minute.
- 5) Repeat from step 2 for 29 cycles.
- 6) Final extension at 72°C for 10 minutes.

7) Hold at 4°C forever.

The PCR product was resolved on 2% agarose gel followed by elution from the gel using Qiagen kit. pTRIPz vector (Open Biosystems) which has Tet CMV promoter to control the expression of Turbo RFP and downstream micro RNA was used for cloning 14-3-3 γ shRNAmir. pTRIPz vector and 14-3-3 γ shRNAmir were digested with EcoRI and XhoI (NEB), gel purified and were then ligated using T4 DNA polymerase (NEB). The clones obtained were screened using BamHI digest as pTRIPz vector has 3 BamHI sites and one of the BamHI sites is lost when shRNAmir is cloned between EcoRI and XhoI sites. The vector map of pTRIPz and pTRIPz 14-3-3 γ shRNAmir is given in Figure 3.3.

Turbo RFP and Turbo RFP-14-3-3 γ shRNAmir segment was PCR amplified from pTRIPz and pTRIPz 14-3-3 γ shRNAmir vector respectively using *Taq* polymerase. Following PCR program was used:

- 1) Initial denaturation at 94°C for 3minutes.
- 2) Denaturation at 94°C for 1 minute.
- 3) Annealing at 65°C for 1 minute.
- 4) Extension at 72°C for 1 minute.
- 5) Repeat from step 2 for 29 cycles.
- 6) Final extension at 72°C for 10 minutes.
- 7) Hold at 4°C forever.

The PCR products amplified using *Taq* polymerase have an A overhang at 3' region, because *Taq* polymerase lacks 3' to 5' proofreading activity, therefore, such PCR products can be easily ligated to TA vector i.e. pTZ57RT/T (InsTA Kit, Thermo Fisher Scientific) which has T overhangs. Turbo RFP or Turbo RFP-14-3-3 γ shRNAmir were ligated to TA vector using T4 DNA ligase. TA Turbo RFP clones and TA Turbo RFP-14-3-3 γ shRNAmir clones were screened using AgeI and SalI sites to identify positive clones.

pCCLK14 GFP vector, a kind gift from Dr. F. Miselli (University of Modena and Reggio Emilia, Italy), was used for cloning Turbo RFP and Turbo RFP-14-3-3 γ shRNAmir. Briefly, pCCLK14 GFP, TA Turbo RFP clone and TA Turbo RFP-14-3-3 γ shRNAmir were digested with AgeI and SalI at 37°C for 4 hours, the digested vectors were then resolved on 1% agarose gel followed by

elution of pCCLK14 vector backbone, Turbo RFP and Turbo RFP-14-3-3 γ shRNAir fragment from the gel. Turbo RFP or Turbo RFP-14-3-3 γ shRNAir were ligated to pCCLK14 vector backbone using T4 DNA ligase. pCCLK14 Turbo RFP and pCCLK14 Turbo RFP-14-3-3 γ shRNAir were screened using AgeI and SalI restriction enzymes. The vector map for pCCLK14 Turbo RFP and pCCLK14 Turbo RFP-14-3-3 γ shRNAir is given in Figure 3.4.

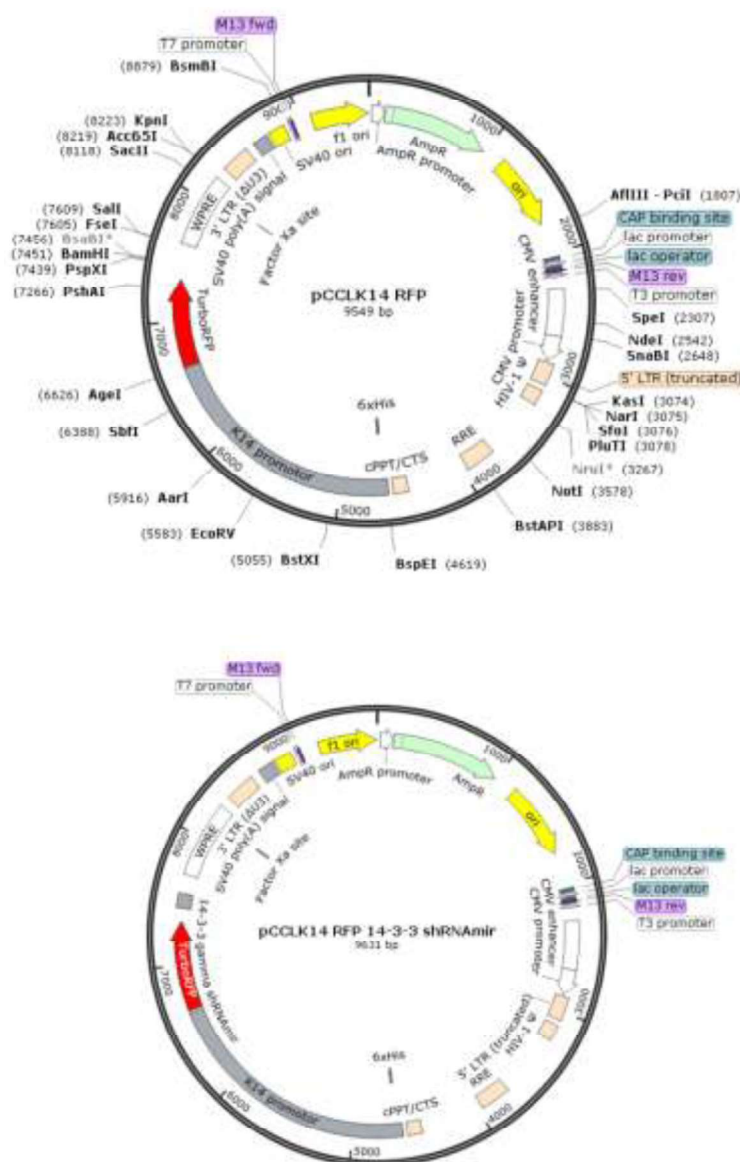


Figure 3.4: Vector map of pCCLK14 Turbo RFP vector and pCCLK14 Turbo RFP 14-3-3 γ shRNAir vector. The unique restriction sites are same in both the vectors.

3.1.3 Cloning 14-3-3 γ gRNA into pLentiCRISPR Cas V1 vector

gRNAs targeting 14-3-3 γ were designed using software developed by crispr.mit.edu. gRNA targeting exon1 was selected for cloning into pLentiCRISPR Cas V1 vector. gRNA forward and reverse oligonucleotides were incubated with T4 PNK enzyme for 1 hour at 37°C using T4 DNA ligase buffer. The phosphorylated oligonucleotides were then annealed using following PCR program:

- 1) 95°C for 5minutes.
- 2) 90°C for 1 minute.
- 3) 85°C for 1 minute.
- 4) 80°C for 1 minute.
- 5) 75°C for 1 minute.
- 6) 70°C for 1 minute.
- 7) 65°C for 1 minute.
- 8) 60°C for 1 minute.
- 9) 55°C for 1 minute.
- 10) 50°C for 1 minute.
- 11) 45°C for 1 minute.
- 12) 40°C for 1 minute.

13) 35°C for 1 minute.

14) 30°C for 1 minute.

15) 25°C for 1 minute.

16) Hold at 25°C forever.

Annealed gRNA oligonucleotides were then diluted (1:200) for ligation. pLentiCRISPR vector, which was digested with restriction enzyme BsmBI (NEB) at 55°C for 4 hours to remove the stuffer sequence present downstream of U6 promoter. Diluted gRNA and BsmBI digested pLentiCRISPR vector was incubated with T4 DNA ligase buffer and T4DNA ligase enzyme for 16 hours at 16°C. The clones obtained were screened using BsmBI digestion.

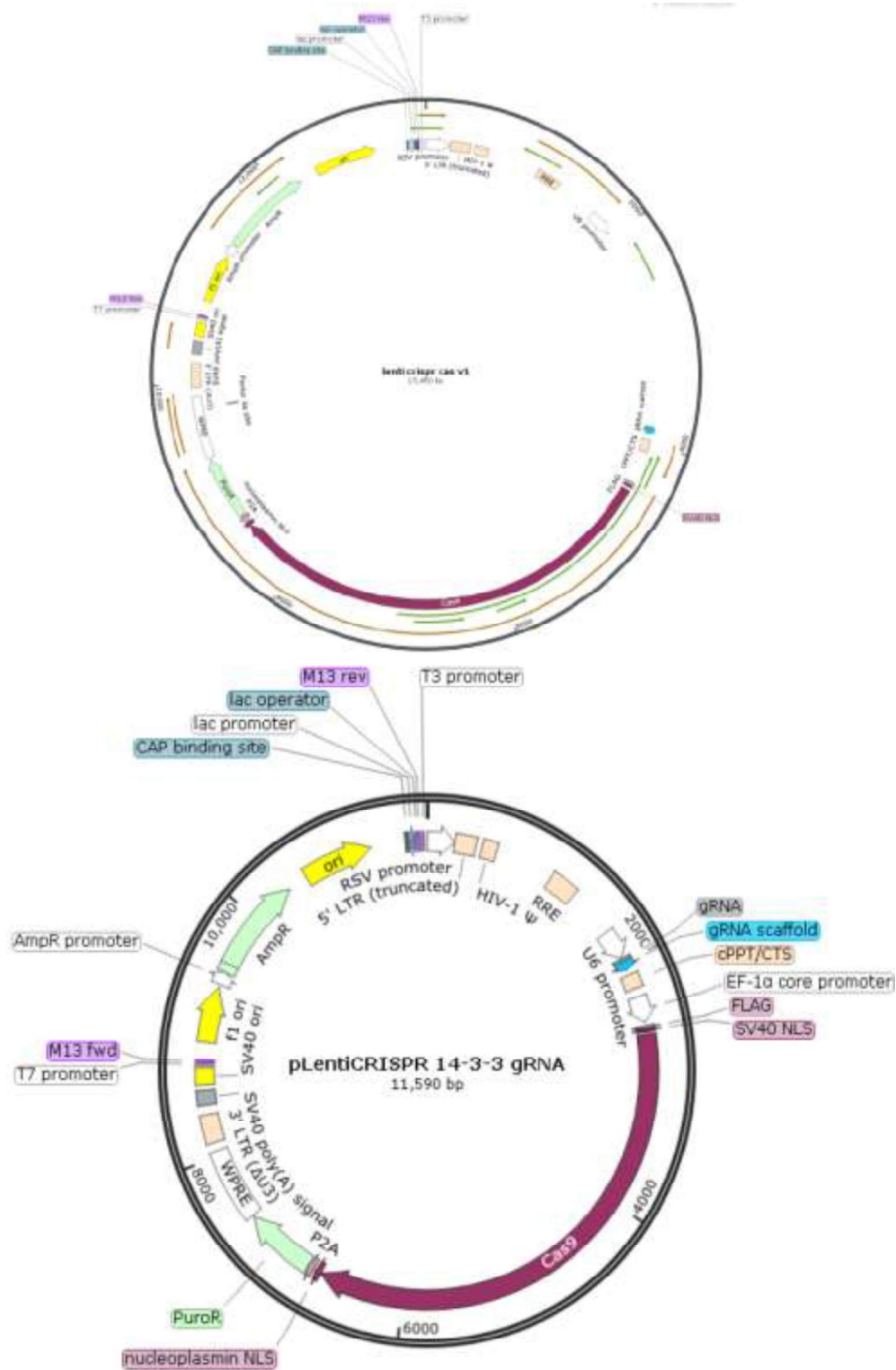


Figure 3.5: Vector map of pLentiCRISPR Cas V1 vector and pLentiCRISPR Cas V1 14-3-3y gRNA vector. The unique restriction sites are same in both the vectors.

3.1.4 Cloning K14 promoter into pLentiCRISPR Cas V1 vector

To achieve epidermis specific Cas9 expression EF1 α promoter, present in pLentiCRISPR Cas V1 vector upstream of Cas9, was replaced with K14 promoter. K14 promoter was PCR amplified from pCCLK14 vector using *Pfu* polymerase (Thermo Fisher Scientific). Following PCR program was used:

- 1) Initial denaturation at 94°C for 3minutes.
- 2) Denaturation at 94°C for 1 minute.
- 3) Annealing at 53°C for 1 minute.
- 4) Extension at 72°C for 5 minutes. (500bp/minute)
- 5) Repeat from step 2 for 29 cycles.
- 6) Final extension at 72°C for 10 minutes.
- 7) Hold at 4°C forever.

PCR product amplified using *Pfu* polymerases are blunt end PCR products and therefore are ligated to pJET vector (Thermo Fisher Scientific), a blunt end linearized vector. The pJET K14 promoter clones were screened using XhoI and BamHI digest as the primer used for amplifying K14 promoter contained these sites. pLentiCRISPR Cas V1 vector and pJET K14 promoter were digested with XhoI and BamHI and K14 promoter was cloned into pLentiCRISPR Cas V1 vector thus replacing EF1 α promoter. Similarly, EF1 α promoter of pLentiCRISPR Cas V1 14-3-3 γ gRNA vector was replaced with K14 promoter.

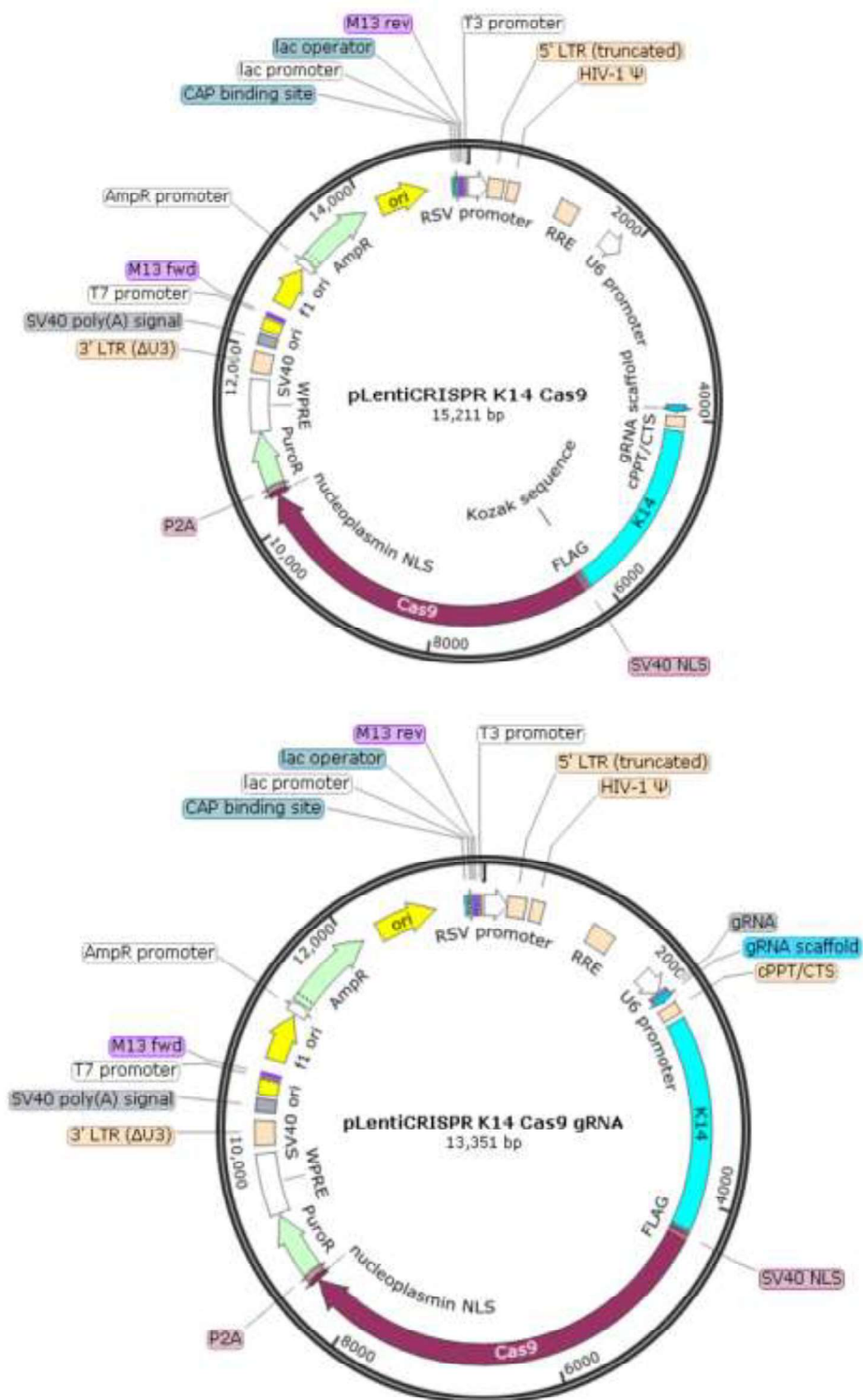


Figure 3.6: Vector map of pLentiCRISPR K14 Cas9 vector and pLentiCRISPR K14 Cas9 14-3-3ygRNA vector. The unique restriction sites are same in both the vectors.

3.1.5 Cloning PKC μ shRNA into pLKO EGFP-f vector

shRNA targeting PKC μ mRNA were designed using pLKO manual. shRNA oligonucleotides were annealed and phosphorylated before ligating to the AgeI and EcoRI digested pLKO EGFP-f vector [53] using T4 DNA ligase. The clones obtained were screened using EcoRV and KpnI digest as KpnI site is lost in shRNA cloning.

3.1.6 Generation of PG S236A mutant

Scansite software predicted that PG binds to 14-3-3 γ by virtue of phosphorylated S236 residue. To validate this prediction, it was necessary to mutate S236 residue of PG and study binding of PG S236A mutant and 14-3-3 γ . To mutate S236 residue to alanine, Myc PG plasmid (Addgene) was used as template. SDM PCR primers were designed in such a way that the S236A mutation will lead to generation of NheI site. PCR mix was prepared as follows:

PCR components	Forward Mix	Reverse Mix
HF Buffer 5X	5.0 μ l	5.0 μ l
Forward Primer (25 pmol)	1.0 μ l	0.0 μ l
Reverse Primer (25 pmol)	0.0 μ l	1.0 μ l
dNTPs 10mM	0.5 μ l	0.5 μ l
DMSO 100%	0.75 μ l	0.75 μ l
Template (100 ng/ μ l)	0.5 μ l	0.5 μ l
Phusion polymerase (2U/ μ l) (Thermo Fisher Scientific)	0.25 μ l	0.25 μ l
MilliQ	17.0 μ l	17.0 μ l

Table 3.2: List of components used in making sited directed mutagenesis (SDM) PCR mix.

SDM PCR program:

- 1) Initial denaturation at 95°C for 5 minutes.
- 2) Denaturation at 95°C for 1 minute.
- 3) Annealing at 50°C for 1 minute.
- 4) Extension at 72°C for 7 minutes. (2kb/min)
- 5) Repeat from step 2 for 9 cycles.
- 6) Hold at 4°C forever.

After the PCR was done, forward and reverse PCR mixtures were mixed and the above PCR program was repeated again. The final PCR product was then digested with DpnI (NEB) to degrade template DNA (methylated DNA). After digestion with DpnI, PCR product was used for transforming competent DH5 α cells. The transformants were grown at 37°C. The clones obtained were screened using SalI and NheI.

The sequence of the S236A PG mutant revealed that Myc PG (Addgene) plasmid had a mutation at 1773 position from A to G which resulted into R to Q mutation, as shown in Figure 3.7. This mutation was reversed using SDM PCR. The SDM primers contained MfeI site and therefore, SalI and MfeI were used for screening R591 PG clones.

ATCCTCGCCCGGACCCCATGAACCGCATGGAGATCTCCGGCTCAACACCATTCCCCTGTTTGTGCGGCTCCTGTACTCGTCGGTGGAGAACATCCAGCGCGTGGC										
1710	1720	1730	1740	1750	1760	1770	1780	1790	1800	1810
ATCCTCGCCCGGACCCCATGAACCGCATGGAGATCTCCGGCTCAACACCATTCCCCTGTTTGTGCGGCTCCTGTACTCGTCGGTGGAGAACATCCAGCGCGTGGC										
ATCCTCGCCCGGACCCCATGAACCGCATGGAGATCTCCGGCTCAACACCATTCCCCTGTTTGTGCGGCTCCTGTACTCGTCGGTGGAGAACATCCAGCGCGTGGC										
ATCCTCGCCCGGACCCCATGAACCGCATGGAGATCTCCGGCTCAACACCATTCCCCTGTTTGTGCGGCTCCTGTACTCGTCGGTGGAGAACATCCAGCGCGTGGC										

Figure 3.7: Sequence analysis of PG cDNA (NCBI), Myc PG WT and Myc PG S236A. The sequencing result showed presence of G at 1773 position in PG WT (middle sequence) and PG S236A (bottom sequence) instead of A (top sequence).

3.1.7 Generation of empty vector carrying Myc tag

In Myc PG plasmid, PG cDNA was cloned downstream of β Actin promoter and therefore we had to generate an empty vector which contains β Actin promoter controlling expression of Myc tag. Myc PG plasmid was digested with SalI and HindIII to remove PG cDNA and the linearized plasmid was then ligated to generate an empty vector.

3.1.8 Cloning GST PG 1-300 WT and GST PG 1-300 S236A

To perform *in vitro* kinase assay GST PG WT was required and as a control GST PG S236A was required which will not be phosphorylated by PKC μ . Full length GST PG was unstable and therefore GST PG 1-300 was generated by amplifying PG using primers containing BamHI and XhoI sites respectively. To generate GST PG S236A 1-300 overlap PCR was done using PG 1-241 and PG 241-300. Briefly, PG 1-241 was PCR amplified using forward primer containing BamHI site and reverse primer containing NheI site and S236A, PG 241-300 was amplified

using forward primer containing NheI site and S236A and reverse primer containing XhoI site, and these two PCR products were then used as template for overlap PCR using forward primer containing BamHI site and reverse primer containing XhoI site to generate PG 1-300 S236A. The PCR product was sub-cloned into pJET vector (blunt end cloning) before cloning it into pGEX4T1 vector using BamHI and XhoI sites.

3.1.9 Generation of PG-EGFP-f and PG-EGFP vector.

To artificially localize PG at the cell border, PG cDNA was cloned upstream of farnesylated GFP i.e. EGFP-f. Briefly, PG cDNA was PCR amplified using Myc PG WT plasmid as template, and cloned into EGFP-f vector using NheI and AgeI sites. To generate a non farnesylated PG-EGFP vector, EGFP-f was replaced with EGFP from EGFP C1 vector in PG-EGFP-f vector using AgeI and EcoRI sites.

3.1.10 Cloning PG-EGFP-f fragment into pCDNA3.1 puro vector

PG-EGFP-f vector contains neomycin as selection marker. Neomycin selection is not efficient in HCT116 cells therefore, PG-EGFP-f fragment was cloned into pCDNA3.1 Puro vector using NheI and EcoRI sites.

3.1.11 Generation of PG6 shRNA resistant PG-EGFP and PG-EGFP-f cDNA

To generate PG6 shRNA resistant PG-EGFP-f and PG-EGFP constructs, the region of the PG cDNA sequence complementary to shRNA was modified by introducing silent mutations to disrupt interaction with the shRNA using SDM PCR. Identification of the shRNA resistant mutants was facilitated by introducing a site for NruI in the primers.

3.1.12 Generation of HA tagged PG deletion mutants

As described previously, structure of PG is made up of three types of domains namely, N terminal domain, Arm domains and C terminal domain. There are total 12 arm domains in PG. To study the interaction of PG with different proteins, HA tagged deletion mutants of PG were generated by PCR amplifying specific domains of PG and cloning the PCR products into pJET vector. The PG deletion mutants from pJET vector were further cloned into pCDNA3.1 HA vector and the transformants were screened using BamHI and XhoI. The primers used for amplifying PG deletion mutants are given in Table 3.1 and the description of the mutants is given in Figure 3.8.

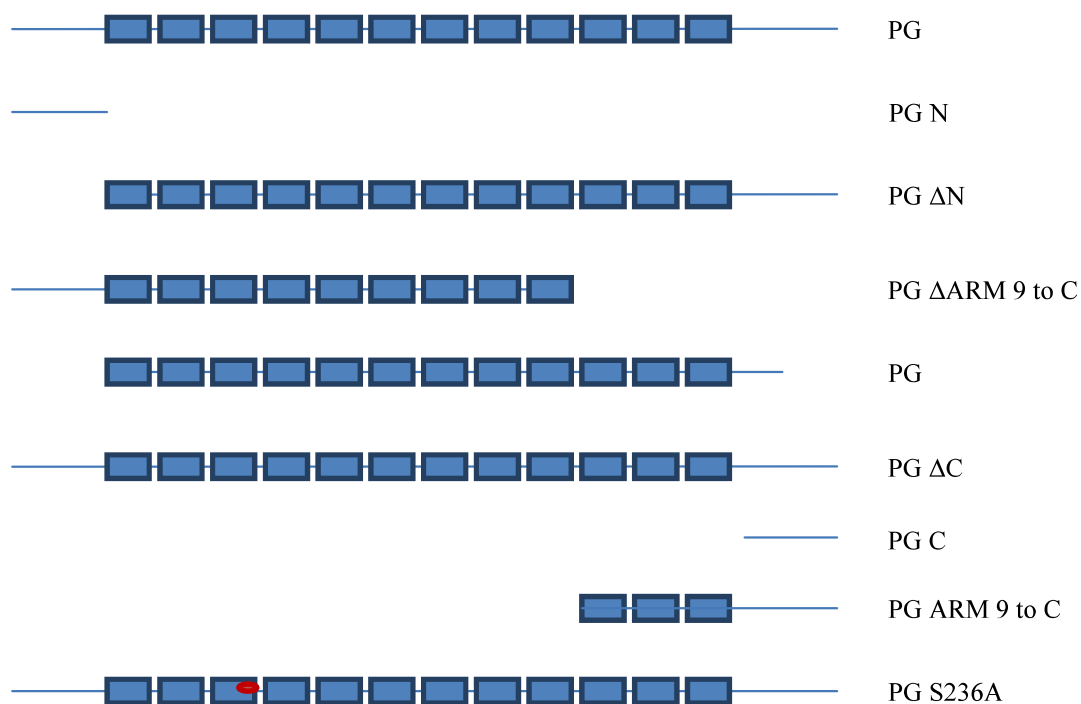


Figure 3.8: A cartoon representing the structure of the PG deletion mutants.

3.1.3 Cloning PG gRNA into pLentiCRISPR Cas V1

PG gRNA targeting exon 1 or exon 2 of PG were phosphorylated and annealed to clone into pLentiCRISPR Cas V1 vector using BsmB1 sites. The sequence of the gRNA is given in Table 3.1. The colonies obtained were screened using BsmBI digestion.

3.2 Cell Lines, transfection and transduction

HCT116 (ATCC) is an epithelial cell line isolated from human colorectal carcinoma. HCT116 derived 14-3-3 γ knockdown, KIF5B knockdown, PG knockdown, PKP3 knockdown cell lines and their respective vector control cell lines were cultured using DMEM (GIBCO) + 10% FBS (GIBCO) medium containing gentamycin, streptomycin and amphotericin B, as described previously [89, 150, 201, 202].

To generate a stable PKC μ knockdown cell line, HCT116 cells were transfected with pLKO.1 EGFP-f Puro or pLKO.1 EGFP-f Puro PKC μ shRNA using Lipofectamine LTX (Invitrogen) according to the manufacturer's protocol. Transfected cells were selected using puromycin (0.5 μ g/ml) and puromycin resistant population was used for further experiments.

The different methods of DNA transfection used in this study are described below:

1. Calcium Phosphate transfection method:

Diameter of the tissue culture dish	Vector DNA (1 μ g/ μ l)	pBSK (1 μ g/ μ l)	Sterile MilliQ	0.5M CaCl ₂	2xBBS
35 mm	2.5 μ l	2.5 μ l	45 μ l	50 μ l	100 μ l
60 mm	5.0 μ l	5.0 μ l	90 μ l	100 μ l	200 μ l
100 mm	15.0 μ l	10.0 μ l	225 μ l	250 μ l	500 μ l

Table 3.3: A table describing different components used for making calcium phosphate DNA transfection mix.

This mixture was incubated at room temperature for 20 minutes before adding dropwise to the cells. Confluency of the cells should be around 40-50% for transfection and cells should be fed with DMEM + 10% FBS medium 1-4 hours before adding transfection mix. After adding transfection mix cells were incubated at 37°C with 5% CO₂. 16 hours post transfection, cells were washed with 1x PBS to calcium phosphate precipitate and DMEM + 10% FBS with antibiotics was added. To induce the shRNA expression in pLKO Tet Puro 14-3-3 γ shRNA transfected HCT116 cells, doxycycline (Sigma) was given at the concentration of 2 μ g/ml after 16 hours of transfection. Doxycycline treated cells were harvested for western blotting after 72 hours of doxycycline addition. For detecting expression of un-inducible shRNA or shRNAmir cells were harvested at 72 hours post transfection and for detecting cDNA expression cells were harvested at 48 hours post transfection.

2. Lipofectamine LTX (Invitrogen) transfection method:

Diameter of the tissue culture dish	OptiMEM/DMEM (-FBS, -Antibiotics)	Plasmid DNA (1 μ g/ μ l)	+ Reagent	Lipofectamine LTX
35 mm	190 μ l	2.0 μ l	2.0 μ l	5 μ l
60 mm	480 μ l	5.0 μ l	5.0 μ l	12.5 μ l
100 mm	930 μ l	15.0 μ l	15.0 μ l	40 μ l

Table 3.4: A table describing the different components used in making DNA:Lipofectamine LTX transfection mix.

After adding + reagent incubate at room temperature for 5 minutes then add lipofectamine LTX. Incubate the transfection mix at room temperature for 30 minutes before adding dropwise to the

cells. Confluency of the cells should be around 40-50% for transfection and cells should be fed with DMEM + 10% FBS medium 1-4 hours before adding transfection mix. After adding transfection mix cells were incubated at 37°C with 5% CO₂. 16 hours post transfection, cells were washed with 1x PBS and DMEM + 10% FBS with antibiotics was added.

3. PEI (Polysciences, Inc.) transfection method:

Diameter of the tissue culture dish	OptiMEM/DMEM (-FBS, -Antibiotics)	Plasmid DNA (1 µg/µl)	PEI Reagent
35 mm	190 µl	2.5 µl	7.5 µl
60 mm	480 µl	5.0 µl	15.0 µl
100 mm	955 µl	15.0 µl	30.0 µl

Table 3.5: A table describing different components used for making DNA:PEI transfection mix.

Incubate the transfection mix at room temperature for 30 minutes before adding dropwise to the cells. Confluency of the cells should be around 40-50% for transfection and cells should be fed with DMEM + 10% FBS medium 1-4 hours before adding transfection mix. After adding transfection mix cells were incubated at 37°C with 5% CO₂. 16 hours post transfection, cells were washed with 1x PBS and DMEM + 10% FBS with antibiotics was added. All the PG-EGFP-f and PG-EGFP transfections were done using PEI.

3.2.1 Lentivirus Packaging

HEK293T cells (ATCC), are human embryonic kidney cell line containing SV40 T antigen, were cultured according to the ViraPower manual (Invitrogen). For viral packaging, ViraPower was used and transfection was done using Lipofectamine LTX (Invitrogen) as per manufacturer's instruction. Composition of a transfection mix for transfecting 80% confluent HEK293 cells in a 100 mm tissue culture dish is given in Table 3.6.

Opti MEM	Lentiviral vector DNA (1 µg/µl)	ViraPower mix (1 µg/µl)	+ Reagent	Lipofectamine LTX
946 µl	3 µl	9 µl	12 µl	30 µl

Table 3.6: Transfection mix for lentiviral packaging using ViraPower.

After adding + reagent incubate at room temperature for 5 minutes then add lipofectamine LTX. After 30 minutes of incubation at room temperature for 30 minutes before adding dropwise to the cells. 16 hours post transfection, media was changed to DMEM + 10% FBS and viral soup was collected at 42 hours and 62 hours post transfection. The viral soup was concentrated by ultracentrifugation at 26,500 rpm at 4°C for 90 minutes.

3.2.2 Lentiviral Transduction

HaCaT (ATCC), an immortalized human keratinocyte cell line, and NIH3T3, an immortalized mouse fibroblast cell line (ATCC) cells were used to determine viral titer. These cell lines were cultured in DMEM + 10% FBS as per the ViraPower manual (Invitrogen). Briefly, 1:100 and

1:1000 diluted viral particles were added to 1×10^5 HaCaT cells (for pCCLK14 Turbo RFP and pCCLK14 Turbo RFP + 14-3-3 γ shRNA_{mir}) or NIH3T3 cells (for pLKO Tet Puro viruses and LentiCRISPR viruses) and incubated at 37°C with 5% CO₂ for 16 hours. 48 hours post transduction, HaCaT cells were examined for Turbo RFP expression by light microscopy and flow cytometry. Viral titre was determined as product of percentage of Turbo RFP positive cells and dilution factor. Viral titre was found to be 7.2×10^8 TU/ml for pCCLK14 Turbo RFP viruses and 1.08×10^9 TU/ml for pCCLK14 Turbo RFP + 14-3-3 γ shRNA_{mir} viruses. Since, pLKO and pLentiCRISPR vector systems lack cDNA for fluorescent proteins, 1×10^5 NIH3T3 cells transduced with pLKO and pLentiCRISPR viruses were selected in puromycin (2mg/ml) for 10 to 15 days to identify the number of puromycin resistant colonies. To count the colonies, the colonies were washed with 1X PBS and fixed with 4% paraformaldehyde in 1X PBS for 20 minutes at room temperature. After fixation, colonies were incubated with 1% crystal violet in methanol for 1 hour at room temperature to stain the colonies, followed by washing the colonies under running tap water, colonies were air dried and the number of colonies was determined. Each colony represents a single transduced cell. Viral titre was determined as product of number of puromycin resistant colonies and dilution factor. Viral titre was found to be 9.15×10^6 TU/ml for pLKO Tet Puro viruses, 4.5×10^6 TU/ml for pLKO Tet Puro 14-3-3 γ shRNA viruses, 2×10^8 TU/ml for LentiCRISPR K14 Cas V1 viruses, 9×10^7 TU/ml and for LentiCRISPR K14 Cas V1 14-3-3 γ shRNA viruses.

3.3 Animal experiments

Swiss mice Crl:CFW(SW), BALB/c mice and FVB mice were bred and maintained in the laboratory animal facility of ACTREC as described previously [196]. Maintenance of the animal facility is as per the national guidelines provided by the Committee for the Purpose of Control and Supervision of the Experiments on Animals (CPCSEA), Ministry of Environment and Forest, Government of India. The animals were housed in a controlled environment with the temperature and relative humidity being maintained at $23\pm 20^{\circ}\text{C}$ and 40-70% respectively and a day night cycle of 12 hours each (7:00 to 19:00 light; 19:00 to 7:00 dark). The animals received an autoclaved balanced diet prepared in-house as per the standard formula and sterile water ad libitum. Mice were housed in Individually Ventilated Cage (IVC) system (M/S Citizen, India) provided with autoclaved rice husk bedding material available locally. Protocols for the experiments were approved by the Institutional Animal Ethics Committee (IAEC) of ACTREC. The animal study proposal numbers are 11/2012 and 1/2014.

3.3.1 Injection of viral particles and generation of transgenic mice

To inject viral particles in testis, protocol developed in the lab was followed [53, 203]. Briefly, 28 day old Crl:CFW(SW) or BALB/c male mice were anesthetized by intra-peritoneal injection of Avertin (Sigma) (2,2 tribromo-ethanol and t-amyl alcohol at the rate of 0.015ml/gm body weight) or by isoflurane vapors. Hair was removed from the inguinal area of mice and the surgical site was cleaned using betadiene. Anterior to the penis, a single midline cutaneous incision of approx. 1-1.5 cm length was made using sterile surgical scissors under aseptic conditions. After making the incision in the muscles, the testes were removed from the scrotal

sac with a curved sterile forceps through the incision by gently pulling the dorsal fat pad associated with the testis. A solution of lentiviruses ($1-5 \times 10^5$ TU/ml) was injected slowly into the inter-tubular space of both the testes using a 30 gauge needle. The pre-founder male mice were co-habitated with wild-type females 35 days post-transduction and the pups obtained were analyzed for the presence of the transgene.

The pre-founder male mice were mated with wild-type females. Pups born were analyzed by PCR using genomic DNA obtained from their tail tip and those positive for the transgene were considered as F1 generation of transgenic animals. F2 generation of mice were produced either by breeding transgene positive animals with wild-type mice or by breeding two mice positive for the presence of the transgene. The pups from these matings were analyzed for the presence of the transgene, i.e. either Turbo RFP or puromycin resistance cDNA, as described below.

3.3.2 Electroporation of DNA into the testicles of mice

pCCLK14Turbo RFP and pCCLK14 Turbo RFP + 14-3-3 γ shRNAmir were digested with PvuI and NdeI to get the plasmid fragment containing K14 promoter-Turbo TFP-WPRE and K14 promoter-Turbo RFP + 14-3-3 γ shRNAmir-WPRE respectively. Briefly, 100 μ g of pCCLK14 Turbo RFP and pCCLK14 Turbo RFP + 14-3-3 γ shRNAmir plasmids were digested with 100 units of PvuI and 100 units of NdeI at 37°C for 16 hours. The digested plasmid were resolved on 1% agarose gel and the fragment containing K14 promoter-Turbo TFP-WPRE and K14 promoter-Turbo RFP + 14-3-3 γ shRNAmir-WPRE were eluted from the gel using the Macherey-Nagel gel elution kit. Eluted fragment was pooled and sent to Dr. Subeer Majumdar's Laboratory at NII for electroporation experiments as described in [48]. The electroporated pro-founder mice

were imported from NII for mating experiments. The electroporated pro-founder mice were of FVB strain.

3.3.3 Isolation of Genomic DNA (gDNA) from tail sections

Tail biopsies (~3mm) from 3 weeks old pups sired by pre-founder males were taken and lysed for 16hours at 55°C in high salt digestion buffer containing 50mM Tris HCl pH 8.0, 1mM EDTA, 1% Tween-20 and 400µg of Proteinase K (Jackson Laboratories). The protein extract was processed for isolation of DNA using phenol-chloroform extraction followed by isopropanol precipitation as described previously [196]. Same protocol was used to isolate DNA from testis, epidermis and cell line.

3.3.4 Genotyping of Animals

The genomic DNA was subjected for PCR analysis using transgene-specific primers whose sequences are listed in Table 3.2. The amplification of the endogenous patched (Ptch) gene from the samples was used as a loading control. Genomic DNA isolated from the human origin cell line, HCT116, was used as a negative control for the Ptch PCR. PCR was done using *Taq* polymerase and PCR program for Ptch PCR was as follows:

- 1) Initial denaturation at 94°C for 5 minutes.
- 2) Denaturation at 94°C for 45 seconds.
- 3) Annealing at 63°C for 30 seconds.

- 4) Extension at 72°C for 30 seconds.
- 5) Repeat from step 2 for 29 cycles.
- 6) Final extension at 72°C for 10 minutes.
- 7) Hold at 4°C forever.

Every PCR reaction set had three controls. The pCCLK14 Turbo RFP plasmid was used as a template for a positive control, genomic DNA obtained from WT mice was used as a negative control. To validate the Turbo RFP PCR results, two sets of primers were used. First set of PCR primer recognizes a part of Turbo RFP sequence whereas second set of primer recognizes the entire Turbo RFP sequence taken from pTRIPz vector.

PCR components	1x
Standard <i>Taq</i> buffer 10X	1.0 µl
Forward Primer (20 pmol)	0.4 µl
Reverse Primer (20 pmol)	0.4 µl
dNTPs 10mM	0.4 µl
MgCl ₂ (25mM)	0.9µl
Template (100 ng/µl)	1.0µl
<i>Taq</i> polymerase (5U/µl) (NEB)	0.3µl
MilliQ	5.6µl

Table 3.7: List of components used in genotyping PCR mix.

PCR program:

- 1) Initial denaturation at 95°C for 3 minutes.
- 2) Denaturation at 95°C for 1 minute.
- 3) Annealing at 70°C for 1 minute.
- 4) Extension at 72°C for 1 minute.
- 5) Repeat from step 2 for 9 cycles.
- 6) Final extension at 72°C for 10 minutes.
- 7) Hold at 4°C forever.

The PCR components and PCR program for both the primer sets were same. To ensure that the PCR product is indeed Turbo RFP sequence, PCR product was cloned into the pTZ57RT/T vector (Thermo Fisher Scientific) and was sequenced using Sanger sequencing.

Similarly, for puromycin resistance cDNA PCR, pLKO Tet Puro or pLentiCRISPR plasmid was used as a template for a positive control and genomic DNA obtained from WT mice was used as a negative control.

- 1) Initial denaturation at 95°C for 3 minutes.
- 2) Denaturation at 95°C for 1 minute.
- 3) Annealing at 66°C for 1 minute.
- 4) Extension at 72°C for 1 minute.

5) Repeat from step 2 for 29 cycles.

6) Final extension at 72°C for 10 minutes.

7) Hold at 4°C forever.

To ensure that the PCR product is indeed puromycin resistance cDNA sequence, PCR product was cloned into the pJET vector (Thermo Fisher Scientific) and was sequenced using Sanger sequencing.

Name of the oligonucleotide	Sequence of the oligonucleotides
Ptch Forward	CTGCGGCAAGTTTTGGTTG
Ptch Reverse	AGGGCTTCTCGTTGGCTACAAG
Turbo RFP Forward	ATGAGCGAGCTGATCAAGG
Turbo RFP Reverse	TTATCTGTGCCCCAGTTTGC
Turbo RFP + shRNAmir Reg Forward	GGACCGGTCGCCACCATGAGC
Turbo RFP + shRNAmir Reg Reverse	GGGTCGACTGGCCGGCCGCATTAGTCT
Puromycin Forward	GCAAGAACTCTTCCTCACGC
Puromycin Reverse	GCCTTCCATCTGTTGCTGCG
14-3-3 γ Exon 1 Forward	CTCTGGACATTCAGGGTCACA
14-3-3 γ Exon 1 Reverse	TCCTCGTCTCAGTAGCTTGC

Table 3.8: List of oligonucleotides used for genotyping.

3.3.5 Histology of epidermis

For histological analysis of epidermis, frozen tissues were used. Using cryotome thin sections of tissues were taken on a glass slide and given for haematoxylin/eosin staining. Images were taken using Zeiss AxioImager Z1 upright microscope.

To detect the Turbo RFP fluorescence in the hair follicle of Turbo RFP positive mice, epidermis was isolated from the tail. Briefly, tail snips were taken and a cut was made longitudinally to remove the cartilage and the skin was incubated with 5mM EDTA solution at room temperature for 16 hours and using forceps epidermis was separated from the dermis as described in [204]. The epidermis was mounted on a glass slide using vectashield (Vector), as per manufacturer's instruction. The epidermis was imaged using LSM 510 confocal microscope. As a control epidermis section from WT mouse was used.

3.3.6 T7 endonuclease assay

14-3-3 γ exon 1 region was PCR amplified from the tail genomic DNA using the primer sequence given in Table 3.8. The PCR components were as follows:

PCR components	1x
Standard <i>Taq</i> buffer 10X	1.0 μ l
Forward Primer (20 pmol)	0.5 μ l
Reverse Primer (20 pmol)	0.5 μ l
dNTPs 10mM	0.4 μ l
MgCl ₂ (25mM)	0.6 μ l
Template (100 ng/ μ l)	2.0 μ l

<i>Taq</i> polymerase (5U/μl) (NEB)	0.3μl
MilliQ	4.7μl

Table 3.9: List of components used in 14-3-3γ exon 1 PCR mix.

PCR Program:

- 1) Initial denaturation at 94°C for 5 minutes.
- 2) Denaturation at 94°C for 45 seconds.
- 3) Annealing at 65°C for 40 seconds.
- 4) Extension at 72°C for 35 seconds.
- 5) Repeat from step 2 for 29 cycles.
- 6) Final extension at 72°C for 10 minutes.
- 7) Hold at 4°C forever.

The PCR product thus obtained was used performing T7 endonuclease assay. The principle of the T7 endonuclease assay is given in Figure 3.9. Briefly, the PCR product from the wild type mice or the vector control mice was mixed with that of the test mouse in the ratio of 1:1. This mixture of PCR product was then denatured at 95°C for 10 minutes and was allowed to re-anneal by gradually cooling it. T7 endonuclease enzyme was then added to cleave the heteroduplex DNA and incubated at 37°C for four hours. After digestion, the mixture was resolved on 2% agarose gel to detect the number and size of the PCR fragments.

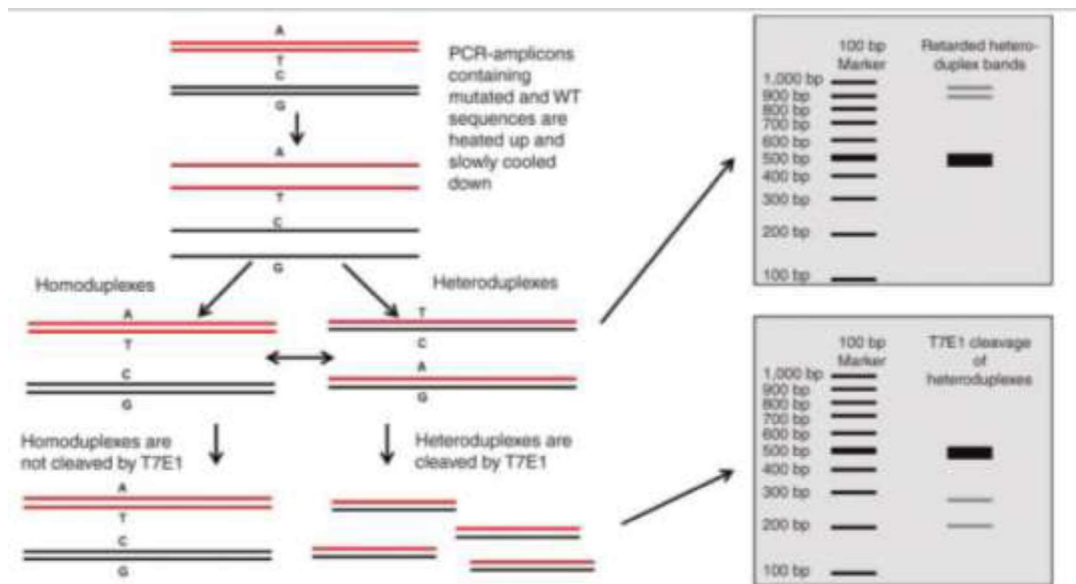


Figure 3.9: The schematic representation of the principle of T7 endonuclease assay [205].

3.3.7 Doxycycline administration

To induce the expression of shRNA in pLKO Tet Puro 14-3-3 γ shRNA transgene positive mice, pLKO Tet Puro 14-3-3 γ shRNA pre-founder mice and wild type mice mated with pLKO Tet Puro 14-3-3 γ shRNA pre-founder mice were given doxycycline in water. Doxycycline (100mg Biodoxi, Biochem Pharmaceutical Industries Ltd.) was mixed with 100 ml of sterile water as described in [206]. To mask the taste of doxycycline, sucrose was added in the water at a final concentration of 5%.

3.3.8 Sertoli cell isolation and culture

Sertoli cell proliferation is observed in new born animals and the rate of Sertoli cell proliferation decreases once the SSC's start proliferating. The protocol used for isolating and culturing Sertoli

cells from rat was described previously [207]. 1-2 week old mice were sacrificed; their testicles were collected in 1X Hank's buffered salt solution (HBSS) (Gibco) and decapsulated using forceps under the dissecting microscope. Decapsulated testes were washed with 1X Hank's buffer and 10% collagenase was added followed by an incubation at room temperature on a rocker for 5 minutes or until tubules are separated. The samples were kept on a test-tube stand and the tubules were allowed to settle and the supernatant was removed. Tubules were washed thrice with 1X HBSS to remove residual collagenase. 1X Trypsin was added to the tubules followed by a 2 minute incubation. The tubules were washed twice with 1X HBSS and 2.5% of trypsin inhibitor was added in the third wash. After the third wash, 1X HBSS containing collagenase (10%), hyaluronidase (20%), DNase (7%) and trypsin inhibitor (2.5%) was added to the tubules and incubated on a rocking platform at RT for 5 minutes. The protease treated tubules were centrifuged at 500 rpm for 4 minutes and the cell pellet was treated with 1:10 diluted 1X HBSS to kill all the SSCs present in the pellet by hypotonic shock..The remaining Sertoli cells were centrifuged at 500 rpm for 4 minutes and plated in F12 DMEM (Gibco) and incubated at 37°C and 5% CO₂. Sertoli cells cannot be passaged and hence once cultured should be used immediately for Western blotting or RT-PCR or immunofluorescence experiments.

3.4 Antibodies and Western blotting

Cell extracts were prepared using 1X sample buffer (Table 3.10) and protein concentration was determined using Folin-Lowry's method of protein estimation. 50 to 100µg of protein was resolved on 6% and 12% step gradient resolving polyacrylamide gel or 7.5% and 10% step gradient resolving polyacrylamide gel. The gel was transferred on nitrocellulose membrane of

0.45 μm pore size (Mdi, Membrane Technologies).For Western blotting, the details of the different antibodies used are given in Table 3.11.

Components	Stock Concentration	Volume
Tris pH 6.8	1.0 M	500 μl
Glycerol	100%	1000 μl
Sodium Dodecyl Sulfate	10%	2000 μl
Distilled Water		6.5 ml

Table 3.10: Composition of 1X Sample buffer.

Antibody	Company	Clone	Raised in	Dilution
DesmoplakinI/II	Abexome	DP 200 1B8	Mouse	1:100
Desmoglein2	Invitrogen	6D8	Mouse	1:250
Desmocollin2/3	Invitrogen	7G6	Mouse	1:250
Plakoglobin	Abcam	15F11	Mouse	1:250
Plakoglobin	Abexome	Monoclonal	Mouse	1:250
Plakophilin3	Thermo Fisher Scientific	23E/4	Mouse	1:2000
KIF5B	Abcam	Polyclonal	Rabbit	1:500
PKC μ	Abcam	Monoclonal	Rabbit	1:500
E-cadherin	BD Biosciences	C-36	Mouse	1:500
α -E-catenin	Santa Cruz Biotechnology	C-19	Goat	1:500
β -catenin	BD Biosciences	C-14	Mouse	1:500
β Actin	Sigma	AC-74	Mouse	1:3000

GFP	Clontech	Monoclonal	Mouse	1:50000
Cytokeratin 8	Sigma	5301	Mouse	1:1000
14-3-3 γ	Abcam	CG31	Mouse	1:500
14-3-3 γ	Enzo Life Sciences	CG31	Mouse	1:2000
14-3-3 ϵ	Santa Cruz Biotechnology	T-16	Mouse	1:500
14-3-3 σ	-	CS-112	Mouse	1:50
HA	-	12CA5	Mouse	1:50

Table 3.11: List of the primary antibodies used for Western blotting experiments.

These antibodies were diluted in 1%BSA solution in TBST containing 0.2% sodium azide. Blocking was performed using 5% milk in TBST. The composition of TBST is given in Table 3.12.

Components	Stock Concentration	Volume
Sodium Chloride	2.5 M	60 ml
Tris pH 8.0	1.0 M	10 ml
Tween20	100%	1 ml
Distilled Water	-	929 ml

Table 3.12: Composition of TBST.

The secondary antibodies were anti-goat antibody (Thermo Fisher Scientific, 1:500), anti-mouse antibody (Thermo Fisher Scientific, 1:2500) and anti-rabbit antibody (Thermo Fisher Scientific, 1:2500) conjugated with horse radish peroxidase. The secondary antibodies were diluted in 2.5% milk in TBST containing 1% goat serum. Western blots were developed using either super signal west pico or super signal west femto (Thermo Fisher Scientific) or Clarity ECL (Bio-Rad) as per the instructions of the manufacturer.

3.4.1 Preparation of tissue extracts.

Tissue extracts of testis, tails and epidermis were prepared using total lysis buffer in mortar and pestle. Briefly, total lysis buffer was added to the tissue followed by liquid nitrogen, to solidify the tissue, and the tissue was crushed in mortar and pestle to obtain a homogeneous suspension. This suspension was then centrifuged at 13,000 rpm for 15 minutes at 4°C and supernatant was collected as the tissue extract. The composition of total lysis buffer is given in Table 3.13.

Component	Stock Concentration	Volume
Tris pH 7.5	1.0 M	500 µl
Sodium Chloride	2.5M	600µl
EGTA	0.5 M	20 µl
EDTA	0.5 M	20 µl
NP-40	100%	50 µl
Triton-X	100%	100 µl
Aprotinin	2.0 mg/ml	50 µl
Leupeptin	1.0 mg/ml	50 µl

Phenylmethane sulfonyl fluoride (PMSF)	50 mM	200 μ l
Sodium orthovanadate	0.2 M	1000 μ l
Sodium fluoride	1.0 M	200 μ l
β -glycerophosphate	1.0 M	10 μ l
Distilled Water		7.2 ml

Table 3.13: Composition of Total lysis buffer.

3.4.2 Soluble and insoluble protein fractionation

Fractionation was done using the protocol given in [208-210]. Briefly, HCT116 monolayer was washed twice with ice-cold 1X PBS, cells were scraped and collected in 1X PBS, centrifuged at 5000 rpm for 3 minutes at 4°C, supernatant was discarded and cells were mixed with cytoskeletal buffer (CSK) and incubated on rocker at 4°C for 20 min. After 20 minutes incubation 2.5 M ammonium sulphate solution (for 200 μ l of CSK buffer 22 μ l of ammonium sulphate solution) was added and the cells were further incubated on rocker at 4°C for 5 min followed by centrifugation at 16000 rpm for 16 minutes at 4°C. Supernatant is soluble fraction and pellet is insoluble fraction. Pellet was dissolved in sample buffer. Insoluble fraction was sonicated to make it homogeneous. Composition of CSK buffer and sample buffer is given in Table 3.14. and 3.15 respectively. Do not boil the soluble fraction

Component	Stock Concentration	Volume
Sucrose	3 M	1000 µl
Sodium Chloride	2.5 M	200 µl
PIPES pH 6.8	0.2 M	1000 µl
MgCl ₂	25mM	120 µl
Triton-X	100%	50 µl
Phenylmethane sulfonyl fluoride (PMSF)	50 mM	24µl
DNaseI	7%	2.8µl
RNase	10 mg/ml	100 µl
Distilled Water		7.5 ml

Table 3.14: Composition of Cytoskeletal buffer.

Component	Stock Concentration	Volume
Tris pH 7.5	1 M	100 µl
Sodium Dodecyl Sulfate	10%	1000 µl
EDTA	0.5 M	100 µl
Distilled Water		8.8 ml

Table 3.15: Composition of sample buffer used for extraction of insoluble fraction.

3.5 Immunofluorescence and confocal microscopy

Cells were fixed with either 4% paraformaldehyde in 1X PBS for 20 minutes at room temperature to image desmosomal proteins or with 100% methanol (chilled) for 10 minutes at -20°C for adherens junction proteins. Cell membrane was permeabilized by incubating cells in 1X PBS containing 0.3% Triton-X for 10 minutes at room temperature. The details of the primary antibodies used for immunofluorescence assay is given in Table 3.16.

Antibody	Company	Clone	Raised in	Dilution
DesmoplakinI/II	Abexome	DP 200 1B8	Mouse	1:7
Desmoglein2	Invitrogen	6D8	Mouse	1:25
Desmocollin2/3	Invitrogen	7G6	Mouse	1:25
Plakoglobin	Abcam	15F11	Mouse	1:25
Plakophilin3	Thermo Fisher Scientific	23E/4	Mouse	1:75
E-cadherin	BD Biosciences	C-36	Mouse	1:50
α -E-catenin	Santa Cruz Biotechnology	C-19	Goat	1:50
β -catenin	BD Biosciences	C-14	Mouse	1:50
Myc	Santa Cruz Biotechnology	9E10	Mouse	1:25

Table 3.16: List of the primary antibodies used for immunofluorescence assay in this study.

Primary and secondary antibodies were diluted in 1% BSA solution prepared in 0.1% NP-40 in 1X PBS. The secondary antibodies were used at 1:100 dilutions. The secondary antibodies used in immunofluorescence assay were conjugated with Alexa Fluor 633 or Alexa Fluor 568, to avoid spectral overlap with GFP. All images were captured using Zeiss LSM 510 confocal microscope or Zeiss LSM 780 confocal microscope or Leica TCS SP8 Confocal Microscope.

3.6 Calcium Switch Assay

The HCT116 derived 14-3-3 γ knockdown cell line was transfected with EGFP-f or PG-EGFP-f cDNA using PEI, 24 hours post transfection cells were incubated in low calcium medium. After 24 hours, the cells were fed with medium containing normal calcium levels and the cells fixed at 0 and 15 minutes post addition were processed for DSG2 staining and confocal microscopy as described previously [150, 211, 212].

3.7 Hanging drop assay

Cells were transfected with either pCDNA3.1 Puromycin EGFP-f or pCDNA3.1 Puromycin PG-EGFP-f PEI. 24 hours post-transfection, the cells were transferred to medium containing 0.5 μ g/ml of puromycin for four days to kill the un-transfected cells. The remaining cells were processed for hanging drop assay as previously described [213]. Images of cell aggregates were obtained with a Zeiss Axiovert 200M inverted microscope with a 5X or 10X objective.

3.8 GST protein preparation

GST protein preparation was done as described in [214]. Briefly, a single colony of BL21 cells transformed with pGEX4T1 (GST) vector pGEX4T1 with PG 300 WT was inoculated in 10 ml of LB broth containing ampicillin(1mg/ml) and incubated at 37°C for 16-18hours at 200 rpm (rotations per minute). This culture broth was used to inoculate 100 ml LB broth containing ampicillin in a 1.0 L flask followed by incubation at 37°C for 1 hour at 200 rpm. After 1 hour of incubation, 10-20 μ l of 1M IPTG was added to and the flasks were further incubated at 37°C for 3-4 hours at 200 rpm. After 3 hours the cells were pelleted by centrifugation at 4000 rpm for 10 minutes at 4°C. The supernatant was discarded and cells were suspended gently in ice cold 0.1%

triton X-100 in PBS, using a 10ml pipette while ensuring that there is minimum frothing. To lyse the bacterial cells suspension was sonicated using sonicator (Branson) at 50 duty cycles for 10 seconds and then placed on ice for 10 seconds. The sonication was repeated 4 times. The suspension was centrifuged at 10,000 rpm for 10 minutes at 4°C. The supernatant was transferred to 15ml screw cap conical tubes and 150µl of 50% slurry of glutathione sepharose beads (Amersham) was added and incubated on a rocker at 4°C for 1 hour. After 1 hour, the beads were pelleted by centrifugation at 3000 rpm for 1 minute at 4°C. The supernatant was discarded, 1ml of NET-N buffer (composition given in Table 3.17) was added and beads were transferred to 1.5ml Eppendorf. The beads were pelleted by centrifugation at 3000 rpm for 1 minute at 4°C. Beads were washed twice with NET-N. After the wash, beads were re-suspended in 150µl of NET-N. To elute the GST tagged fusion protein from the beads 500µl of elution buffer (composition given in Table 3.18) was added and incubated at 4°C for 16 hours. Further, beads were centrifuged at 1500 rpm at 4°C for 5 minutes, supernatant was collected and purified by dialysis in 1X PBS. Briefly, dialysis tubing was incubated in a beaker containing hot water (80°C) for 3 minutes to remove the impurities, then the dialysis tubing was cleaned and again incubated in another beaker containing hot water followed by incubation in 1X PBS. After the 1X PBS wash, the dialysis tubing was clamped at one end and the supernatant obtained after elution was poured from the other end, the other end was clamped, the dialysis tubing containing supernatant was dipped in a beaker containing 1X PBS and incubated on a magnetic stirrer at 4°C for 4 hours. After 4 hours, 1X PBS was changed and dialysis was continued for 16 hours. After dialysis, sample was centrifuged at 13000 rpm for 10 minutes at 4°C. The supernatant was concentrated by loading on centricon tube (50 ml conical screw cap tube with a membrane filter of 3kDa) and centrifuging it at 4000 rpm for 30 minutes at 4°C. 1.5 ml of concentrate was

collected and 10% glycerol was added and stored in -80°C . For determining the protein concentration, 5 μl of the concentrate along with standard BSA solutions were resolved on a 10% SDS-PAGE gel and stained with coomassie blue. For performing protein kinase assay GST and GST PG 300 proteins were sent to Felipe Samaniego's laboratory, University of Texas, MD Anderson Cancer Centre, Houston, Texas, U.S.A.

Component	Stock Concentration	Volume
Tris pH 8.0	1 M	2000 μl
Sodium Chloride	2.5 M	4000 μl
EDTA pH 8.0	0.5 M	200 μl
MgCl_2	25 mM	120 μl
NP-40	100%	500 μl
Distilled Water		93.3 ml

Table 3.17: Composition of NET-N buffer.

Component	Stock Concentration	Volume
Tris pH 7.5	1 M	500 μl
Sodium Chloride	2.5 M	600 μl
Reduced Glutathione	100 mM	1000 μl
Distilled Water		7.9 ml

Table 3.18: Composition of elution buffer.

3.9 RNA isolation and reverse transcriptase PCR

HCT116 cells were transfected with pCDNA3.1 and pCDNA3.1 PG C term using PEI and 48 hours post transfection, 1X PBS wash was given and TRIzol (Thermo Fisher Scientific) was added to the cells (1ml for 35 mm tissue culture plate) and incubated at room temperature for 5 minutes for dissociation of nucleoprotein complex. Samples were collected in an eppendorf 200µl of chloroform was added, vortexed and incubated at room temperature for 2-3 minutes. Samples were centrifuged at 13000 rpm for 15 minutes at 4°C. The aqueous phase was collected in another Eppendorf and 500µl of isopropanol was added and incubated at room temperature for 10 minutes to precipitate the RNA. Samples were centrifuged at 13000 rpm for 15 minutes at 4°C followed by 75% ethanol wash (75ml 100% Ethanol and 25 ml nuclease free water) at 10000 rpm for 5 minutes at 4°C. The RNA pellet was dried for 10 minutes at room temperature and 25µl of commercial water was added. To dissolve the RNA samples were incubated at 55°C for 10 minutes. RNA was stored at -70°C. For mRNA to cDNA conversion High capacity cDNA reverse transcription kit (Applied Biosystems) was used.

PCR components	1x
RT buffer 10X	2.0 µl
RT Random Primers 10X	0.8 µl
dNTPs 10mM	0.4 µl
Template (100 ng/µl)	10.0 µl
Reverse Transcriptase	1.0 µl
Nuclease free water	6.0 µl

Table 3.19: PCR components for mRNA to cDNA conversion.

PCR program:

1) 25°C for 10 minutes.

2) 37°C for 2 hours.

3) 85°C for 5 minutes.

4) Hold at 4°C forever.

1µl of the cDNA was used for the PCR amplification of PG C term mRNA using *Taq* polymerase. Annealing temperature was 60°C. PCR for GAPDH served as a loading control. The sequence of the GAPDH primers is given in Table 3.20. The sequence of the primers used for PCR amplification of PG C term mRNA is given in Table 3.1.

Name of the oligonucleotide	Sequence of the oligonucleotide
GAPDH Forward	TGCACCACCAACTGCTTAGC
GAPDH Reverse	GGCATGGACTGTGGTCATGAG
GAPDH Forward (Mouse)	GGCTGCCCAGAACATCAT
GAPDH Reverse (Mouse)	CGGACACATTGGGGGTAG
14-3-3 γ Forward (Mouse)	GGTCATCAGCAGCATCGAGC
14-3-3 γ Reverse (Mouse)	GTTGTTGCCTTCACCGCCGT

Table 3.20: List of oligonucleotides used for GAPDH reverse transcriptase PCR.

4. Results and Discussion:

**Generate inducible and
epidermis specific knockdown
mice for 14-3-3 γ .**

4. Results

To generate transgenic mice our laboratory developed a novel method in which lentiviruses were injected into the testis of the pre-founder mice and these pre-founder mice sired transgenic mice [53]. To study the role of 14-3-3 γ in the growth and development of mice, lentiviruses expressing 14-3-3 γ shRNA were injected into the testes of the mice but these pre-founder mice became sterile. The sterility observed in these pre-founder mice was due to loss of 14-3-3 γ in the testis, which led to the disruption of desmosome formation and hence cell-cell adhesion between developing spermatocytes and Sertoli cells thereby affecting spermatogenesis [150]. This result also suggested 14-3-3 γ regulates desmosome formation and hence might be important for the development of other epithelial tissues. Hence, we decided to generate inducible or tissue specific 14-3-3 γ knockdown mice.

4.1 Generation of tetracycline inducible 14-3-3 γ knockdown mice

To study the role of 14-3-3 γ in the mammalian development and to prevent the 14-3-3 γ shRNA expression in testis of the pre-founder mice we decided to generate inducible 14-3-3 γ knockdown mice. To generate inducible 14-3-3 γ knockdown mice, we used a tetracycline inducible 14-3-3 γ shRNA system [195]. This system is regulated by doxycycline i.e. 14-3-3 γ shRNA will be expressed only in the presence of doxycycline and therefore this system will not induce sterility in pre-founder mice in the absence of doxycycline, thus permitting the generation of 14-3-3 γ shRNA transgene positive pups. The tetracycline inducible 14-3-3 γ shRNA permits temporal regulation of expression of the 14-3-3 γ shRNA at different stages of development.

4.1.1 Validation of pLKO Tet Puro 14-3-3 γ shRNA vector

Oligonucleotides encoding the 14-3-3 γ shRNA were cloned into the pLKO Tet Puro vector using AgeI and EcoRI sites. To ensure that the 14-3-3 γ shRNA was expressed only in the presence of doxycycline, HCT116 cells were co-transfected with HA-14-3-3 γ and pLKO Tet Puro vector or pLKO Tet Puro 14-3-3 γ shRNA. 24 hours post transfection, doxycycline was added to one set of dishes. 90 hours post transfection, cells were harvested and Western blots performed with antibodies to HA and β Actin. Un-transfected HCT116 cells served as a negative control for HA-14-3-3 γ expression. It was observed that the 14-3-3 γ levels were decreased only in the doxycycline treated HCT116 cells transfected with pLKO Tet Puro 14-3-3 γ shRNA (Figure 4.1).

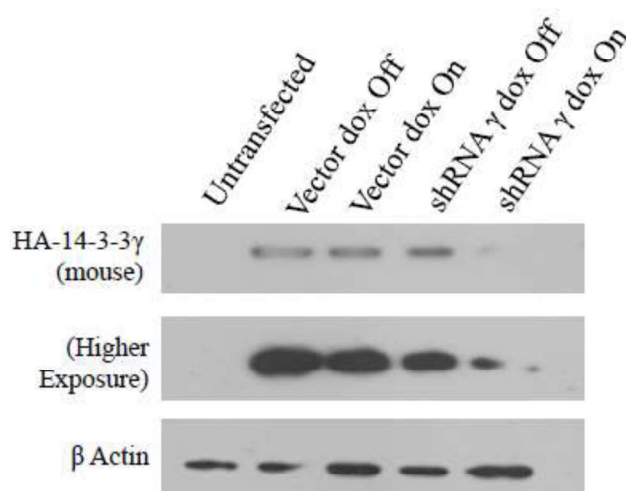


Figure 4.1: Validation of pLKO Tet Puro 14-3-3 γ shRNA construct. Protein extracts of HCT116 cells co-transfected with HA-14-3-3 γ and pLKO Tet Puro vector control or pLKO Tet Puro 14-3-3 γ shRNA, treated (+ Dox) or untreated (- Dox) with doxycycline were resolved on 10% SDS-PAGE gel followed by Western blotting with the indicated antibodies. Western blots for β Actin served as a loading control. Un-transfected HCT116 cells served as a negative control for HA-14-3-3 γ expression.

4.1.2 Generation of pLKO Tet Puro 14-3-3 γ shRNA positive transgenic mice

pLKO Tet Puro vector and pLKO Tet Puro 14-3-3 γ shRNA were packaged using the ViraPower packaging system (Invitrogen). After determining the virus titre as described in materials and methods, the viruses were surgically injected into the testicles of 4 week old BALB/c mice as described previously [53]. Five weeks post-surgery, these pre-founder mice were mated with wild type female mice to obtain transgenic pups. The pups were screened for the presence of puromycin resistance cDNA transgene using genomic DNA isolated from the tail snips of the pups as a template in PCR reactions for the puromycin resistance cDNA (Puro). Genomic DNA from a wild type mouse served as a negative control. All the pups were found to be positive for the puromycin resistance cDNA transgene. A PCR reaction for the mouse Patched (Ptch) gene was performed as a loading control and genomic DNA purified from the human cell line, HCT116, was used as a negative control for the Ptch PCR. The pedigree analysis for the pups obtained from one of the pLKO Tet Puro vector pre-founder mice and pLKO Tet Puro 14-3-3 γ shRNA pre-founder mice along with the Ptch PCR and puromycin resistance cDNA PCR results are shown in Figure 4.2 A and B. Table 4.1 and 4.2 show the gender, number and genotype of the pups obtained from pLKO Tet Puro vector pre-founder mice and pLKO Tet Puro 14-3-3 γ shRNA pre-founder mice respectively.

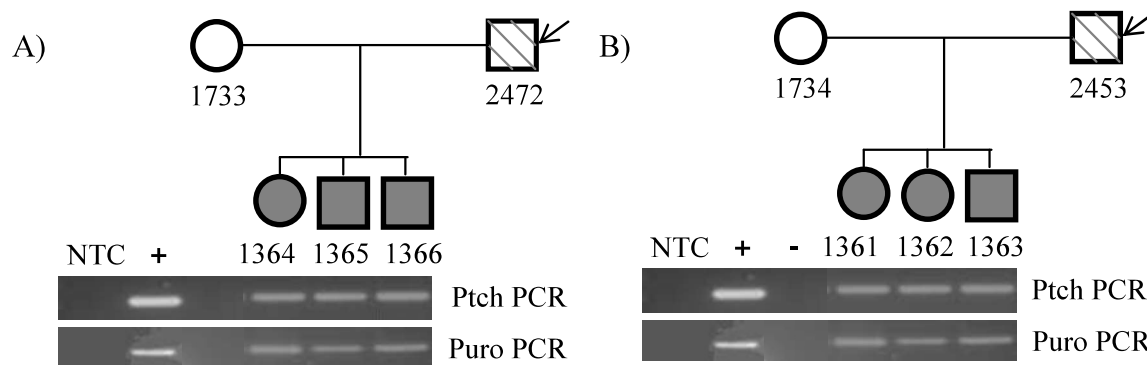


Figure 4.2: Pedigree analysis of the pLKO Tet Puro vector pre-founder mice and pLKO Tet Puro 14-3-3 γ shRNA pre-founder mice [Strain: BALB/c]. A-B. A pedigree analysis for the pre-founder mice (indicated with an arrow) 2472 infected with viruses expressing the pLKO Tet Puro vector control (A) and 2453 (B) infected with viruses expressing the pLKO Tet Puro14-3-3 γ shRNA. Individual mice were assigned numbers for further experiments. Genomic DNA amplification using primers for puromycin resistance DNA (Puro) or Patched (Ptch) as a loading control are shown for each animal. The filled squares and circles indicate transgene positive animals. NTC is the no template control, + is a positive control where the template is the pLKO Tet plasmid and – represents the negative control, which is genomic DNA isolated from WT mice for the puromycin PCR reactions and genomic DNA from HCT116 cells for the Ptch PCR reactions.

Sr. No.	Mother No.	Father No. Pre-founder	Mice No.	Gender	Ptch PCR	Puro PCR	Litter No.
1	48/1733	47/2472	49/1364	F	+	+	I
2			49/1365	M	+	+	I
3			49/1366	M	+	+	I
4	48/1732	47/2471	49/2543	F	+	+	I
5			49/2544	M	+	+	I
6	48/1731	47/2470	49/2536	F	+	+	I
7			49/2537	F	+	+	I
8			49/2538	M	+	+	I
9			49/2539	M	+	+	I
10			49/2540	M	+	+	I
11			49/2541	M	+	+	I
12			49/2542	M	+	+	I

Table 4.1: Pups obtained from pLKO Tet Puro pre-founder mice (F1 generation) [Strain: BALB/c]. (+ is positive and – is negative)

Sr. No.	Mother No.	Father No. Pre-founder	Mice No.	Gender	Ptch PCR	Puro PCR	Litter No.
1	48/1734	47/2453	49/1361	F	+	+	I
2			49/1362	F	+	+	I
3			49/1363	M	+	+	I
4	48/1735	47/2454	49/1359	M	+	+	I
5			49/1360	M	+	+	I
6	48/1736	47/2455	49/2526	F	+	+	I
7			49/2527	F	+	+	I
8			49/2528	M	+	+	I
9	48/2938	47/2455	49/2533	F	+	+	I
10			49/2534	M	+	+	I
11			49/2535	M	+	+	I

Table 4.2: Pups obtained from pLKO Tet Puro14-3-3 γ shRNA pre-founder mice (F1 generation) [Strain: BALB/c]. (+ is positive and – is negative)

Since all the pups were positive puromycin resistance cDNA it was necessary to confirm that the PCR product is indeed puromycin resistance cDNA and not some non-specific PCR product. The PCR product from one of the transgene positive mice was cloned into pJET vector, pJET Puro clones were screened using BglII digest (Figure 4.3 A) and one of the clones was sequenced. The sequence of the PCR product matched with the puromycin resistance cDNA (Figure 4.3 B).

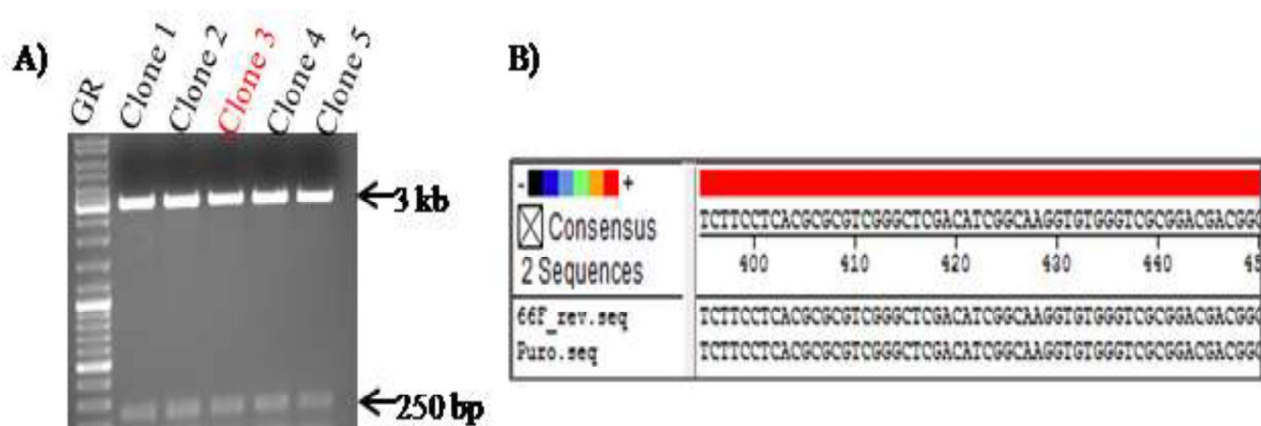


Figure 4.3: Cloning and sequencing of the puromycin resistance cDNA PCR product. A. PCR product of puromycin resistance cDNA obtained from genomic DNA of mouse 49/1366 was cloned into pJET vector and the clones were screened using BglII digest. The clones were resolved using 1% agarose gel. Two bands were seen in all the clones; a 3 kb band corresponding to the size of pJET vector and a 250 bp band corresponding to the size of the PCR product. Clone 3 (highlighted in red) was given for sequencing. **B.** The sequence of the clone B was matched to the puromycin resistance cDNA sequence using MegAlign software. Note that the two sequences showed an exact match.

4.1.3 Stable inheritance of pLKO Tet Puro 14-3-3 γ shRNA from one generation to next generation

To observe if the transgene is stably integrated into the germ line and is being inherited by the next generation the pLKO Tet Puro 14-3-3 γ shRNA transgene positive pups (F1 generation) were weaned and inbred to obtain F2 generation and pups from F2 generation were inbred to generate F3 generation. All the pups from F2 and F3 generations were found to be positive for the puromycin resistant cDNA transgene as shown in Figure 4.4. The gender, number and

genotype of the pups from F2 and F3 generation are shown in Table 4.3 and 4.4 respectively. PCR product of puromycin resistance cDNA obtained from genomic DNA of mouse D/2993 matched with puromycin resistance cDNA sequence.

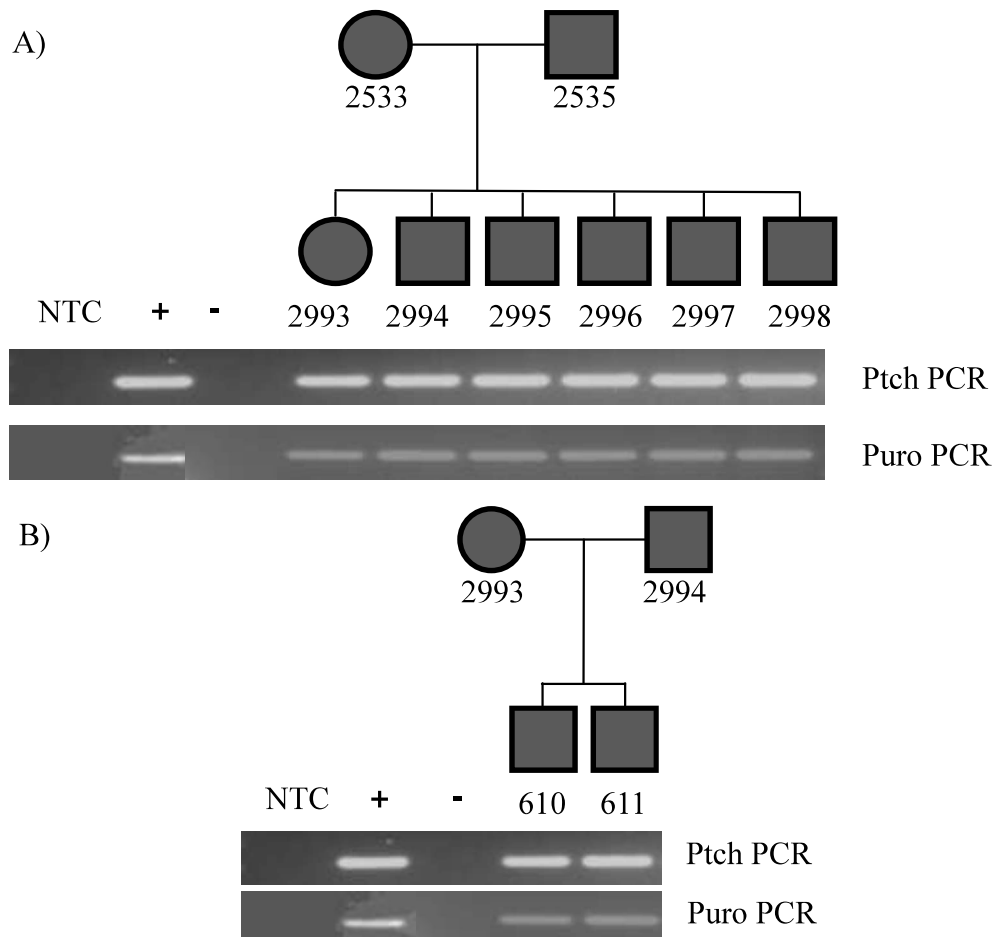


Figure 4.4: Pedigree analysis of F2 and F3 generation obtained from inbreeding of pLKO Tet Puro 14-3-3 γ shRNA positive F1 generation mice [Strain: BALB/c]. **A.** A pedigree analysis for F2 generation mice obtained from inbreeding of pLKO Tet Puro14-3-3 γ shRNA positive F1 generation mice. **B.** A pedigree analysis for F3 generation mice obtained from inbreeding of pLKO Tet Puro14-3-3 γ shRNA positive F2 generation mice. Individual mice were assigned numbers for further experiments. Genomic DNA amplification using primers for

puromycin resistance cDNA (Puro) or Patched (Ptch) as a loading control are shown for each animal. The filled squares and circles indicate transgene positive animals. NTC is the no template control , + is a positive control where the template is the pLKO Tet plasmid and – represents the negative control, which is genomic DNA isolated from WT mice for the puromycin PCR reactions and genomic DNA from HCT116 cells for the Ptch PCR reactions.

Sr. No.	Mother No.	Father No.	Mice No.	Gender	Ptch PCR	Puro PCR	Litter No.
1	49/2533	49/2535	D/2993	F	+	+	I
2			D/2994	M	+	+	I
3			D/2995	M	+	+	I
4			D/2996	M	+	+	I
5			D/2997	M	+	+	I
6			D/2998	M	+	+	I

Table 4.3: Pups obtained from inbreeding of pLKO Tet Puro14-3-3 γ shRNA positive mice (Inbreeding of F1 generation) [Strain: BALB/c]. (+ is positive and – is negative)

Sr. No.	Mother No.	Father No.	Mice No.	Gender	Ptch PCR	Puro PCR	Litter No.
1	D/2993	D/2994	E/610	M	+	+	I
2			E/611	M	+	+	I
3	D/2993	D/2994	G/1221	F	+	+	II
4			G/122	F	+	+	II

Table 4.4: Pups obtained from inbreeding of pLKO Tet Puro14-3-3 γ shRNA positive mice (Inbreeding of F2 generation) [Strain: BALB/c]. (+ is positive and – is negative)

4.1.4 Doxycycline treatment for pLKO Tet Puro 14-3-3 γ shRNA pre-founder mice and transgenic pups

To induce the shRNA expression pLKO Tet Puro positive mice and pLKO Tet Puro 14-3-3 γ shRNA positive mice of F1 generation were given doxycycline in drinking water and the tail snips were collected on day 6 and day 9 of doxycycline treatment for performing reverse transcriptase PCR for 14-3-3 γ and tail snips collected just before initiating doxycycline treatment (day 0) were used as a control. Reverse transcriptase PCR for GAPDH served as a loading control. Since there was no change in the mRNA levels of 14-3-3 γ in tail samples, doxycycline was given for 6 weeks and after that one of the testicles from each animal was surgically removed to isolate RNA to determine the mRNA levels of 14-3-3 γ . As shown in Figure 4.5, no change was observed in the mRNA levels of 14-3-3 γ in any of the testes. Therefore, even after 6

weeks of doxycycline treatment there was no knockdown of 14-3-3 γ in pLKO Tet Puro 14-3-3 γ shRNA positive mice.

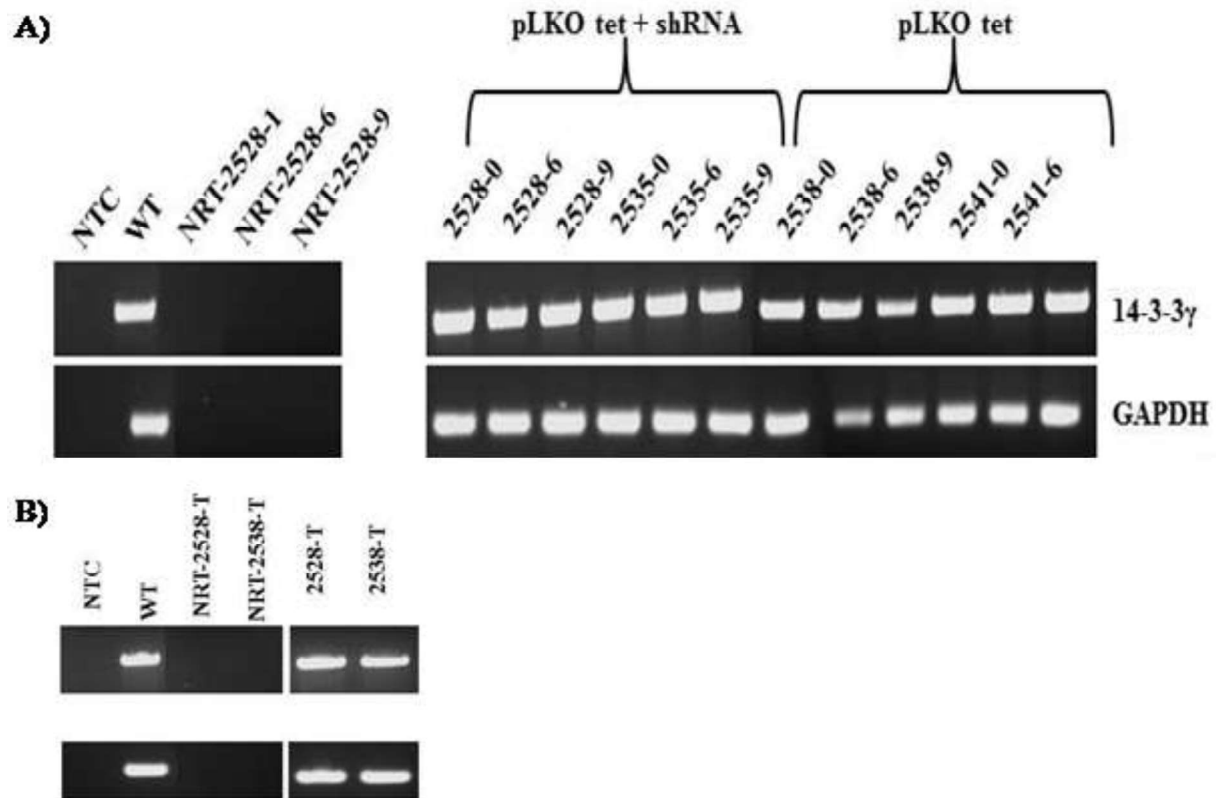


Figure 4.5: Effect of doxycycline treatment on 14-3-3 γ levels in pLKO Tet Puro 14-3-3 γ shRNA positive mice. A. Reverse transcriptase PCR using RNA extracted from tail snips of BALB/c mice pLKO Tet Puro vector positive mice 2538 and 2541 and pLKO Tet Puro 14-3-3 γ shRNA positive mice 2528 and 2535 post 0,6 and 9 days of doxycycline treatment (1mg/ml). No change was observed in the 14-3-3 γ mRNA levels. **B.** RNA was extracted from the doxycycline treated testis of 2528 and 2535. PCR was carried out using primers for 14-3-3 γ and GAPDH (as a loading control).

4.1.5 Effect of 14-3-3 γ knockdown on spermatogenesis in pLKO Tet Puro 14-3-3 γ shRNA pre-founder mice

To study the effect of 14-3-3 γ loss on the process of spermatogenesis, 4 week old Crl:CFW(SW) mice were injected with either pLKO Tet Puro viruses or pLKO Tet Puro 14-3-3 γ shRNA viruses. These pre-founder mice were divided into two groups, three mice in each group, one group was kept on doxycycline and the other group was kept as control. Two mice died after three weeks of surgery one mouse (G/1216) was from the doxycycline treated pLKO Tet Puro pre founder group and the other mouse (G/1213) was from the control pLKO Tet Puro pre-founder because of which only two mice were left in these groups. Five weeks post-surgery doxycycline treated and untreated pre-founder mice were mated to wild type female mice to determine if the doxycycline treated pLKO Tet Puro 14-3-3 γ shRNA pre-founder mice had become sterile. But the doxycycline treated pLKO Tet Puro 14-3-3 γ shRNA pre-founder mice were fertile as they sired pups. We hypothesized that the un-infected SSCs from doxycycline treated pLKO Tet Puro 14-3-3 γ shRNA pre-founder mice must be contributing to the sperm production, therefore, we genotyped the pups obtained from these pre-founder mice. It was observed that all the pups were positive for the puromycin resistance cDNA transgene suggesting that these pups were sired from the transgene positive spermatozoa (Figure 4.6 and table 4.5 and 4.6).

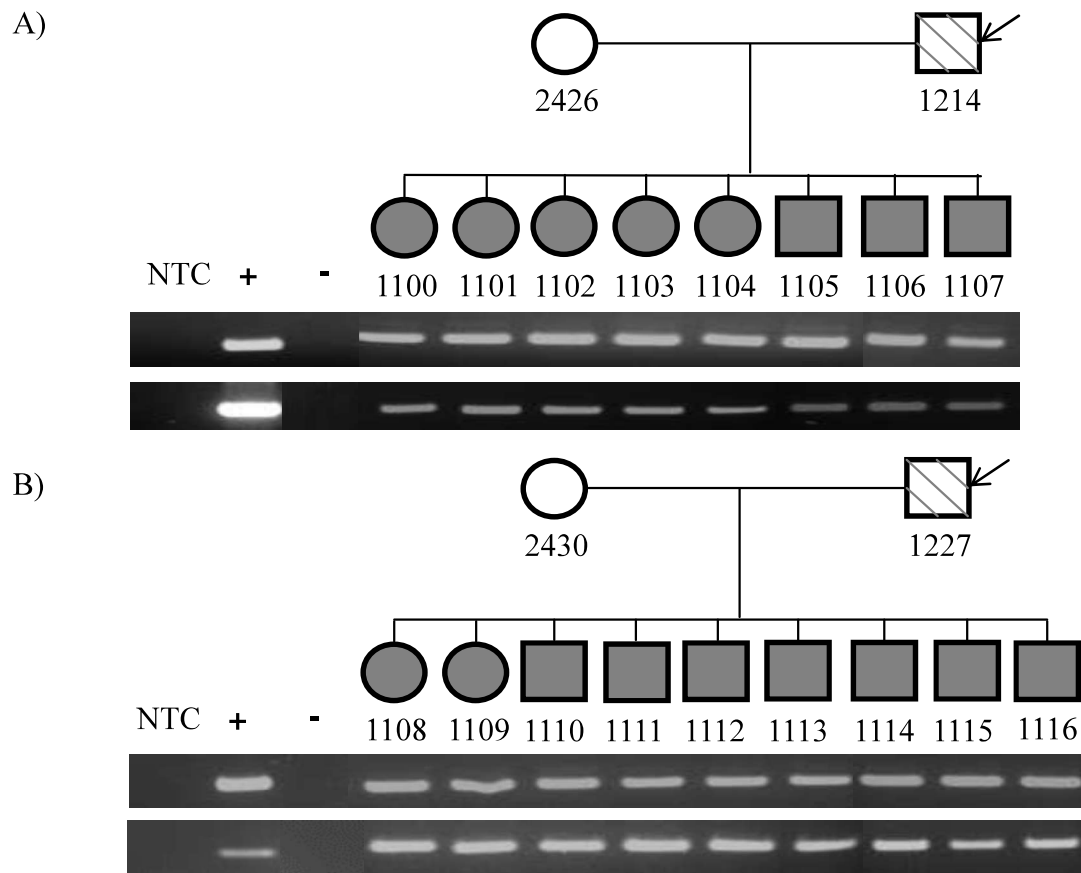


Figure 4.6: Pedigree analysis of the pLKO Tet Puro pre-founder mice and pLKO Tet Puro 14-3-3 γ shRNA pre-founder mice [Strain: Crl:CFW(SW)]. A-B. A pedigree analysis for the pre-founder mice (indicated with an arrow) 1214 infected with viruses expressing the pLKO Tet Puro vector control (A) and 1227 (B) infected with viruses expressing the pLKO Tet Puro14-3-3 γ shRNA. Individual mice were assigned numbers for further experiments. Genomic DNA amplification using primers for puromycin resistance cDNA (Puro) or Patched (Ptch) as a loading control are shown for each animal. The filled squares and circles indicate transgene positive animals. NTC is the no template control , + is a positive control where the template is the pLKO Tet plasmid and – represents the negative control, which is genomic DNA isolated

from WT mice for the puromycin PCR reactions and genomic DNA from HCT116 cells for the Ptch PCR reactions.

Sr. No.	Mother No.	Father No. Pre-founder	Mice No.	Gender	Ptch PCR	Puro PCR	Litter No.
1	G/2426	G/1214 (-Dox)	H/1100	F	+	+	I
2			H/1101	F	+	+	I
3			H/1102	F	+	+	I
4			H/1103	F	+	+	I
5			H/1104	F	+	+	I
6			H/1105	M	+	+	I
7			H/1106	M	+	+	I
8			H/1107	M	+	+	I
9	G/2426	G/1214 (-Dox)	I/1008	F	+	+	II
10			I/1009	F	+	+	II
11			I/1010	F	+	+	II
12			I/1011	F	+	+	II
13			I/1012	F	+	+	II
14			I/1013	F	+	+	II
15			I/1014	M	+	+	II
16			I/1015	M	+	+	II
17			I/1016	M	+	+	II
18	G/2427	G/1215	H/1415	F	+	+	I

19		(-Dox)	H/1416	F	+	+	I
20			H/1417	F	+	+	I
21			H/1418	F	+	+	I
22			H/1419	M	+	+	I
23			H/1420	M	+	+	I
24			H/1421	M	+	+	I
25			H/1422	M	+	+	I
26			H/1423	M	+	+	I
27			H/1424	M	+	+	I
28	G/2427	G/1215	I/682	F	+	+	II
29		(-Dox)	I/683	F	+	+	II
30			I/684	F	+	+	II
31			I/685	F	+	+	II
32			I/686	F	+	+	II
33			I/687	F	+	+	II
34			I/688	F	+	+	II
35			I/689	M	+	+	II
36			I/690	M	+	+	II
37			I/691	M	+	+	II
38			I/692	M	+	+	II
39			I/693	M	+	+	II
40			I/694	M	+	+	II
41	G/2432	G/1220	I/1025	F	+	+	I

42		(+Dox)	I/1026	F	+	+	I
43			I/1027	F	+	+	I
44			I/1028	F	+	+	I
45			I/1029	F	+	+	I
46			I/1030	M	+	+	I
47			I/1031	M	+	+	I
48			I/1032	M	+	+	I
49			I/1033	M	+	+	I
50	G/2432	G/1220 (+Dox)	J/510	F	+	+	II
51			J/511	F	+	+	II
52			J/512	F	+	+	II
53			J/513	F	+	+	II
54			J/514	F	+	+	II
55			J/515	F	+	+	II
56			J/516	M	+	+	II
57			J/517	M	+	+	II
58	G/2431	G/1218	I/871	M	+	+	I
59		(+Dox)	I/872	M	+	+	I

Table 4.5: Pups obtained from pLKO Tet Puro pre-founder mice (F1 generation) [Strain: Crl:CFW (SW)]. (+ is positive and – is negative)

Sr. No.	Mother No.	Father No. Pre-founder	Mice No.	Gender	Ptch PCR	Puro PCR	Litter No.
1	G/2430	G/1227 (- Dox)	H/1108	F	+	+	I
2			H/1109	F	+	+	I
3			H/1110	M	+	+	I
4			H/1111	M	+	+	I
5			H/1112	M	+	+	I
6			H/1113	M	+	+	I
7			H/1114	M	+	+	I
8			H/1115	M	+	+	I
9			H/1116	M	+	+	I
10	G/2430	G/1227 (- Dox)	I/652	F	+	+	II
11			I/653	F	+	+	II
12			I/654	M	+	+	II
13			I/655	M	+	+	II
14			I/656	M	+	+	II
15			I/657	M	+	+	II
16			I/658	M	+	+	II
17			I/659	M	+	+	II
18	G/2428	G/1217 (- Dox)	H/1425	F	+	+	I
19			H/1426	F	+	+	I
20			H/1427	F	+	+	I
21			H/1428	F	+	+	I

22			H/1429	F	+	+	I
23			H/1430	M	+	+	I
24			H/1431	M	+	+	I
25			H/1432	M	+	+	I
26			H/1433	M	+	+	I
27			H/1434	M	+	+	I
28	G/2428	G/1217 (- Dox)	I/672	F	+	+	II
29			I/673	F	+	+	II
30			I/674	F	+	+	II
31			I/675	M	+	+	II
32			I/676	M	+	+	II
33			I/677	M	+	+	II
34			I/678	M	+	+	II
35			I/679	M	+	+	II
36			I/680	M	+	+	II
37			I/681	M	+	+	II
38	G/2429	G/1219 (- Dox)	H/1435	F	+	+	I
39			H/1436	F	+	+	I
40			H/1437	F	+	+	I
41			H/1438	F	+	+	I
42			H/1439	M	+	+	I
43			H/1440	M	+	+	I
44			H/1441	M	+	+	I

45			H/1442	M	+	+	I
46			H/1443	M	+	+	I
47			H/1444	M	+	+	I
48			H/1445	M	+	+	I
49	G/2429	G/1219 (- Dox)	I/660	F	+	+	II
50			I/661	F	+	+	II
51			I/662	F	+	+	II
52			I/663	F	+	+	II
53			I/664	F	+	+	II
54			I/665	F	+	+	II
55			I/666	M	+	+	II
56			I/667	M	+	+	II
57			I/668	M	+	+	II
58			I/669	M	+	+	II
59			I/670	M	+	+	II
60			I/671	M	+	+	II
61	G/2435	G/1226 (+ Dox)	I/1018	F	+	+	I
62			I/1019	F	+	+	I
63			I/1020	F	+	+	I
64			I/1021	M	+	+	I
65			I/1022	M	+	+	I
66			I/1023	M	+	+	I
67			I/1024	M	+	+	I

68	G/2433	G/1224	I/2469	M	+	+	I
69		(+ Dox)	I/2470	M	+	+	I

Table 4.6: Pups obtained from pLKO Tet Puro 14-3-3 γ shRNA pre-founder mice (F1 generation) [Strain: Crl:CFW (SW)]. (+ is positive and – is negative)

Doxycycline treated pLKO Tet Puro 14-3-3 γ shRNA pre-founder mouse G/1225 sired pups but its pups were cannibalized before weaning.

After three months of the lentiviral injections and doxycycline treatment, right testicles of the doxycycline treated and untreated pLKO Tet Puro pre-founder mice and pLKO Tet Puro 14-3-3 γ shRNA pre-founder mice were surgically removed and mRNA levels of 14-3-3 γ were determined using reverse transcriptase PCR. Reverse transcriptase PCR for GAPDH served as a loading control. As shown in Figure 4.7, there was no reduction in 14-3-3 γ mRNA levels in the doxycycline treated and control pLKO Tet Puro 14-3-3 γ shRNA pre-founder mice. The absence of sterility in the doxycycline treated pLKO Tet Puro 14-3-3 γ pre-founder mice could be attributed to the fact that there was no loss of 14-3-3 γ in the testes of these mice.

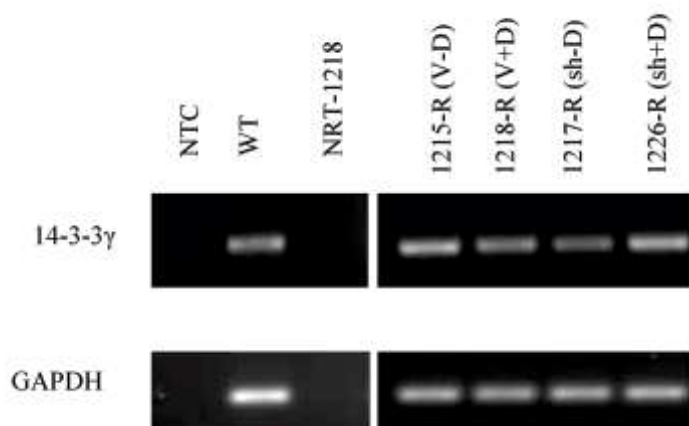


Figure 4.7: The effect of doxycycline treatment on 14-3-3 γ levels in the doxycycline treated and untreated pLKO Tet Puro pre-founder mice and pLKO Tet Puro 14-3-3 γ shRNA pre-founder mice. Reverse transcriptase PCR was done using RNA extracted from the right testicle of Crl:CFW(SW) mice 1215, 1218, 1217 and 1226 post 3 months of doxycycline treatment (1mg/ml). PCR was carried out using primers for 14-3-3 γ and GAPDH (as a loading control). V - pLKO Tet puro Vector, sh - pLKO Tet Puro14-3-3 γ shRNA, +D - Doxycycline administered, -D - Plain water.

4.1.6 Effect of 14-3-3 γ knockdown on the physiology of pLKO Tet Puro 14-3-3 γ shRNA positive mice

The pups obtained from the doxycycline treated pLKO Tet Puro pre-founder mice and pLKO Tet Puro 14-3-3 γ shRNA pre-founder mice were on doxycycline right from the time of fertilization and were kept on doxycycline life long, therefore we wanted to study if the loss of 14-3-3 γ affected the physiology of these animals. The appearance of these animals were same as that of the pups obtained from the control pLKO Tet Puro pre-founder mice and pLKO Tet Puro 14-3-

3 γ shRNA pre-founder mice. The control pLKO Tet Puro positive mice, doxycycline treated pLKO Tet Puro positive mice, control pLKO Tet Puro 14-3-3 γ shRNA positive mice and doxycycline treated pLKO Tet Puro 14-3-3 γ shRNA positive mice were inbred to see if their fertility is compromised. The result of the control pLKO Tet Puro positive mice and control pLKO Tet Puro 14-3-3 γ shRNA positive mice inbreeding experiment is given in Table 4.7 and that of doxycycline untreated pLKO Tet Puro positive mice and doxycycline treated pLKO Tet Puro 14-3-3 γ shRNA positive mice is given in Table 4.8.

Genotype (Swiss)	pLKO Tet Puro (- DOX)		pLKO Tet Puro 14-3-3 γ shRNA (- DOX)		
Female x	H/1101 x	H/1415 x	H/1435 x	H/1425 x	H/1109 x
Male	H/1106	H/1423	H/1445	H/1434	H/1110
I Litter	1	1 (cannibalized)	-	5 (cannibalized)	-
II Litter	2	-	-	1	-

Table 4.7: Pups obtained from the inbreeding of the control pLKO Tet Puro positive mice and control pLKO Tet Puro 14-3-3 γ shRNA positive mice [Strain: Crl:CFW (SW)]. (+ is positive and – is negative)

Genotype (Swiss)	pLKO Tet Puro(+ DOX)			pLKO Tet Puro14-3-3 γ shRNA (+ DOX)		
Female x	J/512 x	J/1025 x	J/510xJ/5	I/1019 x	I/1020 x	I/1029 x
Male	J/516	J/1030	17	I/1021	I/1024	I/1033
I Litter	4 Pups	-	-	-	-	-

Table 4.8: Pups obtained from the inbreeding of the doxycycline untreated pLKO Tet Puro positive mice and doxycycline treated pLKO Tet Puro 14-3-3 γ shRNA positive mice [Strain: Crl:CFW (SW)]. (+ is positive and – is negative)

All the mice of the control pLKO Tet Puro group were fertile whereas out of the three mating pairs of the doxycycline treated pLKO Tet Puro group only one mating pair was found to be fertile. Similarly, out of the three mating pairs of the control pLKO Tet Puro 14-3-3 γ shRNA group only one pair was found to be fertile and all the mice of the doxycycline treated pLKO Tet Puro 14-3-3 γ shRNA group were sterile. It was not clear why some of the animals of the doxycycline treated pLKO Tet Puro group and the control pLKO Tet Puro 14-3-3 γ shRNA were sterile. The levels of 14-3-3 γ in all these animals will be determined to find out if the sterility observed in the control and the doxycycline treated pLKO Tet Puro 14-3-3 γ shRNA was due to the loss of 14-3-3 γ .

4.2 Generation of epidermis specific 14-3-3 γ knockdown mice

Cell-cell adhesion is important for maintenance of tissue structure and function. Loss of 14-3-3 γ disrupted cell-cell adhesion and spermatogenesis in testis by inhibiting desmosome formation [150]. Autoimmune disorders like, pemphigus vulgaris (autoantibodies target DSG3), pemphigus foliaceus (autoantibodies target DSG1) [215] and mutations in DP and PKP1 affect desmosome function and cell-cell adhesion leading to skin fragility and blistering. [216]. Moreover loss of DSC1 in mice led to fragile skin and barrier defects [185] and loss of DSG3 in mouse showed oral lesions and loss of cell-cell adhesion in skin [186] supporting the fact that the rigidity and barrier function of skin is dependent on desmosomes. Since desmosomes regulate epidermal organization and function and 14-3-3 γ regulates desmosome formation, we wanted to observe if loss of 14-3-3 γ in the epidermis would lead to defects in epidermal development.

Skin is divided into two layers dermis and epidermis. Dermis is made up of connective tissues and epidermis is a stratified squamous epithelium mostly made up of keratinocytes. Epidermis is made up of different layers namely basal layer (stratum basale), spinous layer (stratum spinosum), granular layer (stratum granulosum) and stratum corneum [216, 217]. Keratinocytes from the basal layer undergo mitosis and migrate to the spinous layer to undergo differentiation, the keratinocytes in the granular layer starts forming keratohyalin granules (made up of loricrin and profilagrin) and lamellar bodies (to store lipids) and at the stratum corneum keratinocytes lose nucleus, become flattened, cornified and dead (Figure 4.8) [217].

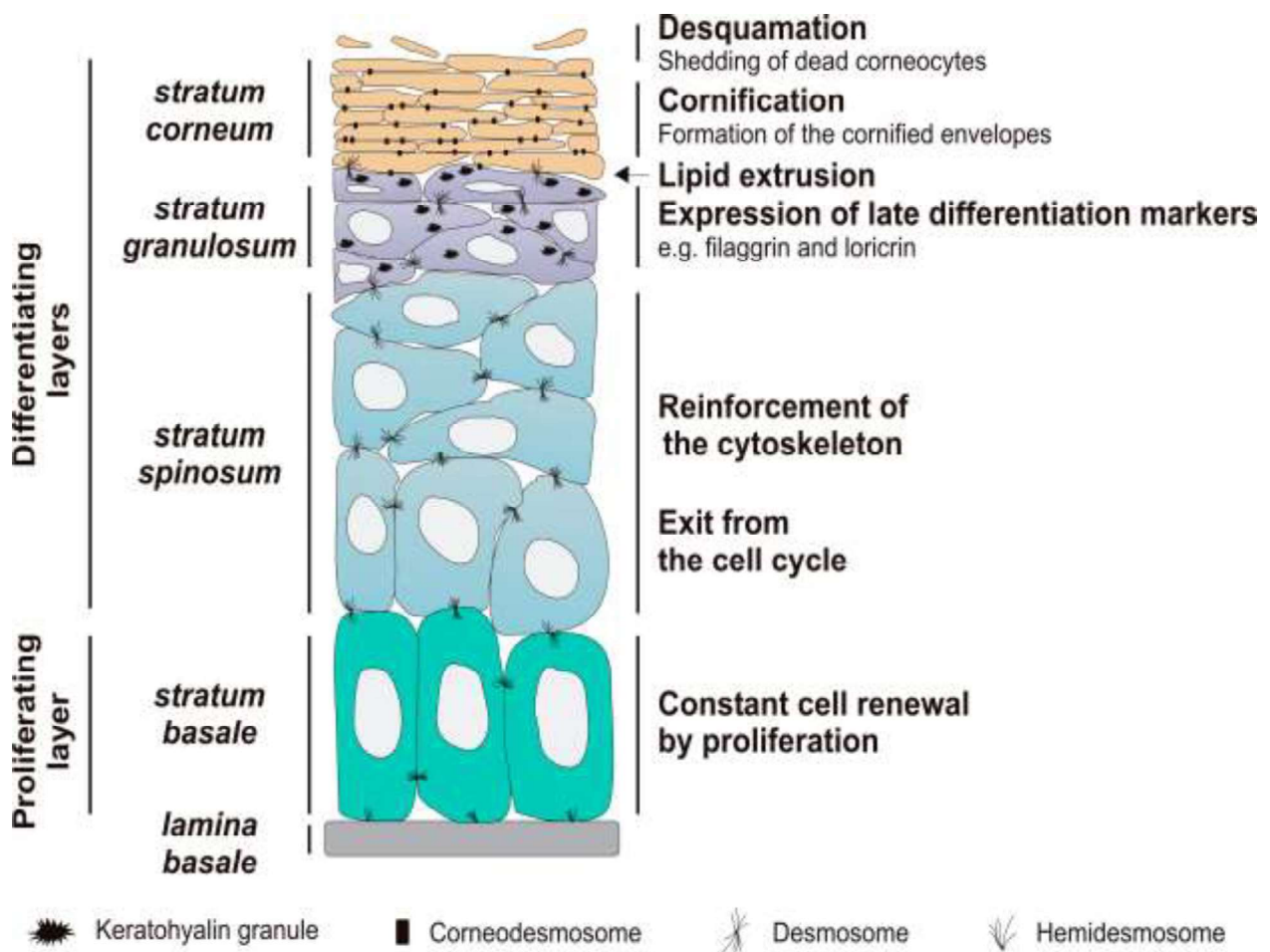


Figure 4.8: Structure of Epidermis [217]. This is a schematic representation of epidermis. Different layers of the epidermis and differentiation of keratinocytes to corneocytes is also shown. Note that these differentiating keratinocytes are attached to each other by desmosomes.

Keratinocytes from different layers express different types of keratins for e.g. cytokeratin 5 (K5) and cytokeratin 14 (K14) are expressed by the basal layer [218] and K1 and K10 in the spinous layer and granular layer and involucrin and loricrin in the cornified layer of the epidermis [219]. Therefore to drive the expression of 14-3-3 γ shRNAmir in the keratinocytes of the basal layer of the epidermis K14 promoter was chosen.

4.2.1 Validation of pCCLK14 Turbo RFP 14-3-3 γ shRNAmir vector

Turbo RFP and Turbo RFP 14-3-3 γ shRNAmir were cloned in pCCLK14 vector using AgeI and SalI sites by replacing GFP. To validate the expression of 14-3-3 γ shRNAmir, HaCaT cells were co-transfected with HA 14-3-3 γ and pCCLK14 Turbo RFP vector or pCCLK14 Turbo RFP 14-3-3 γ shRNAmir. 72 hours post transfection cells were harvested and Western blotting for HA and β Actin was done. Un-transfected HaCaT cells served as a negative control for HA-14-3-3 γ expression. It was observed that the HA-14-3-3 γ levels were decreased only in the HaCaT cells transfected with pCCLK14 Turbo RFP 14-3-3 γ shRNAmir, as shown in Figure 4.9.

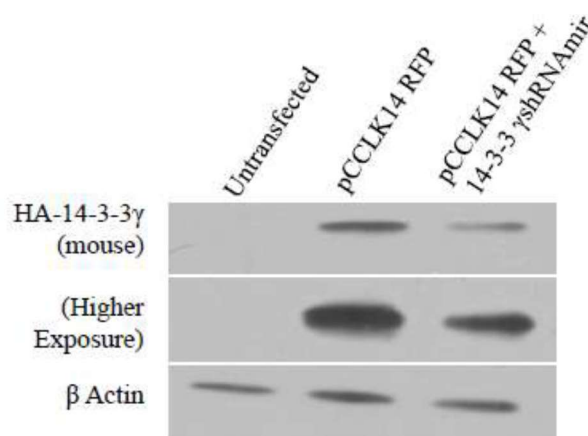


Figure 4.9: Validation of pCCLK14 Turbo RFP 14-3-3 γ shRNAmir construct. Protein extracts of HaCaT cells co-transfected with HA-14-3-3 γ and pCCLK14 Turbo RFP vector control or pCCLK14 Turbo RFP 14-3-3 γ shRNAmir were resolved on 10% SDS-PAGE gel followed by Western blotting with the indicated antibodies. Western blots for β Actin served as a loading control. Un-transfected HaCaT cells served as a negative control for HA-14-3-3 γ expression.

4.2.2 Generation of pCCLK14 Turbo RFP 14-3-3 γ shRNAmir positive transgenic mice

pCCLK14 Turbo RFP vector and pCCLK14 Turbo RFP 14-3-3 γ shRNAmir were packaged using ViraPower. After determining the virus titre as described in materials and methods, the viruses were surgically injected into the testicles of 4 week old Swiss mice as described previously [53]. Five weeks post-surgery, these pre-founder mice were mated to the wild type female mice to obtain transgenic pups. The pups were screened for the presence of Turbo RFP transgene using genomic DNA isolated from the tail snips of the pups as a template for the PCR amplification of Turbo RFP (RFP). Genomic DNA from the wild type mouse served as a negative control. All the pups were found to be positive for the Turbo RFP transgene. Another PCR reaction was performed using genomic DNA isolated from the tail snips as template to amplify Turbo RFP 14-3-3 γ shRNAmir fragment from the Turbo RFP positive mice to detect the presence of 14-3-3 γ shRNAmir but all the pups only showed presence of a band corresponding to the molecular weight of Turbo RFP (~ 980 bp) instead of a band corresponding to the molecular weight of Turbo RFP 14-3-3 γ shRNAmir fragment (~ 1060 bp). The absence of 14-3-3 γ shRNAmir was confirmed by cloning the PCR product into TA vector and sequencing the positive TA clone. A PCR reaction for the mouse Patched (Ptch) gene was performed as a loading control and genomic DNA purified from the human cell line, HCT116, was used as a negative control for the Ptch gene. The pedigree analysis for the pups obtained from one of the pCCLK14 Turbo RFP vector and pCCLK14 Turbo RFP 14-3-3 γ shRNAmir pre-founder mice along with the Ptch PCR and Turbo RFP PCR results are shown in Figure 4.10 A and B. Table 4.9 and 4.10 show the gender, number and genotype of the pups obtained from pCCLK14 Turbo RFP vector control or pCCLK14 Turbo RFP 14-3-3 γ shRNAmir pre-founder mice respectively.

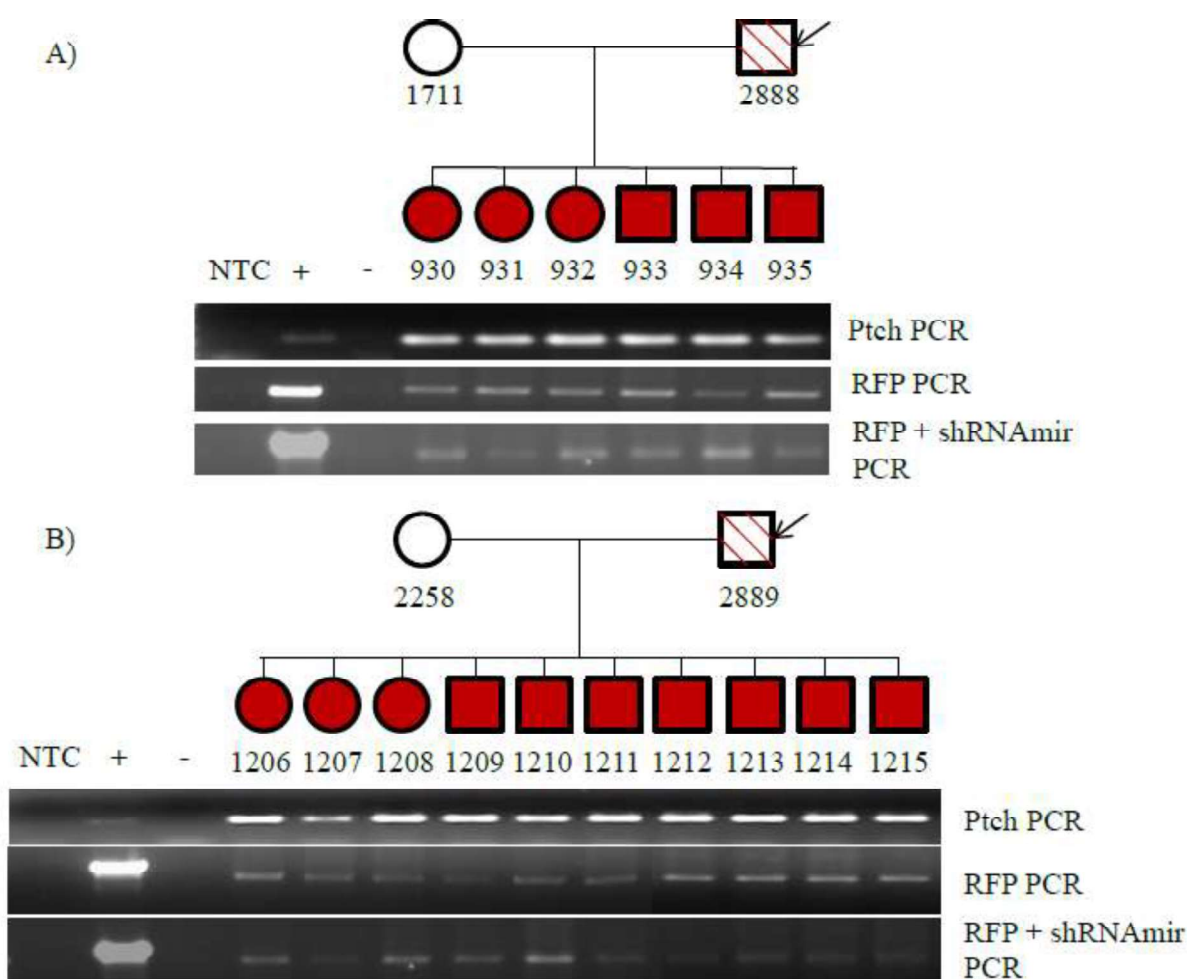


Figure 4.10: Pedigree analysis of the pCCLK14 Turbo RFP vector pre-founder mice and pCCLK14 Turbo RFP 14-3-3 γ shRNA^{mir} pre-founder mice [Strain: Crl:CFW(SW)]. A-B.

A pedigree analysis for the pre-founder mice (indicated with an arrow) 2888 infected with viruses expressing the pCCLK14 Turbo RFP vector control (A) and 2889 (B) infected with viruses expressing the pCCLK14 Turbo RFP14-3-3 γ shRNA^{mir}. Individual mice were assigned numbers for further experiments. Genomic DNA amplification using primers for Turbo RFP (RFP) or Turbo RFP + 14-3-3 γ shRNA^{mir} or Patched (Ptch) as a loading control are shown for each animal. The filled squares and circles indicate transgene positive animals. NTC is the no template control, + is a positive control where the template is the pCCLK14 Turbo RFP or pCCLK14 Turbo RFP 14-3-3 γ shRNA^{mir} and – represents the negative control, which is

genomic DNA isolated from WT mice for the RFP PCR reactions and genomic DNA from HCT116 cells for the Ptch PCR reactions.

Sr. No.	Mother No.	Father No. (Pre-founder)	Mice No.	Gender	Ptch PCR	RFP PCR	RFP + shRNA Amir PCR	Litter No.
1	45/2254	44/2887	46/1190	F	+	+	-	I
2			46/1191	F	+	+	-	I
3			46/1192	F	+	+	-	I
4			46/1193	F	+	+	-	I
5			46/1194	F	+	+	-	I
6			46/1195	F	+	+	-	I
7			46/1196	M	+	+	-	I
8			46/1197	M	+	+	-	I
9			46/1198	M	+	+	-	I
10	45/2253	44/2887	46/1199	F	+	+	-	I
11			46/1200	F	+	+	-	I
12			46/1201	F	+	+	-	I

13			46/1202	F	+	+	-	I
14			46/1203	M	+	+	-	I
15			46/1204	M	+	+	-	I
16			46/1205	M	+	+	-	I
17	45/2256	44/2888	46/1731	F	+	+	-	I
18			46/1732	F	+	+	-	I
19			46/1733	F	+	+	-	I
20			46/1734	F	+	+	-	I
21			46/1735	M	+	+	-	I
22			46/1736	M	+	+	-	I
23			46/1737	M	+	+	-	I
24			46/1738	M	+	+	-	I
25			46/1739	M	+	+	-	I
26	46/1711	44/2888	47/930	F	+	+	-	I
27			47/931	F	+	+	-	I
28			47/932	F	+	+	-	I

29			47/933	M	+	+	-	I
30			47/934	M	+	+	-	I
31			47/935	M	+	+	-	I
32	46/1712	44/2888	47/2376	F	+	+	-	I
33			47/2377	M	+	+	-	I
34			47/2378	M	+	+	-	I

Table 4.9: Pups obtained from pCCLK14 Turbo RFP vector pre-founder mice (F1 generation) [Strain: Crl:CFW(SW)]. (+ is positive and – is negative)

Sr. No.	Mother No.	Father No.(Pre- founder)	Mice No.	Gender	Ptch PCR	RFP PCR	RFP + shRNAmir PCR	Litter No.
1	45/2258	44/2889	46/1206	F	+	+	-	I
2			46/1207	F	+	+	-	I
3			46/1208	F	+	+	-	I
4			46/1209	M	+	+	-	I
5			46/1210	M	+	+	-	I

6			46/1211	M	+	+	-	I
7			46/1212	M	+	+	-	I
8			46/1213	M	+	+	-	I
9			46/1214	M	+	+	-	I
10			46/1215	M	+	+	-	I
11	45/2259	44/2890	46/1216	F	+	+	-	I
12			46/1217	F	+	+	-	I
13			46/1218	F	+	+	-	I
14			46/1219	F	+	+	-	I
15			46/1220	M	+	+	-	I
16			46/1221	M	+	+	-	I
17			46/1222	M	+	+	-	I
18			46/1223	M	+	+	-	I
19	45/2260	44/2890	46/1224	F	+	+	-	I
20			46/1225	F	+	+	-	I
21			46/1226	F	+	+	-	I

22			46/1227	F	+	+	-	I
23			46/1228	F	+	+	-	I
24			46/1229	M	+	+	-	I
25			46/1230	M	+	+	-	I
26			46/1231	M	+	+	-	I
27			46/1232	M	+	+	-	I
28			46/1233	M	+	+	-	I
29			46/1234	M	+	+	-	I
30	46/1715	44/2890	47/927	F	+	+	-	I
31			47/928	F	+	+	-	I
32			47/929	M	+	+	-	I
33	46/1715	44/2890	48/29	F	+	+	-	II
34			48/30	F	+	+	-	II
35			48/31	F	+	+	-	II
36			48/32	M	+	+	-	II
37			48/33	M	+	+	-	II

38			48/34	M	+	+	-	II
39	48/2937	44/2889	49/2529	F	+	+	-	I
40			49/2530	F	+	+	-	I
41			49/2531	M	+	+	-	I
42			49/2532	M	+	+	-	I

Table 4.10: Pups obtained from pCCLK14 Turbo RFP 14-3-3 γ shRNAmir pre-founder mice (F1 generation) [Strain: Crl:CFW(SW)]. (+ is positive and – is negative)

4.2.3 PCR amplification of the 14-3-3 γ shRNAmir from the genomic DNA of the testis of pCCLK14 Turbo RFP 14-3-3 γ shRNAmir pre-founder mice

As mentioned above all the mice were positive for the Turbo RFP PCR, to confirm that the PCR product is indeed Turbo RFP, the Turbo RFP PCR product from the 46/1196 (pCCLK14 Turbo RFP) and 46/1221 (pCCLK14 Turbo RFP + 14-3-3 γ shRNAmir) was cloned into TA vector, the clones obtained were screened using BamHI and KpnI digest, positive clones were given for sequencing and the sequence of the clones matched completely with the Turbo RFP sequence (Figure 4.11 A and B).

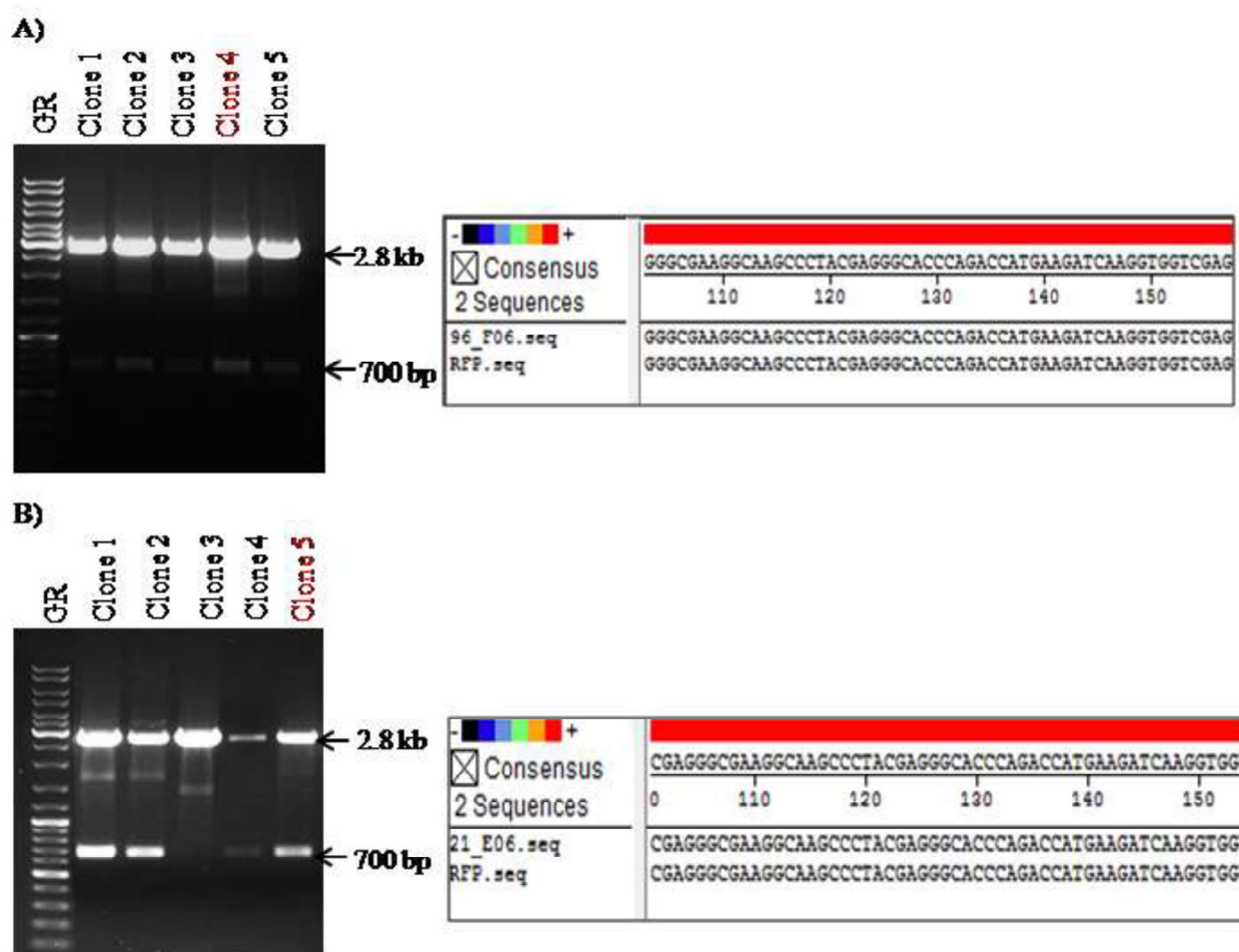


Figure 4.11: PCR amplification of Turbo RFP from transgenic mice and its sequencing. A- B. PCR product of Turbo RFP obtained from the genomic DNA of mice 46/1196 (upper panel) and 46/1221 (lower panel) were cloned into TA vector and the clones were screened using BamHI-KpnI digest. The clones were resolved using 1% agarose gel. Two bands were seen in all the clones; a 2.8 kb band corresponding to the size of TA vector and a 700 bp band corresponding to the size of the PCR product. Clone 4 for 46/1196 (pCCLK14 Turbo RFP) and clone 5 for 46/1221 (pCCLK14 Turbo RFP + 14-3-3 γ shRNA_{mir}) were given for sequencing (highlighted in red). The sequence of the clones matched to the Turbo RFP sequence using MegAlign software. Note that the two sequences showed an exact match to the Turbo RFP.

For the Turbo RFP + 14-3-3 γ shRNAmir PCR all the mice gave the PCR product of smaller size when compared to the positive control (pCCLK14 Turbo RFP 14-3-3 γ shRNAmir vector) (Figure 4.10 A and B). To understand this discrepancy PCR product from 46/1221 (pCCLK14 Turbo RFP + 14-3-3 γ shRNAmir) was cloned into TA vector and as a negative control PCR product from the 46/1736 (pCCLK14 Turbo RFP) was used. The TA clones containing PCR products were screened using BamHI and KpnI digest, positive clones were given for sequencing and the sequence of the TA clones of 46/1221 and 46/1736 was aligned with the 14-3-3 γ shRNAmir sequence but the sequence of the clones did not match with the 14-3-3 γ shRNAmir sequence (Figure 4.12 A and B) suggesting that either the 14-3-3 γ shRNAmir is absent in the pre-founder mice itself or 14-3-3 γ shRNAmir is not inherited by the pups from the pre-founder mice.

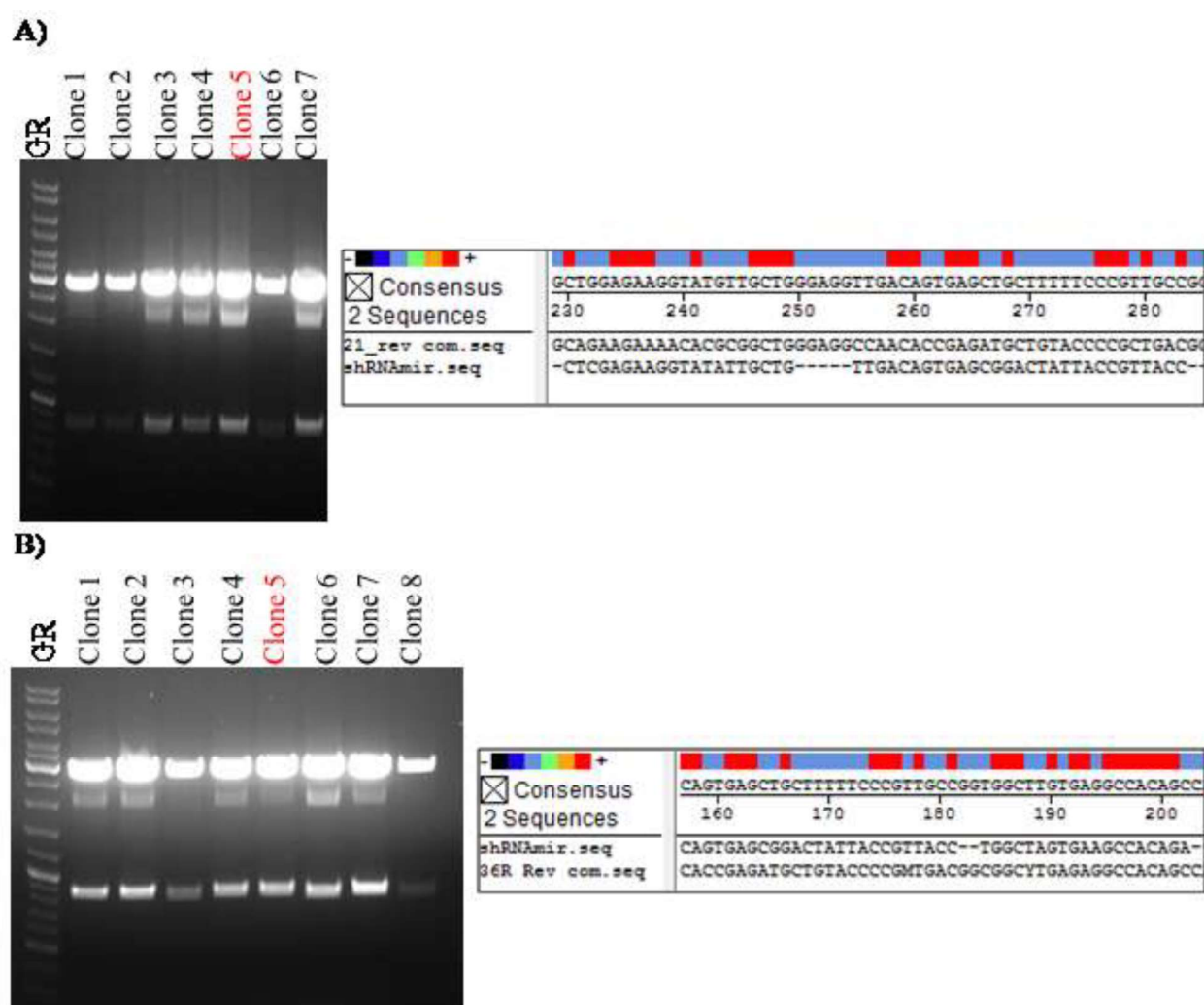


Figure 4.12: PCR amplification of Turbo RFP 14-3-3 γ shRNAmir from transgenic mice and its sequencing. A-B. PCR product of Turbo RFP 14-3-3 γ shRNAmir obtained from the genomic DNA of mice 46/1221 (upper panel) and 46/1736 (lower panel) were cloned into TA vector and the clones were screened using BamHI-KpnI digest. The clones were resolved using 1% agarose gel. Two bands were seen in all the clones; a 2.8 kb band corresponding to the size of TA vector and a 900 bp band corresponding to the size of the PCR product. Clone 5 for 46/1221(pCCLK14 Turbo RFP + 14-3-3 γ shRNAmir) and clone 5 for 46/1736 (pCCLK14 Turbo RFP) were given for sequencing (highlighted in red). The sequence of the clones was aligned to

the 14-3-3 γ shRNAmir sequence using MegAlign software. Note that the sequences of both the clones did not match with the 14-3-3 γ shRNAmir sequence.

To identify whether the pCCLK14 Turbo RFP 14-3-3 γ shRNAmir viruses injected pre-founder mice contain the 14-3-3 γ shRNAmir, pre-founder mice was sacrificed (after 2 years of surgery) to collect the testes. The genomic DNA was isolated from the testis was used as a template to PCR amplify Turbo RFP 14-3-3 γ shRNAmir. The size of the PCR product amplified from the genomic DNA of the testis of pCCLK14 Turbo RFP 14-3-3 γ shRNAmir virus injected pre-founder mice (44/2890) was same as that of the positive control, pCCLK14 Turbo RFP 14-3-3 γ shRNAmir plasmid (Figure 4.13 A). The PCR products were cloned into the TA vector and the TA clones were screened using BamHI-KpnI digest (Figure 4.13 B). A positive clone was sequenced and the sequence matched the Turbo RFP and 14-3-3 γ shRNAmir sequence (Figure 4.13 C and D). These results suggested that the 14-3-3 γ shRNAmir was present in the pre-founder mice but 14-3-3 γ shRNAmir was not inherited by the pups of the pre-founder mice.

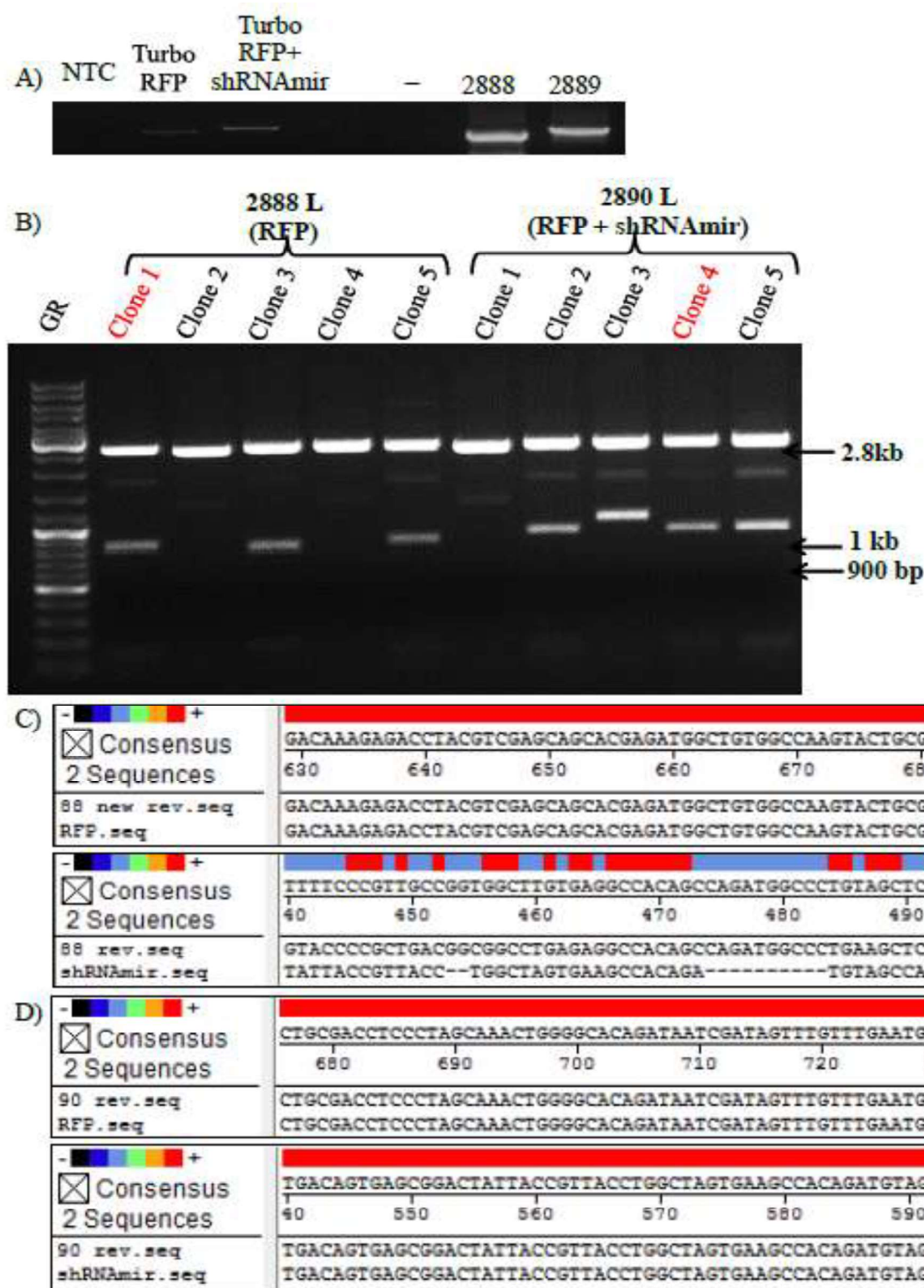


Figure 4.13: PCR amplification of Turbo RFP 14-3-3 γ shRNAmir from the testis of pre-founder mice and its sequencing. A. Turbo RFP 14-3-3 γ shRNAmir PCR amplified from the

genomic DNA obtained from the testis of mice 44/2888 (pCCLK14 Turbo RFP) and 44/2890 (pCCLK14 Turbo RFP 14-3-3 γ shRNAmir). As a positive control pCCLK14 Turbo RFP plasmid and pCCLK14 Turbo RFP 14-3-3 γ shRNAmir plasmid was used, NTC was no template control and – is negative control which was genomic DNA from wild type mouse. Note the difference between the size of the PCR product obtained from pCCLK14 Turbo RFP and pCCLK14 Turbo RFP 14-3-3 γ shRNAmir plasmids and between 44/2888 and 44/2890. The PCR product shown here for 44/2888 and 44/2890 is a re-amplified PCR product because the intensity of the original PCR product was less. **B.** The PCR products were cloned into TA vector and the clones were screened using BamHI-KpnI digest. The clones were resolved using 1% agarose gel. Two bands were seen in all the clones; a 2.8 kb band corresponding to the size of TA vector and a 900 bp band corresponding to the size of the PCR product. Clone 5 for 46/1221(pCCLK14 Turbo RFP + 14-3-3 γ shRNAmir) and clone 5 for 46/1736 (pCCLK14 Turbo RFP) were given for sequencing (highlighted in red). **C.** The sequence of the TA clone obtained from 44/2888 was aligned to the Turbo RFP sequence (upper panel) and 14-3-3 γ shRNAmir sequence (lower panel) using MegAlign software. Note that the sequence matched with the Turbo RFP sequence but did not match with the 14-3-3 γ shRNAmir sequence. **D.** The sequence of the TA clone obtained from 44/2890 was aligned to the Turbo RFP sequence (upper panel) and 14-3-3 γ shRNAmir sequence (lower panel) using MegAlign software. Note that the sequence matched with both Turbo RFP sequence and the 14-3-3 γ shRNAmir sequence.

The pCCLK14 Turbo RFP viruses and pCCLK14 Turbo RFP 14-3-3 γ shRNAmir viruses were again injected in the testes of 4 week old mice to obtain epidermis specific 14-3-3 γ knockdown mice but all the mice pups obtained from these pre-founder mice were negative for the Turbo RFP transgene (Table 4.11 and 4.12).

Sr. No.	Mother No.	Father No. (Pre- founder)	Mice No.	Gender	Ptch PCR	RFP PCR	RFP + shRNAmir PCR	Litter No.
1	I/2912	I/589	J/1549	F	+	-	-	I
2			J/1550	F	+	-	-	I
3			J/1551	F	+	-	-	I
4			J/1552	F	+	-	-	I
5			J/1553	M	+	-	-	I
6			J/1554	M	+	-	-	I
7			J/1555	M	+	-	-	I
8			J/1556	M	+	-	-	I
9			J/1557	M	+	-	-	I
10	I/2914	I/591	J/1564	F	+	-	-	I
11			J/1565	M	+	-	-	I
12			J/1566	M	+	-	-	I
13			J/1567	M	+	-	-	I
14			J/1568	M	+	-	-	I

15			J/1569	M	+	-	-	I
16	I/2913	I/590	J/1890	F	+	-	-	I
17			J/1891	F	+	-	-	I
18			J/1892	F	+	-	-	I
19			J/1893	F	+	-	-	I
20			J/1894	F	+	-	-	I
21			J/1895	M	+	-	-	I
22			J/1896	M	+	-	-	I
23			J/1897	M	+	-	-	I
24	I/2914	I/591	K/643	F	+	-	-	II
25			K/644	F	+	-	-	II
26			K/645	F	+	-	-	II
27			K/646	F	+	-	-	II
28			K/647	F	+	-	-	II
29			K/648	M	+	-	-	II
30			K/649	M	+	-	-	II

31			K/650	M	+	-	-	II
32			K/651	M	+	-	-	II
33	I/2913	I/590	K/1829	F	+	-	-	II
34			K/1830	F	+	-	-	II
35			K/1831	F	+	-	-	II
36			K/1832	F	+	-	-	II
37			K/1833	F	+	-	-	II
38			K/1834	M	+	-	-	II
39			K/1835	M	+	-	-	II
40			K/1836	M	+	-	-	II
41			K/1837	M	+	-	-	II
42			K/1838	M	+	-	-	II
43			K/1839	M	+	-	-	II

Table 4.11: Pups obtained from pCCLK14 Turbo RFP pre-founder mice (F1 generation)

[Strain: Crl:CFW(SW)]. (+ is positive and – is negative)

Sr. No.	Mother No.	Father No.(Pre- founder)	Mice No.	Gender	Ptch PCR	RFP PCR	RFP + shRNAmir PCR	Litter No.
1	E/742	D/1537	E/2261	F	+	-	-	I
2			E/2262	F	+	-	-	I
3			E/2263	F	+	-	-	I
4			E/2264	F	+	-	-	I
5			E/2265	F	+	-	-	I
6			E/2266	F	+	-	-	I
7			E/2267	F	+	-	-	I
8			E/2268	M	+	-	-	I
9			E/2269	M	+	-	-	I
10			E/2270	M	+	-	-	I
11			E/2271	M	+	-	-	I
12	E/744	D/1535	E/2253	F	+	-	-	I
13			E/2254	F	+	-	-	I
14			E/2255	F	+	-	-	I

15			E/2256	F	+	-	-	I
16			E/2257	M	+	-	-	I
17			E/2258	M	+	-	-	I
18			E/2259	M	+	-	-	I
19			E/2260	M	+	-	-	I
20	E/744	D/1535	G/2114	F	+	-	-	II
21			G/2115	F	+	-	-	II
22			G/2116	F	+	-	-	II
23			G/2117	F	+	-	-	II
24			G/2118	M	+	-	-	II
25			G/2119	M	+	-	-	II
26			G/2120	M	+	-	-	I
27	D/2740	D/1531	G/2160	F	+	-	-	I
28			G/2161	F	+	-	-	I
29			G/2162	M	+	-	-	I
30			G/2163	M	+	-	-	I

31			G/2164	M	+	-	-	I
32			G/2165	M	+	-	-	I
33			G/2166	M	+	-	-	I
34			G/2167	M	+	-	-	I
35			G/2168	M	+	-	-	I
36			G/2169	M	+	-	-	I
37	D/2742	D/1536	G/2585	F	+	-	-	I
38			G/2586	F	+	-	-	I
39			G/2587	F	+	-	-	I
40			G/2588	F	+	-	-	I
41			G/2589	F	+	-	-	I
42			G/2590	M	+	-	-	I
43			G/2591	M	+	-	-	I

Table 4.12: Pups obtained from pCCLK14 Turbo RFP 14-3-3 γ shRNAmir pre-founder mice (F1 generation) [Strain: Crl:CFW(SW)]. (+ is positive and – is negative)

To understand why these Turbo RFP 14-3-3 γ shRNAmir pre-founder mice sired only transgene negative pups some of these pre-founder mice such as D/1535 and D/1537 were sacrificed (8 months post-surgery) and testes were collected to isolate the genomic DNA. Turbo RFP 14-3-3 γ

shRNAmir fragment was amplified from the genomic DNA, PCR product was cloned into TA vector and the positive clone was sequenced. The sequence of the TA clone matched with the Turbo RFP and 14-3-3 γ shRNAmir sequence (Figure 4.14). This suggests that even though the pre-founder mice sired transgene negative pups the transgene was stably integrated in the cells of the testis of the pre-founder mice.

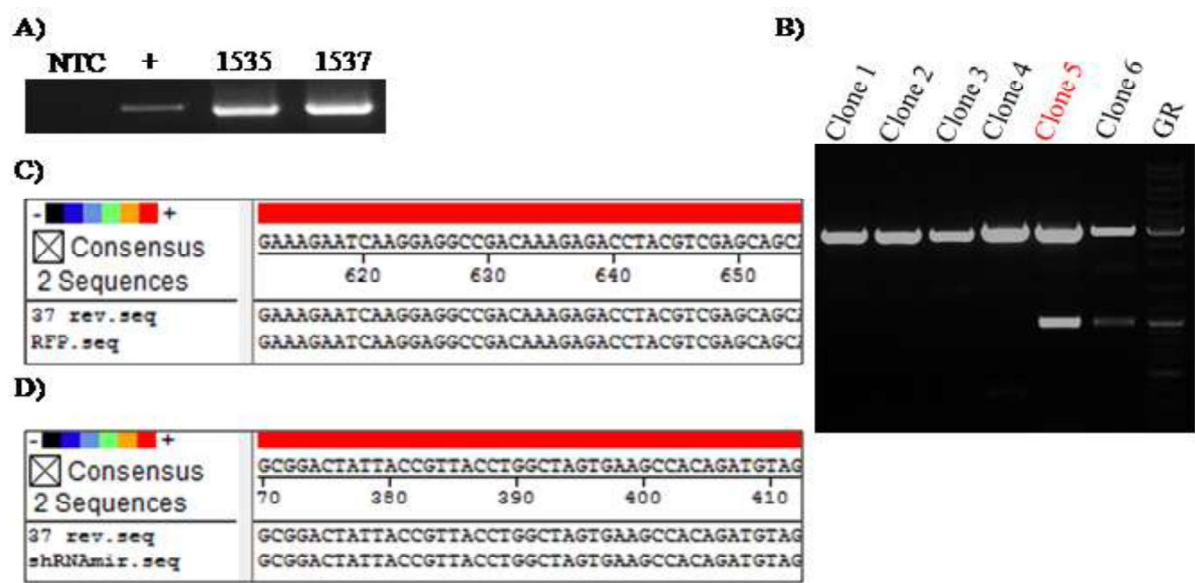


Figure 4.14: PCR amplification of Turbo RFP 14-3-3 γ shRNAmir from the testis of D/1537 and its sequencing. **A.** Turbo RFP 14-3-3 γ shRNAmir PCR amplified from the genomic DNA obtained from the testis of mice D/1535 and D/1537 (pCCLK14Turbo RFP 14-3-3 γ shRNAmir). As a positive control pCCLK14 Turbo RFP 14-3-3 γ shRNAmir plasmid was used, NTC was no template control. The PCR product shown here for D/1535 and D/1537 is a re-amplified PCR product because the intensity of the original PCR product was less. **B.** The PCR product of D/1537 was cloned into TA vector and the clones were screened using BamHI-KpnI digest. The clones were resolved using 1% agarose gel. Two bands were seen in the positive clones (5 and 6); a 2.8 kb band corresponding to the size of TA vector and a 900 bp band corresponding to the

size of the PCR product. Clone 5 was given for sequencing (highlighted in red). **C-D.** The sequence of the TA clone obtained from D/1535 was aligned to the Turbo RFP sequence (upper panel) and 14-3-3 γ shRNAmir sequence (lower panel) using MegAlign software. Note that the sequence matched with the Turbo RFP sequence as well as the 14-3-3 γ shRNAmir sequence.

4.2.4 Stable inheritance of pCCLK14 Turbo RFP from one generation to next generation

To observe if the transgene is stably integrated into the germ line and is being inherited by the next generation, the pCCLK14 Turbo RFP transgene positive pups (F1 generation) were weaned and inbred to obtain F2 generation. All the pups from F2 generations were found to be positive for the Turbo RFP transgene as shown in Figure 4.15. The gender, number and genotype of the pups from F2 generation is shown in Table 4.13.

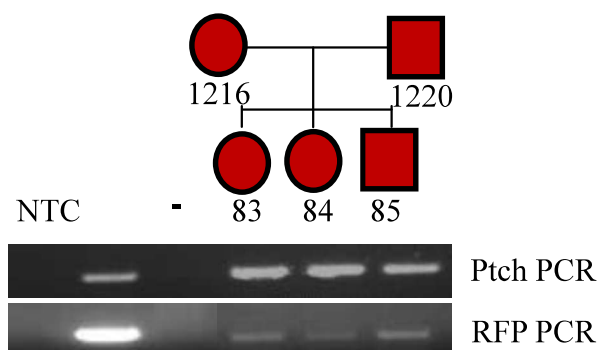


Figure 4.15: Pedigree analysis of F2 generation obtained from inbreeding of Turbo RFP positive F1 generation mice [Strain: Crl:CFW(SW)]. A pedigree analysis for F2 generation mice obtained from inbreeding of Turbo RFP positive F1 generation mice. Individual mice were assigned numbers for further experiments. Genomic DNA amplification using primers for Turbo RFP (RFP) or Patched (Ptch) as a loading control are shown for each animal. The filled squares and circles indicate transgene positive animals. NTC is the no template control , + is a positive

control where the template is the pCCLK14 Turbo RFP plasmid and – represents the negative control, which is genomic DNA isolated from WT mice for the RFP PCR reactions and genomic DNA from HCT116 cells for the Ptch PCR reactions.

Sr. No.	Mother No.	Father No.	Mice No.	Gender	Ptch PCR	RFP PCR	RFP + shRNA mir PCR	Litter No.
1	46/1216	46/1220	D/82	F	+	+	-	I
2			D/83	F	+	+	-	I
3			D/84	M	+	+	-	I

Table 4.13: Pups obtained from inbreeding of Turbo RFP positive mice (Inbreeding of F1 generation) [Strain: Crl:CFW(SW)]. (+ is positive and – is negative)

4.2.5 Stable expression of Turbo RFP in the epidermis of the Turbo RFP positive mice

To determine whether Turbo RFP was expressed in the Turbo RFP positive animals of F1 and F2 generation, tail snips were prepared by separating the epidermis from the muscle and cartilage and the epidermis was examined by confocal microscopy. As shown in Figure 4.16, mice containing the Turbo RFP transgene showed red fluorescence in the bulb region of hair follicle, the root sheath of the hair follicle and the sebaceous glands. The arrangement of hair follicles correlated with that given in literature [220]. The pattern of Turbo RFP expression was similar to that reported for keratin14 [204, 221] suggesting tissue specific transgene expression was

achieved. Further, expression of Turbo RFP was observed in first generation mice (46/1230) as well as second generation mice (D/83), suggesting that the inheritance of the transgene was stable and that expression was maintained over both the generations. The intensity of the Turbo RFP fluorescence is more in second generation when compared to the first generation. Some auto fluorescence was observed in the hair shaft of WT mice, however, this does not overlap with the regions in which keratin 14 is expressed [204, 221]. These results suggest that the transgenic mice expressed Turbo RFP specifically in the epidermis.

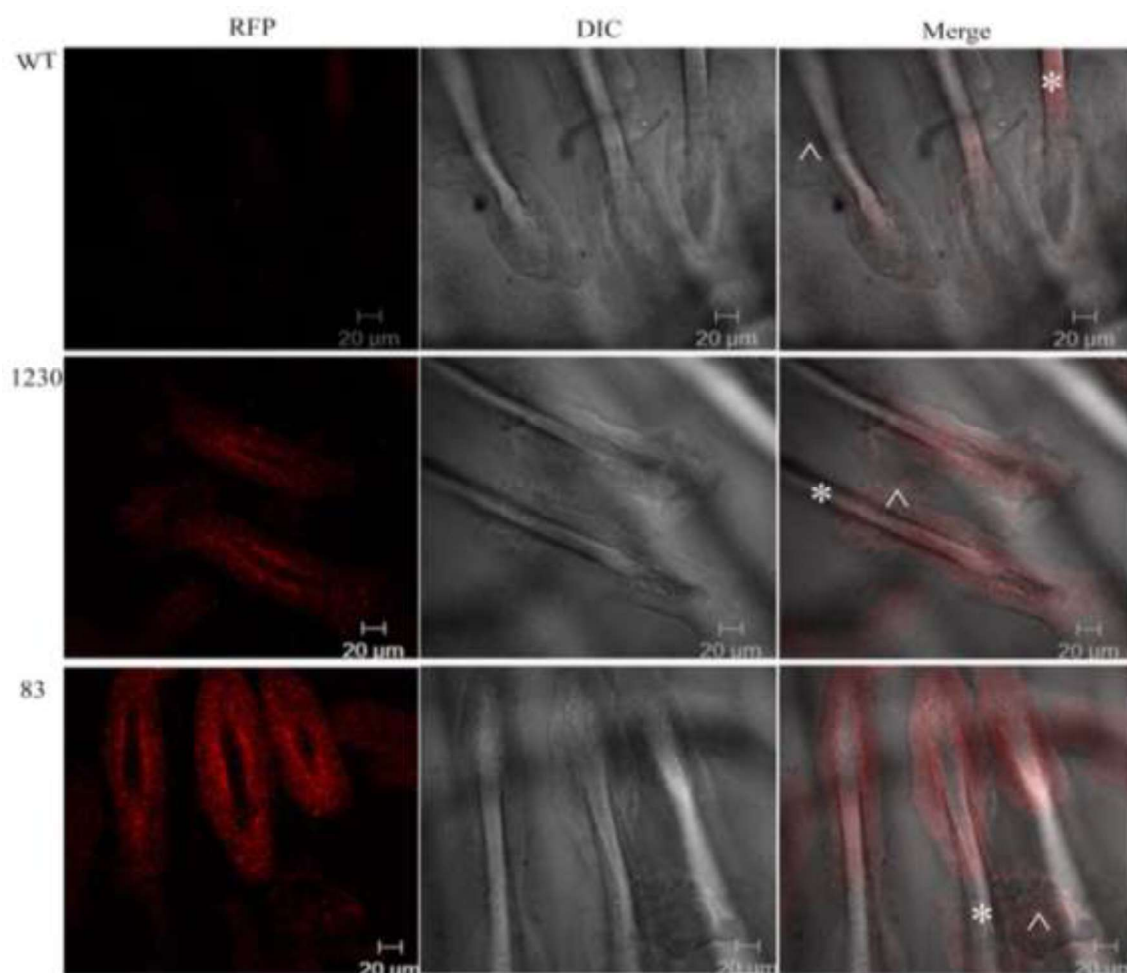


Figure 4.16: Turbo RFP expression in the epidermis of Turbo RFP positive mice. Turbo RFP was expressed in tissues that normally express keratin 14. Epidermis whole mounts from

wild type (WT) or transgenic animals (1230 and 83) were examined by fluorescence microscopy (left panel). A DIC image (middle panel) and a merged image (right panel) are also shown. Note that the turbo RFP fluorescence is more intense in the second generation. Note that the fluorescence in the transgenic animals is observed in the hair follicle and sebaceous glands as previously reported for keratin 14. * indicates Hair Shaft, ^ indicates Sebaceous glands [222].

4.2.6 Generation of epidermis specific 14-3-3 γ knockdown mice using electroporation

pCCLK14 Turbo RFP and pCCLK14 Turbo RFP 14-3-3 γ shRNAmir was digested with PvuI and NdeI to obtain the fragment containing K14 promoter-Turbo RFP-WPRE and K14 promoter-Turbo RFP 14-3-3 γ shRNAmir –WPRE respectively. These fragments were electroporated into the testes of FVB mice to obtain the pro-founder mice as described in [48]. The electroporation was done in Dr. Subeer Majumdar's Laboratory NII. The electroporated mice were imported to ACTREC animal house and then used for further experiments. The K14 Turbo RFP 14-3-3 γ shRNAmir pro-founder mice were mated with wild type FVB mice to obtain pups. One of the pro-founder mice (H/1935) was found to be sterile as it did not sire pups even after mating with multiple fertile female mice. The pups obtained from the remaining pro-founder mouse (H/1936) were genotyped for Turbo RFP and it was found that all the pups were negative for the transgene (Figure 4.17). The gender, number and genotype of the pups obtained from the K14 Turbo RFP 14-3-3 γ shRNAmir is shown in Table 4.14.

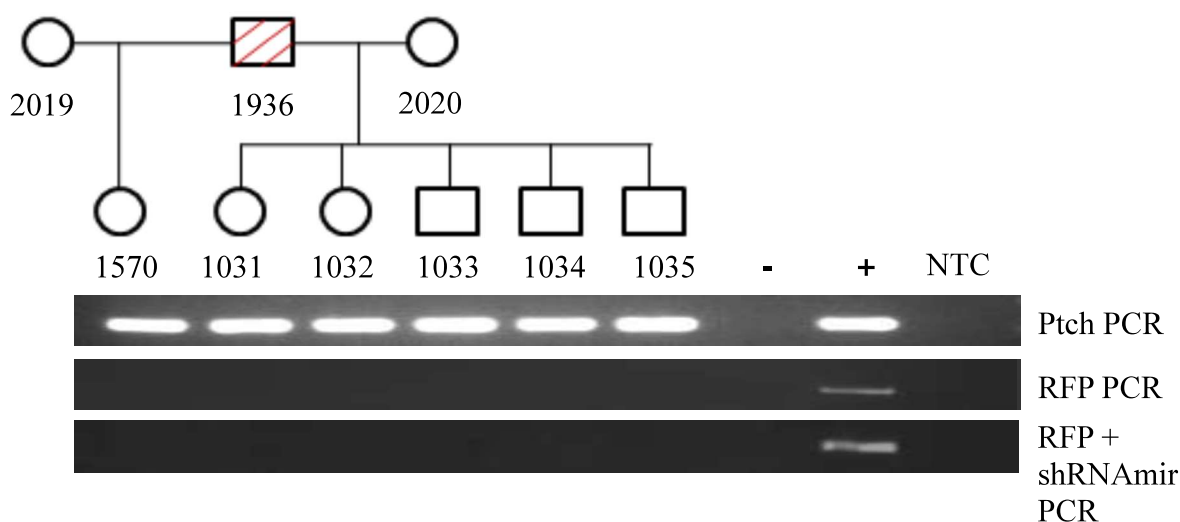


Figure 4.17: Pedigree analysis of pups obtained from the K14 Turbo RFP 14-3-3 γ shRNAmir pro-founder mouse [Strain: FVB]. A pedigree analysis of pups obtained from the K14 Turbo RFP 14-3-3 γ shRNAmir pro-founder mouse. Individual mice were assigned numbers for further experiments. Genomic DNA amplification using primers for Turbo RFP (RFP) or Patched (Ptch) as a loading control are shown for each animal. The empty squares and circles indicate transgene negative animals. NTC is the no template control , + is a positive control where the template is the pCCLK14 Turbo RFP plasmid and – represents the negative control, which is genomic DNA isolated from WT mice for the RFP PCR reactions and genomic DNA from HCT116 cells for the Ptch PCR reactions.

Sr. No.	Mother No.	Father No. (pro-founder)	Mice No.	Gender	Ptch PCR	RFP PCR	RFP + shRNAmir PCR	Litter No.
1	H/2020	H/1936	J/1031	F	+	-	-	I

2			J/1032	F	+	-	-	I
3			J/1033	M	+	-	-	I
4			J/1034	M	+	-	-	I
5			J/1035	M	+	-	-	I
6	H/2019	H/1936	J/1570	F	+	-	-	I
7	H/2019	H/1936	K/638	F	+	-	-	II
8			K/639	F	+	-	-	II
9			K/640	F	+	-	-	II
10			K/641	F	+	-	-	II
11			K/642	M	+	-	-	II
12	J/1570	H/1936	K/660	F	+	-	-	I
13			K/661	F	+	-	-	I
14			K/662	M	+	-	-	I
15			K/663	M	+	-	-	I
16			K/664	M	+	-	-	I
17			K/665	M	+	-	-	I

18	H/2019	H/1936	K/666	F	+	-	-	III
19			K/667	M	+	-	-	III
20			K/668	M	+	-	-	III
21			K/669	M	+	-	-	III

Table 4.14: Pups obtained from the K14 Turbo RFP14-3-3 γ shRNAmir pro-founder mouse [Strain: FVB]. (+ is positive and – is negative)

4.2.7 Generation of epidermis specific 14-3-3 γ knockout mice

To generate an epidermis specific knockout of 14-3-3 γ , we attempted to generate a knockout using a tissue specific CRISPR/Cas system [223]. A gRNA targeting 14-3-3 γ was cloned into pLentiCRISPR Cas V1 using BsmBI sites. To test the efficiency of 14-3-3 γ gRNA pLentiCRISPR Cas V1 and pLentiCRISPR Cas V1 14-3-3 γ gRNA were packaged using ViraPower; NIH3T3 cells were transduced by pLentiCRISPR Cas V1 and pLentiCRISPR Cas V1 14-3-3 γ gRNA viruses and selected in puromycin. Puromycin resistant cells were harvested and Western blots for 14-3-3 γ and β Actin was done. pLentiCRISPR Cas V1 14-3-3 γ gRNA transduced cells expressed reduced levels of 14-3-3 γ (Figure 4.18A). The exon 1 region of 14-3-3 γ was PCR amplified from the pLentiCRISPR Cas V1 14-3-3 γ gRNA transduced cells (Figure 4.18 B) and cloned into TA vector. The TA clones were given for sequencing and it was found that the exon1 region of the pLentiCRISPR Cas V1 14-3-3 γ gRNA transduced cells had a

transversion and a frame shift mutation which resulted into a nonsense mutation thereby expressing a truncated 14-3-3 γ protein (1-26 amino acid) which may not be stable (Figure 4.18 D and E).

The EF1 α promoter of pLentiCRISPR Cas V1 and pLentiCRISPR Cas V1 14-3-3 γ gRNA which drives the Cas9 expression was replaced by the K14 promoter to drive the expression of Cas9 specifically in the basal layer of epidermis such that the knockout of 14-3-3 γ is achieved only in the epidermis. The pLentiCRISPR K14 Cas9 and pLentiCRISPR K14 Cas9 14-3-3 γ gRNA were packaged using ViraPower. Viruses were used to transduce NIH3T3 cells as previously published data suggests that the K14 promoter is active in NIH3T3 cells grown in culture, as previously published data suggests that the K14 promoter cloned from the pCCLK14 promoter is a minimal promoter and can be used for expressing cDNA in different cell lines [224], selected in puromycin for 15 days and after puromycin selection cell extracts were prepared. Cell extracts were resolved on 10% acrylamide gel and Western blot was done for 14-3-3 γ and β Actin. As shown in Figure 4.18 F, here was loss of 14-3-3 γ in the NIH3T3 cells transduced with pLentiCRISPR K14 Cas9 14-3-3 γ gRNA viruses.

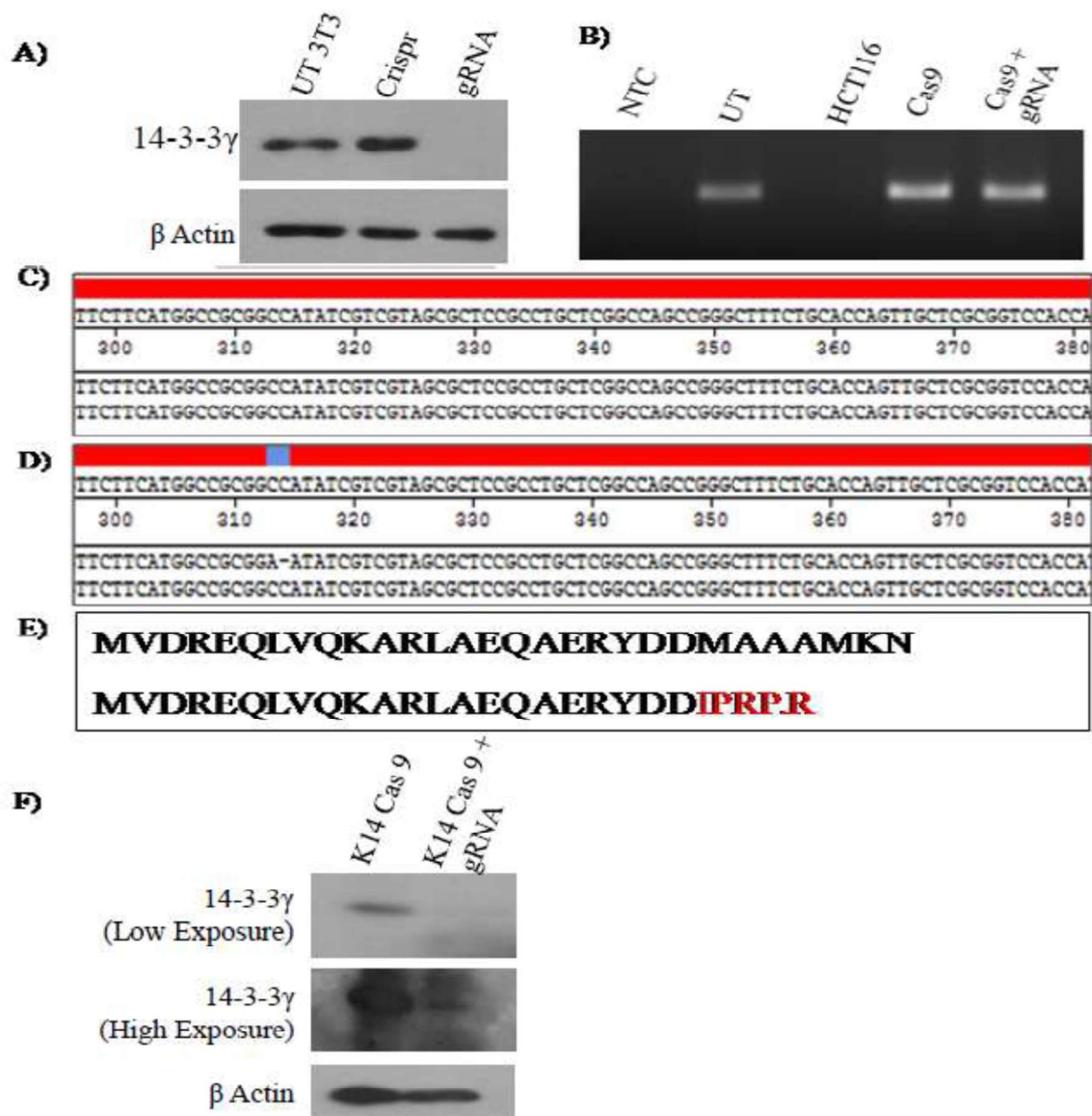


Figure 4.18: Validation of 14-3-3 γ gRNA. **A.** Protein extracts of NIH3T3 cells transduced with pLentiCRISPR Cas V1 viruses or pLentiCRISPR Cas V1 14-3-3 γ gRNA viruses were resolved on 10% SDS-PAGE gel followed by Western blotting with the indicated antibodies. Protein extracts of un-transduced NIH3T3 served as a control. Western blots for β Actin served as a loading control. **B.** The 14-3-3 γ exon1 region flanked by 5' UTR and the intron 1 was PCR amplified from the genomic DNA of un-transduced NIH3T3 cells, pLentiCRISPR Cas V1 and pLentiCRISPR Cas V1 14-3-3 γ gRNA transduced NIH3T3 cells. The genomic DNA from the

HCT116 served as a negative control and NTC was no template control. **C.** The 14-3-3 γ exon 1 region amplified from the genomic DNA of pLentiCRISPR Cas V1 and pLentiCRISPR Cas V1 14-3-3 γ gRNA transduced NIH3T3 cells was cloned into TA vector and sequenced. The 14-3-3 γ exon 1 sequence obtained from pLentiCRISPR Cas V1 transduced NIH3T3 cells (top sequence) and the sequence of 14-3-3 γ exon 1 from NCBI (bottom sequence) was aligned using MegAlign software. Note there is a complete match between the two sequences. **D.** The 14-3-3 γ exon 1 sequence obtained from pLentiCRISPR Cas V1 14-3-3 γ gRNA transduced NIH3T3 cells (top sequence) and the sequence of 14-3-3 γ exon 1 from NCBI (bottom sequence) was aligned using MegAlign software. Note that there is a frame shift mutation in top strand as C at 314 position is deleted and a transversion mutation at the 313 position C is converted to A. **E.** The sequence of the exon 1 was translated using SeqBuilder software to identify the effect of transversion and frame shift mutation on the amino acid sequence. Top strand is the amino acid sequence for the WT 14-3-3 γ obtained from NCBI and the bottom strand is the amino acid sequence translated from the 14-3-3 γ exon 1 sequence of pLentiCRISPR Cas V1 14-3-3 γ gRNA transduced NIH3T3 cells. **F.** Protein extracts of NIH3T3 cells transduced with pLentiCRISPR K14 Cas9 viruses or pLentiCRISPR K14 Cas9 14-3-3 γ gRNA viruses were resolved on 10% SDS-PAGE gel followed by Western blotting with the indicated antibodies. Western blots for β Actin served as a loading control.

pLentiCRISPR K14 Cas9 viruses or pLentiCRISPR K14 Cas9 14-3-3 γ gRNA viruses were surgically injected into the testes of the 4 week old Swiss [CrI:CFW (SW)] mice and five weeks post-surgery these mice were mated with the wild type female mice to obtain transgene positive pups. The pups were screened for the presence of puromycin resistance cDNA using genomic DNA obtained from the tail snips of the pups. PCR for patched (Ptch) served as a loading

control. The pedigree analysis for the pups obtained from one of the pLentiCRISPR K14 Cas9 and pLentiCRISPR K14 Cas9 14-3-3 γ gRNA pre-founder mice along with the Ptch PCR and Turbo RFP PCR results are shown in Figure 4.19 A and B. The gender, number and genotype of the pups obtained from the K14 Turbo RFP 14-3-3 γ shRNAmir is shown in Table 4.15.

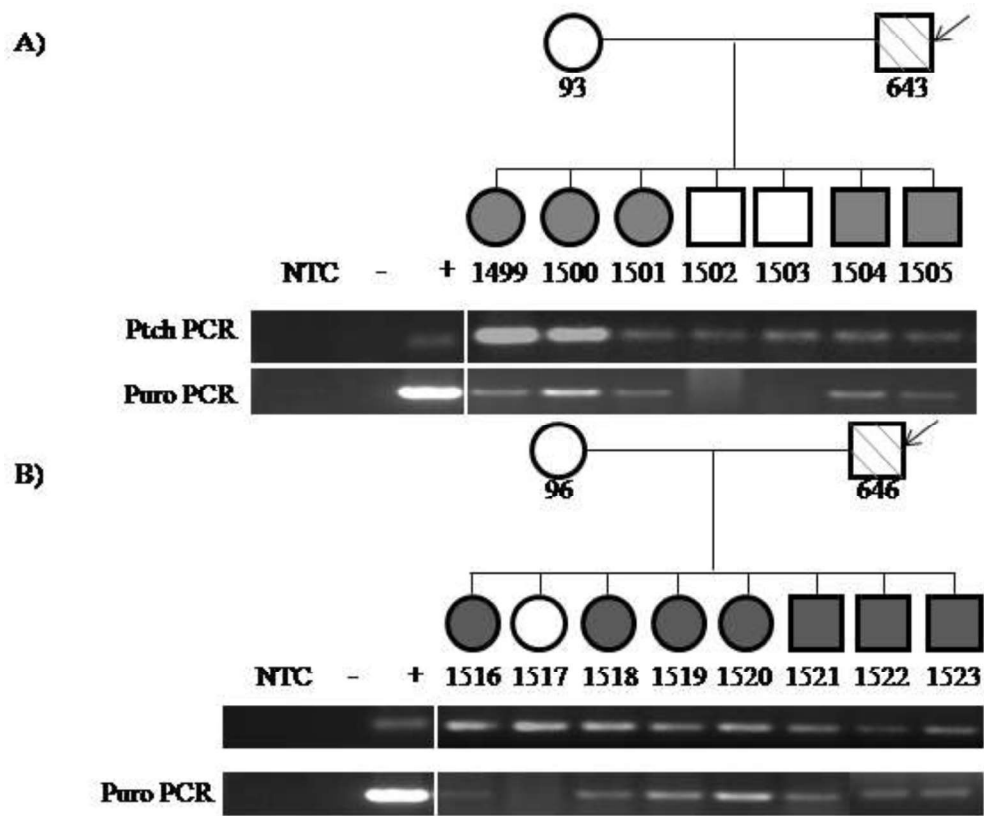


Figure 4.19: Pedigree analysis of the pLentiCRISPR K14 Cas9 and pLentiCRISPR K14 Cas9 14-3-3 γ gRNA pre-founder mice [Strain: Crl:CFW(SW)]. A-B. A pedigree analysis for the pre-founder mice (indicated with an arrow) 643 infected with viruses expressing the pLentiCRISPR K14 Cas9 (A) and 646 (B) infected with viruses expressing and pLentiCRISPR K14 Cas9 14-3-3 γ gRNA. Individual mice were assigned numbers for further experiments. Genomic DNA amplification using primers for puromycin resistance cDNA (Puro) or Patched (Ptch) as a loading control are shown for each animal. The filled squares and circles indicate

transgene positive animals. NTC is the no template control , + is a positive control where the template is the genomic DNA of the pLKO Tet Puro positive mice and – represents the negative control, which is genomic DNA isolated from WT mice for the puromycin resistance cDNA PCR reactions and genomic DNA from HCT116 cells for the Ptch PCR reactions.

Sr. No.	Mother No.	Father No. (Pre-founder)	Mice No.	Gender	Ptch PCR	Puro PCR	Litter No.
1	O/93	N/643	O/1499	F	+	+	I
2			O/1500	F	+	+	I
3			O/1501	F	+	+	I
4			O/1502	M	+	-	I
5			O/1503	M	+	-	I
6			O/1504	M	+	+	I
7			O/1505	M	+	+	I
8	O/94	N/644	O/1506	F	+	+	I
9			O/1507	F	+	+	I
10			O/1508	F	+	+	I
11			O/1509	F	+	-	I
12			O/1510	F	+	+	I
13			O/1511	M	+	+	I
14			O/1512	M	+	-	I
15			O/1513	M	+	-	I
16			O/1514	M	+	-	I

17	O/95	N/645	O/1515	F	+	-	I
18	O/95	N/645	O/2112	F	+	+	II
19			O/2113	F	+	+	II
20			O/2114	F	+	-	II
21			O/2115	F	+	+	II
22			O/2116	F	+	+	II
23			O/2117	F	+	+	II
24			O/2118	M	+	+	II
25			O/2119	M	+	+	II

Table 4.15: Pups obtained from the pLentiCRISPR K14 Cas9 pre-founder mice [Strain: Crl:CFW(SW)]. (+ is positive and – is negative)

Sr. No.	Mother No.	Father No. (Pre-founder)	Mice No.	Gender	Ptch PCR	Puro PCR	Litter No.
1	O/96	N/646	O/1516	F	+	+	I
2			O/1517	F	+	-	I
3			O/1518	F	+	+	I
4			O/1519	F	+	+	I
5			O/1520	F	+	+	I
6			O/1521	M	+	+	I
7			O/1522	M	+	+	I
8			O/1523	M	+	+	I

9	O/97	N/647	O/1524	F	+	-	I
10			O/1525	F	+	+	I
11			O/1526	F	+	+	I
12			O/1527	F	+	+	I
13			O/1528	F	+	-	I
14			O/1529	M	+	+	I
15			O/1530	M	+	+	I
16			O/1531	M	+	+	I
17	O/98	N/648	O/1532	F	+	+	I
18			O/1533	F	+	+	I
19			O/1534	F	+	-	I
20			O/1535	M	+	+	I
21			O/1536	M	+	+	I
22			O/1537	M	+	+	I
23			O/1538	M	+	-	I
24			O/1539	M	+	+	I

Table 4.16: Pups obtained from the pLentiCRISPR K14 Cas914-3-3 γ gRNA pre-founder mice [Strain: Crl:CFW(SW)]. (+ is positive and – is negative)

To identify the mice which expressed reduced levels of 14-3-3 γ in the epidermis, epidermis was isolated from the tail skin of the pLentiCRISPR K14 Cas9 14-3-3 γ gRNA positive pups and used for making protein extracts. To ensure that epidermis was properly separated from the dermis

cryosections of the epidermis were stained with hematoxylin and eosin and observed using the upright microscope (Figure 4.20A). Protein extracts of the epidermis were prepared in lysis buffer and were resolved on a 12% gel and the levels of 14-3-3 γ determined by Western blot analysis. Western blots for β Actin served as a loading control. The levels of the 14-3-3 γ were reduced in some of the pLentiCRISPR K14 Cas9 14-3-3 γ gRNA positive mice when compared to that of pLentiCRISPR K14 Cas9 mice.

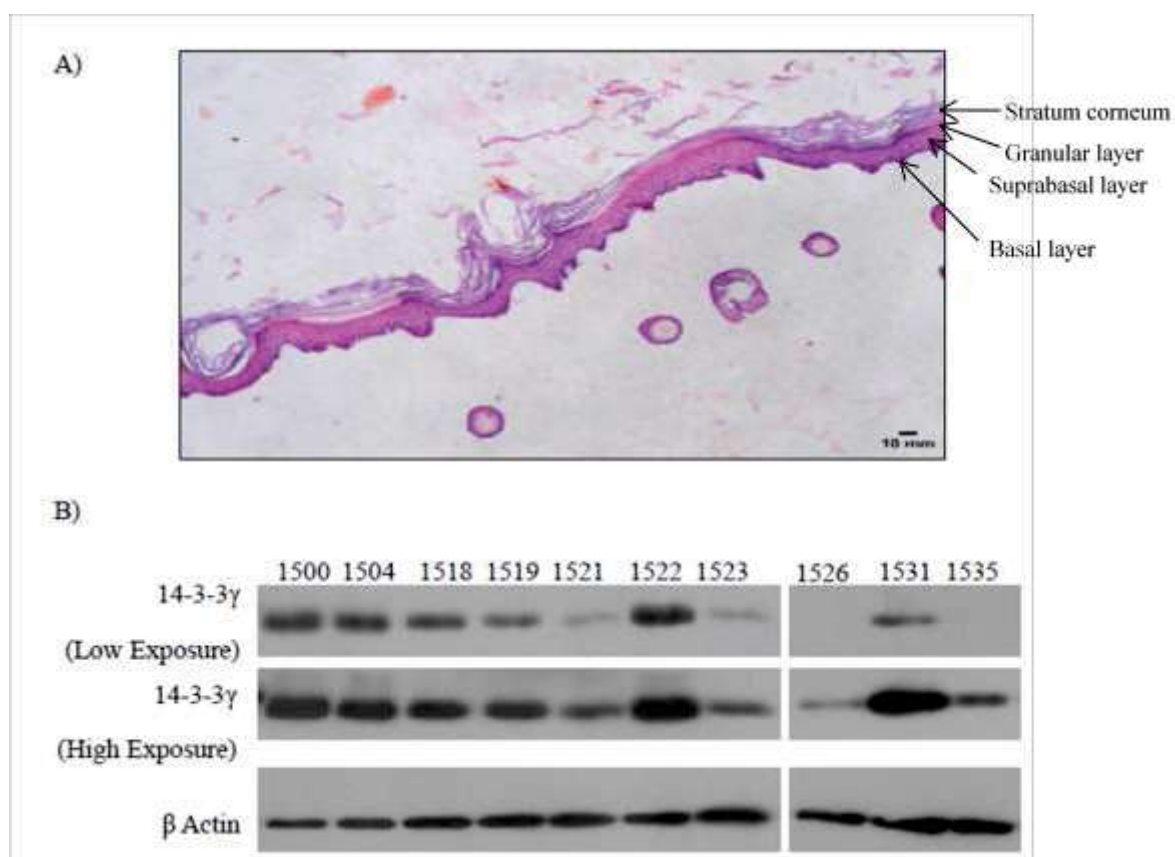


Figure 4.20: Levels of 14-3-3 γ in the epidermis of pLentiCRISPR K14 Cas9 14-3-3 γ gRNA positive mice. **A.** The hematoxylin and eosin stained cryosection of epidermis was imaged using Zeiss Axioimager Z1 upright microscope. The different layers of the epidermis can be observed in the image. **B.** Epidermis was separated from the tail snips of the transgene positive mice using EDTA. Epidermal extracts was made using total lysis buffer. Epidermal extracts were resolved

on to 12% acrylamide gel Western blots for 14-3-3 γ and β Actin were done. 1500 and 1504 are epidermal extracts of pLentiCRISPR K14 Cas9 positive mice and 1518, 1519, 1521, 1522, 1523, 1526, 1531 and 1535 are epidermal extracts of pLentiCRISPR K14 Cas9 14-3-3 γ gRNA mice.

To identify the pups with the mutation in 14-3-3 γ gene sequence, exon1 region was amplified from the genomic DNA isolated from the epidermis of the pLentiCRISPR K14 Cas9 positive mice (Control) and pLentiCRISPR K14 Cas9 14-3-3 γ gRNA positive mice (Test) which expressed reduced levels of 14-3-3 γ in the epidermis. The PCR product obtained from the control mice and the test mice was mixed in the 1:1 ratio followed by denaturation and renaturation, the renatured product was treated with T7 endonuclease enzyme to cleave the heteroduplex DNA. After the T7 endonuclease digestion, PCR products were resolved on 2% agarose gel to identify the pups with mutation in the exon 1 region of 14-3-3 γ . The result of the T7 endonuclease assay for some of the samples is shown in Figure 4.21. It was found that there was no change in the 14-3-3 γ exon1 sequence in any of the pLentiCRISPR K14 Cas9 14-3-3 γ gRNA positive mice. To confirm the results of T7 endonuclease assay 14-3-3 γ exon 1 PCR product was gel purified and sequenced. All the transgene positive animals were found to have wild type exon 1 sequence. Figure 4.21 C shows the sequence of the 14-3-3 γ exon 1 obtained from one of the pLentiCRISPR K14 Cas9 14-3-3 γ gRNA positive mice (O/1535) completely aligned with the wild type 14-3-3 γ exon 1 sequence.

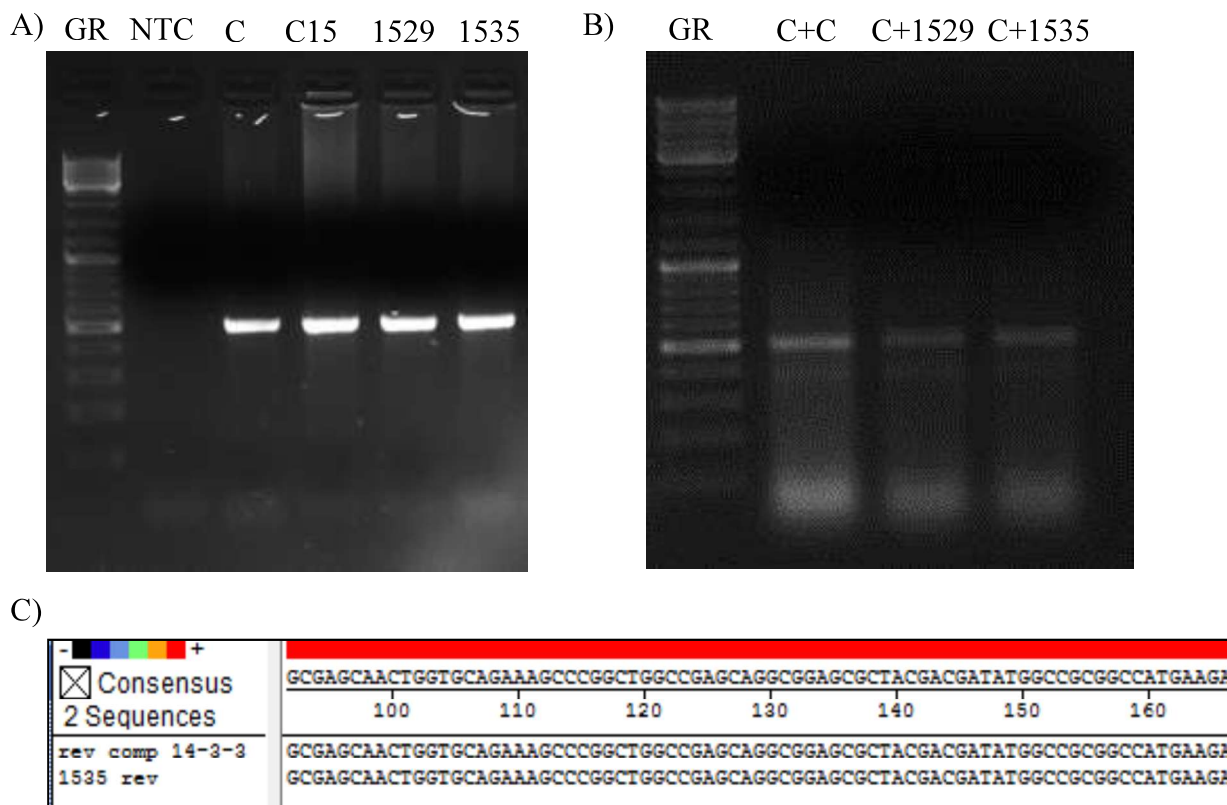


Figure 4.21: PCR amplification of 14-3-3 γ exon 1 sequence from the pLentiCRISPR K14 Cas9 14-3-3 γ gRNA positive pups. A. The 14-3-3 γ exon1 region flanked by 5' UTR and the intron 1 was PCR amplified from the genomic DNA isolated from the epidermis of pLentiCRISPR K14 Cas9 (C) and pLentiCRISPR K14 Cas9 14-3-3 γ gRNA positive transgenic mice. NTC was no template control. **B.** T7 endonuclease assay was done on the 14-3-3 γ exon1 region amplified from the genomic DNA isolated from the epidermis of pLentiCRISPR K14 Cas9 and pLentiCRISPR K14 Cas9 14-3-3 γ gRNA positive pups. Note that the size and the number of bands in all the test lanes were same as that of in the control + control lane. **C.** The 14-3-3 γ exon 1 PCR product amplified from the genomic DNA isolated from the epidermis of O/1535 was given for sequencing. The sequence obtained from O/1535 (bottom sequence) and the sequence of 14-3-3 γ exon 1 from NCBI (top sequence) was aligned using MegAlign software. Note that there is a complete match between the two sequences.

4.3. Discussion

14-3-3 γ plays an important role in different pathways like cell cycle regulation, centrosome duplication, apoptosis, ion channel transport, neuronal migration, desmosome formation, translation and splicing. To understand the function of 14-3-3 γ in the growth and development of mammals we tried to generate an inducible 14-3-3 γ knockdown mice using pLKO Tet Puro system. This is the first report in which pLKO Tet Puro system was used to generate transgenic mice and therefore nothing is known about how the pLKO Tet Puro system functions *in vivo*.

pLKO Tet Puro lentiviral system was utilized for virus mediated transgenesis and it was observed that the efficiency of obtaining transgenic animal using this system was 100% in both the BALB/c strain and in the Crl:CFW(SW) strain of mice. However, the puromycin resistance cDNA positive pups obtained from the pLKO Tet Puro pre-founder mice and pLKO Tet Puro 14-3-3 γ shRNA pre-founder mice (strain: BALB/c) did not show any difference in the mRNA levels of 14-3-3 γ even after 6 weeks of doxycycline treatment suggesting that the pLKO Tet Puro system was silenced or inactivated by the host cells in the pre-founder mice. The pLKO Tet Puro system even though silenced or inactivated was stably integrated into the spermatocytes of the pre-founder mice because the transgene was stably inherited by the next two generations of the mice.

The unaltered levels of 14-3-3 γ mRNA in the pLKO Tet Puro positive mice and pLKO Tet Puro 14-3-3 γ shRNA positive mice could be the reason for the absence of phenotype in these animals. Moreover, these mice were administered doxycycline after they had become sexually mature suggesting inaccessibility of RNA polymerase to the H1 Tet promoter might have resulted into the silencing of the lentiviral fragment. An alternative explanation is 14-3-3 γ is required only for

the first few cycles of spermatogenesis after which the levels of 14-3-3 γ does not affect process of spermatogenesis.

To test the hypothesis that 14-3-3 γ is required for the first few cycles of spermatogenesis, pLKO Tet 14-3-3 γ shRNA viruses were injected in the pre-pubescent Swiss mice and one set of pre-founder mice were administered doxycycline. We observed that both the doxycycline treated and untreated pre-founder mice were fertile and the testes from these pre founder mice did not show loss of 14-3-3 γ . But the fertility of the pups, obtained from the doxycycline treated and untreated pLKO Tet 14-3-3 γ shRNA pre-founder mice, was affected. Levels of 14-3-3 γ will be determined in these mice to ascertain that the loss of fertility is associated with the loss of 14-3-3 γ . Also, the sterility observed in the doxycycline treated pLKO Tet Puro positive mice raises the question about the safety of pLKO Tet Puro system and doxycycline treatment in mice.

To study the role of 14-3-3 γ in regulating desmosome assembly, cell-cell adhesion and in epidermis function *in vivo*, we tried to generate epidermis specific 14-3-3 γ knockdown mice using pCCLK14 vector system. pCCLK14 vector system was previously used to correct mutations in human epidermal stem cells, these modified stem cells were used in the xenograft models and it was observed that the expression of transgene was restricted to the basal layer of epidermis [225].

In this study, we showed this vector system can be used in SMGT technique for generating transgenic animals with epidermis specific transgene expression. The transgenic animals showed the Turbo RFP expression specifically in the epidermal regions which K14. The Turbo RFP was stably integrated in the pre-founder mice and was stably inherited by the F1 and F2 generation.

Moreover the Turbo RFP expression was more prominent in F2 generation as compared to the F1 region.

We were unable to generate K14 specific 14-3-3 γ knockdown mice because of the absence of 14-3-3 γ shRNA_{mir} sequence in the Turbo RFP positive pups obtained from the pCCLK14 Turbo RFP 14-3-3 γ shRNA_{mir} pre-founder mice. The genomic DNA isolated from the testis of these pre-founder mice (2 years post-surgery) showed the presence of 14-3-3 γ shRNA_{mir} suggesting that the 14-3-3 γ shRNA_{mir} was stably integrated into the spermatocytes of the pre-founder mice. The absence of shRNA_{mir} in the transgene positive pups could have happened during the embryonic development. There are no reports available in literature where shRNA_{mir} or microRNA sequences were deleted during embryogenesis. This deletion could be the result of lentiviral recombination. Alternatively, it is possible that in the pre-founder mice the 14-3-3 γ shRNA_{mir} positive SSCs and developing spermatocytes with diploid DNA content might have lost the 14-3-3 γ shRNA_{mir} while differentiating into spermatozoa because it is reported that palindromic AT rich regions, which might form hairpin or cruciform structure, are prone to undergo double strand breaks in the spermatocytes undergoing meiosis [226]. 14-3-3 γ shRNA_{mir} used in this study has a palindromic sequence and is also rich in A and T nucleotides.

Electroporation of the K14 Turbo RFP 14-3-3 γ shRNA_{mir} fragment into the testes of mice [48] was done in collaboration with Dr. Subeer Majumdar, but the electroporated mouse did not sire any transgene positive pup. The similar results were obtained with eight out of ten pre-founder mice which were injected with the pCCLK14 Turbo RFP 14-3-3 γ shRNA_{mir} viruses. These pre-founder mice also had stable integration of Turbo RFP 14-3-3 γ shRNA_{mir} fragment into the spermatocytes as shown by PCR amplification of Turbo RFP 14-3-3 γ shRNA_{mir} but why the transgene was not inherited by any of the pups was not clear.

We also attempted to generate epidermis specific 14-3-3 γ knockout using CRISPR Cas system by driving Cas9 expression from K14 promoter. The 14-3-3 γ gRNA cloned into pLentiCRISPR Cas V1 vector and the pLentiCRISPR K14 Cas 9 14-3-3 γ gRNA construct were validated using NIH3T3 cells. The K14 promoter cloned into the pLentiCRISPR from pCCLK14 vector is a minimal promoter and is capable of driving cDNA expression in cell lines which do not express K14 [224] but the transgene expression driven by this promoter *in vivo* is specific [227].

pLentiCRISPR K14 Cas 9 and pLentiCRISPR K14 Cas 9 14-3-3 γ gRNA pre-founder mice sired pups which contained puromycin resistance cDNA. The epidermis of the pLentiCRISPR K14 Cas 9 14-3-3 γ gRNA positive pups was isolated and it was observed that some of the transgene positive mice expressed reduced levels of 14-3-3 γ . The genomic DNA was isolated from the epidermis of these mice to identify mutations in the 14-3-3 γ gene sequence using T7 endonuclease assay and Sanger sequencing but none of the mice had any mutation in 14-3-3 γ gene sequence. The only explanation for this result is that the double stranded break caused by Cas9 nuclease in keratinocytes was efficiently repaired by the DNA repair pathways. Therefore, we were unable to generate epidermis specific 14-3-3 γ knockout mice using CRISPR Cas system. This is disappointing as results from our laboratory demonstrate that loss of 14-3-3 γ in the human skin keratinocyte cell line HaCaT leads to defects in desmosome formation [228]. Hence, it is possible that if we had been successful in generating a tissue specific knockout of 14-3-3 γ , we would have observed defects in epidermal differentiation in mice. As mice with floxed alleles of 14-3-3 γ are not available, we might generate such animals in the future to determine the role played by 14-3-3 γ in desmosome formation in the epidermis.

5. Results and Discussion: Determine the mechanisms by which 14-3-3 γ loss leads to defect in the desmosome formation.

5.1 Results:

It was observed that the loss of 14-3-3 γ affects cell-cell adhesion *in vitro* and *in vivo*. The loss of cell-cell adhesion was because of a disruption in desmosome assembly due to a defect in the transport of PG to the cell border [150]. In addition to PG, 14-3-3 γ binds to DP and PKP3 in GST pulldown assays [150]. The experiments in this section are designed to identify the mechanisms by which 14-3-3 γ affects desmosome assembly through its interaction with desmosomal proteins.

5.1.1 PKC μ phosphorylates PG

14-3-3 proteins bind to their ligands using one of the three consensus binding motifs [80-83]. To identify the 14-3-3 consensus binding motif in PG, the PG sequence was analyzed using the Scansite software and a putative mode I motif was identified in PG. PKP3 and DP showed presence of multiple 14-3-3 binding motifs. Scansite software also predicted that the 14-3-3 binding site present in PG was phosphorylated by PKC μ at S236 position (Figure 5.1 A). To validate this prediction it was necessary to show that PG is the substrate of PKC μ . GST tagged full length PG was expressed and resolved on a 10% SDS PAGE gels. It was observed that the GST PG with the expected molecular weight of 108 kDa (PG is 82 kDa and GST is 26 kDa) was getting degraded as the purified GST PG showed a number of bands ranging from 92 kDa to 26 kDa (Figure 5.1 B). As the Scansite software predicted PKC μ would phosphorylate S236, the first 300 amino acids of PG were cloned downstream of GST tag using BamHI and XhoI sites. GST (26 kDa) and GST PG 300 (~59 kDa = ~33 kDa + 26 kDa) were expressed in bacteria and purified using glutathione conjugated sepharose beads (Figure 5.1 C). GST and GST PG 300

were eluted from the glutathione sepharose beads (Figure 5.1 C), dialyzed and concentrated before determining the concentration using a 10% SDS PAGE gel (Figure 5.1 D). The concentration of the purified GST protein was $\sim 1 \mu\text{g}/\mu\text{l}$ whereas the concentration of the purified GST PG 300 was $\sim 1.5 \mu\text{g}/\mu\text{l}$. Concentrated GST and GST PG 300 were sent to Dr. Felipe Samaniego's laboratory, University of Texas, MD Anderson Cancer Centre, Houston, Texas, U.S.A. where an *in vitro* kinase assay was performed. Briefly, GST and GST PG were used as substrates to determine the kinase activity of recombinant PKC μ (Signal Chem.) using ADP glow assay kit (Promega) according to manufacturer's instruction. Recombinant kinase and the purified substrate were incubated with $1 \mu\text{M}$ ATP, after a short incubation all the remaining ATP was depleted and a substrate was added which will convert ADP generated by the kinase activity into luminescent ATP and the luminescence was measured which determines the kinase activity. It was observed that with the increase in the GST PG 300 concentration there was an increase in the PKC μ kinase activity whereas the PKC μ kinase activity did not increase significantly when the concentration of GST protein was increased. This suggested PG is a substrate for PKC μ kinase activity.

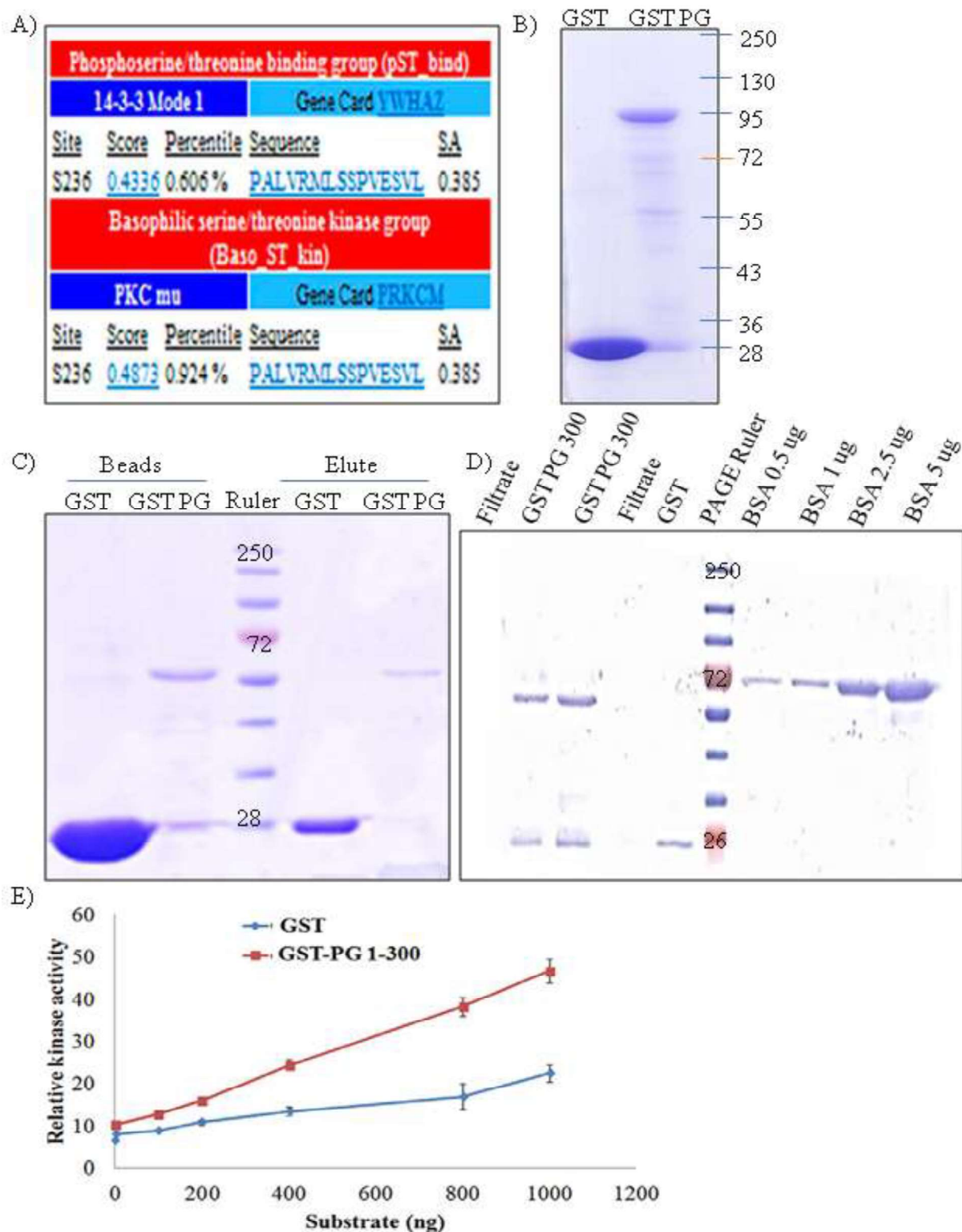


Figure 5.1: PKC μ phosphorylates PG. A. Analysis of amino acid sequence of PG to identify the putative 14-3-3 binding site using Scansite software. Putative kinase which might

phosphorylate the 14-3-3 binding site is also shown. **B.** Purified GST and GST PG (full length) resolved on 10% SDS PAGE gel and stained with brilliant blue. **C.** GST and GST PG 300 proteins bound to the glutathione coated sepharose beads and eluted from the sepharose beads were resolved on the 10% SDS PAGE gel and stained using coomassie brilliant blue. **D.** GST and GST PG 300 eluted from the glutathione coated sepharose beads were dialyzed and concentrated before resolving on a 10% SDS PAGE gel to determine the protein concentration using BSA solutions of different concentrations as a reference. **E.** The kinase activity of PKC μ was measured using ADP glow assay kit. The kinase activity of PKC μ (Y axis) was plotted against the substrate concentration (X axis) to determine if the activity increased with the increase in substrate concentration [150].

5.1.2 Mutation of PG serine 236 to alanine and its effect on PG localization

The results above suggested that S236A was phosphorylated by PKC μ . To determine if phosphorylation of S236 was required for PG transport to the border and complex formation with 14-3-3 γ , the S236 residue in PG was altered to Alanine (PG S236A). PG S236A failed to bind to 14-3-3 γ in a GST pull down assay suggesting that the phosphorylation of PG at S236 residue is important for its binding to 14-3-3 γ [150]. To study the effect of S236A mutation on PG transport the localization of S236A PG mutant was studied. Briefly, Myc tagged PG (WT) and Myc tagged S236A PG were transfected into HCT116 cells, 48 hours post transfection cells were fixed and stained with antibodies to Myc. The cells were imaged using LSM 510 confocal microscope and it was observed that the Myc PG WT mostly localized at the cell border whereas the cell border localization of S236A PG was highly reduced and PS236A PG localized mostly

to the cytoplasm (Figure 5.2). This data suggests that the phosphorylation of S236 is important for the 14-3-3 binding and for the PG transport from cytoplasm to the cell border.

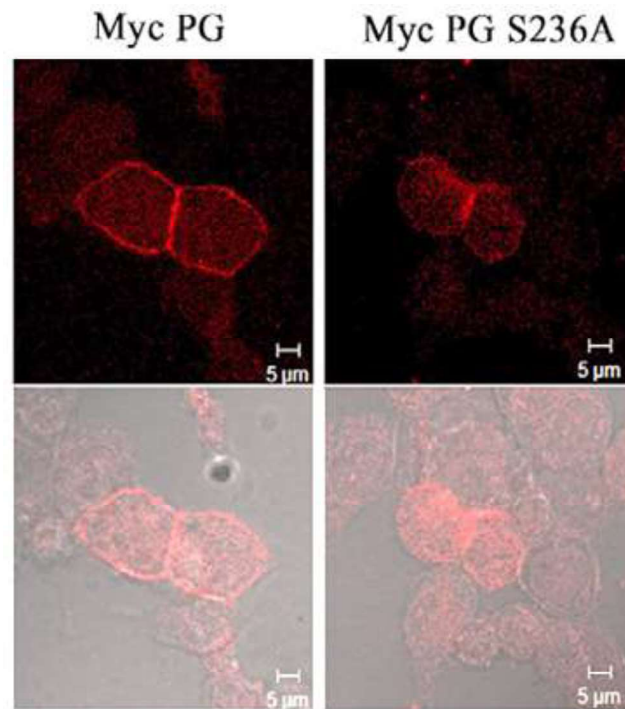


Figure 5.2: Cytoplasmic localization of S236A PG. HCT116 cells expressing Myc PG WT and Myc PG S236A were stained with the Myc antibody and imaged using LSM 510 confocal microscope using 63X objective. Representative images are shown and scale bars are shown in each panel [150].

5.1.3 Effect of PKC μ loss on desmosome formation

PKC μ phosphorylates PG and generates a 14-3-3 γ binding site in PG. Complex formation between PG and 14-3-3 γ is crucial for PG transport from the cytoplasm to the cell border. Previous results had indicated that an inhibitor that targets both PKC α and PKC μ could inhibit desmosome formation [150]. To determine if loss of just PKC μ led to defects in desmosome

formation, a, HCT116 derived PKC μ knockdown cell line was generated and the protein levels and localization of the desmosomal proteins were studied. A Western blot showing the levels of PKC μ and the desmosomal proteins is shown in figure 5.3 A. The levels of PG and DP upon the PKC μ knockdown were reduced whereas the levels of PKP3 were largely unaltered. It was observed that upon the loss of PKC μ , PG, PKP3 and DP did not localize to the cell border (Figure 5.3 B). This data suggests that PKC μ plays an important role in the transport of desmosomal proteins and in the desmosome assembly [150].

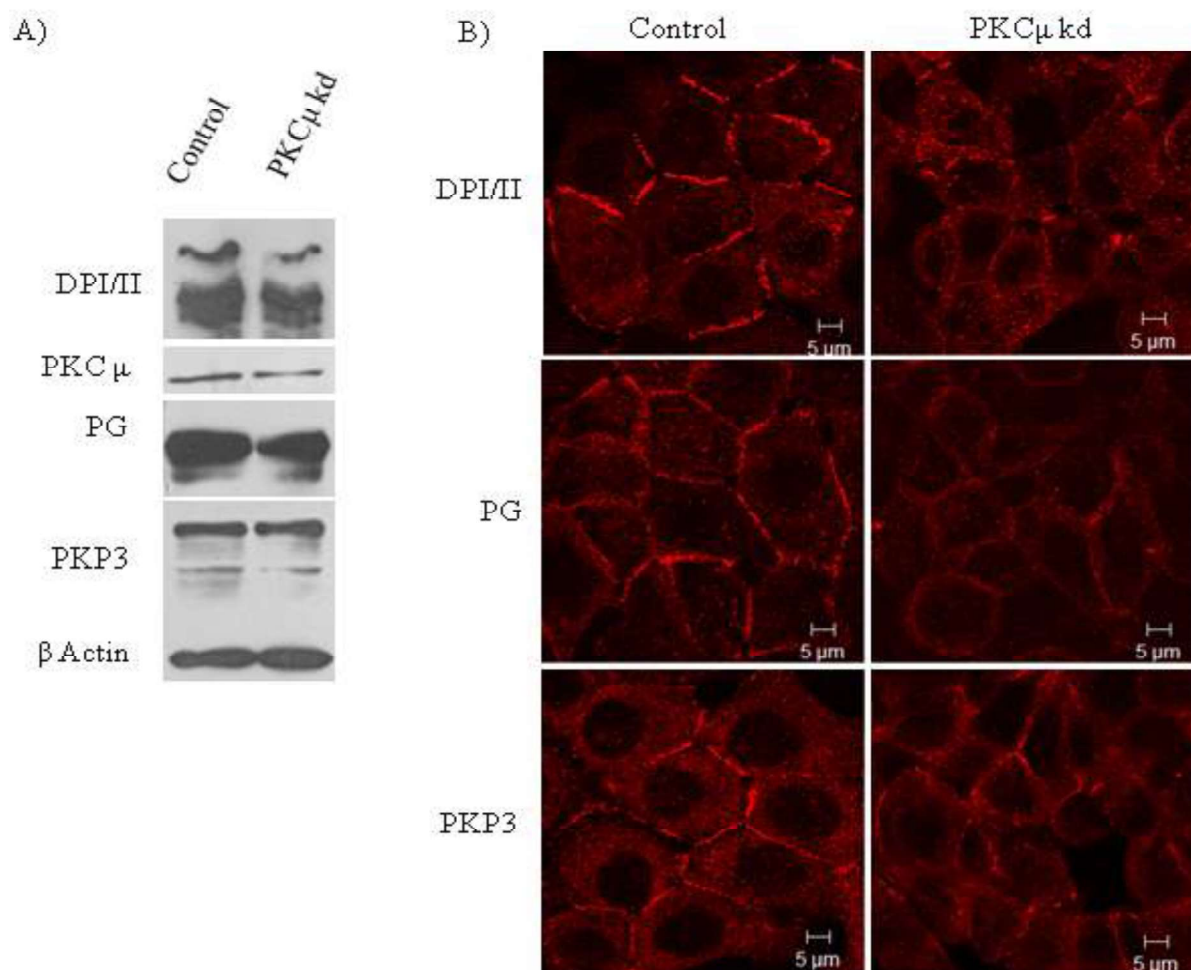


Figure 5.3: The loss of PKC μ affects desmosome assembly and the levels of desmosomal proteins. A. The protein extracts of HCT116 derived vector control and PKC μ knockdown cells

were resolved using 7.5 % acrylamide gel and Western blots for PKC μ , DP, PG and PKP3 were done. Western blots for β Actin served as a loading control. **B.** HCT116 derived vector control and PKC μ knockdown cells were fixed and stained with the antibodies to the indicated proteins. Cells were imaged using LSM 510 confocal microscope at 63X. Representative images are shown and scale bars are shown in each panel [150].

5.1.4 Sertoli cell isolation to study desmosomes

Loss of 14-3-3 γ led to the loss of cell-cell adhesion and disruption of spermatogenesis in testis [150]. 14-3-3 γ regulates desmosome formation by regulating PG transport [150]. The Sertoli cells and developing spermatocytes are connected to each other by different cell-cell adhesion junctions one of which is the desmosome. Therefore, to study localization of different desmosomal proteins in the Sertoli cells, Sertoli cells were isolated using a protocol described by Anway *et al.*, [207] and stained with the antibodies to PG. The cultured Sertoli cells were imaged using inverted microscope (Figure 5.4 A). The Sertoli cells cannot be passaged and therefore with the few isolated Sertoli cells were stained with Nile red dye which stains the lipid droplets present in the Sertoli cells as shown in Figure 5.4 B [229]. The lipid droplets are not seen in SSCs and spermatocytes because of which lipid droplets are considered as a Sertoli cell specific marker [229]. Vimentin, Sox9, Anti-mullerian hormone, Wilm's tumor suppressor 1 and Androgen binding protein are the markers of immature Sertoli cells (at neonatal stage) [230]. To study desmosome formation in Sertoli cells is not feasible as large number of mice will have to be sacrificed to obtain enough Sertoli cells to perform the Western blotting and staining for desmosomal proteins.

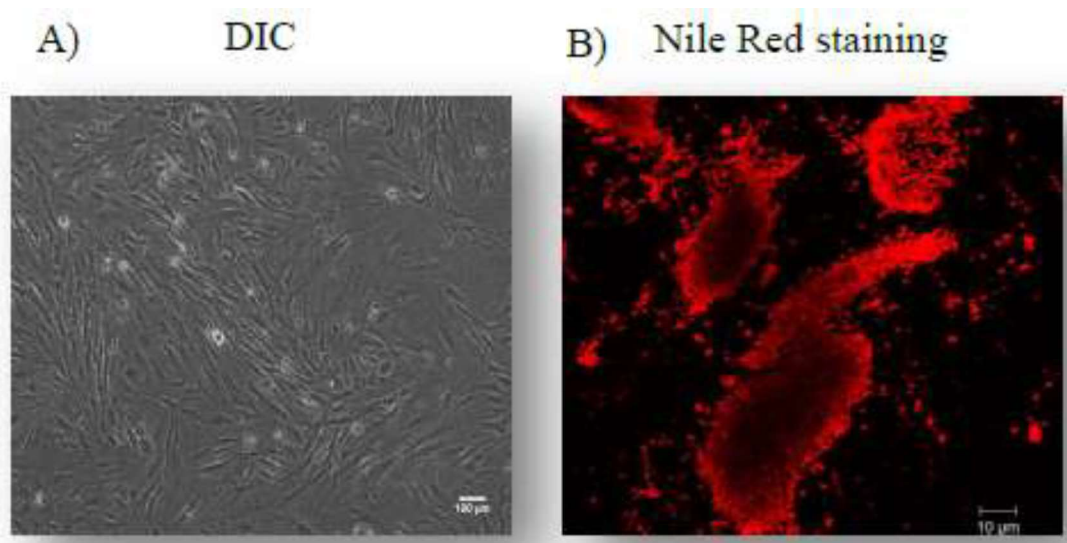


Figure 5.4: Sertoli cell isolation and culture. **A.** Sertoli cells isolated from the neonatal mouse was cultured in F12 medium. The cells were imaged using Zeiss Axiovert 200 M inverted microscope at 10X objective. **B.** Sertoli cells were stained with Nile Red to identify lipid droplets and imaged using LSM 510 confocal microscope at 63X objective. Representative images are shown. Scale bars are shown in each panel.

5.1.5 Generation of HA tagged PG deletion constructs

To identify the functions of the different domains of PG, HA tagged PG deletion constructs were generated by cloning different domains of PG into pCDNA3.1 HA vector. HCT116 cells were transfected with the HA pCDNA3.1 vector control or with one of the following HA tagged PG deletion constructs:

Name of the PG deletion mutant	Expected molecular weight in kDa
HA PG Wild type	83
HA PG S236A	83
HA PG N term	15
HA PG Arm	58
HA PG C term	11
HA PG N term to 9 th Arm	57
HA PG 10 th Arm to C term	26
HA PG Δ N term	73
HA PG Δ C term	69

Table 5.1: A table showing different types of HA tagged PG deletion constructs with the expected molecular weight.

48 hours post transfection cell extracts were prepared, the cell extracts were resolved on a SDS PAGE gel and Western blots were done using antibodies for HA. As shown in Figure 5.5 A, the expression of all the PG deletion mutants except the HA tagged PG C term mutant was detected using Western blotting. The HA tagged PG C term mutant has the molecular weight of 10 kDa and this protein may not be stable *in vitro*. To detect the expression of the PG C term mutant, mRNA was isolated from the HCT116 cells transfected with pCDNA3.1 HA construct or the HA tagged PG C term construct and the reverse transcriptase PCR was done to amplify the HA tagged PG C term mRNA. As shown in Figure 5.5 B HCT116 cells transfected with the HA tagged PG C term mutant expressed the HA tagged PG C term mRNA.

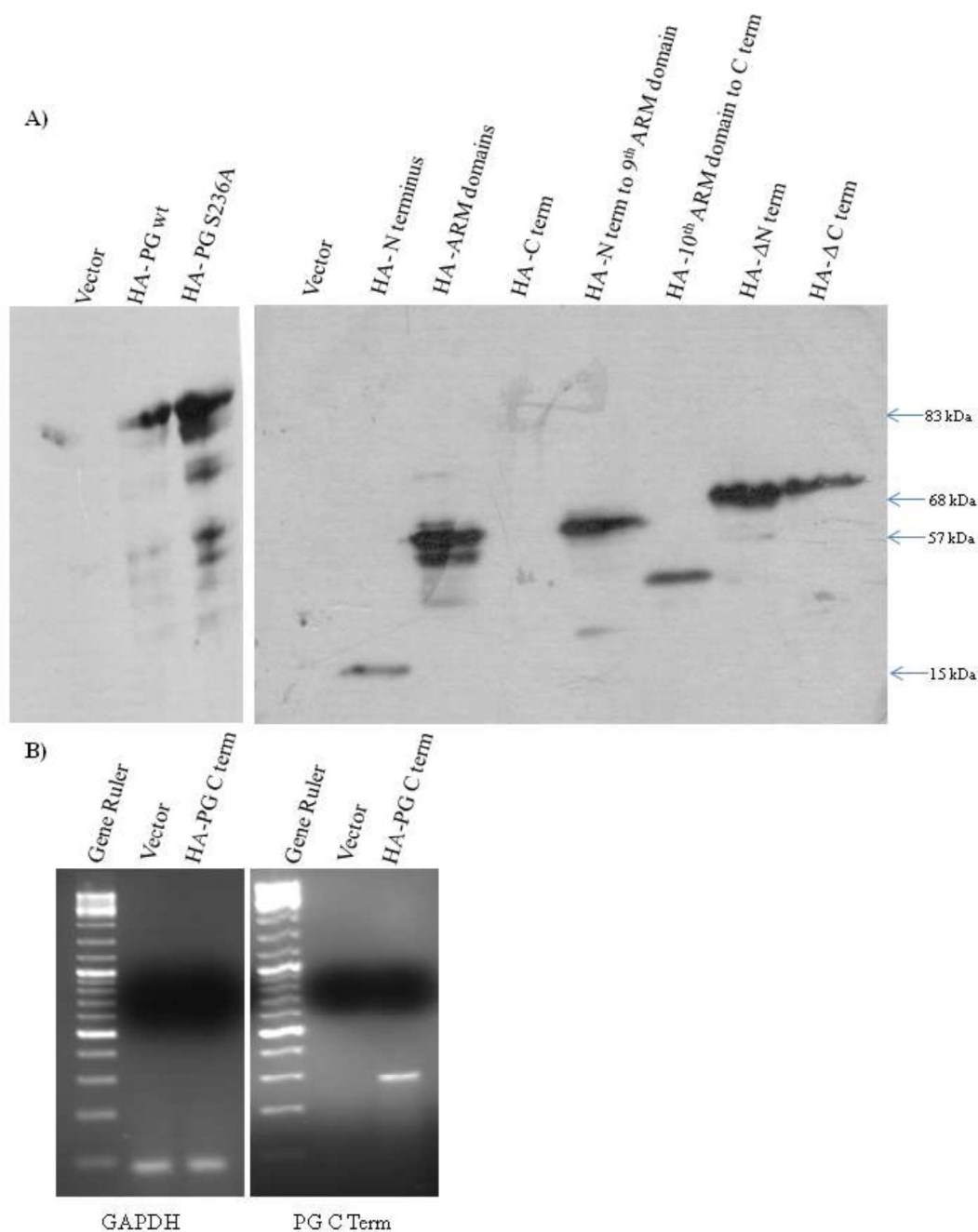


Figure 5.5: Expression of HA tagged PG deletion constructs. **A.** HCT116 cells were transfected with the HA tagged PG deletion constructs using PEI, 48 hours post-transfection cell extracts were prepared and resolved using a 12% (left) and a 10% SDS PAGE gel (right). Western blotting was done using HA antibody. Note that the expression of HA-PG C term was not detected on the blot. **B.** HCT116 cells were transfected with the pCDNA3.1 HA vector or

HA tagged PG C term constructs, 48 hours post-transfection mRNA was extracted and reverse transcriptase PCR was done to amplify PG C term mRNA.

5.1.6 Validation of pLentiCRISPR PG gRNA constructs

To generate a PG knockout cell lines in which different PG deletion mutants can be expressed to identify the functions of the each domain of PG, PG gRNA 1 (targeting exon 1) and PG gRNA (targeting exon 2) were cloned into pLentiCRISPR Cas V1 vector using BsmBI sites. The pLentiCRISPR Cas V1 clones containing gRNA targeting exon 1 of PG was termed as PG gRNA 1 and the pLentiCRISPR Cas V1 clones containing gRNA targeting exon 2 of PG were termed as PG gRNA 2.1, PG gRNA 2.2, PG gRNA 2.3 and PG gRNA 2.4. The PG gRNA clones were transfected into HCT116 using PEI, 72 hours post-transfection cell extracts were prepared, resolved on a 10% SDS PAGE gel and Western blots were done using antibodies for PG and β Actin. As shown in Figure 5.6, reduction in PG levels were seen with the both the PG gRNA clones.

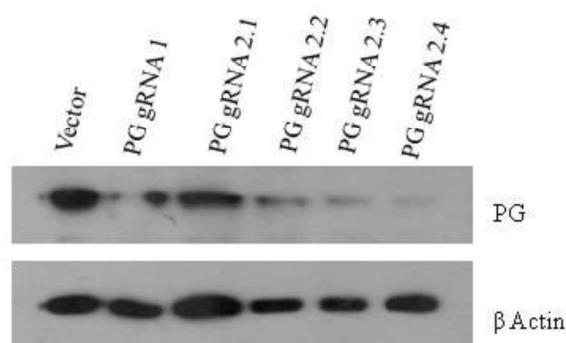


Figure 5.6: The validation of PG gRNA clones in HCT116 cells. HCT116 cells were transfected with PG 1 gRNA and PG 2 gRNA clones (2.1-2.4) using PEI, 72 hours post

transfection cell extracts were prepared and resolved on a 10% SDS PAGE gel. Western blot was done using PG antibody. Western blot for β Actin served as a loading control.

5.1.7 Validation of PG-EGFP and PG-EGFP-f constructs

It was previously shown in the lab that in HCT116 derived PKP3 knockdown cells none of the desmosomal proteins were present at the cell border except PG, suggesting PG is recruited to the cell border to initiate desmosome formation [211]. Loss of 14-3-3 γ in HCT116 cells led to the reduction in the cell border localization of all the desmosomal proteins thereby disrupting desmosome formation. 14-3-3 γ binds to DP, PG and PKP3 and regulates transport of PG from cytoplasm to the cell border [150]. It was not clear that the disruption of desmosome assembly in 14-3-3 γ knockdown cells was caused by the disrupted PG transport or 14-3-3 γ plays an important role in the desmosome formation irrespective of PG transport to the cell border. To test this hypothesis, a farnesylated GFP tagged PG (PG-EGFP-f) construct was expressed in 14-3-3 γ knockdown cells and desmosome formation was studied. As a control, non-farnesylated GFP tagged PG (PG-EGFP) was expressed in 14-3-3 γ knockdown cells to study the effect of PG over-expression on desmosome formation.

PG cDNA was cloned into pEGFP-f N1 vector to generate PG-EGFP-f. To generate PG-EGFP vector EGFP-f fragment from PG-EGFP-f was replaced by EGFP fragment from EGFP C1. To validate the expression of PG-EGFP-f and PG-EGFP, HCT116 cells were transfected with PG-EGFP-f /EGFP-f or PG-EGFP/EGFP using PEI. 48 hours post transfection cell extracts were prepared and resolved on a 10% SDS PAGE gel. Western blotting was performed using antibodies to PG, β Actin and GFP. As shown in Figure 5.7 HCT116 cells transfected with PG-

EGFP-f and PG-EGFP showed the presence of two bands, one band is endogenous PG and the second band is PG-EGFP-f and PG-EGFP respectively.

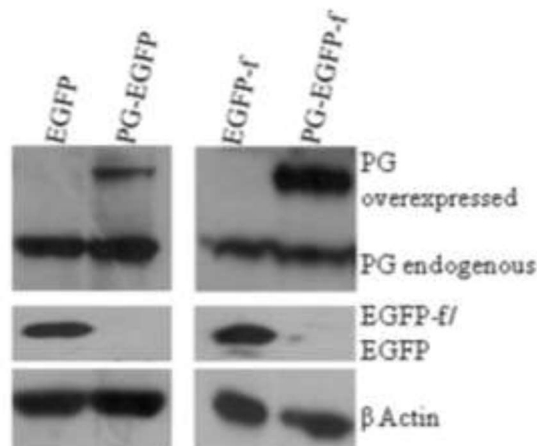


Figure 5.7: Expression of PG-EGFP-f and PG-EGFP in HCT116 cells. HCT116 cells were transfected with EGFP or PG-EGFP or EGFP-f or PG-EGFP-f using PEI, 48 hours post transfection cell extracts were prepared, cell extracts were resolved on a 10% SDS PAGE gel and Western blotting was done using PG, β Actin and GFP antibodies.

5.1.8 PG-EGFP-f recruits desmosomal proteins to the cell border in the absence of 14-3-3 γ

To study the effect of 14-3-3 γ loss on desmosome assembly, HCT116 derived vector control and 14-3-3 γ knockdown cells were stained with the antibodies to PG. A Western blot showing the levels of 14-3-3 γ in the HCT116 derived vector control cells and 14-3-3 γ knockdown cells is shown in Figure 5.8 A. As shown in Figure 5.8 B, PG localized to the cell border in the vector control cells whereas in the 14-3-3 γ knockdown cells PG mostly localized to the cytoplasm.

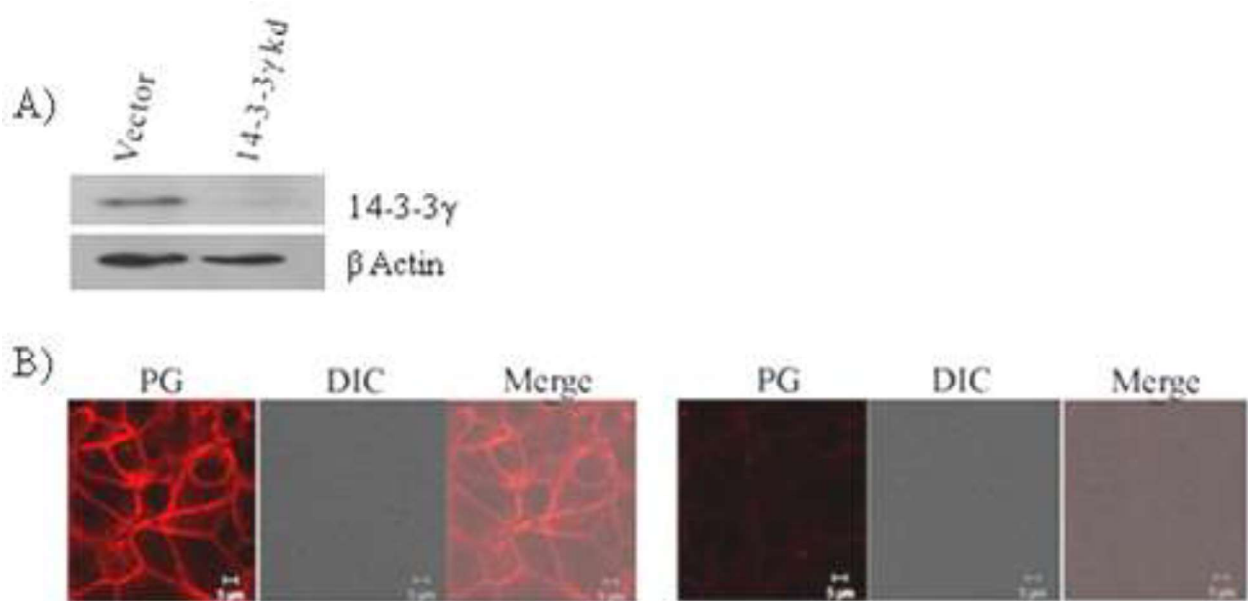
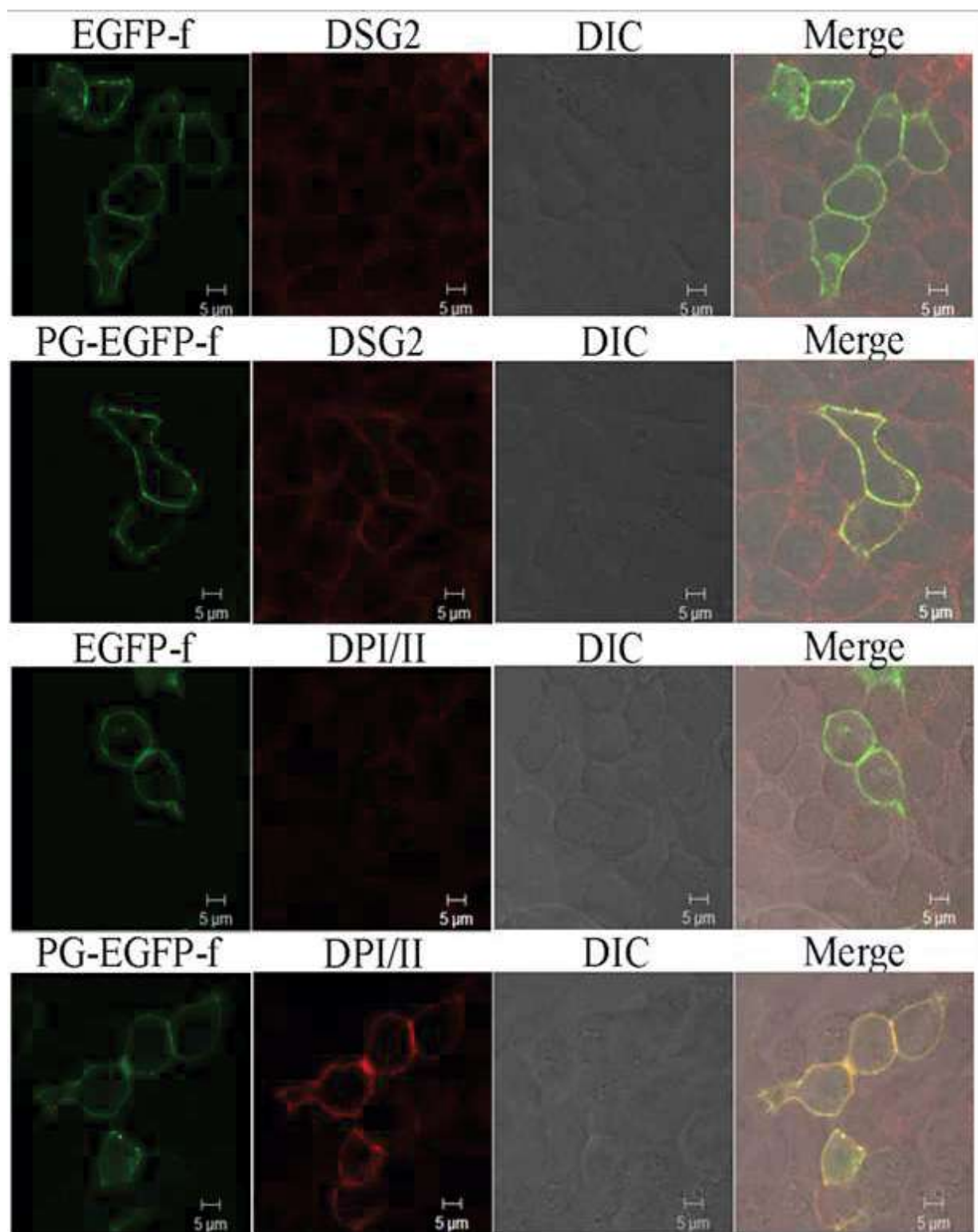


Figure 5.8: Cell border localization of PG is altered upon loss of 14-3-3 γ . **A.** Protein extracts of HCT116 derived vector control and 14-3-3 γ knockdown cells were resolved on a 10% SDS PAGE gel and Western blotting was done with the indicated antibodies. **B.** HCT116 derived vector control and 14-3-3 γ knockdown cells were stained with the PG antibody and imaged using Zeiss LSM 780 confocal microscope at 40X objective. Representative images are shown and scale bars are shown in each panel [228].

To rescue the defect in PG transport in the absence of 14-3-3 γ , HCT116 derived 14-3-3 γ knockdown cells were transfected with the PG-EGFP-f or PG-EGFP and the localization of different desmosomal proteins were studied. As shown in Figure 5.9, PG-EGFP-f completely restored DPI/II and DSG2 to the cell border; partially restored PKP3 to the cell border and did not restore DSC2/3 to the cell border.



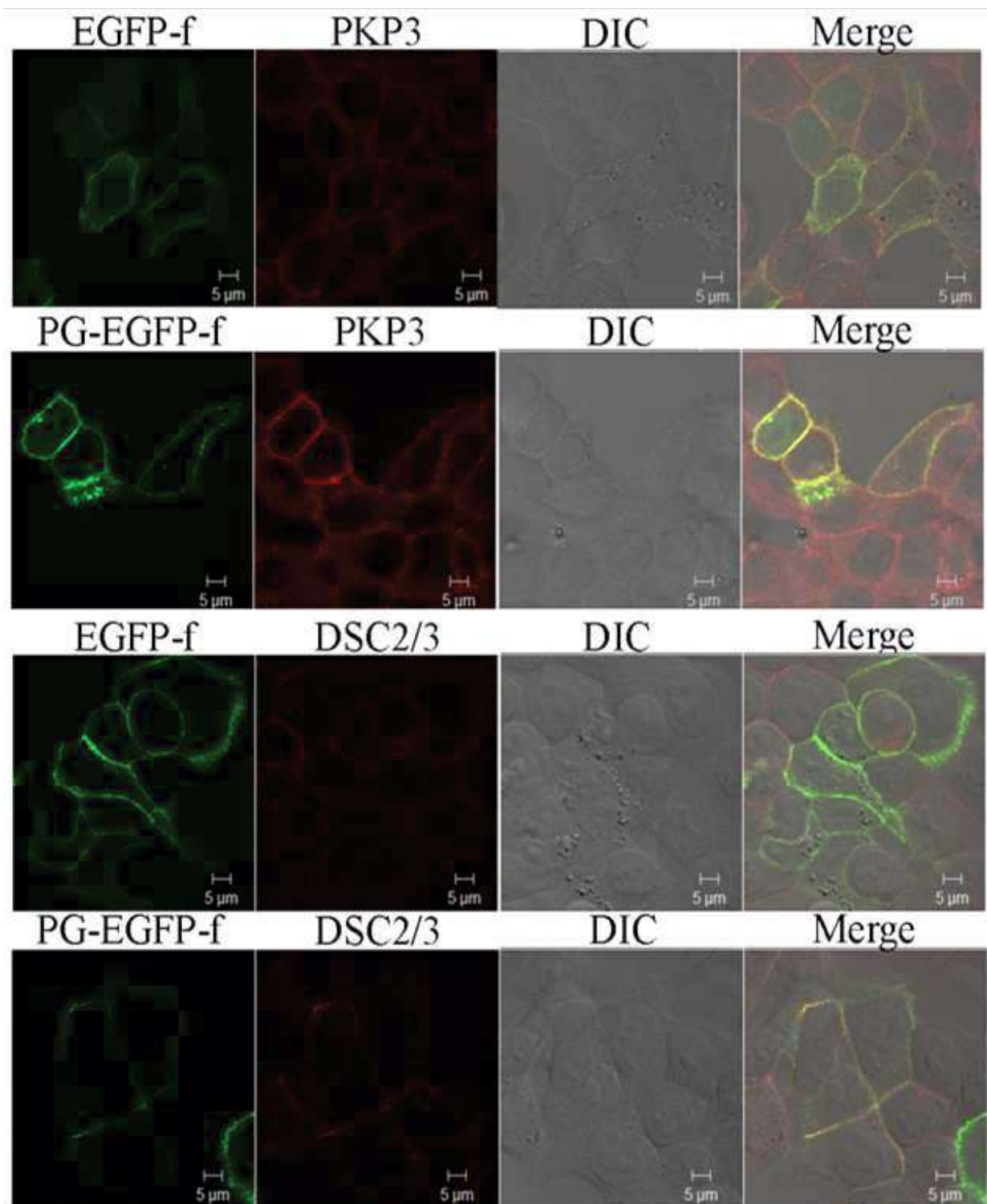


Figure 5.9: PG-EGFP-f rescues cell border localization of DSG2, DP and PKP3 upon 14-3-3 γ loss. HCT116 derived 14-3-3 γ knockdown cells were transfected with EGFP-f or PG-EGFP-f using PEI. 48 hours post transfection cells were fixed with paraformaldehyde and stained with

the indicated antibodies. The images were acquired using Zeiss LSM 780 confocal microscope at 63X objective and 2X zoom. Representative images are shown and scale bars are shown in each panel [228].

To observe if there was a significant increase in the cell border staining of the desmosomal protein in the cells expressing PG-EGFP-f the intensity of the staining for each of the desmosomal protein at the cell border was measured and plotted (Figure 5.10). There was a significant increase in the cell border staining of DPI/II and DSG2 in the 14-3-3 γ knockdown cells expressing PG-EGFP-f when compared to the 14-3-3 γ knockdown cells expressing EGFP-f.

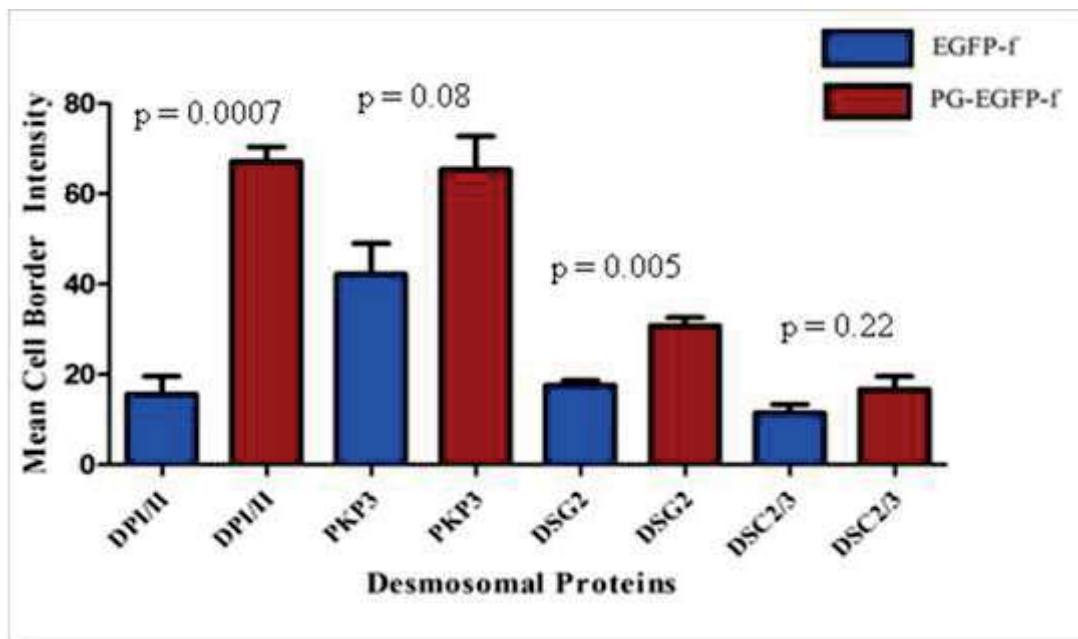


Figure 5.10: PG-EGFP-f expression in 14-3-3 γ knockdown cells led to the increase in the cell border localization of DP and DSG2. The intensity of border staining for different desmosomal proteins was measured using ImageJ software for 33 transfected cells from each experiment. The mean cell border intensity and standard error from three different experiments is plotted. *p value* was calculated using student's t-test [228].

To determine if the cell border localization of the desmosomal proteins observed upon PG-EGFP-f expression was because of the PG over-expression, PG-EGFP was expressed in the 14-3-3 γ knockdown cells and stained with the antibodies to DPI/II. As shown in Figure 5.11 A and B, expression of PG-EGFP did not restore DPI/II to the cell border suggesting that the PG over-expression cannot restore the cell border localization of desmosomal proteins.

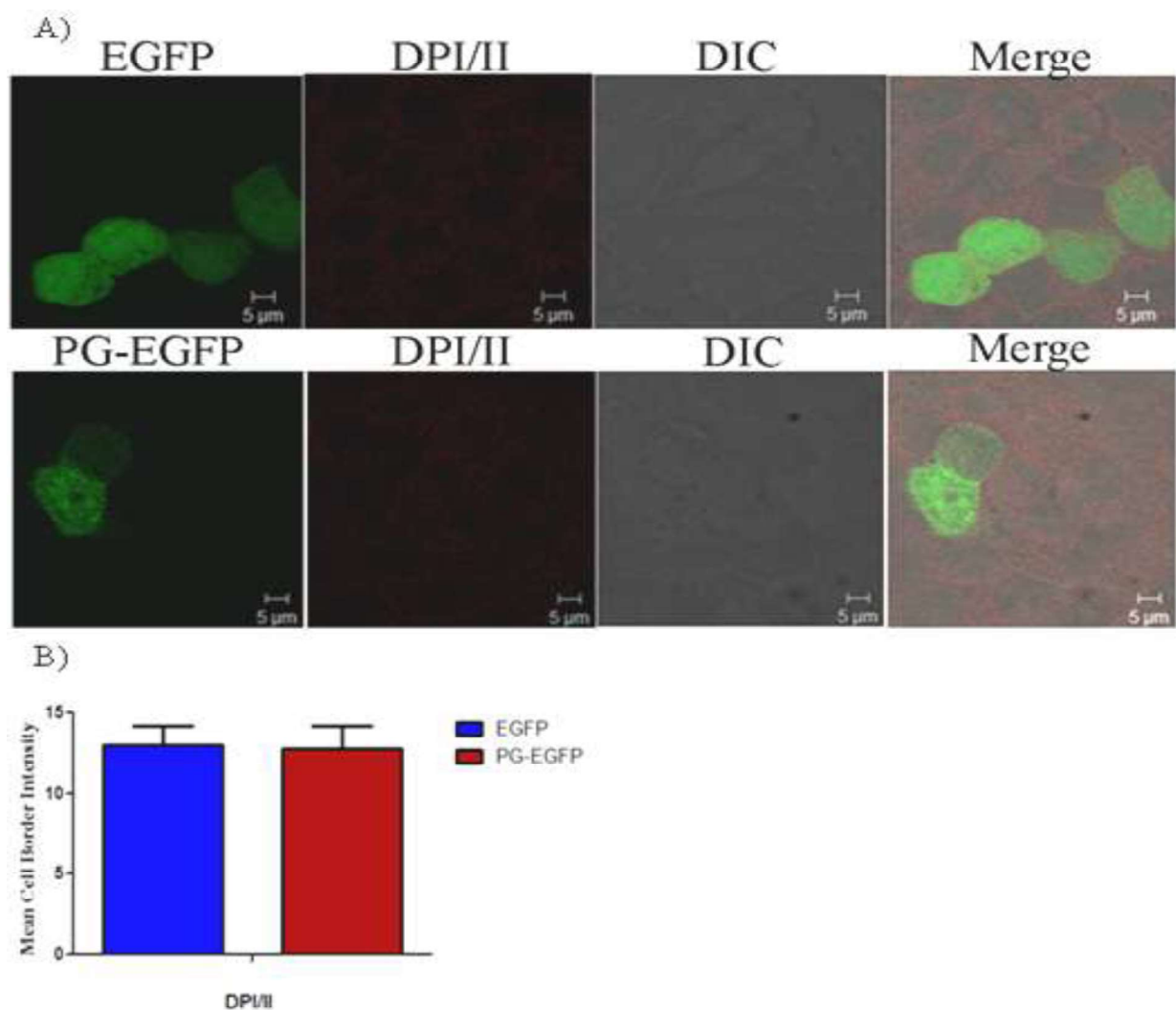


Figure 5.11: PG-EGFP does not restore DP to the cell border upon 14-3-3 γ loss. A. HCT116 derived 14-3-3 γ knockdown cells were transfected with EGFP or PG-EGFP using PEI. 48 hours post transfection cells were fixed with paraformaldehyde and stained with the antibody. The

images were acquired using Zeiss LSM 780 confocal microscope at 63X objective and 2X zoom. Representative images are shown and scale bars are shown in each panel. **B.** The intensity of border staining for DPI/II was measured using ImageJ software for 33 transfected cells from each experiment. The mean cell border intensity and standard error from three different experiments is plotted. Note there is no difference in the mean cell border intensity of DPI/II in cells expressing EGFP and cells expressing PG-EGFP [228].

5.1.9 PG-EGFP-f increased DPI/II protein levels in 14-3-3 γ knockdown cells

As reported previously, loss of 14-3-3 γ in HCT116 does not affect the desmosomal protein levels and the desmosomal proteins in the HCT116 derived vector control and 14-3-3 γ knockdown cells were mostly present in the insoluble fraction [150]. To determine if the increase in the border localization of DP and DSG2 observed upon PG-EGFP-f expression in 14-3-3 γ knockdown cells led to the increase in the protein levels of DP and DSG2, cell extracts of 14-3-3 γ knockdown cells transfected with EGFP-f/PG-EGFP-f or EGFP/PG-EGFP were resolved on a 7.5% and 10% step gradient resolving gel and Western blotting was done with the antibodies to desmosomal proteins. Western blots for β Actin served as a loading control. As shown in Figure 5.12 A, the PG-EGFP-f expression led to the increase in the levels of DPI/II whereas PG-EGFP expression did not lead to the change in the expression of DPI/II. The increase in the DPI/II protein levels upon PG-EGFP-f expression was also observed in the insoluble fraction (Figure 5.12 B). The increase in the DPI/II levels in the insoluble fraction could be attributed to the fact that the cell border localization of desmosomal proteins at an intact desmosome increases the

stability of the desmosomal proteins as compared to the desmosomal proteins present in the cytoplasmic pool [209, 212, 231].

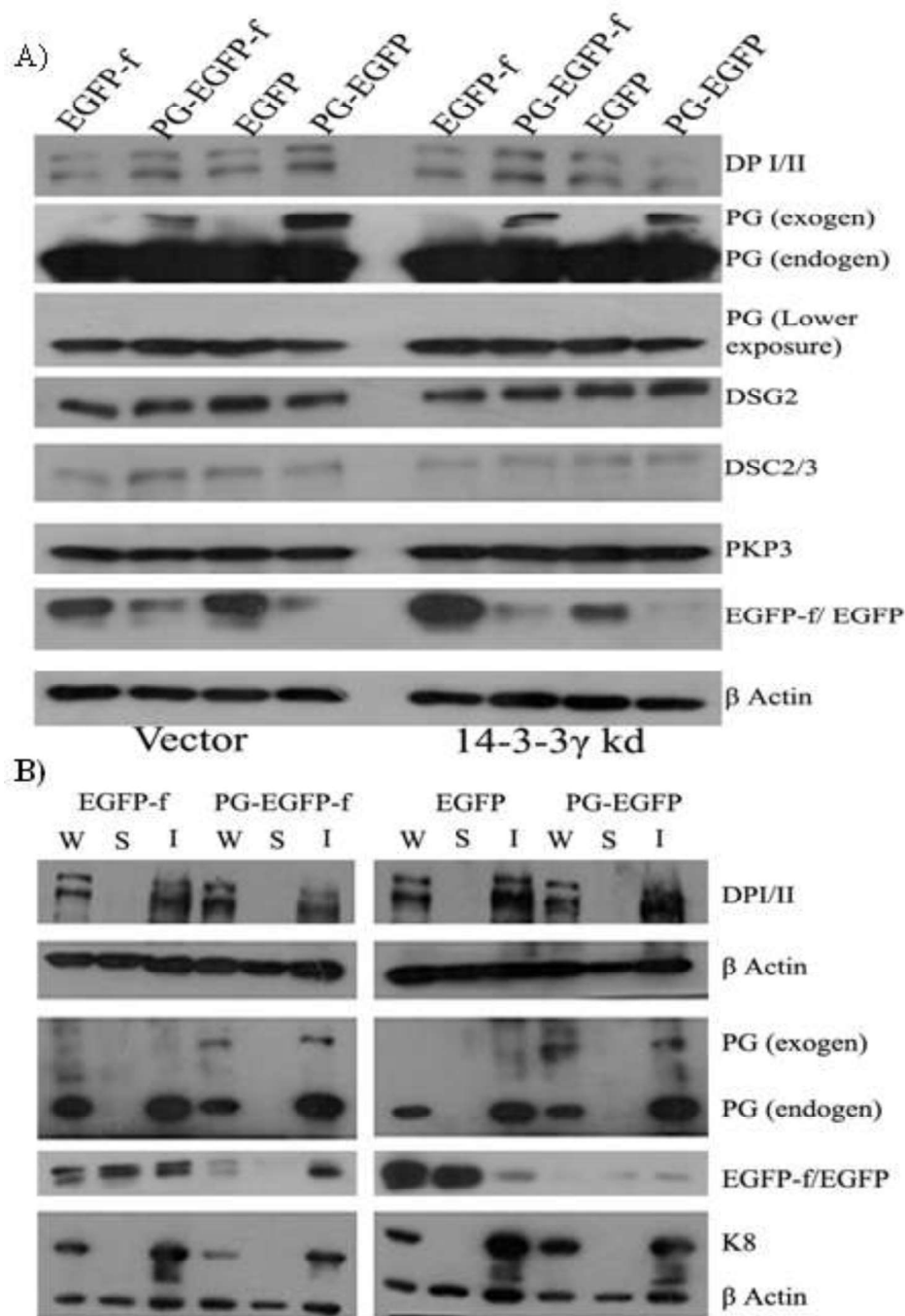


Figure 5.12: The expression of PG-EGFP-f in 14-3-3γ knockdown cells led to the increase in the DPI/II protein levels. A. Protein extracts prepared from HCT116 derived vector control and

14-3-3 γ knockdown cell lines expressing EGFP-f/PG-EGFP-f or EGFP /PG-EGFP were resolved on SDS-PAGE gels followed by Western blotting with the indicated antibodies. Western blots for β Actin served as a loading control. Lane 1 and 2 are vector control cells expressing EGFP-f or PG-EGFP-f respectively. Lane 3 and 4 are vector control cells expressing EGFP or PG-EGFP respectively. Lane 5 and 6 are 14-3-3 γ knockdown cells expressing EGFP-f or PG-EGFP-f respectively. Lane 7 and 8 are 14-3-3 γ knockdown cells expressing EGFP or PG-EGFP respectively. **B.** Cytoskeletal buffer soluble [S] and insoluble [I] fractions were prepared from HCT116 derived 14-3-3 γ knockdown cell line expressing EGFP-f or PG-EGFP-f or EGFP or PG-EGFP were resolved on SDS-PAGE gels followed by Western blotting with the indicated antibodies. Western blots for β Actin served as a loading control and Western blot for Keratin 8 (K8) served as control for insoluble fraction. Whole cell extracts [W] served as a control [228].

5.1.10 PG-EGFP-f stabilizes DSG2 at the cell border in the absence of 14-3-3 γ

Desmosomes are calcium dependent cell-cell adhesion junctions. The desmosomal cadherins require calcium for their interaction with the desmosomal cadherins present on the neighboring cells and in the absence of the calcium desmosomal cadherins are unstable at the border [232]. The stable interaction of desmosomal cadherins also requires PG and PG targets desmosomal cadherins to the cell-cell junctions [233]. It was shown previously that in the 14-3-3 γ knockdown cells in the absence of calcium, PG and desmosomal cadherins were not localized to the cell border and upon calcium addition some of the desmosomal cadherins localized to the border but at a slower rate compared to the vector control cells [150]. To determine if the PG-EGFP-f expression stabilized desmosomal cadherins at the cell border in the absence of calcium, calcium

switch assays were done on the HCT116 derived 14-3-3 γ knockdown cells transfected with EGFP-f or PG-EGFP-f as described in the materials and methods. As shown in Figure 5.13, upon PG-EGFP-f expression in 14-3-3 γ knockdown cells some of the DSG2 was seen at the cell border even at the 0 minutes of calcium addition whereas EGFP-f expressing 14-3-3 γ knockdown cells DSG2 was seen only in the cytoplasm. After 15 minutes of calcium addition, DSG2 localization at the cell border increased in the PG-EGFP-f expressing 14-3-3 γ knockdown cells and in the EGFP-f expressing 14-3-3 γ knockdown cells DSG2 localization at the cell border was barely visible. The results of the calcium switch assay suggests that the PG-EGFP-f stabilized the DSG2 at the cell border to some extent even in the absence of calcium and in the presence of calcium PG-EGFP-f stimulated the cell border localization of DSG2 and provided stability to DSG2 preventing cycling of DSG2 to the cytoplasm. In the 14-3-3 γ knockdown cells even in the presence of the calcium DSG2 is not seen at the cell border because DSG2 is not stabilized at the border due to the absence of plakin family of proteins at the cell border.

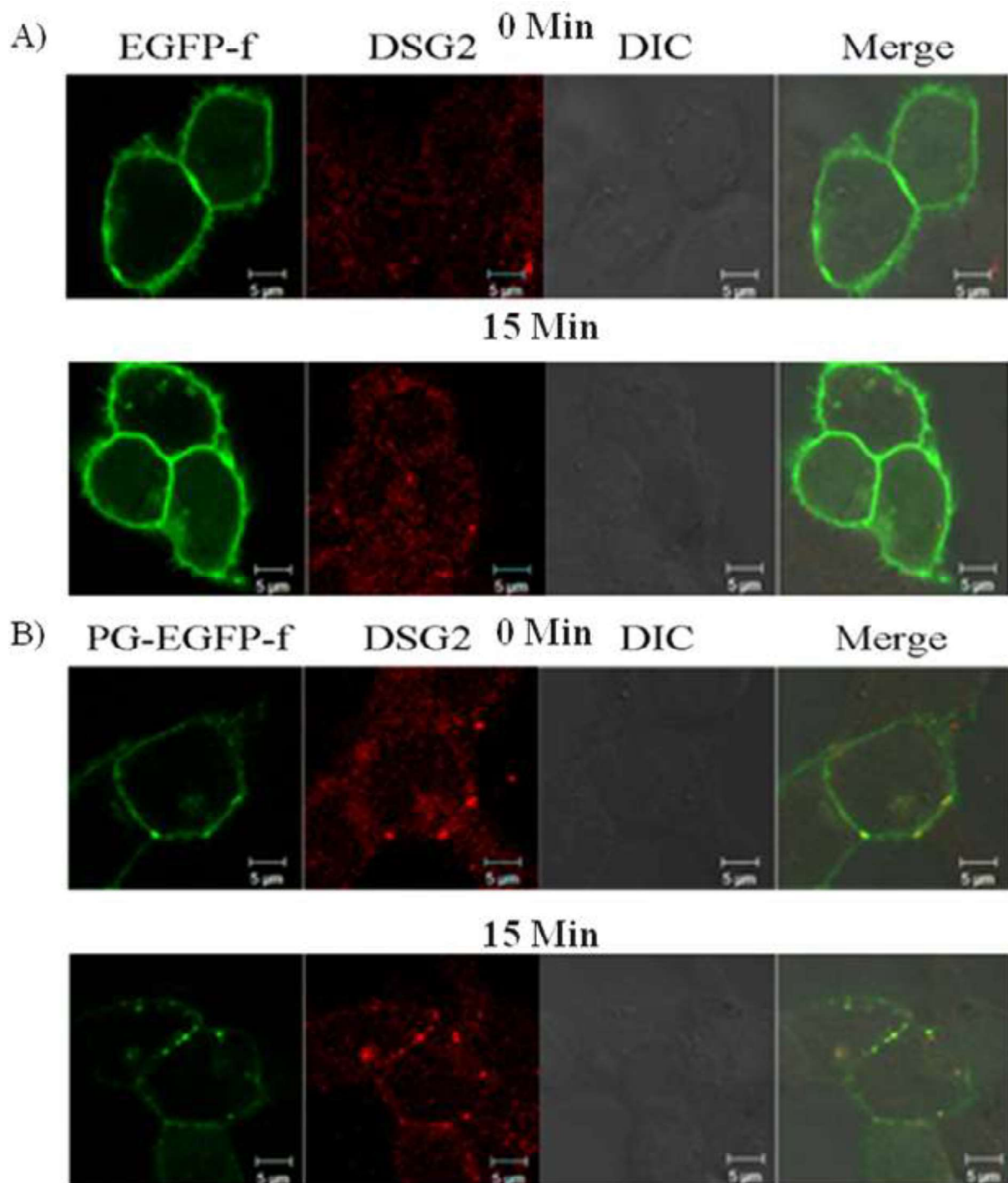
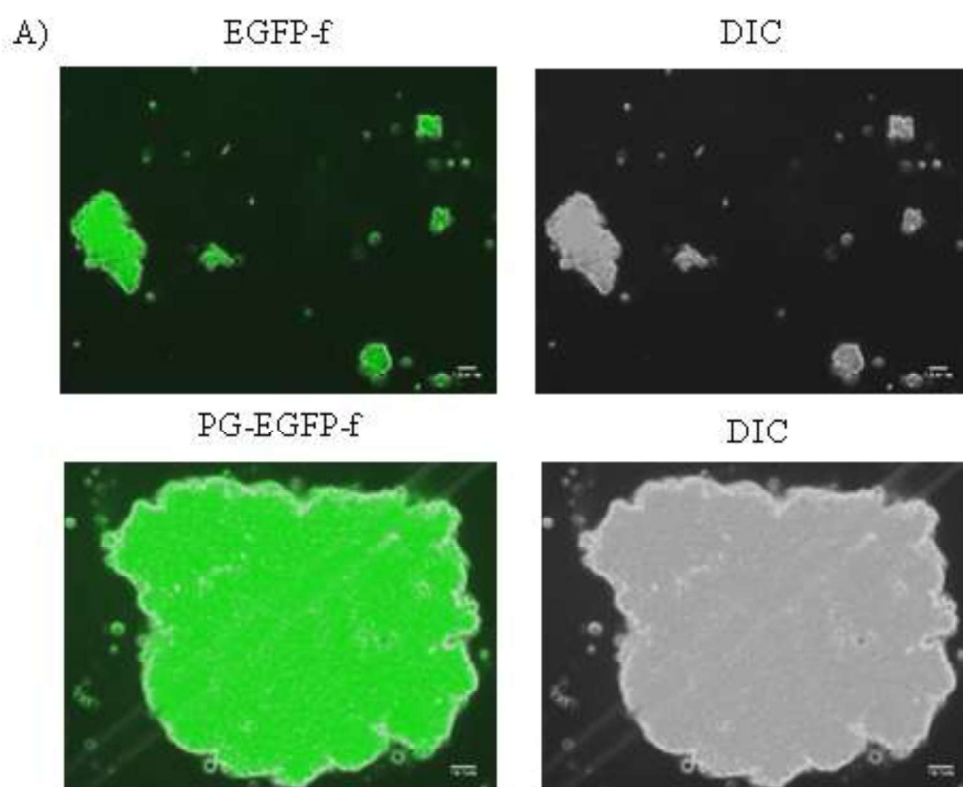


Figure 5.13: PG-EGFP-f stabilizes the DSG2 at the cell border and stimulates DSG2 transport. A-B. Calcium switch assays were performed on 14-3-3 γ knockdown cells transfected with pEGFP-f (A) or PG-EGFP-f (B) (green) as described. Cells were fixed at 0 and 15 minutes

post calcium addition and stained for DSG2 (red). Images were obtained on a Zeiss LSM 780 confocal microscope using a 63X objective and 4X optical zoom. Scale bars are indicated in the image panels [228].

5.1.11 PG-EGFP-f restores desmosome formation in the 14-3-3 γ knockdown cells

It is reported that a desmosomal cadherin and a plaque protein along with the DP can form functional desmosomes [234]. HCT116 derived 14-3-3 γ knockdown cells did not form the desmosomes because of the reduced cell border localization of desmosomal proteins which resulted into reduced cell-cell adhesion [150]. PG-EGFP-f expression in the 14-3-3 γ knockdown cells restored DPI/II and DSG2 to the cell border and to determine if the PG-EGFP-f expressing 14-3-3 γ knockdown cells formed functional desmosomes and had increased cell-cell adhesion, hanging drop assay was done. Briefly, HCT116 derived 14-3-3 γ knockdown cells were transfected with pCDNA3.1 EGFP-f Puro and pCDNA3.1 PG-EGFP-f Puro and 24 hours post transfection puromycin was added. After 3 days in puromycin selection, cells were used for performing hanging drop assay as described in [201]. As shown in Figure 5.14, it was observed that the PG-EGFP-f expressing cells formed fewer but larger cell aggregates when compared to the cells expressing EGFP-f. The formation of cell aggregates is dependent on cell-cell adhesion and therefore PG-EGFP-f expressing cells formed desmosomes which led to the increase in cell-cell adhesion.



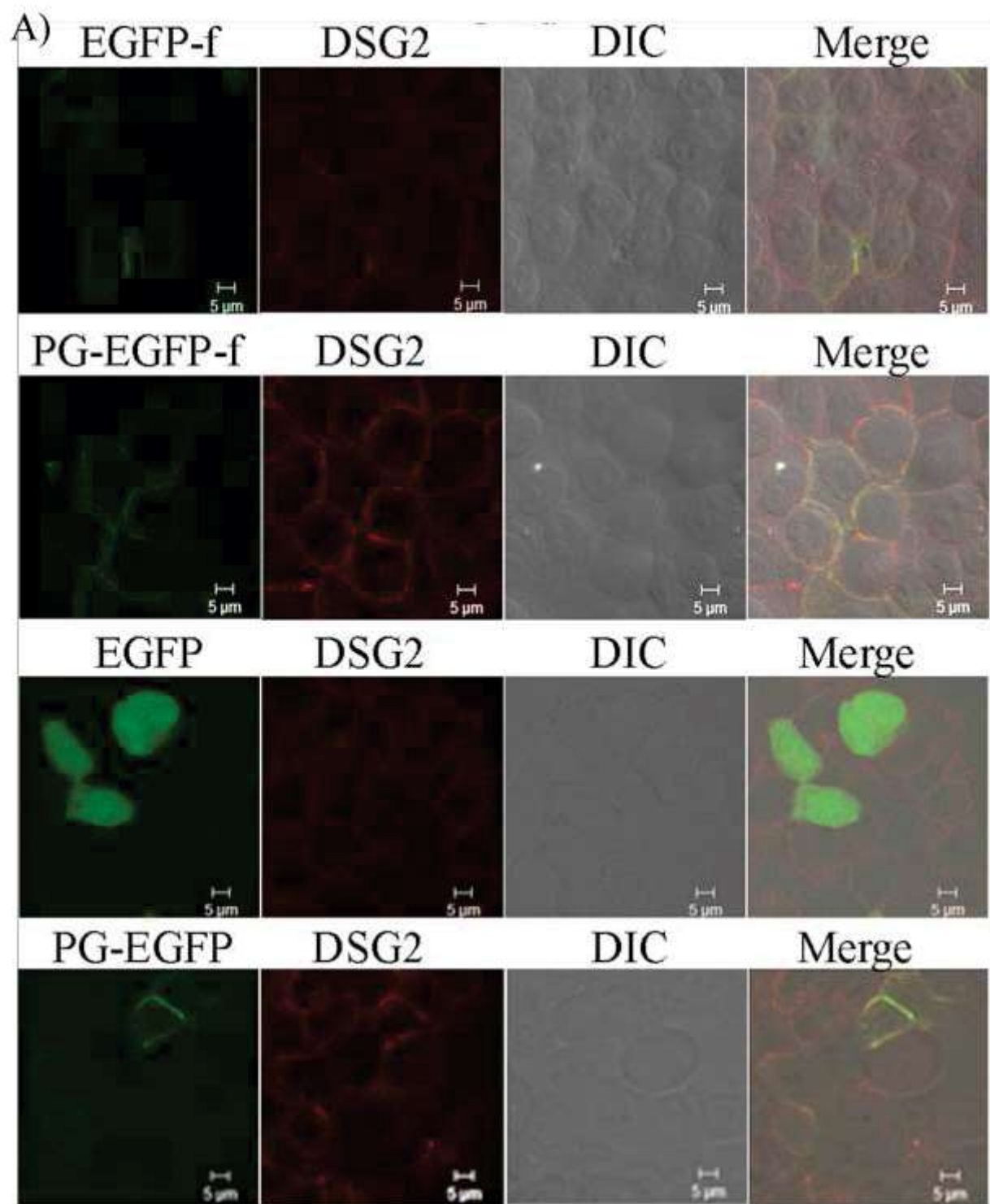
B)

Cell line	Aggregates per field			
	$<2.5 \cdot 10^4 - 1 \cdot 10^4 \mu\text{m}^2$	$<1 \cdot 10^4 - 1.5 \cdot 10^3 \mu\text{m}^2$	$<1.5 \cdot 10^3 - 0.35 \cdot 10^3 \mu\text{m}^2$	$<0.35 \cdot 10^3 \mu\text{m}^2$
14-3-3 γ kd EGFP-f	0	2	20	28
14-3-3 γ kd PG-EGFP-f	1	5	15	10

Figure 5.14: HCT116 derived 14-3-3 γ knockdown cells expressing PG-EGFP-f have increased cell-cell adhesion. A-B. Hanging drop assays were performed to determine cell-cell adhesion in HCT116 derived 14-3-3 γ knockdown cells expressing EGFP-f or PG-EGFP-f. Images of cell aggregates were obtained with a Zeiss Axiovert 200M inverted microscope with a 10X objective. Representative images are shown and scale bars are shown in each panel. The size and number of clusters is indicated in the table [228].

5.1.12 PG-EGFP-f/PG-EGFP restores desmosome formation in PG knockdown cells

Cells with a knockdown of PG cannot form desmosomes and the transport of other desmosomal proteins is disrupted in the PG knockdown cells [202]. To ascertain that the PG-EGFP-f does not require the endogenous PG to stimulate transport of desmosomal proteins to the cell border or to stabilize desmosomal proteins, PG knockdown cells were transfected with the EGFP-for shRNA resistant PG-EGFP-f or EGFP or shRNA resistant PG-EGFP and stained with the antibodies to DSG2. As shown in Figure 5.15 A, both PG-EGFP-f and PG-EGFP could restore the cell border localization of DSG2 in PG knockdown cells. A western blot showing the levels of different desmosomal proteins is shown in the Figure 5.15 B. PG knockdown cells have reduced levels of DP, DSG2 and DSC2/3 when compared to the vector control cells and there was a slight increase in the DPI/II levels in the PG knockdown cells upon PG-EGFP-f or PG-EGFP expression. These results suggested that the PG-EGFP-f did not require endogenous PG to restore desmosomal protein transport to the cell border. PG-EGFP did not localize to the cell border in 14-3-3 γ knockdown cells but PG-EGFP localized to the cell border in the PG knockdown cells supporting the fact that in the presence of 14-3-3 γ PG is transported to the cell border [150].



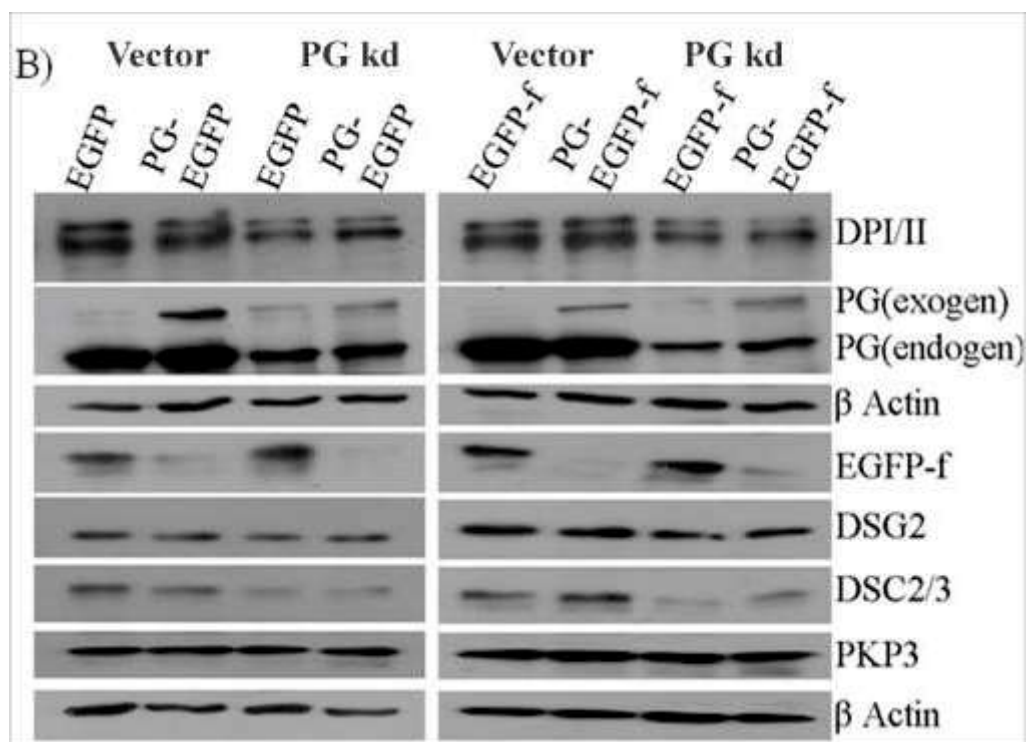
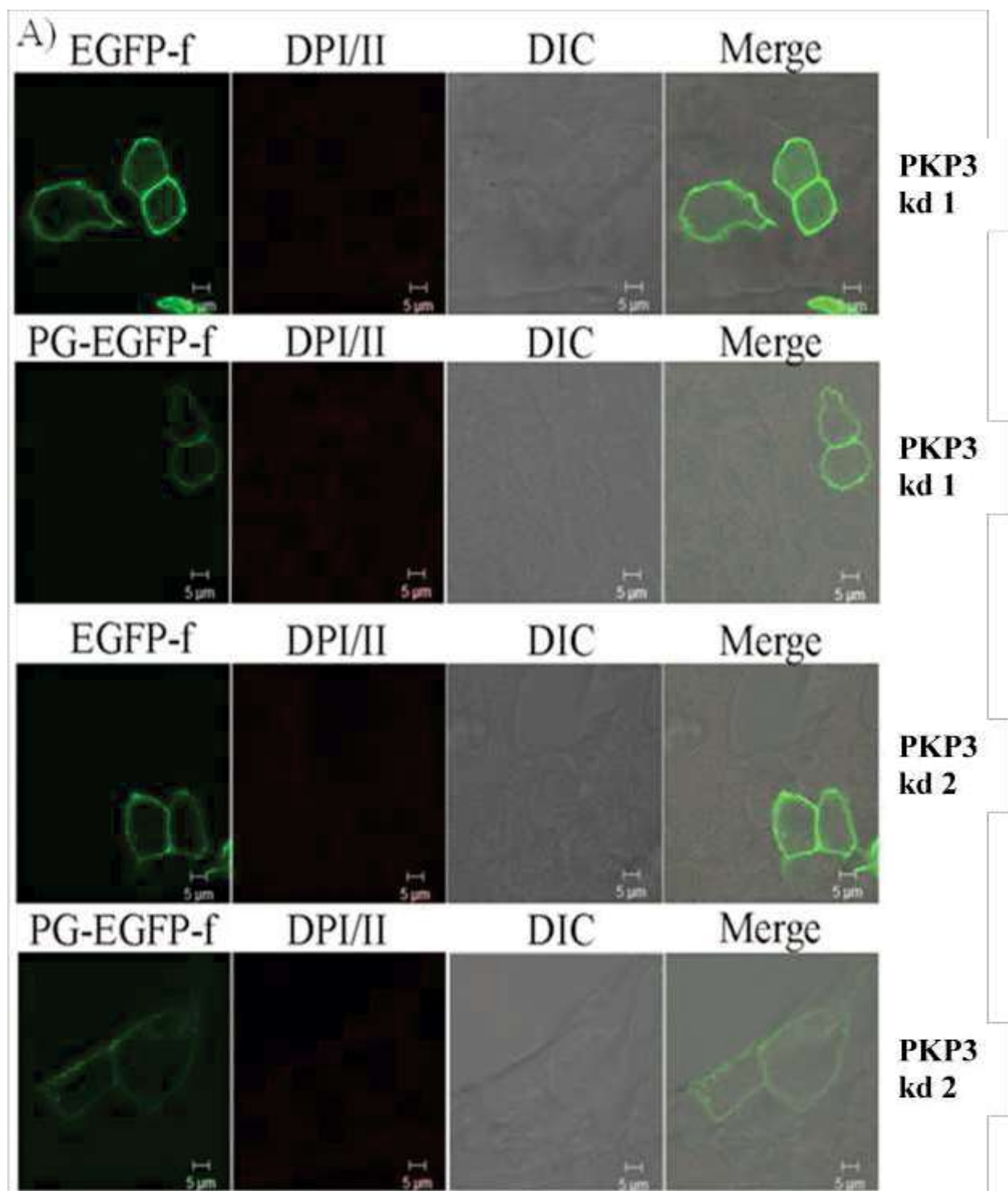
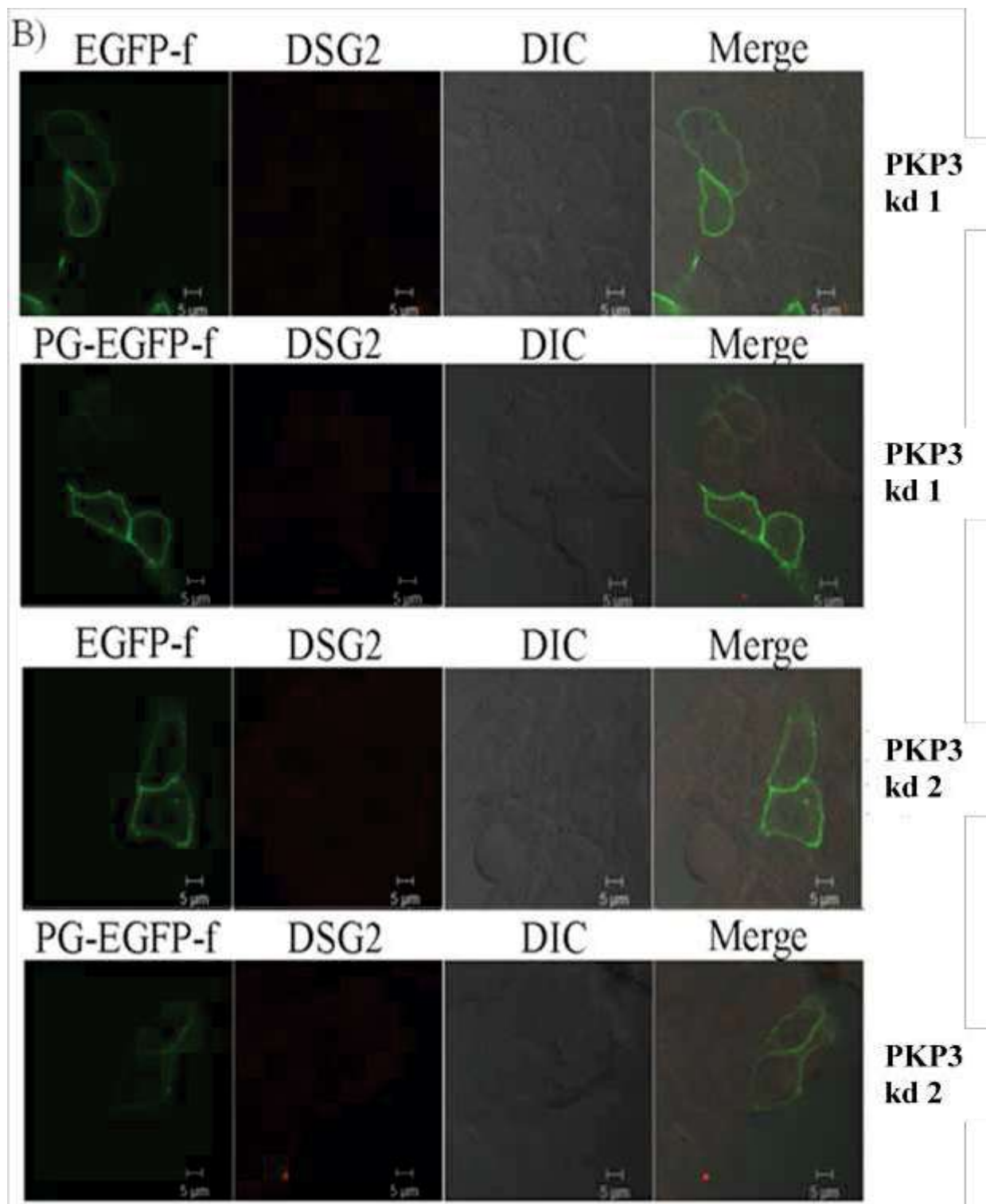


Figure 5.15: PG-EGFP-f rescued desmosomal protein localization in the PG knockdown cells. **A.** HCT116 derived PG knockdown clone was transfected with either EGFP-f or PG-EGFP-f or EGFP or PG-EGFP (green) and were stained with antibodies to DSG2 (red) followed by confocal microscopy. Representative images are shown and scale bars are shown in each panel. **B.** Protein extracts of HCT116 derived PG knockdown clones were transfected with either EGFP-f or PG-EGFP-f or EGFP or PG-EGFP were prepared and resolved on SDS-PAGE gels followed by Western blotting with the indicated antibodies. Western blots for β Actin served as a loading control. PG (exogen) is over expressed/exogenous PG and PG (endogen) is endogenous PG [228].

5.1.13 PG-EGFP-f requires PKP3 to restore desmosome formation

PG-EGFP-f could restore desmosome formation in the cells lacking endogenous PG to determine whether PG-EGFP-f requires PKP3 for rescuing desmosome formation, PKP3 knockdown cells, which does not form desmosomes because in these cells only PG is localized to the cell border [202], were transfected with EGFP-f or PG-EGFP-f and stained with the antibodies to DP and DSG2. As shown in Figure 5.16 A-C, PG-EGFP-f could not restore DP and DSG2 to the cell border suggesting that PG-EGFP-f just like endogenous PG requires PKP3 for desmosome assembly [202]. A Western blot showing the levels of different desmosomal proteins is shown in the Figure 5.16 D. The transfection efficiency for the PG-EGFP-f in vector control cell was less because of which PG-EGFP-f expression was not detected with Western blotting.





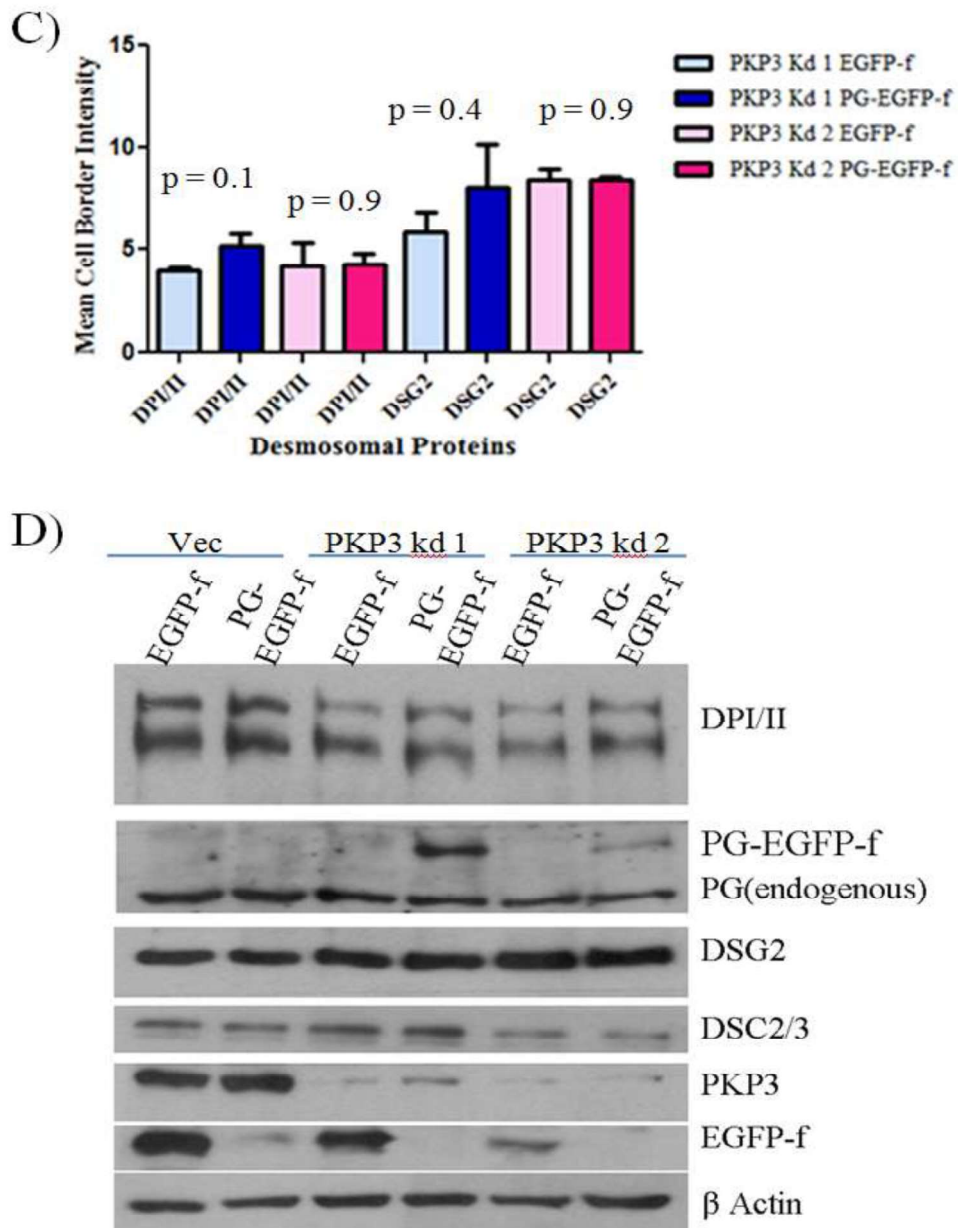


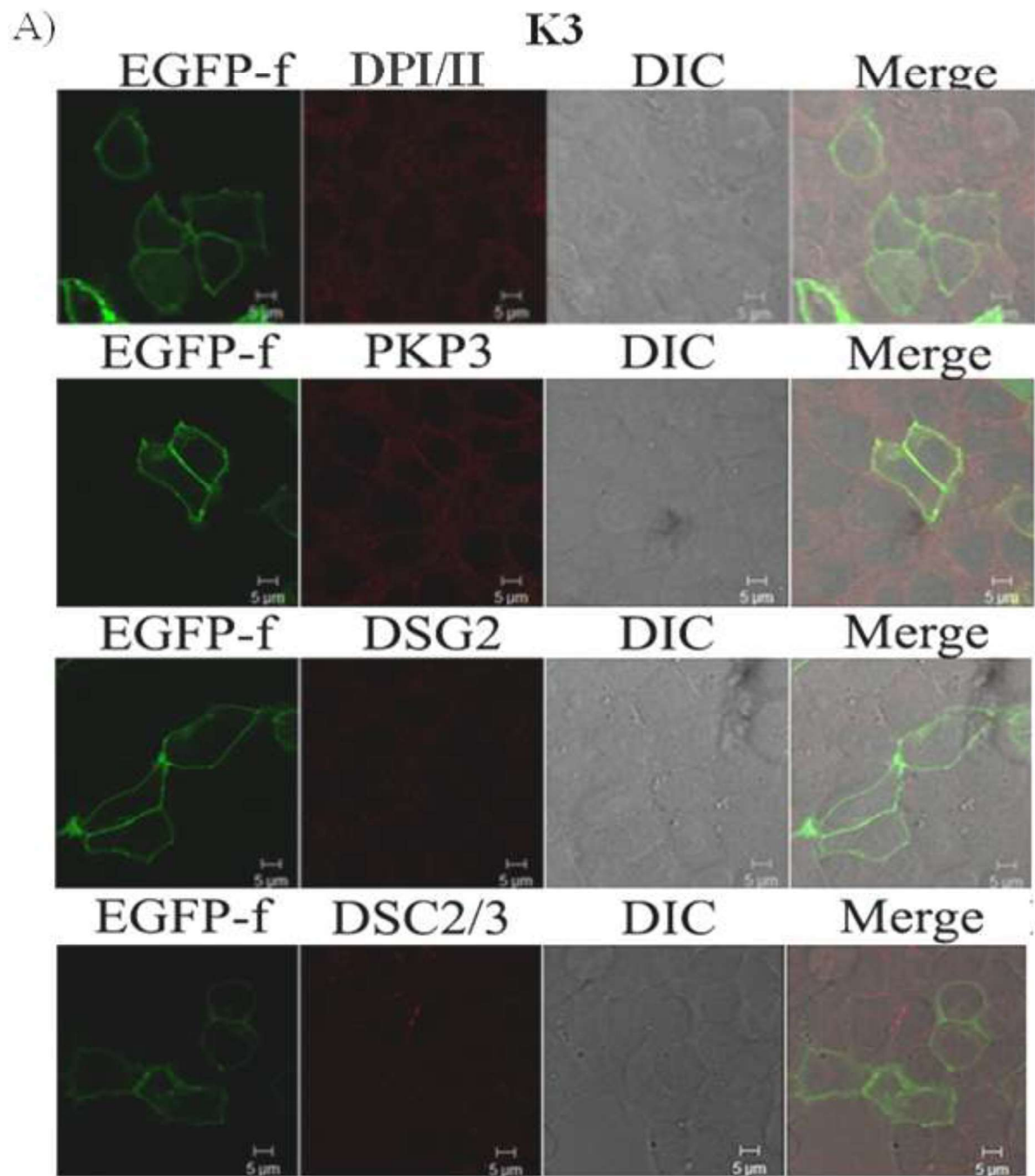
Figure 5.16: PG-EGFP-f requires PKP3 to restore desmosomal protein to the cell border.

A-B. HCT116 derived PKP3 knockdown clones were transfected with either EGFP-f or PG-EGFP-f (green) and were stained with antibodies to DPI/II (red) [A] or DSG2 [B] followed by confocal microscopy. Images were obtained on a Zeiss LSM 780 confocal microscope using a 63X objective and 2X optical zoom. Representative images are shown and scale bars are shown in each panel. **C.** The intensity of border staining, for the different desmosomal proteins, was

measured for 33 transfected cells in three different experiments and the mean cell border intensity and standard error from three different experiments is plotted. *p value* was calculated using student's t-test **D**. Protein extracts prepared from HCT116 derived vector control and PKP3 knockdown clones expressing EGFP-f or PG-EGFP-f were resolved on SDS-PAGE gels followed by Western blotting with the indicated antibodies. Western blots for β Actin served as a loading control [228].

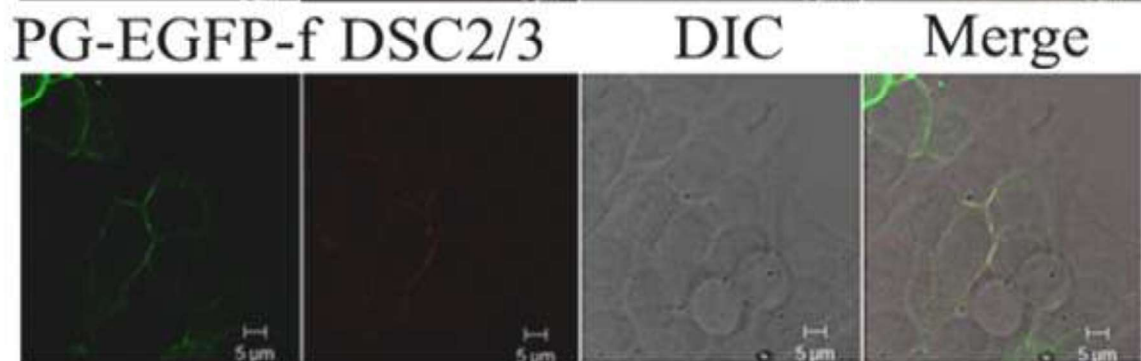
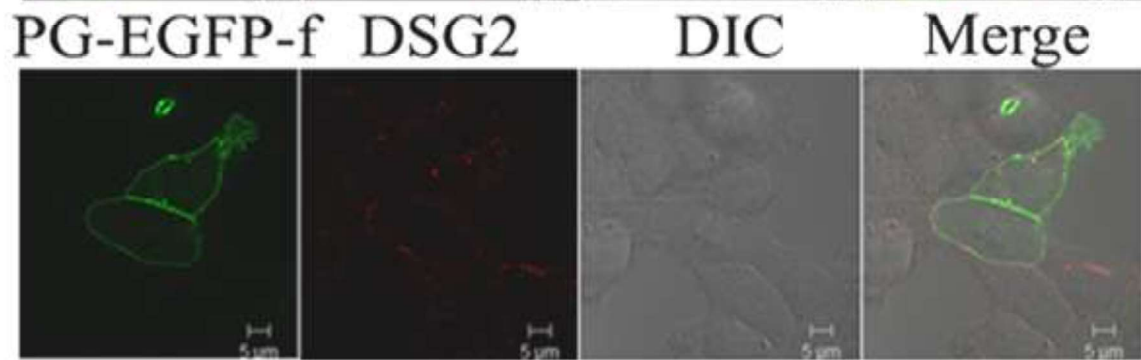
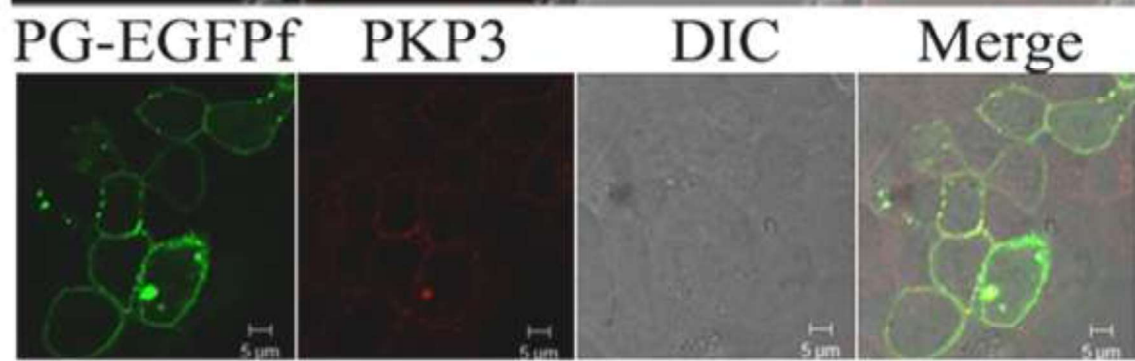
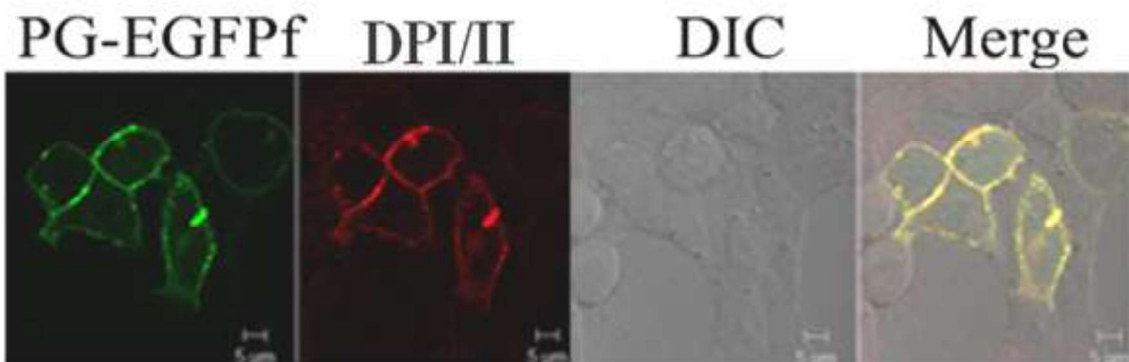
5.1.14 PG-EGFP-f requires KIF5B to restore DSG2 to the cell border

It was shown previously that γ 14-3-3 binds to PG and loads PG on to the motor protein KIF5B and KIF5B transports PG from cytoplasm to the cell border. In the absence of KIF5B desmosomal proteins are not transported to the cell border and cell-cell adhesion is decreased [150]. To determine if the role of KIF5B is just to mediate transport of PG to initiate desmosome assembly, KIF5B knockdown cells were transfected with EGFP-f or PG-EGFP-F and stained with the antibodies for the desmosomal proteins. As shown in Figure 5.17 A to E, PG restored DPI/II to the cell border but failed to restore other desmosomal proteins to the cell border suggesting that the cell border localization of DSG2, DSC2/3 and PKP3 is dependent on KIF5B. The Western blot analysis of the KIF5B knockdown cells transfected with EGFP-f or PG-EGFP-f showed that there was an increase in DPI/II levels in the PG-EGFP-f expressing KIF5B knockdown cells (Figure 5.17 F). Western blots also showed that as compared to the vector control cells KIF5B knockdown cells had reduced levels of desmosomal cadherins. All these results support the fact that the PG localization is required for the DPI/II cell border localization but to recruit desmosomal cadherins KIF5B and PKP3 are required.



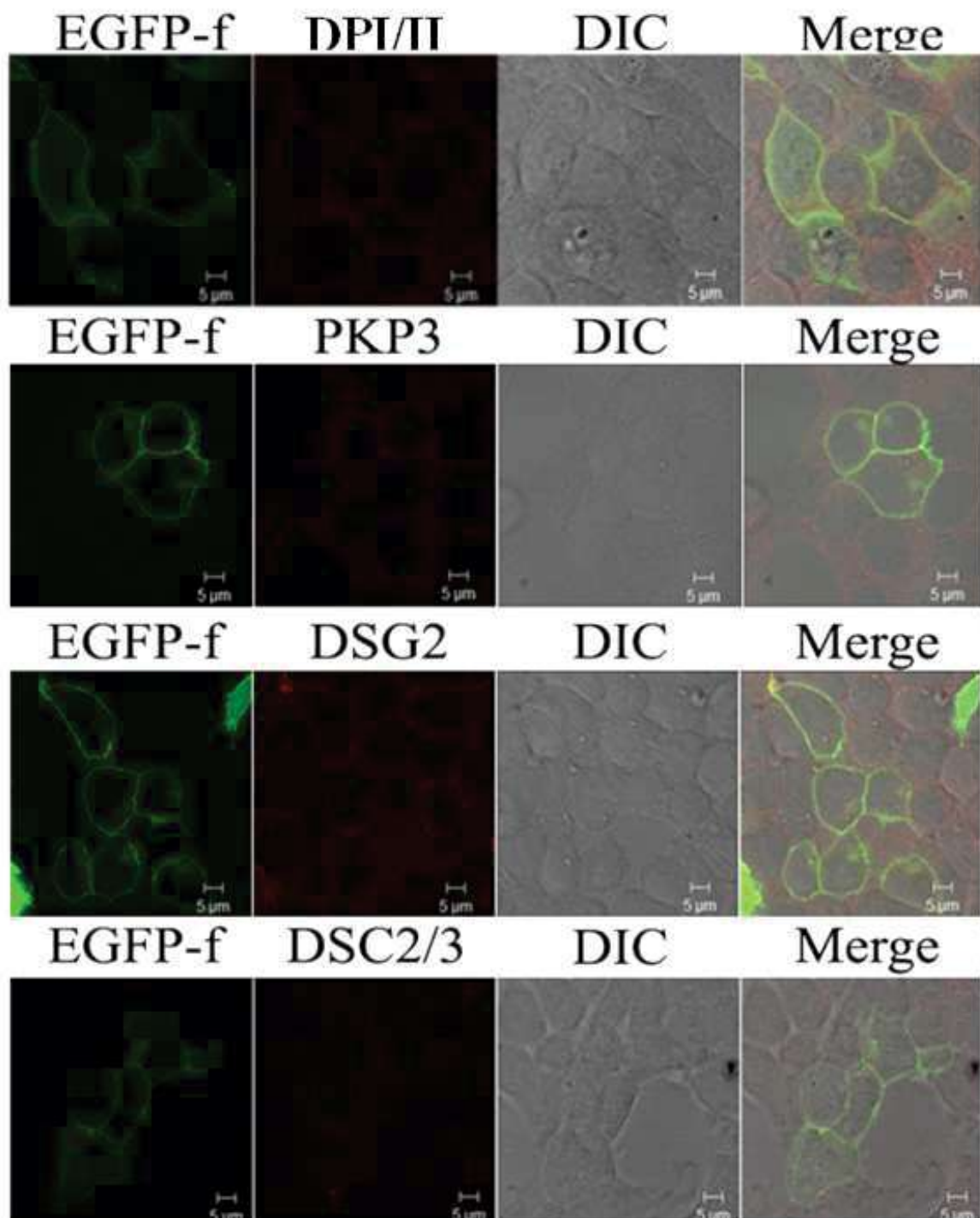
B)

K3



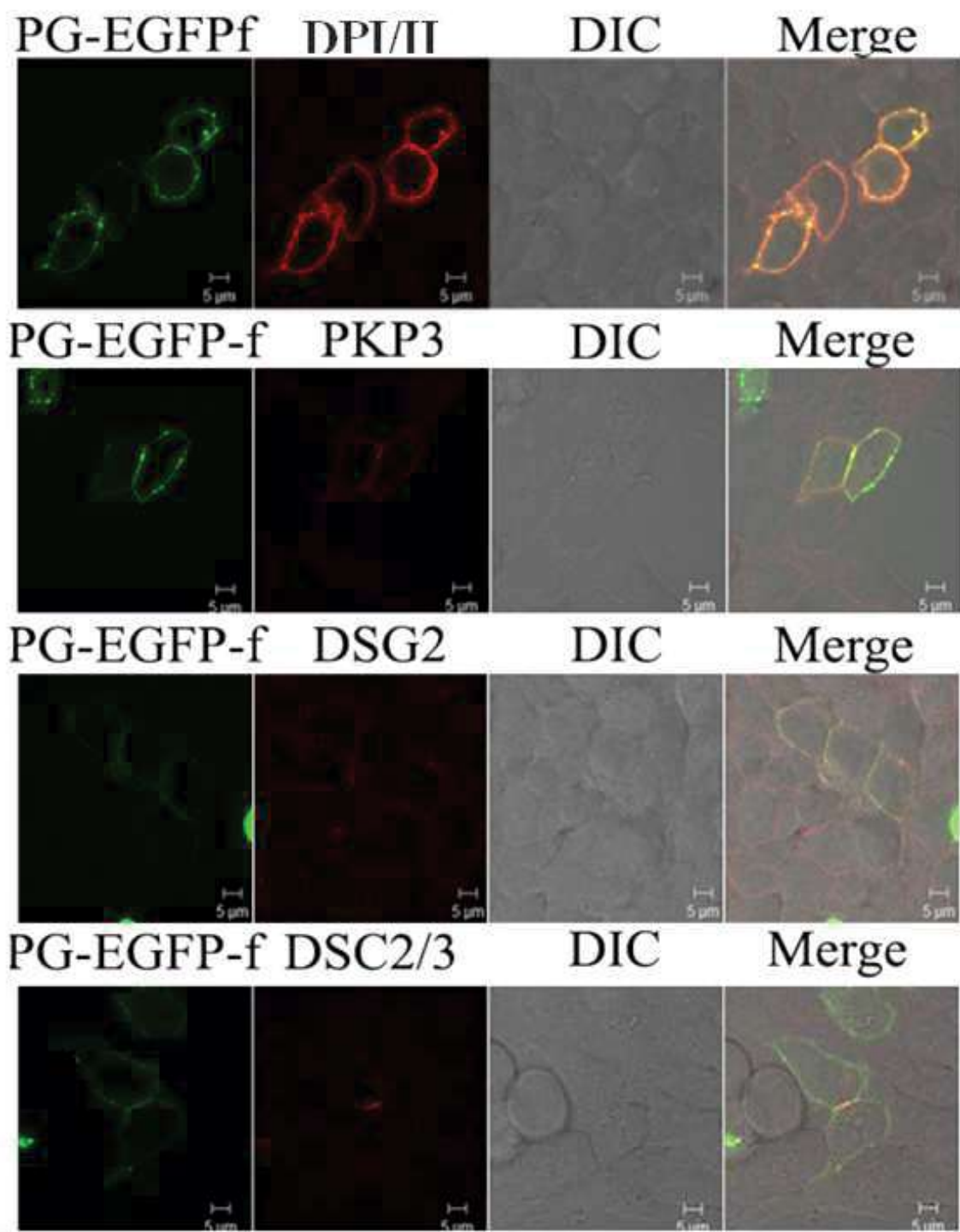
C)

K5



D)

K5



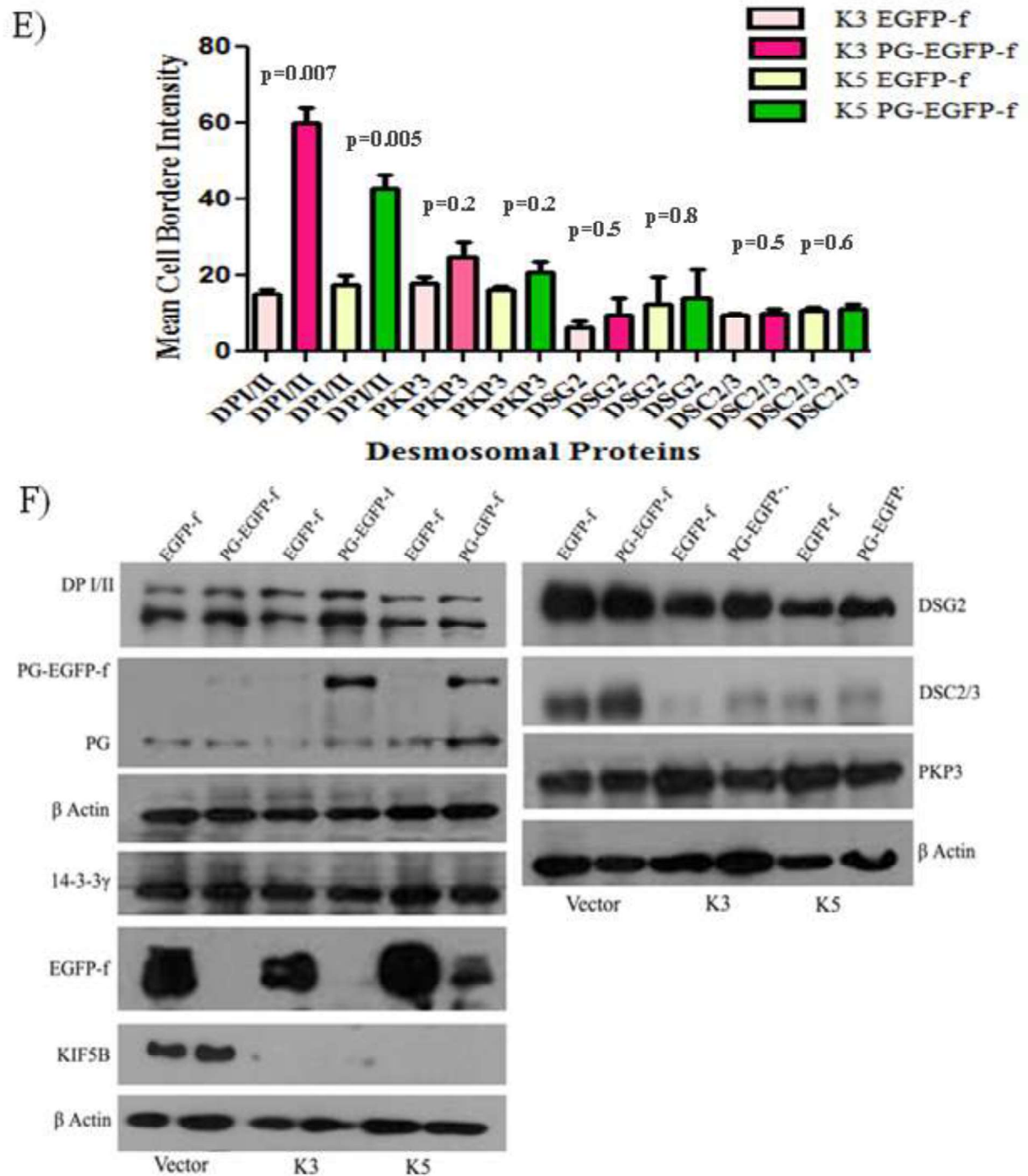


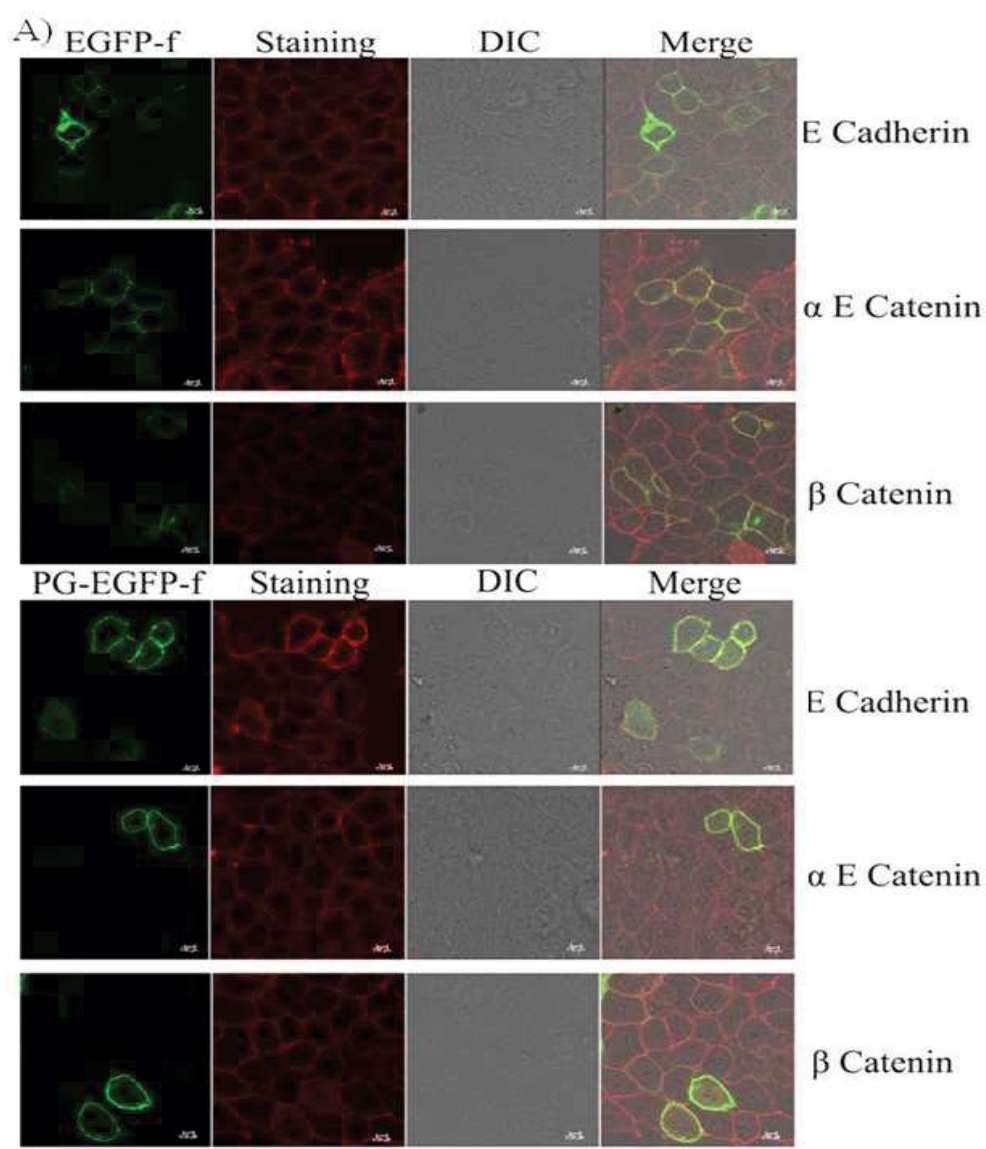
Figure 5.17: PG-EGFP-f requires KIF5B to restore desmosomal cadherins to the cell border. **A.** HCT116 derived KIF5B knockdown clone K3 was transfected with EGFP-f (green) and was stained with indicated antibodies (red) followed by confocal microscopy. **B.** HCT116

derived KIF5B knockdown clone K3 was transfected with PG-EGFP-f (green) and was stained with indicated antibodies (red) followed by confocal microscopy. **C.** HCT116 derived KIF5B knockdown clone K5 was transfected with EGFP-f (green) and was stained with indicated antibodies (red) followed by confocal microscopy. **D.** HCT116 derived KIF5B knockdown clone K5 was transfected with PG-EGFP-f (green) and was stained with indicated antibodies (red) followed by confocal microscopy. Images were obtained on a Zeiss LSM 780 confocal microscope using a 63X objective and 2X optical zoom. Representative images are shown and scale bars are shown in each panel. **E.** The intensity of border staining, for the different desmosomal proteins, was measured for 33 transfected cells in three different experiments and the mean cell border intensity and standard error from three different experiments is plotted. *p value* was calculated using student's t-test **F.** Protein extracts prepared from HCT116 derived vector control and PKP3 knockdown clones expressing EGFP-f or PG-EGFP-f were resolved on SDS-PAGE gels followed by Western blotting with the indicated antibodies. Western blots for β Actin served as a loading control.

5.1.15 PG-EGFP-f expression does not alter the localization or levels of adherens junction proteins

PG is a component of adherens junction and therefore, change in localization of PG might affect the adherens junction but it was observed that the loss of 14-3-3 γ did not affect the levels or localization of adherens junction proteins [150]. To determine if the PG-EGFP-f expression in 14-3-3 γ knockdown cells altered the levels or localization of adherens junction proteins, 14-3-3 γ knockdown cells were transfected with EGFP-f or PG-EGFP-f and stained with the antibodies to

adherens junction proteins. As shown in Figure 5.18 A and B, the localization of the adherens junction proteins did not change upon PG-EGFP-f expression but some PG-EGFP-f expressing cells showed pan-cellular staining for β catenin. A Western blot showing the levels of different adherens junction proteins is shown in the Figure 5.18C. A slight increase in β catenin levels are seen in the cells expressing PG-EGFP-f. These results suggested that the PG-EGFP-f expression in 14-3-3 γ knockdown cells does not majorly affect adherens junction protein expression or localization.



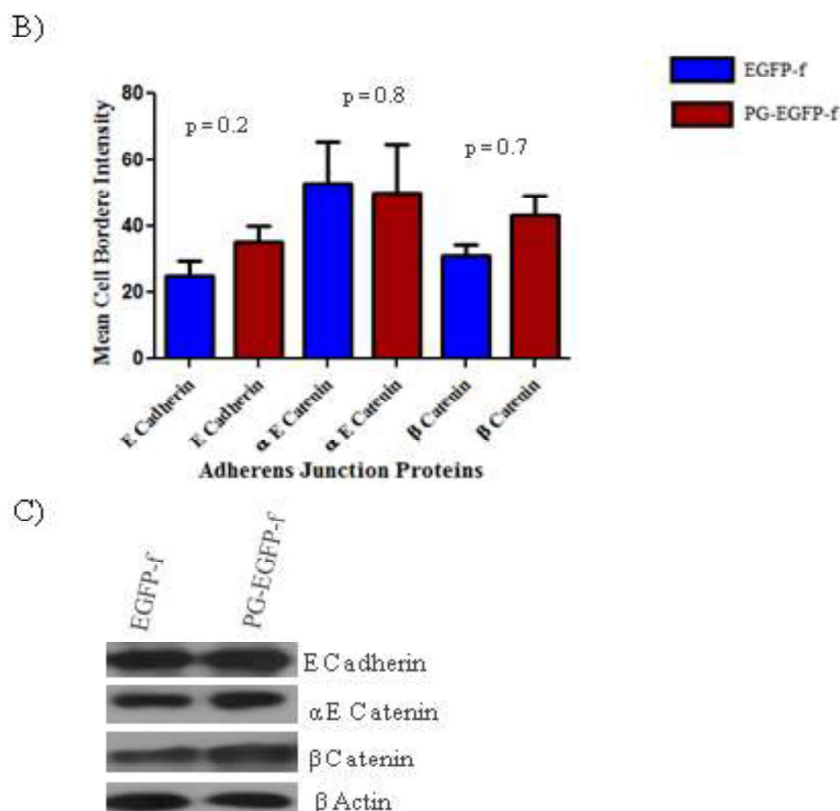


Figure 5.18: PG-EGFP-f does not affect adherens junction protein localization. A. HCT116 derived 14-3-3 γ knockdown cells were transfected with either EGFP-f or PG-EGFP-f (green) and were stained with indicated antibodies (red) followed by confocal microscopy. Images were obtained on a confocal microscope using Leica TCS SP8 Confocal microscope using a 63X objective and 2x optical zoom. Representative images are shown and scale bars are shown in each panel. **B.** The intensity of border staining, for the different adherens junction proteins, was measured for 33 transfected cells in three different experiments and the mean cell border intensity and standard error from three different experiments is plotted. *p* value was calculated using student's t-test **C.** Protein extracts prepared from HCT116 derived 14-3-3 γ knockdown clones expressing EGFP-f or PG-EGFP-f were resolved on SDS-PAGE gels followed by

Western blotting with the indicated antibodies. Western blots for β Actin served as a loading control.

5.2 Discussion

It was observed that the loss of 14-3-3 γ disrupted spermatogenesis and cell-cell adhesion in testis. To identify the mechanism by which 14-3-3 γ regulates cell-cell adhesion, interacting partners of 14-3-3 γ were identified by GST pulldown assay and it was found that 14-3-3 γ interacts with PG, DP and PKP3 [150]. Moreover, transport of the desmosomal proteins was compromised in the HCT116 cells lacking 14-3-3 γ suggesting 14-3-3 γ regulates transport of desmosomal proteins [150]. To understand the mechanism by which 14-3-3 γ regulated the transport of desmosomal proteins this study was carried out.

Scansite software predicted that DP and PKP3 had multiple 14-3-3 binding sites making it difficult to identify the function of each of the 14-3-3 binding site present on these proteins. Scansite software predicted that the PG had a single 14-3-3 γ binding site which is S236 and is phosphorylated by PKC μ . To test the predictions of Scansite software GST PG 1-300 was made and using recombinant PKC μ *in vitro* protein kinase assay was performed. It was observed that the GST PG 1-300 is a substrate of the recombinant PKC μ . In the absence of PKC μ PG did not localize to the cell border and the levels of PG were also affected suggesting PKC μ is important for the PG transport and stability. The S236A mutant which will not be phosphorylated by PKC μ failed to bind 14-3-3 γ and failed to localize to the cell border supporting the fact that the PG phosphorylated at S236 residue by PKC μ binds to 14-3-3 γ and is transported to the cell border. It was shown in the lab that the kinesin motor protein KIF5B is an interacting partner of 14-3-3 γ [150]. Loss of KIF5B in testis also led to disrupted spermatogenesis and cell-cell adhesion.

KIF5B loss in HCT116 cells led to the loss of desmosome formation due to disrupted desmosomal protein transport[150]. On the basis of these results it was suggested that PG-14-3-3 γ complex is loaded on to the KIF5B to transport PG from cytoplasm to the cell border [150].

This was the first report which highlighted the role of 14-3-3 γ in transport of desmosomal proteins DP, PG, PKP3, DSG2 and DSC2/3. The effect on DSG2 and DSC2/3 transport observed upon 14-3-3 γ loss could be the result of the defect in transport of PKP3, DP and PG as these proteins are important to stabilize desmosomal cadherins. Shafraz O., *et al.*, recently showed that when the E-cadherin is stabilized on the cell border after the formation of adherens junctions between the two cells, E-cadherin interacts laterally with DSG2 on the same cell to stabilize DSG2 and initiate nascent desmosome formation [235]. Similarly, the localization and initial stabilization of DSG2 at the cell border could be mediated by the E-cadherin in 14-3-3 γ knockdown cells but the absence of armadillo proteins and plaque proteins at the cell border inhibits desmosome formation and DSG2 is transported back to the cytoplasm, as shown in Figure 5.19B. To determine if the major function of 14-3-3 γ was to mediate PG transport in desmosome assembly, PG-EGFP-f was expressed in the 14-3-3 γ knockdown cells. The results in this report indicated that targeting PG to the cell border in 14-3-3 γ knockdown cells resulted in an increase in the localization of desmosomal proteins to the cell border, an increase in cell-cell adhesion and an increase in desmosome formation. These results suggest that the major role of 14-3-3 γ in regulating desmosome formation is to stimulate the KIF5B mediated transport of PG to the cell border. The formation of 14-3-3 γ -PG-KIF5B complex is important for PG transport and recruitment of PG to the cell border. The disruption of this complex affects desmosome assembly as seen in 14-3-3 γ , KIF5B and PG knockdown cells. In 14-3-3 γ and PG knockdown cells rescuing PG localization helps in restoring desmosome formation.

14-3-3 γ formed a complex with PKP3, PG and DP [150]. Therefore, the defects in desmosome formation in HCT116 cell line could have resulted from the mis-localization of both PG and PKP3 to the cell border. PG is required for the recruitment of PKP3 and other desmosomal proteins to the cell border [202] and the results in this report indicate that localizing PG to the cell border is sufficient to restore cell-cell adhesion in the 14-3-3 γ knockdown cells. Importantly, the over-expression of PG-EGFP, which does not localize to the cell border in 14-3-3 γ knockdown and KIF5B knockdown cells, did not restore the localization of DP to the cell border. However, consistent with previously published data [150, 202, 236] the farnesylated PG could not stimulate desmosome formation in cells lacking PKP3. These results lend further credence to the model that 14-3-3 γ is required for transport of PG to the cell border, which is followed by the 14-3-3 γ mediated transport and recruitment of PKP3 resulting in the formation of an intact desmosome.

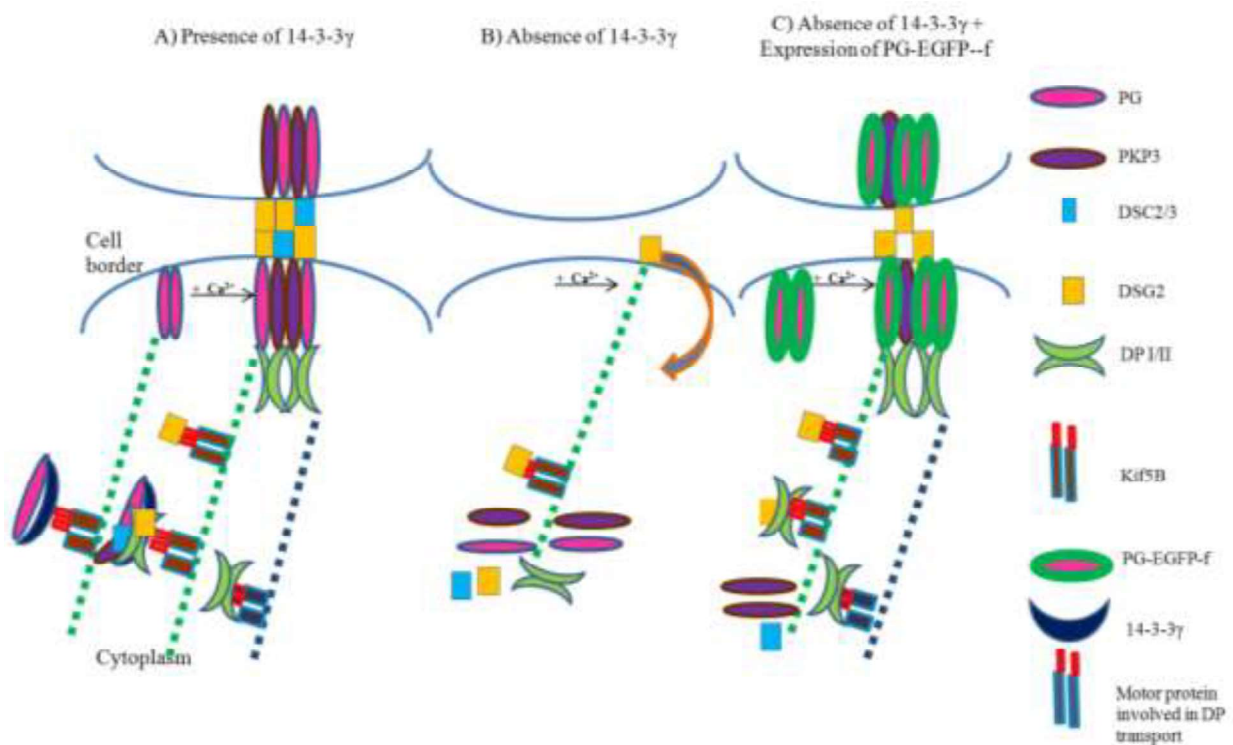


Figure 5.19: Model illustrating the role of PG and 14-3-3 γ in regulating desmosome assembly. A) In low calcium media, PG is localized to the cell border but the other desmosomal components remain in the cytoplasm. Upon calcium addition, the other components are transported to the cell border (either in complex with one another or individually) by KIF5B to form an intact desmosome. DP could be transported by some other motor protein. B) In the absence of 14-3-3 γ , PG is not transported to the border, either in the presence or absence of calcium, leading to a decrease in desmosome formation. The desmosomal cadherins might be transported to the border but might not be retained at the border due to the absence of PG and other plaque proteins. C) When PG is artificially targeted to the cell border (PG-EGFP-f) in HCT116 cells lacking 14-3-3 γ , a restoration of desmosome function is observed with the desmosomal proteins being transported either in complex with one another or individually to the cell border. Adapted from [228].

The presence of PG at the cell border resulted in the recruitment of DP, DSG2 and PKP3 to the cell border, but could not recruit DSC2/3 to the cell border. These results are consistent with a previously published report which suggests that localization of PG at the cell border is required for DP localization at the cell border [237]. Further, the retention of DP at the cell border in cells lacking KIF5B suggests that motor proteins other than KIF5B are required for the transport of DP to the cell border. PG has been demonstrated to form a strong complex *in vitro* with DSG2, but its interaction with DSC2 is weak [238] and loss of PG affected localization of DSG2 to the border [237]. PG might form a complex with DSG2 and transport DSG2 to the cell border as PG has been shown to bind another DSG family member, DSG3, which results in the localization of DSG3 to the cell border [238, 239]. Alternatively, DSG2 retention at the cell border may not be stable in the absence of PG because its cytoplasmic tail is not anchored to an Armadillo family

protein. DSG2 is not localized to the cell border in cells lacking KIF5B even after expressing PG-EGFP-f. This is consistent with previous studies which have demonstrated that KIF5B is required for the transport of DSG2 to the cell border [240]. Thus increasing PG levels at the cell border is sufficient to induce desmosome formation in cells lacking 14-3-3 γ but not in cells lacking KIF5B.

The recruitment of DSC2/3 to the cell border might be dependent on the presence of PKP3 at the cell border [202, 241, 242] and since the increase in PKP3 levels at the cell border is partially attenuated in the PG-EGFP-f expressing cells, this might be the reason why DSC2/3 does not localize to the border in these cells. These results are consistent with previously published reports suggesting that the presence of DSC2 with PKP2 or PKP3 is sufficient to induce desmosome formation in cells [241]. Alternatively, it is possible that the recruitment of PKP3 to the cell border in cells expressing PG-EGFP-f is normal but its retention at the border is compromised in the absence of DSC2/3 at the cell border. This is consistent with our observations suggesting that the retrograde transport of PG and PKP3 occurs via vastly different mechanisms in HCT116 cells [243].

The loss of KIF5B in HCT116 cells led to the disruption of desmosome formation and cytoplasmic localization of all the desmosomal proteins (DP, PG, PKP3, DSG2 and DSC2/3) but it was not clear if KIF5B is required for the transport of all the desmosomal proteins [150]. Previous report suggested that the DSC2 transport is mediated by Kinesin 2 i.e. KIF3A [240] but the loss of KIF5B affected the DSC2 transport as well. In order to understand the role KIF5B in transporting all the desmosomal components we expressed PG-EGFP-f in the KIF5B knockdown cells and observed that PG-EGFP-f could not rescue the cell border localization of PKP3, DSG2 and DSC2/3. This data highlighted the importance of KIF5B in DSG2, PKP3 and DSC2/3

transport. As mentioned above DSC2/3 transport is mediated by the KIF3A [240] but DSC2/3 transport is also dependent on PKP3 localization at the cell border [211, 241, 242] and therefore, it will be interesting to study if rescuing PKP3 localization to the cell border could rescue the transport of DSC2/3 in the KIF5B knockdown cells. The recruitment of DP to the cell border in PG-EGFP-f expressing KIF5B knockdown cells also suggests that if PG is stabilized at the border then DP is stabilized at the cell border. DP connects intermediate filaments to the desmosome and therefore it remains elusive whether DP connects the intermediate filaments to PG-EGFP-f in the KIF5B knockdown cells. Also, it is not clear whether DP is transported to the cell border in the absence of KIF5B and recycled back because the armadillo proteins are not present at the border (Figure 5.20 B).

The loss of KIF5B in HCT116 cells also affected the protein levels of desmosomal cadherins suggesting that the cytoplasmic localization of the desmosomal cadherins affected the protein stability of desmosomal cadherins. This supports the finding that stability of desmosomal proteins increases when localized to the cell border. Similarly, KIF5B knockdown cells expressing PG-EGFP-f showed increased DP levels which could be due to the increased cell border localization of DP in these cells [209, 212, 231].

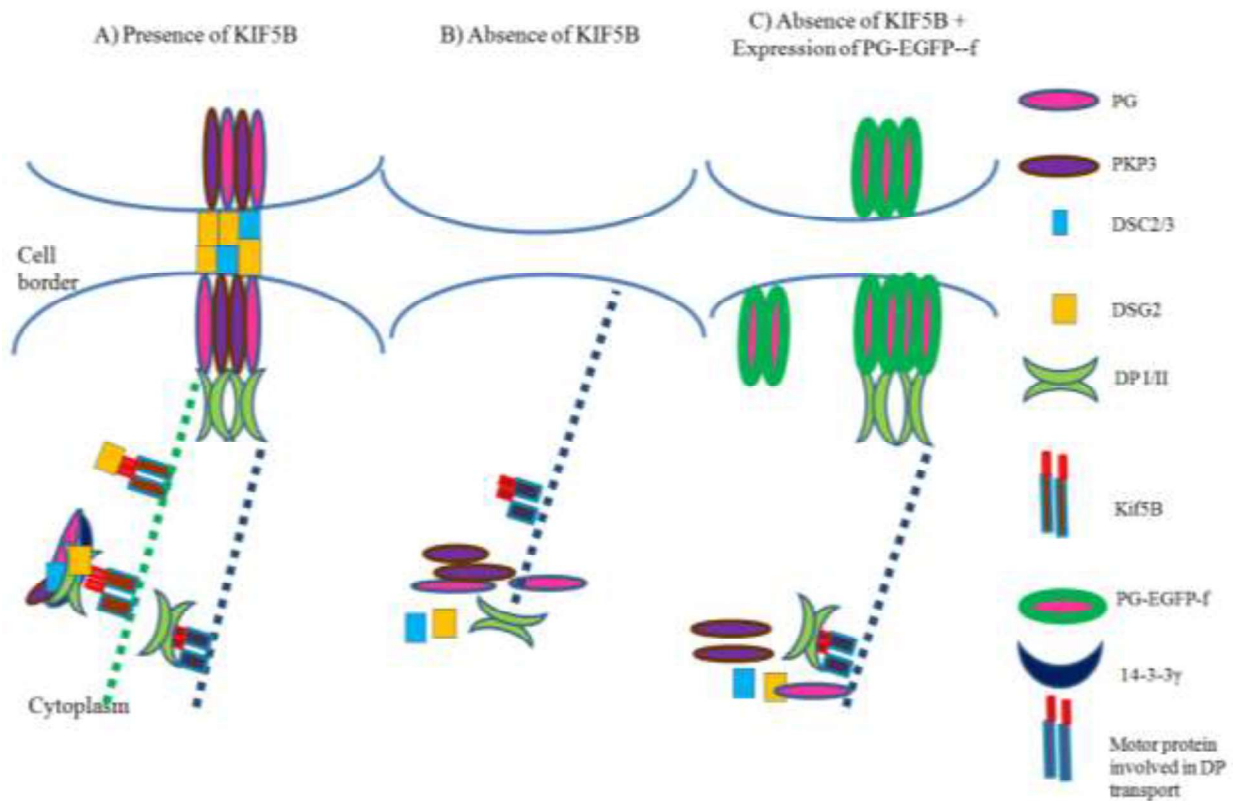


Figure 5.20: Model illustrating the role of PG and KIF5B in regulating desmosome assembly. **A)** Desmosome assembly in the wild type HCT116 cells, where PG and the other desmosomal components are transported to the cell border (either in complex with one another or individually) by KIF5B to form an intact desmosome. DP could be transported by some other motor protein. **B)** In the absence of KIF5B, none of the desmosomal proteins are transported at the cell border. **C)** When PG is artificially targeted to the cell border (PG-EGFP-f) in HCT116 cells lacking KIF5B, DP is transported to the cell border and stabilized by PG-EGFP-f.

Given the data in this thesis and previous results about the role of the Armadillo proteins in desmosome assembly, we would like to propose the following model (Figure 5.19). 14-3-3 γ and KIF5B are required for the transport of PG to the cell border [150]. The forced localization of PG to the cell border in cells lacking 14-3-3 γ , results in the localization of DSG2, PKP3 and DP at

the cell border thus stimulating desmosome formation. Previous reports from multiple laboratories have suggested a hierarchy in the accumulation of desmosome formation where PKP3 is required to recruit DP to the desmosome precursors, PKP2 is required to recruit the DP containing desmosome precursors to the cell border and DP recruitment to cell border is further stimulated by PKP3 recruitment to the border [244]. Our previous results suggest that PG is required for the recruitment of PKP3 to the cell border to initiate desmosome formation [202]. The inability of PG-EGFP-f to recruit DSC2/3 to the cell border might be due to the incomplete recruitment of PKP3 to the cell border as while an increase in PKP3 levels is observed at the cell border in 14-3-3 γ knockdown cells expressing PG-EGFP-f, a complete restoration of PKP3 levels at the cell border is not observed in these cells. This might be due to the fact that an artificial targeting construct has been used to localize PG to the cell border in these cells. Alternatively, as PKP3 also forms a complex with 14-3-3 γ [150], the absence of 14-3-3 γ could result in a defect in either the transport of or retention of PKP3 at the cell border. This is consistent with our data suggesting that cells lacking KIF5B do not induce PKP3 transport to the cell border. Taken together our results suggest that the different components of the desmosome might be transported independently to the cell border to initiate the process of desmosome formation following which complexes containing pre-assembled desmosome components can integrate with the initial structure as previously described [238]. To conclude, our results suggest that one major role of the 14-3-3 γ /KIF5B complex is to mediate the transport of PG to the cell border and the 14-3-3 γ /KIF5B complex also play a role in the transport of PKP3 to the cell border.

On the basis of the present study we propose that in physiological conditions, the KIF5B mediated transport of PG by 14-3-3 γ is the first step in desmosome assembly. Presence of PG at

the cell border then signals for the motor protein mediated transport of DP and PKP3 at the border individually or in complex with other desmosomal cadherins to form desmosomes. Alternatively, desmosomal cadherins could be transported before the initiation of desmosome formation [235] and recruitment of PG and PKP3 stabilizes the desmosomal cadherins to initiate desmosome assembly.

6. Conclusions

6. Conclusions

Previous work from the laboratory demonstrated that 14-3-3 γ is required for spermatogenesis and cell to cell adhesion. On the basis of these findings, the work presented in this study aimed to elucidate the function of 14-3-3 γ in growth and development of mice, the development of epidermis and the molecular mechanisms by which 14-3-3 γ regulates these processes.

To study the function of 14-3-3 γ in growth and development of mice we attempted to generate doxycycline inducible 14-3-3 γ knockdown mice. However, we obtained only transgene positive animals which did not show loss of 14-3-3 γ even after doxycycline administration for months. Similarly, to study the function of 14-3-3 γ in development of epidermis we attempted to generate epidermis specific 14-3-3 γ knockdown animals we obtained animals which showed transgene expression specifically in the epidermis [222] but none of the transgene positive animals inherited the 14-3-3 γ shRNAmir. We also attempted to generate epidermis specific 14-3-3 γ knockout animals using the CRISPR/Cas system but we did not obtain any animal with a mutation in or a knockout of the 14-3-3 γ gene. In the future, we propose to generate mice with floxed alleles for 14-3-3 γ , which will be crossed with mice expressing either a doxycycline inducible Cre allele or with transgenic mice expressing Cre under the control of the K14 promoter to study the function of 14-3-3 γ in growth and development of mice and in the development of epidermis respectively.

Epidermis is made up of keratinocytes. To study if the loss of 14-3-3 γ affects cell-cell adhesion in the keratinocytes, a HaCaT derived 14-3-3 γ knockout cell line was generated using the CRISPR/Cas system. Loss of 14-3-3 γ in HaCaT led to decrease in cell-cell adhesion characterized by reduction in the desmosome size due to decreased cell border localization of desmosomal proteins and reduction in levels of desmosomal proteins [245]. These observations suggested that 14-3-3 γ is crucial for desmosome formation in keratinocytes *in vitro* and might

affect epidermis function *in vivo*. We will try to generate epidermis specific 14-3-3 γ knockout/knockdown mice to demonstrate that 14-3-3 γ is required for epidermis formation and function.

To understand the mechanisms by which 14-3-3 γ regulates desmosome formation, we studied 14-3-3 γ binding to desmosomal proteins. We observed 14-3-3 γ binds to DP, PG and PKP3 and regulates the transport of all the desmosomal proteins as loss of 14-3-3 γ in HCT116 cells led to the disruption of desmosomal protein transport from cytoplasm to the cell border[150].

To understand the mechanism of 14-3-3 γ -PG complex formation, we identified that PG is phosphorylated by PKC μ and this phosphorylation generates 14-3-3 binding site. Disruption of the 14-3-3 binding site in PG inhibited transport of PG from cytoplasm to the cell border. PG-14-3-3 γ complex formation is therefore necessary for transporting PG to the cell border [150]. PG-14-3-3 γ complex is transported from cytoplasm to the cell border by the motor protein KIF5B[150].

To understand if the loss of desmosome formation observed upon 14-3-3 γ loss was because of a disruption in PG transport, we expressed farnesylated PG in the 14-3-3 γ knockdown cells and studied the localization of desmosomal proteins. We observed that farnesylated PG restored DPI/II and DSG2 localization to the cell border but did not restore PKP3 and DSC2/3 localization to the cell border. This result suggested that 14-3-3 γ is required for both PG and PKP3 transport from cytoplasm to the cell border and recruitment of PKP3 to the cell border is necessary for transporting DSC2/3 to the cell border [211, 241, 242]. Even though farnesylated PG could not restore cell border localization of PKP3 and DSC2/3 in 14-3-3 γ knockdown cells

but farnesylated PG restored the desmosome formation in 14-3-3 γ knockdown cells which led to the increase in cell-cell adhesion in the 14-3-3 γ knockdown cells.

The results presented in this study unraveled the molecular mechanism by which 14-3-3 γ mediates transport of PG from cytoplasm to the cell border. The results also demonstrate the importance of recruitment of PG at the cell border for initiating desmosome formation by recruiting DSG2 and DP as the aggregation of DSG2 to the cell-cell adhesion is dependent on PG [246]. Farnesylated PG was also expressed in the KIF5B knockdown cells but its expression only rescued DP transport suggesting DP localization at the cell border is dependent on presence of PG at the cell border. The transport of DSG2 is dependent on KIF5B [240], and therefore DSG2 was not recruited to the cell border by PG in the absence of KIF5B. These observations prove that 14-3-3 γ -PG complex formation and the transport of this complex by KIF5B is one of the important steps in initiating desmosome formation and recruiting DP and DSG2.

The study also highlighted the importance of 14-3-3 γ in PKP3 transport. Further studies are required to understand the molecular mechanisms by which PKP3 interacts with 14-3-3 γ and regulates DSC2/3 transport.

7. Bibliography

- [1] R.L. Brinster, A Method for in Vitro Cultivation of Mouse Ova from Two-Cell to Blastocyst, *Exp Cell Res*, 32 (1963) 205-208.
- [2] R.L. Brinster, The effect of cells transferred into the mouse blastocyst on subsequent development, *J Exp Med*, 140 (1974) 1049-1056.
- [3] B. Mintz, K. Illmensee, Normal genetically mosaic mice produced from malignant teratocarcinoma cells, *Proc Natl Acad Sci U S A*, 72 (1975) 3585-3589.
- [4] J.W. Gordon, G.A. Scangos, D.J. Plotkin, J.A. Barbosa, F.H. Ruddle, Genetic transformation of mouse embryos by microinjection of purified DNA, *Proc Natl Acad Sci U S A*, 77 (1980) 7380-7384.
- [5] R.L. Brinster, H.Y. Chen, M. Trumbauer, A.W. Senear, R. Warren, R.D. Palmiter, Somatic expression of herpes thymidine kinase in mice following injection of a fusion gene into eggs, *Cell*, 27 (1981) 223-231.
- [6] D. Jahner, K. Haase, R. Mulligan, R. Jaenisch, Insertion of the bacterial gpt gene into the germ line of mice by retroviral infection, *Proc Natl Acad Sci U S A*, 82 (1985) 6927-6931.
- [7] D. Huszar, R. Balling, R. Kothary, M.C. Magli, N. Hozumi, J. Rossant, A. Bernstein, Insertion of a bacterial gene into the mouse germ line using an infectious retrovirus vector, *Proc Natl Acad Sci U S A*, 82 (1985) 8587-8591.
- [8] A. Gossler, T. Doetschman, R. Korn, E. Serfling, R. Kemler, Transgenesis by means of blastocyst-derived embryonic stem cell lines, *Proc Natl Acad Sci U S A*, 83 (1986) 9065-9069.
- [9] R.L. Brinster, H.Y. Chen, M.E. Trumbauer, M.K. Yagle, R.D. Palmiter, Factors affecting the efficiency of introducing foreign DNA into mice by microinjecting eggs, *Proc Natl Acad Sci U S A*, 82 (1985) 4438-4442.

- [10] B.G. Brackett, W. Baranska, W. Sawicki, H. Koprowski, Uptake of heterologous genome by mammalian spermatozoa and its transfer to ova through fertilization, *Proc Natl Acad Sci U S A*, 68 (1971) 353-357.
- [11] M. Lavitrano, A. Camaioni, V.M. Fazio, S. Dolci, M.G. Farace, C. Spadafora, Sperm cells as vectors for introducing foreign DNA into eggs: genetic transformation of mice, *Cell*, 57 (1989) 717-723.
- [12] M. Riaz-Ul-Haq, D.E. Mahdi, E.U. Elhassan, Neonatal testicular torsion; a review article, *Iranian journal of pediatrics*, 22 (2012) 281-289.
- [13] D.M. de Kretser, K.L. Loveland, A. Meinhardt, D. Simorangkir, N. Wreford, Spermatogenesis, *Hum Reprod*, 13 Suppl 1 (1998) 1-8.
- [14] Saggital section of testis.
- [15] D.G. de Rooij, L.D. Russell, All you wanted to know about spermatogonia but were afraid to ask, *J Androl*, 21 (2000) 776-798.
- [16] C.W. Feng, J. Bowles, P. Koopman, Control of mammalian germ cell entry into meiosis, *Molecular and cellular endocrinology*, 382 (2014) 488-497.
- [17] S.Z. Jan, G. Hamer, S. Repping, D.G. de Rooij, A.M. van Pelt, T.L. Vormer, Molecular control of rodent spermatogenesis, *Biochimica et biophysica acta*, 1822 (2012) 1838-1850.
- [18] S. Schlatt, J. Ehmcke, Regulation of spermatogenesis: an evolutionary biologist's perspective, *Seminars in cell & developmental biology*, 29 (2014) 2-16.
- [19] S.S.D. Vishal, S. N., Transgenesis: Embryo modification to sperm mediated gene transfer, *Indian Journal of Biotechnology*, 15 (2016) 459-466.

- [20] M. Zani, M. Lavitrano, D. French, V. Lulli, B. Maione, S. Sperandio, C. Spadafora, The mechanism of binding of exogenous DNA to sperm cells: factors controlling the DNA uptake, *Exp Cell Res*, 217 (1995) 57-64.
- [21] M. Lavitrano, B. Maione, E. Forte, M. Francolini, S. Sperandio, R. Testi, C. Spadafora, The interaction of sperm cells with exogenous DNA: a role of CD4 and major histocompatibility complex class II molecules, *Exp Cell Res*, 233 (1997) 56-62.
- [22] K.R. Smith, Sperm cell mediated transgenesis: a review, *Anim Biotechnol*, 10 (1999) 1-13.
- [23] N. Xin, T. Liu, H. Zhao, Z. Wang, J. Liu, Q. Zhang, J. Qi, The impact of exogenous DNA on the structure of sperm of olive flounder (*Paralichthys olivaceus*), *Anim Reprod Sci*, 149 (2014) 305-310.
- [24] A.W. Chan, C.M. Luetjens, T. Dominko, J. Ramalho-Santos, C.R. Simerly, L. Hewitson, G. Schatten, Foreign DNA transmission by ICSI: injection of spermatozoa bound with exogenous DNA results in embryonic GFP expression and live rhesus monkey births, *Mol Hum Reprod*, 6 (2000) 26-33.
- [25] M. Lavitrano, M.L. Bacci, M. Forni, D. Lazzereschi, C. Di Stefano, D. Fioretti, P. Giancotti, G. Marfe, L. Pucci, L. Renzi, H. Wang, A. Stoppacciaro, G. Stassi, M. Sargiacomo, P. Sinibaldi, V. Turchi, R. Giovannoni, G. Della Casa, E. Seren, G. Rossi, Efficient production by sperm-mediated gene transfer of human decay accelerating factor (hDAF) transgenic pigs for xenotransplantation, *Proc Natl Acad Sci U S A*, 99 (2002) 14230-14235.
- [26] N.L. Webster, M. Forni, M.L. Bacci, R. Giovannoni, R. Razzini, P. Fantinati, A. Zannoni, L. Fusetti, L. Dalpra, M.R. Bianco, M. Papa, E. Seren, M.S. Sandrin, I.F. Mc Kenzie, M. Lavitrano, Multi-transgenic pigs expressing three fluorescent proteins produced with high efficiency by sperm mediated gene transfer, *Mol Reprod Dev*, 72 (2005) 68-76.

- [27] K.L. Kroll, E. Amaya, Transgenic *Xenopus* embryos from sperm nuclear transplantations reveal FGF signaling requirements during gastrulation, *Development*, 122 (1996) 3173-3183.
- [28] A.C. Perry, T. Wakayama, H. Kishikawa, T. Kasai, M. Okabe, Y. Toyoda, R. Yanagimachi, Mammalian transgenesis by intracytoplasmic sperm injection, *Science*, 284 (1999) 1180-1183.
- [29] B.A. Ball, K. Sabeur, W.R. Allen, Liposome-mediated uptake of exogenous DNA by equine spermatozoa and applications in sperm-mediated gene transfer, *Equine Vet J*, 40 (2008) 76-82.
- [30] E. Harel-Markowitz, M. Gurevich, L.S. Shore, A. Katz, Y. Stram, M. Shemesh, Use of sperm plasmid DNA lipofection combined with REMI (restriction enzyme-mediated insertion) for production of transgenic chickens expressing eGFP (enhanced green fluorescent protein) or human follicle-stimulating hormone, *Biol Reprod*, 80 (2009) 1046-1052.
- [31] H.S.C. C. C. Yang, C. J. Lin, C. C. Hsu, J. I. Cheung, L. Hwu and W. T. K. Cheng, Cock Spermatozoa Serve as the Gene Vector for Generation of Transgenic Chicken (*Gallus gallus*), *Asian-Australasian Journal of Animal Sciences*, 17 (2004) 885-891.
- [32] R.R. Churchil, J. Gupta, A. Singh, D. Sharma, Exogenous DNA internalisation by sperm cells is improved by combining lipofection and restriction enzyme mediated integration, *Br Poult Sci*, 52 (2011) 287-291.
- [33] T.S. Kim, S.H. Lee, G.T. Gang, Y.S. Lee, S.U. Kim, D.B. Koo, M.Y. Shin, C.K. Park, D.S. Lee, Exogenous DNA uptake of boar spermatozoa by a magnetic nanoparticle vector system, *Reprod Domest Anim*, 45 (2010) e201-206.
- [34] V.F. Campos, P.M. de Leon, E.R. Komninou, O.A. Dellagostin, J.C. Deschamps, F.K. Seixas, T. Collares, NanoSMGT: transgene transmission into bovine embryos using halloysite clay nanotubes or nanopolymer to improve transfection efficiency, *Theriogenology*, 76 (2011) 1552-1560.

- [35] N. Barkalina, C. Jones, J. Kashir, S. Coote, X. Huang, R. Morrison, H. Townley, K. Coward, Effects of mesoporous silica nanoparticles upon the function of mammalian sperm in vitro, *Nanomedicine*, 10 (2014) 859-870.
- [36] V.F. Campos, E.R. Komninou, G. Urtiaga, P.M. de Leon, F.K. Seixas, O.A. Dellagostin, J.C. Deschamps, T. Collares, NanoSMGT: transfection of exogenous DNA on sex-sorted bovine sperm using nanopolymer, *Theriogenology*, 75 (2011) 1476-1481.
- [37] R.L. Brinster, J.W. Zimmermann, Spermatogenesis following male germ-cell transplantation, *Proc Natl Acad Sci U S A*, 91 (1994) 11298-11302.
- [38] R.L. Brinster, M.R. Avarbock, Germline transmission of donor haplotype following spermatogonial transplantation, *Proc Natl Acad Sci U S A*, 91 (1994) 11303-11307.
- [39] M. Nagano, T. Shinohara, M.R. Avarbock, R.L. Brinster, Retrovirus-mediated gene delivery into male germ line stem cells, *FEBS Lett*, 475 (2000) 7-10.
- [40] M. Nagano, D.J. Watson, B.Y. Ryu, J.H. Wolfe, R.L. Brinster, Lentiviral vector transduction of male germ line stem cells in mice, *FEBS Lett*, 524 (2002) 111-115.
- [41] Z. Ivics, Z. Izsvak, K.M. Chapman, F.K. Hamra, Sleeping Beauty transposon mutagenesis of the rat genome in spermatogonial stem cells, *Methods*, 53 (2011) 356-365.
- [42] T. Sato, K. Katagiri, A. Gohbara, K. Inoue, N. Ogonuki, A. Ogura, Y. Kubota, T. Ogawa, In vitro production of functional sperm in cultured neonatal mouse testes, *Nature*, 471 (2011) 504-507.
- [43] I.R. Sato M, Kasai K, Tada N., Direct injection of foreign DNA into mouse testis as a possible alternative of sperm-mediated gene transfer, *Anim Biotechnol*, 5 (1994) 19-31.

- [44] T. Muramatsu, O. Shibata, S. Ryoki, Y. Ohmori, J. Okumura, Foreign gene expression in the mouse testis by localized in vivo gene transfer, *Biochemical and biophysical research communications*, 233 (1997) 45-49.
- [45] Y. Yamazaki, H. Fujimoto, H. Ando, T. Ohyama, Y. Hirota, T. Noce, In vivo gene transfer to mouse spermatogenic cells by deoxyribonucleic acid injection into seminiferous tubules and subsequent electroporation, *Biol Reprod*, 59 (1998) 1439-1444.
- [46] Z. Huang, M. Tamura, T. Sakurai, S. Chuma, T. Saito, N. Nakatsuji, In vivo transfection of testicular germ cells and transgenesis by using the mitochondrially localized jellyfish fluorescent protein gene, *FEBS Lett*, 487 (2000) 248-251.
- [47] S. Dhup, S.S. Majumdar, Transgenesis via permanent integration of genes in repopulating spermatogonial cells in vivo, *Nat Methods*, 5 (2008) 601-603.
- [48] A. Usmani, N. Ganguli, H. Sarkar, S. Dhup, S.R. Batta, M. Vimal, S. Basu, P. Nagarajan, S.S. Majumdar, A non-surgical approach for male germ cell mediated gene transmission through transgenesis, *Sci Rep*, 3 (2013) 3430.
- [49] M. Nagano, C.J. Brinster, K.E. Orwig, B.Y. Ryu, M.R. Avarbock, R.L. Brinster, Transgenic mice produced by retroviral transduction of male germ-line stem cells, *Proc Natl Acad Sci U S A*, 98 (2001) 13090-13095.
- [50] A. Pfeifer, M. Ikawa, Y. Dayn, I.M. Verma, Transgenesis by lentiviral vectors: lack of gene silencing in mammalian embryonic stem cells and preimplantation embryos, *Proc Natl Acad Sci U S A*, 99 (2002) 2140-2145.
- [51] F.K. Hamra, J. Gatlin, K.M. Chapman, D.M. Grellhesl, J.V. Garcia, R.E. Hammer, D.L. Garbers, Production of transgenic rats by lentiviral transduction of male germ-line stem cells, *Proc Natl Acad Sci U S A*, 99 (2002) 14931-14936.

- [52] M. Kanatsu-Shinohara, S. Toyokuni, T. Shinohara, Transgenic mice produced by retroviral transduction of male germ line stem cells in vivo, *Biol Reprod*, 71 (2004) 1202-1207.
- [53] L. Sehgal, R. Thorat, N. Khapare, A. Mukhopadhaya, M. Sawant, S.N. Dalal, Lentiviral mediated transgenesis by in vivo manipulation of spermatogonial stem cells, *PLoS One*, 6 (2011) e21975.
- [54] M. Takehashi, M. Kanatsu-Shinohara, K. Inoue, N. Ogonuki, H. Miki, S. Toyokuni, A. Ogura, T. Shinohara, Adenovirus-mediated gene delivery into mouse spermatogonial stem cells, *Proc Natl Acad Sci U S A*, 104 (2007) 2596-2601.
- [55] A. Chandrasekran, R. Sarkar, A. Thrasher, S.E. Fraser, N. Dibb, C. Casimir, R. Winston, C. Readhead, Efficient generation of transgenic mice by lentivirus-mediated modification of spermatozoa, *Faseb J*, 28 (2014) 569-576.
- [56] M. Kanatsu-Shinohara, M. Ikawa, M. Takehashi, N. Ogonuki, H. Miki, K. Inoue, Y. Kazuki, J. Lee, S. Toyokuni, M. Oshimura, A. Ogura, T. Shinohara, Production of knockout mice by random or targeted mutagenesis in spermatogonial stem cells, *Proc Natl Acad Sci U S A*, 103 (2006) 8018-8023.
- [57] B. Davies, G. Davies, C. Preece, R. Puliyadi, D. Szumska, S. Bhattacharya, Site specific mutation of the *Zic2* locus by microinjection of TALEN mRNA in mouse CD1, C3H and C57BL/6J oocytes, *PloS one*, 8 (2013) e60216.
- [58] V. Ponce de Leon, A.M. Merillat, L. Tesson, I. Anegon, E. Hummler, Generation of TALEN-mediated GRdim knock-in rats by homologous recombination, *PloS one*, 9 (2014) e88146.

- [59] L. Tesson, C. Usal, S. Menoret, E. Leung, B.J. Niles, S. Remy, Y. Santiago, A.I. Vincent, X. Meng, L. Zhang, P.D. Gregory, I. Anegón, G.J. Cost, Knockout rats generated by embryo microinjection of TALENs, *Nat Biotechnol*, 29 (2011) 695-696.
- [60] P. Reddy, A. Ocampo, K. Suzuki, J. Luo, S.R. Bacman, S.L. Williams, A. Sugawara, D. Okamura, Y. Tsunekawa, J. Wu, D. Lam, X. Xiong, N. Montserrat, C.R. Esteban, G.H. Liu, I. Sancho-Martinez, D. Manau, S. Civico, F. Cardellach, M. Del Mar O'Callaghan, J. Campistol, H. Zhao, J.M. Campistol, C.T. Moraes, J.C. Izpisua Belmonte, Selective elimination of mitochondrial mutations in the germline by genome editing, *Cell*, 161 (2015) 459-469.
- [61] D.A. Fanslow, S.E. Wirt, J.C. Barker, J.P. Connelly, M.H. Porteus, C.T. Dann, Genome editing in mouse spermatogonial stem/progenitor cells using engineered nucleases, *PloS one*, 9 (2014) e112652.
- [62] T. Sato, T. Sakuma, T. Yokonishi, K. Katagiri, S. Kamimura, N. Ogonuki, A. Ogura, T. Yamamoto, T. Ogawa, Genome Editing in Mouse Spermatogonial Stem Cell Lines Using TALEN and Double-Nicking CRISPR/Cas9, *Stem Cell Reports*, (2015).
- [63] H. Yang, H. Wang, C.S. Shivalila, A.W. Cheng, L. Shi, R. Jaenisch, One-step generation of mice carrying reporter and conditional alleles by CRISPR/Cas-mediated genome engineering, *Cell*, 154 (2013) 1370-1379.
- [64] A.Y. Lee, K.C. Lloyd, Conditional targeting of *Ispid* using paired Cas9 nickase and a single DNA template in mice, *FEBS Open Bio*, 4 (2014) 637-642.
- [65] A. Honda, M. Hirose, T. Sankai, L. Yasmin, K. Yuzawa, K. Honsho, H. Izu, A. Iguchi, M. Ikawa, A. Ogura, Single-Step Generation of Rabbits Carrying a Targeted Allele of the Tyrosinase Gene Using CRISPR/Cas9, *Exp Anim*, (2014).

- [66] Y. Wu, H. Zhou, X. Fan, Y. Zhang, M. Zhang, Y. Wang, Z. Xie, M. Bai, Q. Yin, D. Liang, W. Tang, J. Liao, C. Zhou, W. Liu, P. Zhu, H. Guo, H. Pan, C. Wu, H. Shi, L. Wu, F. Tang, J. Li, Correction of a genetic disease by CRISPR-Cas9-mediated gene editing in mouse spermatogonial stem cells, *Cell Res*, 25 (2015) 67-79.
- [67] F.A. Ran, P.D. Hsu, C.Y. Lin, J.S. Gootenberg, S. Konermann, A.E. Trevino, D.A. Scott, A. Inoue, S. Matoba, Y. Zhang, F. Zhang, Double nicking by RNA-guided CRISPR Cas9 for enhanced genome editing specificity, *Cell*, 154 (2013) 1380-1389.
- [68] T. Ichimura, T. Isobe, T. Okuyama, N. Takahashi, K. Araki, R. Kuwano, Y. Takahashi, Molecular cloning of cDNA coding for brain-specific 14-3-3 protein, a protein kinase-dependent activator of tyrosine and tryptophan hydroxylases, *Proc Natl Acad Sci U S A*, 85 (1988) 7084-7088.
- [69] S. Comparot, G. Lingiah, T. Martin, Function and specificity of 14-3-3 proteins in the regulation of carbohydrate and nitrogen metabolism, *J Exp Bot*, 54 (2003) 595-604.
- [70] A.K. Gardino, S.J. Smerdon, M.B. Yaffe, Structural determinants of 14-3-3 binding specificities and regulation of subcellular localization of 14-3-3-ligand complexes: a comparison of the X-ray crystal structures of all human 14-3-3 isoforms, *Seminars in cancer biology*, 16 (2006) 173-182.
- [71] D.H. Jones, S. Ley, A. Aitken, Isoforms of 14-3-3 protein can form homo- and heterodimers in vivo and in vitro: implications for function as adapter proteins, *FEBS Lett*, 368 (1995) 55-58.
- [72] A.K. Gardino, S.J. Smerdon, M.B. Yaffe, Structural determinants of 14-3-3 binding specificities and regulation of subcellular localization of 14-3-3-ligand complexes: a comparison of the X-ray crystal structures of all human 14-3-3 isoforms, *Semin Cancer Biol*, 16 (2006) 173-182.

- [73] G. Tzivion, Y.H. Shen, J. Zhu, 14-3-3 proteins; bringing new definitions to scaffolding, *Oncogene*, 20 (2001) 6331-6338.
- [74] A. Aitken, 14-3-3 proteins: a historic overview, *Seminars in cancer biology*, 16 (2006) 162-172.
- [75] S.F. Pietromonaco, G.A. Seluja, A. Aitken, L. Elias, Association of 14-3-3 proteins with centrosomes, *Blood cells, molecules & diseases*, 22 (1996) 225-237.
- [76] Y. Li, K. Inoki, R. Yeung, K.L. Guan, Regulation of TSC2 by 14-3-3 binding, *The Journal of biological chemistry*, 277 (2002) 44593-44596.
- [77] E.W. Wilker, R.A. Grant, S.C. Artim, M.B. Yaffe, A structural basis for 14-3-3sigma functional specificity, *The Journal of biological chemistry*, 280 (2005) 18891-18898.
- [78] A. Aitken, 14-3-3 and its possible role in co-ordinating multiple signalling pathways, *Trends Cell Biol*, 6 (1996) 341-347.
- [79] X. Yang, W.H. Lee, F. Sobott, E. Papagrigoriou, C.V. Robinson, J.G. Grossmann, M. Sundstrom, D.A. Doyle, J.M. Elkins, Structural basis for protein-protein interactions in the 14-3-3 protein family, *Proc Natl Acad Sci U S A*, 103 (2006) 17237-17242.
- [80] M.B. Yaffe, K. Rittinger, S. Volinia, P.R. Caron, A. Aitken, H. Leffers, S.J. Gamblin, S.J. Smerdon, L.C. Cantley, The structural basis for 14-3-3:phosphopeptide binding specificity, *Cell*, 91 (1997) 961-971.
- [81] A.J. Muslin, J.W. Tanner, P.M. Allen, A.S. Shaw, Interaction of 14-3-3 with signaling proteins is mediated by the recognition of phosphoserine, *Cell*, 84 (1996) 889-897.
- [82] B. Coblitz, M. Wu, S. Shikano, M. Li, C-terminal binding: an expanded repertoire and function of 14-3-3 proteins, *FEBS Lett*, 580 (2006) 1531-1535.

- [83] B. Coblitz, S. Shikano, M. Wu, S.B. Gabelli, L.M. Cockrell, M. Spieker, Y. Hanyu, H. Fu, L.M. Amzel, M. Li, C-terminal recognition by 14-3-3 proteins for surface expression of membrane receptors, *The Journal of biological chemistry*, 280 (2005) 36263-36272.
- [84] M. Horie, M. Suzuki, E. Takahashi, A. Tanigami, Cloning, expression, and chromosomal mapping of the human 14-3-3gamma gene (YWHAG) to 7q11.23, *Genomics*, 60 (1999) 241-243.
- [85] P. Steinacker, P. Schwarz, K. Reim, P. Brechlin, O. Jahn, H. Kratzin, A. Aitken, J. Wiltfang, A. Aguzzi, E. Bahn, H.C. Baxter, N. Brose, M. Otto, Unchanged survival rates of 14-3-3gamma knockout mice after inoculation with pathological prion protein, *Mol Cell Biol*, 25 (2005) 1339-1346.
- [86] C.Y. Peng, P.R. Graves, R.S. Thoma, Z. Wu, A.S. Shaw, H. Piwnica-Worms, Mitotic and G2 checkpoint control: regulation of 14-3-3 protein binding by phosphorylation of Cdc25C on serine-216, *Science*, 277 (1997) 1501-1505.
- [87] S.N. Dalal, C.M. Schweitzer, J. Gan, J.A. DeCaprio, Cytoplasmic localization of human cdc25C during interphase requires an intact 14-3-3 binding site, *Mol Cell Biol*, 19 (1999) 4465-4479.
- [88] S.N. Dalal, M.B. Yaffe, J.A. DeCaprio, 14-3-3 family members act coordinately to regulate mitotic progression, *Cell Cycle*, 3 (2004) 672-677.
- [89] A.S. Hosing, S.T. Kundu, S.N. Dalal, 14-3-3 Gamma is required to enforce both the incomplete S phase and G2 DNA damage checkpoints, *Cell Cycle*, 7 (2008) 3171-3179.
- [90] B. Furnari, N. Rhind, P. Russell, Cdc25 mitotic inducer targeted by chk1 DNA damage checkpoint kinase, *Science*, 277 (1997) 1495-1497.

- [91] Y. Sanchez, C. Wong, R.S. Thoma, R. Richman, Z. Wu, H. Piwnica-Worms, S.J. Elledge, Conservation of the Chk1 checkpoint pathway in mammals: linkage of DNA damage to Cdk regulation through Cdc25, *Science*, 277 (1997) 1497-1501.
- [92] S. Dunaway, H.Y. Liu, N.C. Walworth, Interaction of 14-3-3 protein with Chk1 affects localization and checkpoint function, *J Cell Sci*, 118 (2005) 39-50.
- [93] K. Kasahara, H. Goto, M. Enomoto, Y. Tomono, T. Kiyono, M. Inagaki, 14-3-3gamma mediates Cdc25A proteolysis to block premature mitotic entry after DNA damage, *EMBO J*, 29 (2010) 2802-2812.
- [94] K. Shimuta, N. Nakajo, K. Uto, Y. Hayano, K. Okazaki, N. Sagata, Chk1 is activated transiently and targets Cdc25A for degradation at the *Xenopus* midblastula transition, *EMBO J*, 21 (2002) 3694-3703.
- [95] I. Blomberg, I. Hoffmann, Ectopic expression of Cdc25A accelerates the G(1)/S transition and leads to premature activation of cyclin E- and cyclin A-dependent kinases, *Mol Cell Biol*, 19 (1999) 6183-6194.
- [96] T. Abbas, A. Dutta, CRL4Cdt2: master coordinator of cell cycle progression and genome stability, *Cell Cycle*, 10 (2011) 241-249.
- [97] A. Dar, D. Wu, N. Lee, E. Shibata, A. Dutta, 14-3-3 proteins play a role in the cell cycle by shielding cdt2 from ubiquitin-mediated degradation, *Mol Cell Biol*, 34 (2014) 4049-4061.
- [98] A. Mukhopadhyay, L. Sehgal, A. Bose, A. Gulvady, P. Senapati, R. Thorat, S. Basu, K. Bhatt, A.S. Hosing, R. Balyan, L. Borde, T.K. Kundu, S.N. Dalal, 14-3-3gamma Prevents Centrosome Amplification and Neoplastic Progression, *Sci Rep*, 6 (2016) 26580.

- [99] S.I. Han, M.A. Kawano, K. Ishizu, H. Watanabe, M. Hasegawa, S.N. Kanesashi, Y.S. Kim, A. Nakanishi, K. Kataoka, H. Handa, Rep68 protein of adeno-associated virus type 2 interacts with 14-3-3 proteins depending on phosphorylation at serine 535, *Virology*, 320 (2004) 144-155.
- [100] M.J. Waterman, E.S. Stavridi, J.L. Waterman, T.D. Halazonetis, ATM-dependent activation of p53 involves dephosphorylation and association with 14-3-3 proteins, *Nature genetics*, 19 (1998) 175-178.
- [101] E.S. Stavridi, N.H. Chehab, A. Malikzay, T.D. Halazonetis, Substitutions that compromise the ionizing radiation-induced association of p53 with 14-3-3 proteins also compromise the ability of p53 to induce cell cycle arrest, *Cancer research*, 61 (2001) 7030-7033.
- [102] S. Rajagopalan, A.M. Jaulent, M. Wells, D.B. Veprintsev, A.R. Fersht, 14-3-3 activation of DNA binding of p53 by enhancing its association into tetramers, *Nucleic acids research*, 36 (2008) 5983-5991.
- [103] S. Rajagopalan, R.S. Sade, F.M. Townsley, A.R. Fersht, Mechanistic differences in the transcriptional activation of p53 by 14-3-3 isoforms, *Nucleic acids research*, 38 (2010) 893-906.
- [104] V.M. Radhakrishnan, C.W. Putnam, W. Qi, J.D. Martinez, P53 suppresses expression of the 14-3-3 gamma oncogene, *BMC cancer*, 11 (2011) 378.
- [105] D.Y. Chen, D.F. Dai, Y. Hua, W.Q. Qi, p53 suppresses 14-3-3gamma by stimulating proteasome-mediated 14-3-3gamma protein degradation, *International journal of oncology*, 46 (2015) 818-824.
- [106] L. Strohlic, A. Cartaud, A. Mejat, R. Grailhe, L. Schaeffer, J.P. Changeux, J. Cartaud, 14-3-3 gamma associates with muscle specific kinase and regulates synaptic gene transcription at vertebrate neuromuscular synapse, *Proc Natl Acad Sci U S A*, 101 (2004) 18189-18194.

- [107] L. Storchlic, A. Cartaud, J. Cartaud, [14-3-3 gamma, a novel partner of MuSK downregulates synaptic gene transcription at the neuromuscular junction], *Medecine sciences : M/S*, 21 (2005) 467-469.
- [108] W.W. Ge, K. Volkening, C. Leystra-Lantz, H. Jaffe, M.J. Strong, 14-3-3 protein binds to the low molecular weight neurofilament (NFL) mRNA 3' UTR, *Molecular and cellular neurosciences*, 34 (2007) 80-87.
- [109] P. Silveyra, M. Raval, B. Simmons, S. Diangelo, G. Wang, J. Floros, The untranslated exon B of human surfactant protein A2 mRNAs is an enhancer for transcription and translation, *American journal of physiology. Lung cellular and molecular physiology*, 301 (2011) L795-803.
- [110] G.T. Noutsios, P. Ghattas, S. Bennett, J. Floros, 14-3-3 isoforms bind directly exon B of the 5'-UTR of human surfactant protein A2 mRNA, *American journal of physiology. Lung cellular and molecular physiology*, 309 (2015) L147-157.
- [111] T.A. Yacoubian, S.R. Slone, A.J. Harrington, S. Hamamichi, J.M. Schieltz, K.A. Caldwell, G.A. Caldwell, D.G. Standaert, Differential neuroprotective effects of 14-3-3 proteins in models of Parkinson's disease, *Cell death & disease*, 1 (2010) e2.
- [112] K. Muda, D. Bertinetti, F. Gesellchen, J.S. Hermann, F. von Zweydtorf, A. Geerlof, A. Jacob, M. Ueffing, C.J. Gloeckner, F.W. Herberg, Parkinson-related LRRK2 mutation R1441C/G/H impairs PKA phosphorylation of LRRK2 and disrupts its interaction with 14-3-3, *Proc Natl Acad Sci U S A*, 111 (2014) E34-43.
- [113] Y.H. Weng, C.Y. Chen, K.J. Lin, Y.L. Chen, T.H. Yeh, I.T. Hsiao, I.J. Chen, C.S. Lu, H.L. Wang, (R1441C) LRRK2 induces the degeneration of SN dopaminergic neurons and alters the expression of genes regulating neuronal survival in a transgenic mouse model, *Experimental neurology*, 275 Pt 1 (2016) 104-115.

- [114] J. Schapansky, S. Khasnavis, M.P. DeAndrade, J.D. Nardoizzi, S.R. Falkson, J.D. Boyd, J.B. Sanderson, T. Bartels, H.L. Melrose, M.J. LaVoie, Familial knockin mutation of LRRK2 causes lysosomal dysfunction and accumulation of endogenous insoluble alpha-synuclein in neurons, *Neurobiology of disease*, 111 (2017) 26-35.
- [115] M. Zannis-Hadjopoulos, W. Yahyaoui, M. Callejo, 14-3-3 cruciform-binding proteins as regulators of eukaryotic DNA replication, *Trends in biochemical sciences*, 33 (2008) 44-50.
- [116] V. Brazda, J. Cechova, J. Coufal, S. Rumpel, E.B. Jagelska, Superhelical DNA as a preferential binding target of 14-3-3gamma protein, *Journal of biomolecular structure & dynamics*, 30 (2012) 371-378.
- [117] Z. Xu, Z. Fulop, G. Wu, E.J. Pone, J. Zhang, T. Mai, L.M. Thomas, A. Al-Qahtani, C.A. White, S.R. Park, P. Steinacker, Z. Li, J. Yates, 3rd, B. Herron, M. Otto, H. Zan, H. Fu, P. Casali, 14-3-3 adaptor proteins recruit AID to 5'-AGCT-3'-rich switch regions for class switch recombination, *Nature structural & molecular biology*, 17 (2010) 1124-1135.
- [118] T. Lam, L.M. Thomas, C.A. White, G. Li, E.J. Pone, Z. Xu, P. Casali, Scaffold functions of 14-3-3 adaptors in B cell immunoglobulin class switch DNA recombination, *PLoS One*, 8 (2013) e80414.
- [119] B. Pierrat, M. Ito, W. Hinz, M. Simonen, D. Erdmann, M. Chiesi, J. Heim, Uncoupling proteins 2 and 3 interact with members of the 14.3.3 family, *European journal of biochemistry*, 267 (2000) 2680-2687.
- [120] G. Czirjak, D. Vuity, P. Enyedi, Phosphorylation-dependent binding of 14-3-3 proteins controls TRESK regulation, *The Journal of biological chemistry*, 283 (2008) 15672-15680.

- [121] B. Sokolowski, S. Orchard, M. Harvey, S. Sridhar, Y. Sakai, Conserved BK channel-protein interactions reveal signals relevant to cell death and survival, *PLoS One*, 6 (2011) e28532.
- [122] X. Liang, A.C. Da Paula, Z. Bozoky, H. Zhang, C.A. Bertrand, K.W. Peters, J.D. Forman-Kay, R.A. Frizzell, Phosphorylation-dependent 14-3-3 protein interactions regulate CFTR biogenesis, *Molecular biology of the cell*, 23 (2012) 996-1009.
- [123] J. Fernandez-Orth, P. Ehling, T. Ruck, S. Pankratz, M.S. Hofmann, P. Landgraf, D.C. Dieterich, K.H. Smalla, T. Kahne, G. Seebohm, T. Budde, H. Wiendl, S. Bittner, S.G. Meuth, 14-3-3 Proteins regulate K2P 5.1 surface expression on T lymphocytes, *Traffic*, 18 (2017) 29-43.
- [124] X. Feng, Z. Li, Y. Du, H. Fu, J.D. Klein, H. Cai, J.M. Sands, G. Chen, Downregulation of urea transporter UT-A1 activity by 14-3-3 protein, *American journal of physiology. Renal physiology*, 309 (2015) F71-78.
- [125] S.J. Oh, J. Woo, Y.S. Lee, M. Cho, E. Kim, N.C. Cho, J.Y. Park, A.N. Pae, C. Justin Lee, E.M. Hwang, Direct interaction with 14-3-3gamma promotes surface expression of Best1 channel in astrocyte, *Molecular brain*, 10 (2017) 51.
- [126] C.H. Cho, E. Kim, Y.S. Lee, O. Yarishkin, J.C. Yoo, J.Y. Park, S.G. Hong, E.M. Hwang, Depletion of 14-3-3gamma reduces the surface expression of Transient Receptor Potential Melastatin 4b (TRPM4b) channels and attenuates TRPM4b-mediated glutamate-induced neuronal cell death, *Molecular brain*, 7 (2014) 52.
- [127] H.J. Bustad, L. Skjaerven, M. Ying, O. Halskau, A. Baumann, D. Rodriguez-Larrea, M. Costas, J. Underhaug, J.M. Sanchez-Ruiz, A. Martinez, The peripheral binding of 14-3-3gamma to membranes involves isoform-specific histidine residues, *PLoS One*, 7 (2012) e49671.

- [128] Y. Miyamoto, N. Kitamura, Y. Nakamura, M. Futamura, T. Miyamoto, M. Yoshida, M. Ono, S. Ichinose, H. Arakawa, Possible existence of lysosome-like organelle within mitochondria and its role in mitochondrial quality control, *PLoS One*, 6 (2011) e16054.
- [129] N. Kitamura, Y. Nakamura, Y. Miyamoto, T. Miyamoto, K. Kabu, M. Yoshida, M. Futamura, S. Ichinose, H. Arakawa, Mieap, a p53-inducible protein, controls mitochondrial quality by repairing or eliminating unhealthy mitochondria, *PLoS One*, 6 (2011) e16060.
- [130] T. Miyamoto, N. Kitamura, M. Ono, Y. Nakamura, M. Yoshida, H. Kamino, R. Murai, T. Yamada, H. Arakawa, Identification of 14-3-3gamma as a Mieap-interacting protein and its role in mitochondrial quality control, *Sci Rep*, 2 (2012) 379.
- [131] P. Anderson, N. Kedersha, RNA granules, *J Cell Biol*, 172 (2006) 803-808.
- [132] C.J. Decker, R. Parker, P-bodies and stress granules: possible roles in the control of translation and mRNA degradation, *Cold Spring Harbor perspectives in biology*, 4 (2012) a012286.
- [133] N. Okada, N. Yabuta, H. Suzuki, Y. Aylon, M. Oren, H. Nojima, A novel Chk1/2-Lats2-14-3-3 signaling pathway regulates P-body formation in response to UV damage, *J Cell Sci*, 124 (2011) 57-67.
- [134] Q. Shen, X. Hu, L. Zhou, S. Zou, L.Z. Sun, X. Zhu, Overexpression of the 14-3-3gamma protein in uterine leiomyoma cells results in growth retardation and increased apoptosis, *Cell Signal*, 45 (2018) 43-53.
- [135] Y. Song, Z. Yang, Z. Ke, Y. Yao, X. Hu, Y. Sun, H. Li, J. Yin, C. Zeng, Expression of 14-3-3gamma in patients with breast cancer: correlation with clinicopathological features and prognosis, *Cancer Epidemiol*, 36 (2012) 533-536.

- [136] B.S. Ko, I.R. Lai, T.C. Chang, T.A. Liu, S.C. Chen, J. Wang, Y.J. Jan, J.Y. Liou, Involvement of 14-3-3gamma overexpression in extrahepatic metastasis of hepatocellular carcinoma, *Hum Pathol*, 42 (2011) 129-135.
- [137] P. Raungrut, A. Wongkotsila, K. Lirdprapamongkol, J. Svasti, S.L. Geater, M. Phukaoloun, S. Suwiwat, P. Thongsuksai, Prognostic significance of 14-3-3gamma overexpression in advanced non-small cell lung cancer, *Asian Pac J Cancer Prev*, 15 (2014) 3513-3518.
- [138] B.S. Ajjappala, Y.S. Kim, M.S. Kim, M.Y. Lee, K.Y. Lee, H.Y. Ki, D.H. Cha, K.H. Baek, 14-3-3 gamma is stimulated by IL-3 and promotes cell proliferation, *J Immunol*, 182 (2009) 1050-1060.
- [139] V.M. Radhakrishnan, J.D. Martinez, 14-3-3gamma induces oncogenic transformation by stimulating MAP kinase and PI3K signaling, *PLoS One*, 5 (2010) e11433.
- [140] V.M. Radhakrishnan, C.W. Putnam, J.D. Martinez, Activation of phosphatidylinositol 3-kinase (PI3K) and mitogen-activated protein kinase (MAPK) signaling and the consequent induction of transformation by overexpressed 14-3-3gamma protein require specific amino acids within 14-3-3gamma N-terminal variable region II, *The Journal of biological chemistry*, 287 (2012) 43300-43311.
- [141] P. Wang, Y. Deng, X. Fu, MiR-509-5p suppresses the proliferation, migration, and invasion of non-small cell lung cancer by targeting YWHAG, *Biochem Biophys Res Commun*, 482 (2017) 935-941.
- [142] P. Raungrut, A. Wongkotsila, N. Champoochana, K. Lirdprapamongkol, J. Svasti, P. Thongsuksai, Knockdown of 14-3-3gamma Suppresses Epithelial-Mesenchymal Transition and

Reduces Metastatic Potential of Human Non-small Cell Lung Cancer Cells, *Anticancer Res*, 38 (2018) 3507-3514.

[143] R. Perdigao-Henriques, F. Petrocca, G. Altschuler, M.P. Thomas, M.T. Le, S.M. Tan, W. Hide, J. Lieberman, miR-200 promotes the mesenchymal to epithelial transition by suppressing multiple members of the Zeb2 and Snail1 transcriptional repressor complexes, *Oncogene*, 35 (2016) 158-172.

[144] N. Park, J.C. Yoo, J. Ryu, S.G. Hong, E.M. Hwang, J.Y. Park, Copine1 enhances neuronal differentiation of the hippocampal progenitor HiB5 cells, *Mol Cells*, 34 (2012) 549-554.

[145] J. Cheal Yoo, N. Park, B. Lee, A. Nashed, Y.S. Lee, T. Hwan Kim, D. Yong Lee, A. Kim, E. Mi Hwang, G.S. Yi, J.Y. Park, 14-3-3gamma regulates Copine1-mediated neuronal differentiation in HiB5 hippocampal progenitor cells, *Exp Cell Res*, 356 (2017) 85-92.

[146] T. Wachi, B. Cornell, C. Marshall, V. Zhukarev, P.W. Baas, K. Toyo-oka, Ablation of the 14-3-3gamma Protein Results in Neuronal Migration Delay and Morphological Defects in the Developing Cerebral Cortex, *Developmental neurobiology*, 76 (2016) 600-614.

[147] B. Cornell, T. Wachi, V. Zhukarev, K. Toyo-Oka, Overexpression of the 14-3-3gamma protein in embryonic mice results in neuronal migration delay in the developing cerebral cortex, *Neuroscience letters*, 628 (2016) 40-46.

[148] I. Guella, M.B. McKenzie, D.M. Evans, S.E. Buerki, E.B. Toyota, M.I. Van Allen, S. Epilepsy Genomics, M. Suri, F. Elmslie, S. Deciphering Developmental Disorders, M.E.H. Simon, K.L.I. van Gassen, D. Heron, B. Keren, C. Nava, M.B. Connolly, M. Demos, M.J. Farrer, De Novo Mutations in YWHAG Cause Early-Onset Epilepsy, *American journal of human genetics*, 101 (2017) 300-310.

- [149] L.L. Arthur, J.J. Chung, P. Jankirama, K.M. Keefer, I. Kolotilin, S. Pavlovic-Djuranovic, D.L. Chalker, V. Grbic, R. Green, R. Menassa, H.L. True, J.B. Skeath, S. Djuranovic, Rapid generation of hypomorphic mutations, *Nature communications*, 8 (2017) 14112.
- [150] L. Sehgal, A. Mukhopadhyay, A. Rajan, N. Khapare, M. Sawant, S.S. Vishal, K. Bhatt, S. Ambatipudi, N. Antao, H. Alam, M. Gurjar, S. Basu, R. Mathur, L. Borde, A.S. Hosing, M.M. Vaidya, R. Thorat, F. Samaniego, U. Kolthur-Seetharam, S.N. Dalal, 14-3-3gamma-Mediated transport of plakoglobin to the cell border is required for the initiation of desmosome assembly in vitro and in vivo, *J Cell Sci*, 127 (2014) 2174-2188.
- [151] K.M. Yamada, B. Geiger, Molecular interactions in cell adhesion complexes, *Current opinion in cell biology*, 9 (1997) 76-85.
- [152] J.J. Jefferson, C.L. Leung, R.K. Liem, Plakins: goliaths that link cell junctions and the cytoskeleton, *Nature reviews. Molecular cell biology*, 5 (2004) 542-553.
- [153] W.Y. Lui, W.M. Lee, Regulation of junction dynamics in the testis--transcriptional and post-translational regulations of cell junction proteins, *Molecular and cellular endocrinology*, 250 (2006) 25-35.
- [154] D.D. Mruk, C.Y. Cheng, The Mammalian Blood-Testis Barrier: Its Biology and Regulation, *Endocrine reviews*, 36 (2015) 564-591.
- [155] C.Y. Cheng, D.D. Mruk, The blood-testis barrier and its implications for male contraception, *Pharmacological reviews*, 64 (2012) 16-64.
- [156] M.W. Li, D.D. Mruk, W.M. Lee, C.Y. Cheng, Connexin 43 and plakophilin-2 as a protein complex that regulates blood-testis barrier dynamics, *Proc Natl Acad Sci U S A*, 106 (2009) 10213-10218.

- [157] Y. Toyama, M. Ohkawa, R. Oku, M. Maekawa, S. Yuasa, Neonatally administered diethylstilbestrol retards the development of the blood-testis barrier in the rat, *J Androl*, 22 (2001) 413-423.
- [158] C.H. Wong, D.D. Mruk, W.Y. Lui, C.Y. Cheng, Regulation of blood-testis barrier dynamics: an in vivo study, *J Cell Sci*, 117 (2004) 783-798.
- [159] H.T. Wan, D.D. Mruk, C.K. Wong, C.Y. Cheng, Perfluorooctanesulfonate (PFOS) perturbs male rat Sertoli cell blood-testis barrier function by affecting F-actin organization via p-FAK-Tyr(407): an in vitro study, *Endocrinology*, 155 (2014) 249-262.
- [160] M.W. Li, D.D. Mruk, W.M. Lee, C.Y. Cheng, Disruption of the blood-testis barrier integrity by bisphenol A in vitro: is this a suitable model for studying blood-testis barrier dynamics?, *The international journal of biochemistry & cell biology*, 41 (2009) 2302-2314.
- [161] W. Meng, M. Takeichi, Adherens junction: molecular architecture and regulation, *Cold Spring Harbor perspectives in biology*, 1 (2009) a002899.
- [162] C.M. Niessen, C.J. Gottardi, Molecular components of the adherens junction, *Biochimica et biophysica acta*, 1778 (2008) 562-571.
- [163] L. Larue, M. Ohsugi, J. Hirchenhain, R. Kemler, E-cadherin null mutant embryos fail to form a trophectoderm epithelium, *Proc Natl Acad Sci U S A*, 91 (1994) 8263-8267.
- [164] G.L. Radice, H. Rayburn, H. Matsunami, K.A. Knudsen, M. Takeichi, R.O. Hynes, Developmental defects in mouse embryos lacking N-cadherin, *Developmental biology*, 181 (1997) 64-78.
- [165] G.L. Radice, M.C. Ferreira-Cornwell, S.D. Robinson, H. Rayburn, L.A. Chodosh, M. Takeichi, R.O. Hynes, Precocious mammary gland development in P-cadherin-deficient mice, *J Cell Biol*, 139 (1997) 1025-1032.

- [166] H. Haegel, L. Larue, M. Ohsugi, L. Fedorov, K. Herrenknecht, R. Kemler, Lack of beta-catenin affects mouse development at gastrulation, *Development*, 121 (1995) 3529-3537.
- [167] C. Bierkamp, K.J. McLaughlin, H. Schwarz, O. Huber, R. Kemler, Embryonic heart and skin defects in mice lacking plakoglobin, *Developmental biology*, 180 (1996) 780-785.
- [168] M. Torres, A. Stoykova, O. Huber, K. Chowdhury, P. Bonaldo, A. Mansouri, S. Butz, R. Kemler, P. Gruss, An alpha-E-catenin gene trap mutation defines its function in preimplantation development, *Proc Natl Acad Sci U S A*, 94 (1997) 901-906.
- [169] R.G. Oas, K. Xiao, S. Summers, K.B. Wittich, C.M. Chiasson, W.D. Martin, H.E. Grossniklaus, P.A. Vincent, A.B. Reynolds, A.P. Kowalczyk, p120-Catenin is required for mouse vascular development, *Circulation research*, 106 (2010) 941-951.
- [170] W. Ikeda, H. Nakanishi, J. Miyoshi, K. Mandai, H. Ishizaki, M. Tanaka, A. Togawa, K. Takahashi, H. Nishioka, H. Yoshida, A. Mizoguchi, S. Nishikawa, Y. Takai, Afadin: A key molecule essential for structural organization of cell-cell junctions of polarized epithelia during embryogenesis, *J Cell Biol*, 146 (1999) 1117-1132.
- [171] S.M. Troyanovsky, Mechanism of cell-cell adhesion complex assembly, *Current opinion in cell biology*, 11 (1999) 561-566.
- [172] P.P. Lie, C.Y. Cheng, D.D. Mruk, The biology of the desmosome-like junction a versatile anchoring junction and signal transducer in the seminiferous epithelium, *International review of cell and molecular biology*, 286 (2011) 223-269.
- [173] K.J. Green, C.L. Simpson, Desmosomes: new perspectives on a classic, *J Invest Dermatol*, 127 (2007) 2499-2515.

- [174] D.K. Armstrong, K.E. McKenna, P.E. Purkis, K.J. Green, R.A. Eady, I.M. Leigh, A.E. Hughes, Haploinsufficiency of desmoplakin causes a striate subtype of palmoplantar keratoderma, *Hum Mol Genet*, 8 (1999) 143-148.
- [175] D.M. Hunt, L. Rickman, N.V. Whittock, R.A. Eady, D. Simrak, P.J. Dopping-Hepenstal, H.P. Stevens, D.K. Armstrong, H.C. Hennies, W. Kuster, A.E. Hughes, J. Arnemann, I.M. Leigh, J.A. McGrath, D.P. Kelsell, R.S. Buxton, Spectrum of dominant mutations in the desmosomal cadherin desmoglein 1, causing the skin disease striate palmoplantar keratoderma, *Eur J Hum Genet*, 9 (2001) 197-203.
- [176] D. Li, Y. Liu, M. Maruyama, W. Zhu, H. Chen, W. Zhang, S. Reuter, S.F. Lin, L.S. Haneline, L.J. Field, P.S. Chen, W. Shou, Restrictive loss of plakoglobin in cardiomyocytes leads to arrhythmogenic cardiomyopathy, *Hum Mol Genet*, 20 (2011) 4582-4596.
- [177] G. McKoy, N. Protonotarios, A. Crosby, A. Tsatsopoulou, A. Anastasakis, A. Coonar, M. Norman, C. Baboonian, S. Jeffery, W.J. McKenna, Identification of a deletion in plakoglobin in arrhythmogenic right ventricular cardiomyopathy with palmoplantar keratoderma and woolly hair (Naxos disease), *Lancet*, 355 (2000) 2119-2124.
- [178] E.E. Norgett, S.J. Hatsell, L. Carvajal-Huerta, J.C. Cabezas, J. Common, P.E. Purkis, N. Whittock, I.M. Leigh, H.P. Stevens, D.P. Kelsell, Recessive mutation in desmoplakin disrupts desmoplakin-intermediate filament interactions and causes dilated cardiomyopathy, woolly hair and keratoderma, *Hum Mol Genet*, 9 (2000) 2761-2766.
- [179] L. Rickman, D. Simrak, H.P. Stevens, D.M. Hunt, I.A. King, S.P. Bryant, R.A. Eady, I.M. Leigh, J. Arnemann, A.I. Magee, D.P. Kelsell, R.S. Buxton, N-terminal deletion in a desmosomal cadherin causes the autosomal dominant skin disease striate palmoplantar keratoderma, *Hum Mol Genet*, 8 (1999) 971-976.

- [180] N.V. Whittock, M. Haftek, N. Angoulvant, F. Wolf, H. Perrot, R.A. Eady, J.A. McGrath, Genomic amplification of the human plakophilin 1 gene and detection of a new mutation in ectodermal dysplasia/skin fragility syndrome, *J Invest Dermatol*, 115 (2000) 368-374.
- [181] B.V. Desai, R.M. Harmon, K.J. Green, Desmosomes at a glance, *J Cell Sci*, 122 (2009) 4401-4407.
- [182] W.W. Franke, Discovering the molecular components of intercellular junctions--a historical view, *Cold Spring Harbor perspectives in biology*, 1 (2009) a003061.
- [183] L. Eshkind, Q. Tian, A. Schmidt, W.W. Franke, R. Windoffer, R.E. Leube, Loss of desmoglein 2 suggests essential functions for early embryonic development and proliferation of embryonal stem cells, *Eur J Cell Biol*, 81 (2002) 592-598.
- [184] Z. Den, X. Cheng, M. Merched-Sauvage, P.J. Koch, Desmocollin 3 is required for pre-implantation development of the mouse embryo, *J Cell Sci*, 119 (2006) 482-489.
- [185] M. Chidgey, C. Brakebusch, E. Gustafsson, A. Cruchley, C. Hail, S. Kirk, A. Merritt, A. North, C. Tselepis, J. Hewitt, C. Byrne, R. Fassler, D. Garrod, Mice lacking desmocollin 1 show epidermal fragility accompanied by barrier defects and abnormal differentiation, *J Cell Biol*, 155 (2001) 821-832.
- [186] P.J. Koch, M.G. Mahoney, H. Ishikawa, L. Pulkkinen, J. Uitto, L. Shultz, G.F. Murphy, D. Whitaker-Menezes, J.R. Stanley, Targeted disruption of the pemphigus vulgaris antigen (desmoglein 3) gene in mice causes loss of keratinocyte cell adhesion with a phenotype similar to pemphigus vulgaris, *J Cell Biol*, 137 (1997) 1091-1102.
- [187] E. Delva, D.K. Tucker, A.P. Kowalczyk, The desmosome, *Cold Spring Harbor perspectives in biology*, 1 (2009) a002543.

- [188] A. Schmidt, L. Langbein, S. Pratzel, M. Rode, H.R. Rackwitz, W.W. Franke, Plakophilin 3--a novel cell-type-specific desmosomal plaque protein, *Differentiation; research in biological diversity*, 64 (1999) 291-306.
- [189] C. Bierkamp, K.J. McLaughlin, H. Schwarz, O. Huber, R. Kemler, Embryonic heart and skin defects in mice lacking plakoglobin, *Dev Biol*, 180 (1996) 780-785.
- [190] K.S. Grossmann, C. Grund, J. Huelsken, M. Behrend, B. Erdmann, W.W. Franke, W. Birchmeier, Requirement of plakophilin 2 for heart morphogenesis and cardiac junction formation, *J Cell Biol*, 167 (2004) 149-160.
- [191] T. Sklyarova, S. Bonne, P. D'Hooge, G. Denecker, S. Goossens, R. De Rycke, G. Borgonie, M. Bosl, F. van Roy, J. van Hengel, Plakophilin-3-deficient mice develop hair coat abnormalities and are prone to cutaneous inflammation, *J Invest Dermatol*, 128 (2008) 1375-1385.
- [192] K. Rietscher, A. Wolf, G. Hause, A. Rother, R. Keil, T.M. Magin, M. Glass, C.M. Niessen, M. Hatzfeld, Growth Retardation, Loss of Desmosomal Adhesion, and Impaired Tight Junction Function Identify a Unique Role of Plakophilin 1 In Vivo, *J Invest Dermatol*, 136 (2016) 1471-1478.
- [193] K.J. Green, D.A. Parry, P.M. Steinert, M.L. Virata, R.M. Wagner, B.D. Angst, L.A. Nilles, Structure of the human desmoplakins. Implications for function in the desmosomal plaque, *The Journal of biological chemistry*, 265 (1990) 11406-11407.
- [194] G.I. Gallicano, P. Kouklis, C. Bauer, M. Yin, V. Vasioukhin, L. Degenstein, E. Fuchs, Desmoplakin is required early in development for assembly of desmosomes and cytoskeletal linkage, *J Cell Biol*, 143 (1998) 2009-2022.

- [195] D. Wiederschain, S. Wee, L. Chen, A. Loo, G. Yang, A. Huang, Y. Chen, G. Caponigro, Y.M. Yao, C. Lengauer, W.R. Sellers, J.D. Benson, Single-vector inducible lentiviral RNAi system for oncology target validation, *Cell Cycle*, 8 (2009) 498-504.
- [196] L. Sehgal, Generation of knockdown mice that lack 14-3-3 ϵ and 14-3-3 γ using RNA interference., Life Sciences, Homi Bhabha National Institute, Advanced Centre for Treatment Research and Education in Cancer (ACTREC), Cancer Research Institute (CRI), Navi Mumbai., 2012, pp. 221.
- [197] P.A. Coulombe, R. Kopan, E. Fuchs, Expression of keratin K14 in the epidermis and hair follicle: insights into complex programs of differentiation, *J Cell Biol*, 109 (1989) 2295-2312.
- [198] R. Christensen, L. Alhonen, J. Wahlfors, M. Jakobsen, T.G. Jensen, Characterization of transgenic mice with the expression of phenylalanine hydroxylase and GTP cyclohydrolase I in the skin, *Exp Dermatol*, 14 (2005) 535-542.
- [199] J.M. Arbeit, K. Munger, P.M. Howley, D. Hanahan, Progressive squamous epithelial neoplasia in K14-human papillomavirus type 16 transgenic mice, *J Virol*, 68 (1994) 4358-4368.
- [200] T. Kopp, J.D. Kieffer, A. Rot, S. Strommer, G. Stingl, T.S. Kupper, Inflammatory skin disease in K14/p40 transgenic mice: evidence for interleukin-12-like activities of p40, *J Invest Dermatol*, 117 (2001) 618-626.
- [201] S.T. Kundu, P. Gosavi, N. Khapare, R. Patel, A.S. Hosing, G.B. Maru, A. Ingle, J.A. DeCaprio, S.N. Dalal, Plakophilin3 downregulation leads to a decrease in cell adhesion and promotes metastasis, *International journal of cancer*, 123 (2008) 2303-2314.
- [202] P. Gosavi, S.T. Kundu, N. Khapare, L. Sehgal, M.S. Karkhanis, S.N. Dalal, E-cadherin and plakoglobin recruit plakophilin3 to the cell border to initiate desmosome assembly, *Cellular and molecular life sciences : CMLS*, 68 (2011) 1439-1454.

- [203] L. Sehgal, A. Usmani, S.N. Dalal, S.S. Majumdar, Generation of transgenic mice by exploiting spermatogonial stem cells in vivo, *Methods in molecular biology*, 1194 (2014) 327-337.
- [204] K.M. Braun, C. Niemann, U.B. Jensen, J.P. Sundberg, V. Silva-Vargas, F.M. Watt, Manipulation of stem cell proliferation and lineage commitment: visualisation of label-retaining cells in wholemounts of mouse epidermis, *Development*, 130 (2003) 5241-5255.
- [205] E.B. Ehrke-Schulz, T.; Schiwon, M.; Doerner, J.; Saydaminova, K.; Lieber, A.; Ehrhardt, A., Quantification of designer nuclease induced mutation rates: a direct comparison of different methods., *Mol Ther Methods Clin Dev*, (2016).
- [206] N.R. Leitner, C. Lassnig, R. Rom, S. Heider, Z. Bago-Horvath, R. Eferl, S. Muller, T. Kolbe, L. Kenner, T. Rulicke, B. Strobl, M. Muller, Inducible, dose-adjustable and time-restricted reconstitution of STAT1 deficiency in vivo, *PLoS One*, 9 (2014) e86608.
- [207] M.D. Anway, J. Folmer, W.W. Wright, B.R. Zirkin, Isolation of sertoli cells from adult rat testes: an approach to ex vivo studies of Sertoli cell function, *Biol Reprod*, 68 (2003) 996-1002.
- [208] E.G. Fey, K.M. Wan, S. Penman, Epithelial cytoskeletal framework and nuclear matrix-intermediate filament scaffold: three-dimensional organization and protein composition, *J Cell Biol*, 98 (1984) 1973-1984.
- [209] M. Pasdar, W.J. Nelson, Kinetics of desmosome assembly in Madin-Darby canine kidney epithelial cells: temporal and spatial regulation of desmoplakin organization and stabilization upon cell-cell contact. I. Biochemical analysis, *J Cell Biol*, 106 (1988) 677-685.
- [210] K.T. Trevor, L.S. Steben, Distribution of desmosomal proteins in F9 embryonal carcinoma cells and epithelial cell derivatives, *J Cell Sci*, 103 (Pt 1) (1992) 69-80.

- [211] P. Gosavi, S.T. Kundu, N. Khapare, L. Sehgal, M.S. Karkhanis, S.N. Dalal, E-cadherin and plakoglobin recruit plakophilin3 to the cell border to initiate desmosome assembly, *Cell Mol Life Sci*, 68 (2011) 1439-1454.
- [212] M. Pasdar, W.J. Nelson, Kinetics of desmosome assembly in Madin-Darby canine kidney epithelial cells: temporal and spatial regulation of desmoplakin organization and stabilization upon cell-cell contact. II. Morphological analysis, *J Cell Biol*, 106 (1988) 687-695.
- [213] S.T. Kundu, P. Gosavi, N. Khapare, R. Patel, A.S. Hosing, G.B. Maru, A. Ingle, J.A. Decaprio, S.N. Dalal, Plakophilin3 downregulation leads to a decrease in cell adhesion and promotes metastasis, *Int J Cancer*, 123 (2008) 2303-2314.
- [214] A.S. Hosing, Regulation of the G2/M DNA damage checkpoint by 14-3-3 proteins in human cells., Mumbai University, Advanced Centre for Treatment Research and Education in Cancer (ACTREC), Cancer Research Institute (CRI), Navi Mumbai., 2009, pp. 213.
- [215] M.A. Brooke, D. Nitoiu, D.P. Kelsell, Cell-cell connectivity: desmosomes and disease, *The Journal of pathology*, 226 (2012) 158-171.
- [216] M.D. Kottke, E. Delva, A.P. Kowalczyk, The desmosome: cell science lessons from human diseases, *J Cell Sci*, 119 (2006) 797-806.
- [217] G. Denecker, P. Ovaere, P. Vandenabeele, W. Declercq, Caspase-14 reveals its secrets, *J Cell Biol*, 180 (2008) 451-458.
- [218] A.K. Wilson, P.A. Coulombe, E. Fuchs, The roles of K5 and K14 head, tail, and R/K L L E G E domains in keratin filament assembly in vitro, *J Cell Biol*, 119 (1992) 401-414.
- [219] H.H. Bragulla, D.G. Homberger, Structure and functions of keratin proteins in simple, stratified, keratinized and cornified epithelia, *Journal of anatomy*, 214 (2009) 516-559.

- [220] J. Schweizer, F. Marks, A developmental study of the distribution and frequency of Langerhans cells in relation to formation of patterning in mouse tail epidermis, *J Invest Dermatol*, 69 (1977) 198-204.
- [221] J.G. Nijhof, K.M. Braun, A. Giangreco, C. van Pelt, H. Kawamoto, R.L. Boyd, R. Willemze, L.H. Mullenders, F.M. Watt, F.R. de Gruijl, W. van Ewijk, The cell-surface marker MTS24 identifies a novel population of follicular keratinocytes with characteristics of progenitor cells, *Development*, 133 (2006) 3027-3037.
- [222] S.S.T. Vishal, S.; Dalal, S. N., Generation of mice with tissue specific transgene expression using sperm mediated gene transfer., *International Journal of Pharma and Bio Sciences.*, 8 (2017) 324-329.
- [223] J. Ablain, E.M. Durand, S. Yang, Y. Zhou, L.I. Zon, A CRISPR/Cas9 vector system for tissue-specific gene disruption in zebrafish, *Developmental cell*, 32 (2015) 756-764.
- [224] A. Leask, C. Byrne, E. Fuchs, Transcription factor AP2 and its role in epidermal-specific gene expression, *Proc Natl Acad Sci U S A*, 88 (1991) 7948-7952.
- [225] F. Di Nunzio, G. Maruggi, S. Ferrari, E. Di Iorio, V. Poletti, M. Garcia, M. Del Rio, M. De Luca, F. Larcher, G. Pellegrini, F. Mavilio, Correction of laminin-5 deficiency in human epidermal stem cells by transcriptionally targeted lentiviral vectors, *Molecular therapy : the journal of the American Society of Gene Therapy*, 16 (2008) 1977-1985.
- [226] H. Kurahashi, B.S. Emanuel, Long AT-rich palindromes and the constitutional t(11;22) breakpoint, *Hum Mol Genet*, 10 (2001) 2605-2617.
- [227] X. Wang, S. Zinkel, K. Polonsky, E. Fuchs, Transgenic studies with a keratin promoter-driven growth hormone transgene: prospects for gene therapy, *Proc Natl Acad Sci U S A*, 94 (1997) 219-226.

- [228] S.S. Vishal, S. Tilwani, S.N. Dalal, Plakoglobin localization to the cell border restores desmosome function in cells lacking 14-3-3gamma, *Biochem Biophys Res Commun*, 495 (2018) 1998-2003.
- [229] J.P. Mather, K.M. Attie, T.K. Woodruff, G.C. Rice, D.M. Phillips, Activin stimulates spermatogonial proliferation in germ-Sertoli cell cocultures from immature rat testis, *Endocrinology*, 127 (1990) 3206-3214.
- [230] R.M. Sharpe, C. McKinnell, C. Kivlin, J.S. Fisher, Proliferation and functional maturation of Sertoli cells, and their relevance to disorders of testis function in adulthood, *Reproduction*, 125 (2003) 769-784.
- [231] M. Pasdar, W.J. Nelson, Regulation of desmosome assembly in epithelial cells: kinetics of synthesis, transport, and stabilization of desmoglein I, a major protein of the membrane core domain, *J Cell Biol*, 109 (1989) 163-177.
- [232] N.A.T. Chitaev, S. M., Direct Ca^{2+} -dependent Heterophilic Interaction between Desmosomal Cadherins, Desmoglein and Desmocollin, Contributes to Cell–Cell Adhesion, *Journal of Cell Biology*, 138 (1997) 193-201.
- [233] R.B.C. Troyanovsky, N. A.; Troyanovsky, S. M., Cadherin binding sites of plakoglobin: localization, specificity and role in targeting to adhering junctions, *Journal of cell science*, 109 (1996) 3069-3078.
- [234] A.P. Kowalczyk, E.A. Bornslaeger, J.E. Borgwardt, H.L. Palka, A.S. Dhaliwal, C.M. Corcoran, M.F. Denning, K.J. Green, The amino-terminal domain of desmoplakin binds to plakoglobin and clusters desmosomal cadherin-plakoglobin complexes, *J Cell Biol*, 139 (1997) 773-784.

- [235] O. Shafraz, M. Rubsam, S.N. Stahley, A.L. Caldara, A.P. Kowalczyk, C.M. Niessen, S. Sivasankar, E-cadherin binds to desmoglein to facilitate desmosome assembly, *Elife*, 7 (2018).
- [236] C. Michels, T. Buchta, W. Bloch, T. Krieg, C.M. Niessen, Classical cadherins regulate desmosome formation, *J Invest Dermatol*, 129 (2009) 2072-2075.
- [237] T. Yin, S. Getsios, R. Caldelari, L.M. Godsel, A.P. Kowalczyk, E.J. Muller, K.J. Green, Mechanisms of plakoglobin-dependent adhesion: desmosome-specific functions in assembly and regulation by epidermal growth factor receptor, *The Journal of biological chemistry*, 280 (2005) 40355-40363.
- [238] N.A. Chitaev, R.E. Leube, R.B. Troyanovsky, L.G. Eshkind, W.W. Franke, S.M. Troyanovsky, The binding of plakoglobin to desmosomal cadherins: patterns of binding sites and topogenic potential, *J Cell Biol*, 133 (1996) 359-369.
- [239] C.D. Andl, J.R. Stanley, Central role of the plakoglobin-binding domain for desmoglein 3 incorporation into desmosomes, *J Invest Dermatol*, 117 (2001) 1068-1074.
- [240] O.E. Nekrasova, E.V. Amargo, W.O. Smith, J. Chen, G.E. Kreitzer, K.J. Green, Desmosomal cadherins utilize distinct kinesins for assembly into desmosomes, *J Cell Biol*, 195 (2011) 1185-1203.
- [241] M. Fujiwara, A. Nagatomo, M. Tsuda, S. Obata, T. Sakuma, T. Yamamoto, S.T. Suzuki, Desmocollin-2 alone forms functional desmosomal plaques, with the plaque formation requiring the juxtamembrane region and plakophilins, *J Biochem*, 158 (2015) 339-353.
- [242] M. Gurjar, K. Raychaudhuri, S. Mahadik, D. Reddy, A. Atak, T. Shetty, K. Rao, M.S. Karkhanis, P. Gosavi, L. Sehgal, S. Gupta, S.N. Dalal, Plakophilin3 increases desmosome assembly, size and stability by increasing expression of desmocollin2, *Biochem Biophys Res Commun*, 495 (2018) 768-774.

- [243] K. Raychudhuri, Gurjar, M., and Dalal, S.N., Plakophilin3 and Plakoglobin recycling are differentially regulated during the disassembly of desmosomes., *Journal of Bioscience And Technology*, 6 (2015) 634-642.
- [244] V. Todorovic, J.L. Koetsier, L.M. Godsel, K.J. Green, Plakophilin 3 mediates Rap1-dependent desmosome assembly and adherens junction maturation, *Molecular biology of the cell*, 25 (2014) 3749-3764.
- [245] S.S.T. Vishal, S.; Dalal, S. N., Plakoglobin localization to the cell border restores desmosome function in cells lacking 14-3-3 γ ., *Biochem Biophys Res Commun*, 495 (2018) 1998-2003.
- [246] R.B.C. Troyanovsky, N. A.; Troyanovsky S. M., Cadherin binding sites of plakoglobin: localization, specificity and role in targeting to adhering junctions., *J Cell Sci*, 109 (1996) 3069-3078.

Publications

RESEARCH ARTICLE

14-3-3 γ -mediated transport of plakoglobin to the cell border is required for the initiation of desmosome assembly *in vitro* and *in vivo*

Lalit Sehgal^{1,2}, Amitabha Mukhopadhyay¹, Anandi Rajan^{1,*}, Nileema Khapare^{1,*}, Mugdha Sawant^{1,*}, Sonali S. Vishal¹, Khyati Bhatt¹, Srikant Ambatipudi¹, Noelle Antao¹, Hunain Alam¹, Mansa Gurjar¹, Srikanta Basu¹, Rohit Mathur², Lalit Borde³, Amol S. Hosing¹, Milind M. Vaidya¹, Rahul Thorat¹, Felipe Samaniego², Ullas Kolthur-Seetharam³ and Sorab N. Dalal^{1,†}

ABSTRACT

The regulation of cell–cell adhesion is important for the processes of tissue formation and morphogenesis. Here, we report that loss of 14-3-3 γ leads to a decrease in cell–cell adhesion and a defect in the transport of plakoglobin and other desmosomal proteins to the cell border in HCT116 cells and cells of the mouse testis. 14-3-3 γ binds to plakoglobin in a PKC μ -dependent fashion, resulting in microtubule-dependent transport of plakoglobin to cell borders. Transport of plakoglobin to the border is dependent on the KIF5B–KLC1 complex. Knockdown of KIF5B in HCT116 cells, or in the mouse testis, results in a phenotype similar to that observed upon 14-3-3 γ knockdown. Our results suggest that loss of 14-3-3 γ leads to decreased desmosome formation and a decrease in cell–cell adhesion *in vitro*, and in the mouse testis *in vivo*, leading to defects in testis organization and spermatogenesis.

KEY WORDS: 14-3-3 γ , Desmosome, Plakoglobin, KIF5B, Spermatogenesis

INTRODUCTION

Desmosomes are adherens-like junctions that anchor intermediate filaments, leading to the generation of a tissue-wide intermediate filament network. Three different protein families contribute to desmosome structure and function – the desmosomal cadherins desmocollins (DSCs) and desmogleins (DSGs), the armadillo (ARM) proteins and the plakins (Green and Gaudry, 2000). Desmosome composition varies with respect to tissue type and differentiation status, as the cadherins and the associated ARM family members show tissue- and cell-type-specific expression (Bass-Zubek et al., 2009; Dusek et al., 2007), leading to changes in the organization and function of desmosomes in different tissues.

The ARM proteins participate in the regulation of desmosome assembly and cell–cell adhesion (Marcozzi et al., 1998; Palka and Green, 1997). Plakoglobin (encoded by *JUP*) localizes to both

desmosomes and adherens junctions and is required for the initiation of desmosome formation by adherens junctions (Acehan et al., 2008; Knudsen and Wheelock, 1992; Lewis et al., 1997). Decreases in DSG3, the density of the plaque and the levels of plakophilin 1 (PKP1) at the cell border have been observed in plakoglobin-null keratinocytes (Acehan et al., 2008; Caldelari et al., 2001), suggesting that plakoglobin is required for desmosome formation and function in cultured keratinocytes. Plakoglobin-knockout mice die during embryogenesis owing to defects in desmosome formation in cardiac tissue (Ruiz et al., 1996). Some discrepancies exist in the literature regarding the effects of plakoglobin loss on desmosome formation in the epidermis. Ruiz and colleagues have reported that the epidermis of embryos at 11.5 days post coitum are normal upon loss of plakoglobin (Ruiz et al., 1996), whereas others have reported that defects in epidermal organization and desmosome function are observed in mice lacking plakoglobin at 17.5 days post coitum (Bierkamp et al., 1996). Plakoglobin has been reported to form a complex with both P-cadherin and E-cadherin, and the total levels of the classical cadherins dictate desmosome formation and organization (Lewis et al., 1997; Michels et al., 2009; Tinkle et al., 2008). These results suggest that plakoglobin and other ARM proteins might serve as a link between adherens junction formation and desmosome formation. Consistent with this hypothesis, plakoglobin and E-cadherin are independently required for the recruitment of plakophilin 3 (PKP3) to the cell border in order to initiate desmosome formation in HCT116 cells (Gosavi et al., 2011), whereas plakoglobin and the plakophilin family members collaborate with the desmoplakin N-terminus to regulate the clustering of the desmosomal cadherins at the cell surface (Chen et al., 2002). These data are indicative of plakoglobin being required for the initiation of desmosome formation and maintenance. However, the mechanisms by which the ARM proteins are transported to the cell border to initiate the process of desmosome formation remain unclear.

Spermatogenesis occurs in seminiferous tubules in the testis and is intrinsically dependent upon cell–cell adhesion between spermatocytes and Sertoli cells, and the formation of the blood–testis barrier between two Sertoli cells (Russell et al., 1990). These adhesive interactions are crucial for the progression of spermatogenesis. The blood–testis barrier comprises tight junctions, basal ectoplasmic specializations, gap junctions and desmosome-like junctions (Cheng and Mruk, 2002; Lie et al., 2011). Disruption of cell–cell adhesion perturbs the normal progression of spermatogenesis (Wong et al., 2004). Importantly,

¹KS215, ACTREC, Tata Memorial Centre Kharghar Node, Navi Mumbai 410210, India. ²Department of Lymphoma/Myeloma, The University of Texas MD Anderson Cancer Center, 1515 Holcombe Boulevard, Houston, TX 77030, USA. ³Department of Biological Sciences, Tata Institute of Fundamental Research, Homi Bhabha Road, Mumbai 400005, India.

*These authors contributed equally to this work

[†]Author for correspondence (sdalal@actrec.gov.in)

decreasing the expression of PKP2, DSG2 and DSC2 affects cell–cell adhesion, indicating that the development of spermatozoa is regulated by the formation of desmosome-like junctions in the testis (Li et al., 2009; Lie et al., 2010).

The 14-3-3 protein family is a family of small acidic proteins (Yaffe, 2002) that bind to proteins that contain a phosphorylated serine residue in a consensus motif (Muslin et al., 1996; Yaffe et al., 1997). Loss of 14-3-3 ϵ and 14-3-3 γ leads to the overriding of checkpoint function and premature entry into mitosis (Hosing et al., 2008; Telles et al., 2009). Therefore, we wanted to determine whether loss of 14-3-3 γ in the mouse led to defects in checkpoint function. When we attempted to generate 14-3-3 γ -knockdown mice by using a novel transgenic protocol that had been developed in our laboratory (Sehgal et al., 2011), we observed that loss of 14-3-3 γ led to sterility in male mice due to a decrease in cell–cell adhesion and a defect in the transport of plakoglobin and other desmosomal proteins to the cell border in the seminiferous tubules of mice. Similar results were obtained in the human HCT116 colorectal cancer cell line. Furthermore, our results demonstrate that 14-3-3 γ might load plakoglobin onto the KIF5B–KLC1 complex in order to transport plakoglobin to the cell border to initiate desmosome formation, both in HCT116 cells in culture and in the mouse testis, thus demonstrating that 14-3-3 γ is required for desmosome formation.

RESULTS

Loss of 14-3-3 γ leads to sterility in male mice

To determine whether loss of 14-3-3 γ leads to a loss of checkpoint regulation *in vivo*, we attempted to generate knockdown mice for 14-3-3 γ by using a sperm-mediated gene transfer protocol that was developed in our laboratory (Sehgal et al., 2011). However, when mice that had been injected with viruses expressing the shRNA construct against 14-3-3 γ were mated with female mice, no pups were obtained. The levels of 14-3-3 γ were substantially decreased in the testis of mice that had been injected with viruses expressing the shRNA construct against 14-3-3 γ (sh14-3-3 γ) in comparison with the mice that had been injected with the vector control (Vec, Fig. 1A). Loss of 14-3-3 γ led to an almost complete absence of mature spermatozoa in the epididymis in comparison with the control mice (Fig. 1B,C). In addition, the organization of the seminiferous tubule was severely disrupted upon 14-3-3 γ knockdown, as evidenced by individual sections of the seminiferous tubule being dissociated from one another in comparison with those of control mice (Fig. 1B). Furthermore, primary germ cells and Sertoli cells were detached from the basal lamina. This did not lead to a large increase in transferase dUTP nick end labeling (TUNEL)-positive cells (supplementary material Fig. S1A). Finally, histological examination revealed an abrogation of cell–cell adhesion between Sertoli cells, and between Sertoli cells and germ cells, in the testis, upon knockdown of 14-3-3 γ (Fig. 1D), which was confirmed by electron microscopy (Fig. 1E). Thus, these results suggest that loss of 14-3-3 γ leads to a decrease in cell–cell adhesion *in vivo*.

14-3-3 γ loss leads to defects in cell adhesion and desmosome assembly

To identify the mechanisms that lead to a decrease in cell–cell adhesion, we used a HCT116 cell line model in which 14-3-3 γ had been knocked down (sh14-3-3 γ) (described previously by Hosing et al., 2008). 14-3-3 γ mRNA and protein levels were lower in the sh14-3-3 γ cells in comparison with the control cells

(Fig. 2A,B). The protein levels of 14-3-3 ϵ and 14-3-3 σ , or the mRNA levels of 14-3-3 ϵ , 14-3-3 β , 14-3-3 τ and 14-3-3 ζ (Fig. 2A,B) were not altered in the sh14-3-3 γ cells in comparison with vector control cells (Fig. 2A). In comparison with the control cells, the sh14-3-3 γ cells showed a decrease in cell–cell adhesion in hanging-drop assays (Fig. 2C,D), and cell adhesion to fibronectin and collagen IV was also diminished in these cells (supplementary material Fig. S1B), which is consistent with the detachment of cells in the testis from the basal lamina.

To determine whether the defect in cell–cell adhesion was induced specifically by the loss of 14-3-3 γ , cells that had been subjected to 14-3-3 ϵ knockdown were generated (sh14-3-3 ϵ). Western blot analysis demonstrated that, although 14-3-3 ϵ protein levels were decreased in sh14-3-3 ϵ cells, the levels of 14-3-3 γ were unaltered. No substantial difference was observed in cell–cell adhesion in the sh14-3-3 ϵ -knockdown cells in comparison with the control cells (Fig. 2F,G). These results suggest that the differences in cell–cell adhesion that are observed upon knockdown of 14-3-3 γ are specific to the 14-3-3 γ isoform.

To determine the causes of the decrease in cell–cell adhesion, the levels of adhesion proteins in the control and sh14-3-3 γ cells were determined by western blot analysis or reverse transcription PCR (RT-PCR) (Fig. 3A–C). The levels of these proteins or mRNAs were not decreased upon 14-3-3 γ knockdown. However, in the case of DSG2, and DSC2 and DSC3, increased protein levels were observed in the 14-3-3 γ knockdown cells (Fig. 3B), although no substantial increase was observed in mRNA levels (Fig. 3C). PKP2 mRNA levels were not altered substantially in the sh14-3-3 γ cells in comparison with the control cells (Fig. 3C), and our previous reports have suggested that HCT116 cells do not express PKP1 (Kundu et al., 2008). Notably, the levels of the desmosomal proteins plakoglobin, PKP3, desmoplakin, DSC2 and DSC3, DSG2 and PKP2 were significantly lower at the cell borders in sh14-3-3 γ cells than in control cells (Fig. 3E,F), even though the total levels of these proteins were unaltered in the sh14-3-3 γ cells. Intensity profiles for the staining are shown in supplementary material Fig. S2. Importantly, no change in the detergent solubility of the desmosomal proteins was observed in the 14-3-3 γ -knockdown cells when compared with the control cells (supplementary material Fig. S4D).

By contrast, the levels of adherens junction components [E-cadherin (also known as CDH1), P-cadherin (also known as CDH3), β -catenin, p120-catenin (also known as CTNND1) and α -E-catenin], tight junction components (ZO-1) and polarity proteins (Par-3, also known as PARD3) were not reduced at the cell border in sh14-3-3 γ cells (supplementary material Fig. S1D,E). Loss of 14-3-3 ϵ did not result in a decrease in the levels of plakoglobin at the cell border (Fig. 3D). HCT116 cells that lacked both copies of 14-3-3 σ (Chan et al., 1999) showed a decrease in plakoglobin levels (supplementary material Fig. S4A) and a decrease in cell–cell adhesion (supplementary material Fig. S4B). However, there was no defect in localization of plakoglobin to the border in these cells (supplementary material Fig. S4C), suggesting that 14-3-3 σ is required to maintain plakoglobin protein levels, but not plakoglobin localization to the border.

Expression of a green fluorescent protein (GFP)-tagged shRNA-resistant 14-3-3 γ cDNA (GFP-14-3-3 γ R) resulted in the recruitment of plakoglobin to the cell border in sh14-3-3 γ cells in contrast with cells transfected with GFP alone (Fig. 4A). To determine whether the desmosomal proteins formed a complex with 14-3-3 γ , protein extracts from HCT116 cells

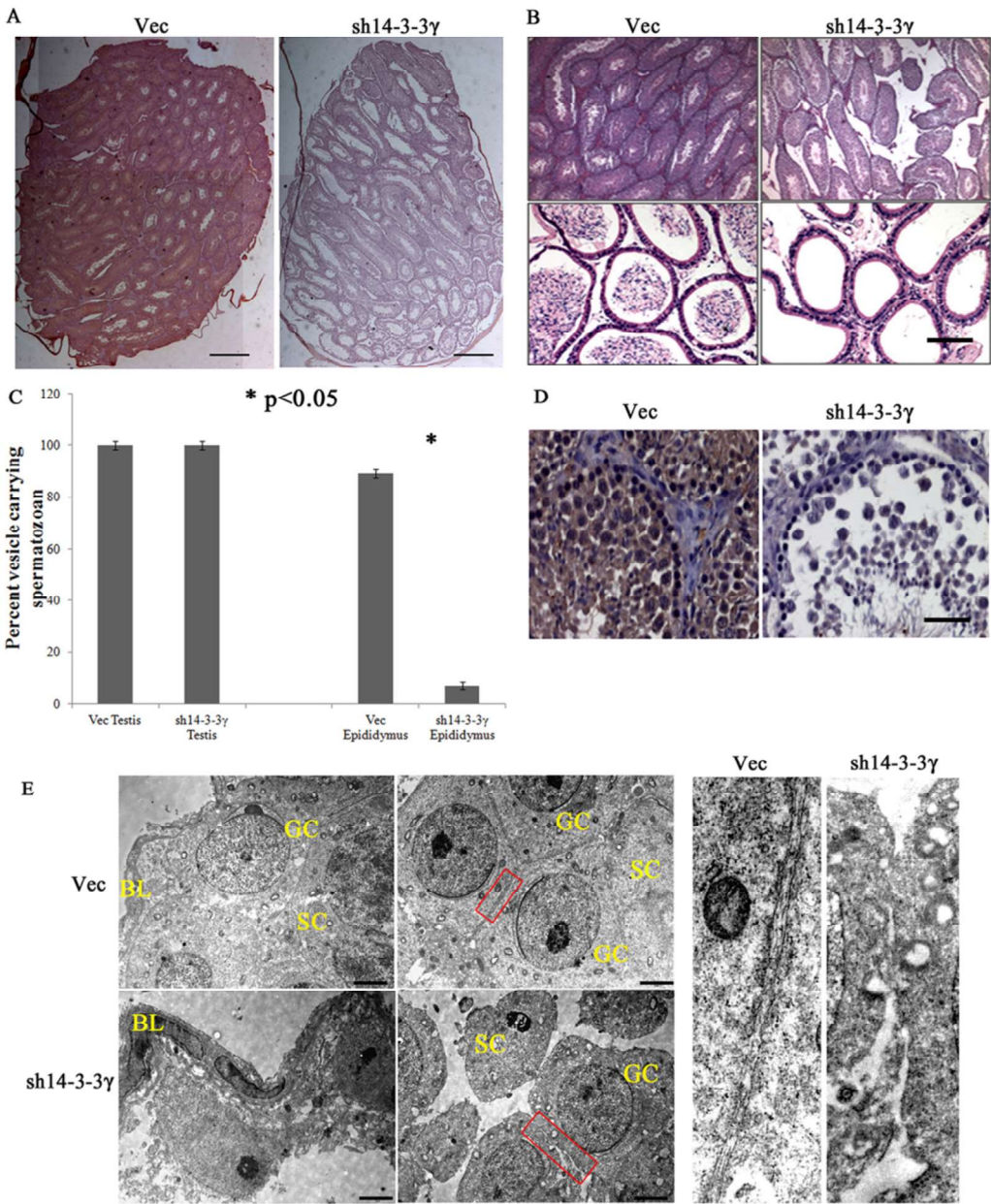


Fig. 1. Loss of 14-3-3 γ leads to disruption of cell-cell adhesion. (A–D) Tissue sections from mouse testis that had been injected with either the 14-3-3 γ -knockdown construct (sh14-3-3 γ) or the vector control (Vec) were stained with antibodies against 14-3-3 γ and visualized by using light microscopy (A shows the entire testis, D shows a single seminiferous tubule), or were stained with hematoxylin and eosin (B) to visualize either the seminiferous tubules (top panels) or the epididymis (bottom panels). The percentage of vesicles that contained spermatozoa in the epididymis is shown and the error bars represent the mean \pm s.d. for three different animals (C). (E) Electron micrographs of testis that had been injected with either the 14-3-3 γ knockdown virus or the vector control. Sertoli cells (SC), and germ cells (GC) are indicated. The panels on the far right are higher magnification images of the boxed areas indicated. Scale bars: 5 μ m (A,B,D); 2 μ m (E).

were incubated with either glutathione S-transferase (GST) alone or GST–14-3-3 γ . 14-3-3 γ formed a complex with plakoglobin, PKP3 and desmoplakin but not with DSG2 or adherens junction proteins, such as E-cadherin (Fig. 4B). Our previous results have suggested that plakoglobin is present at the cell border in low-calcium medium, and that plakoglobin is required for the recruitment of other desmosomal proteins to the cell border in HCT116 cells and for the initiation of desmosome formation upon the addition of calcium (Gosavi et al., 2011). Therefore, to determine whether 14-3-3 γ is required for the initiation of desmosome formation, calcium-switch assays were performed. Plakoglobin was present at the cell border in low-calcium medium and the levels at the border increased upon the addition of calcium in the vector control cells. DSC2 and DSC3 were not detectable at the border in the control cells in low-calcium medium. However, DSC2 and DSC3 localized to the border 60 minutes after the addition of calcium in the control cells. By contrast, in the sh14-3-3 γ cells, plakoglobin, DSC2 and DSC3

were not present at the border in low-calcium medium and accumulated at significantly lower levels at the border upon the addition of calcium in comparison with the control cells (Fig. 4C). E-cadherin levels at the border were unaffected in the sh14-3-3 γ cells in comparison with the control cells (Fig. 4C). These results suggest that 14-3-3 γ specifically is required for the localization of plakoglobin to cell borders and is required for the initiation of desmosome formation.

We observed that, although the levels of DSC2 and DSC3 at the cell borders were lower in 14-3-3 γ -knockdown cells than in the control cells, a substantial fraction of DSC2 and DSC3, nevertheless still localized to the borders in the knockdown cells. These results suggested that, to some extent, localization of DSC2 and DSC3 to the border might be independent of the presence of 14-3-3 γ and plakoglobin at the cell border. We have previously shown that, in this cell system, plakoglobin is required to recruit PKP3 and desmoplakin to the cell border (Gosavi et al., 2011). To determine whether plakoglobin is required for the recruitment of

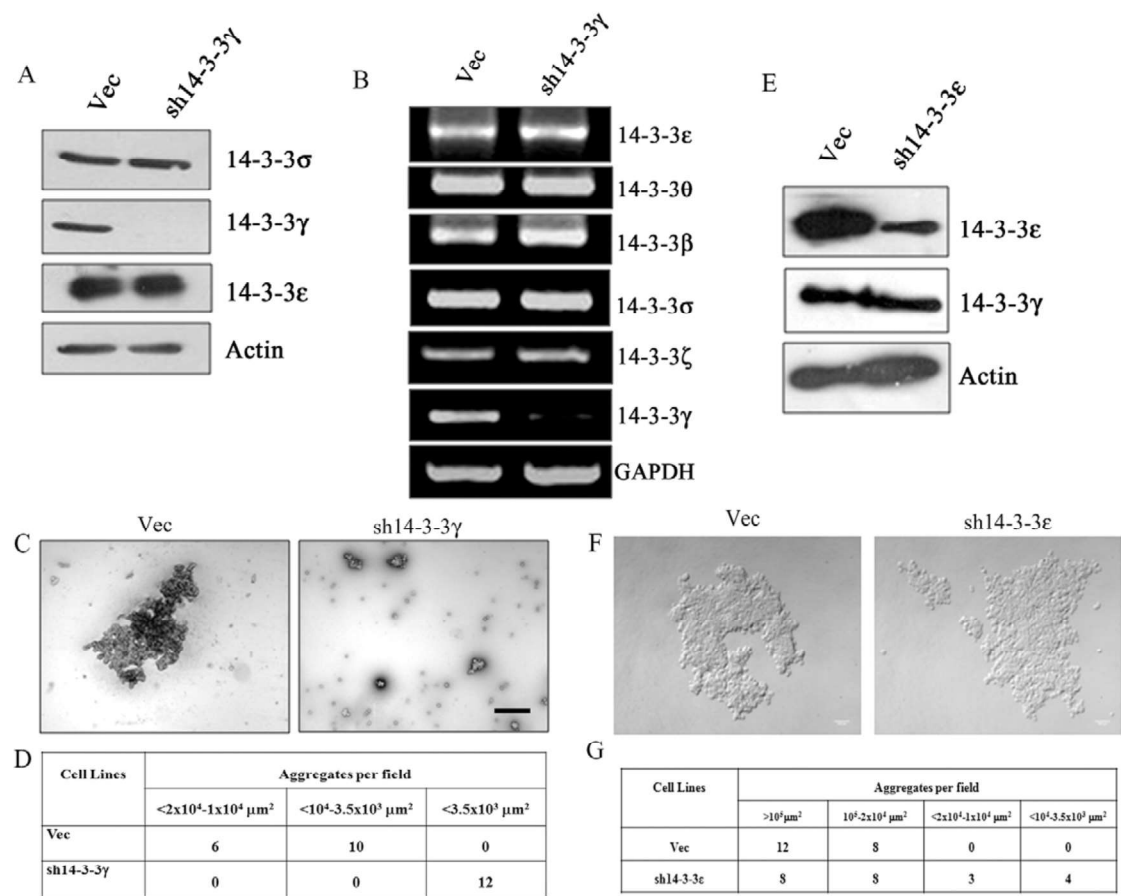


Fig. 2. Loss of 14-3-3γ leads to a decrease in cell–cell adhesion. (A) Protein extracts from the vector control (Vec) and 14-3-3γ-knockdown (sh14-3-3γ) cells were resolved on SDS-PAGE gels followed by western blotting with the indicated antibodies. Actin served as a loading control. (B) mRNA was prepared from the control and sh14-3-3γ cells and RT-PCR reactions were performed with oligonucleotide pairs specific for the indicated genes. GAPDH served as a reaction control. (C,D) Hanging-drop assays were performed on the control and sh14-3-3γ cells. The images (C) of the clumps and the quantification (D) of cluster number and size are shown. (E) Protein extracts from the control and sh14-3-3ε cells were resolved on SDS-PAGE gels followed by western blotting with the indicated antibodies. Actin served as a loading control. (F,G) Hanging-drop assays were performed on the control and sh14-3-3γ cells. The images (F) of the clumps and the quantification (G) of cluster number and size are shown. Scale bar: 200 μM.

desmosomal cadherins to the border, the localization of these cadherins was studied in HCT116-derived plakoglobin-knockdown cells, which have been described previously (Gosavi et al., 2011). The levels of DSC2 and DSC3, and DSG2, were not reduced at the border in the plakoglobin-knockdown cells (supplementary material Fig. S1C), suggesting that 14-3-3γ, in addition to being required for plakoglobin localization to the border, might have other functions in desmosome formation. These data are consistent with the observation that 14-3-3γ forms a complex with PKP3 and desmoplakin (Fig. 4B).

Complex formation between plakoglobin and 14-3-3γ requires PKCμ

Analysis of the plakoglobin amino acid sequence led to the identification of a potential 14-3-3 binding site at serine residue 236 (S236) (supplementary material Fig. S3A) (Obenauer et al., 2003). To determine whether S236 is required for an interaction between plakoglobin and 14-3-3γ and to mediate the targeting of plakoglobin to the surface, residue S236 was replaced with alanine (S236A), and the ability of this mutant to bind to 14-3-3γ and to localize to the border was investigated. GST–14-3-3γ formed a complex with wild-type plakoglobin but not with that of the S236A mutant (Fig. 5A). In contrast with wild-type plakoglobin, which

localized to the cell border, we observed reduced levels of the S236A protein at the border and an increased pan-cellular localization (Fig. 5B). Although some of the S236A mutant protein still localized to the border, the localization to the border was attenuated in comparison with that of the wild-type protein, suggesting that binding of plakoglobin to 14-3-3γ is required for the efficient localization of plakoglobin to the border.

The S236 residue is a potential site for phosphorylation by PKCμ (supplementary material Fig. S3A), suggesting that phosphorylation of plakoglobin by PKCμ is required for plakoglobin localization to the border. HCT116 cells were treated with the vehicle control dimethyl sulfoxide (DMSO), a pan PKC inhibitor that doesn't inhibit PKCμ (bisindolylmaleimide I, BisI) or an inhibitor that is specific for PKCμ and PKCα (Go6976). A GST pull-down assay was then performed using 14-3-3γ. Importantly, GST–14-3-3γ was unable to pull down plakoglobin from protein extracts that had been prepared from cells treated with Go6976, in contrast to cells that had been treated with DMSO (Fig. 5C), suggesting that the activity of either PKCα or PKCμ is required for complex formation with 14-3-3γ and localization of plakoglobin to the cell border. However, 14-3-3γ formed a complex with desmoplakin and PKP3 in extracts that had been derived from cells treated with the inhibitor (Fig. 5C),

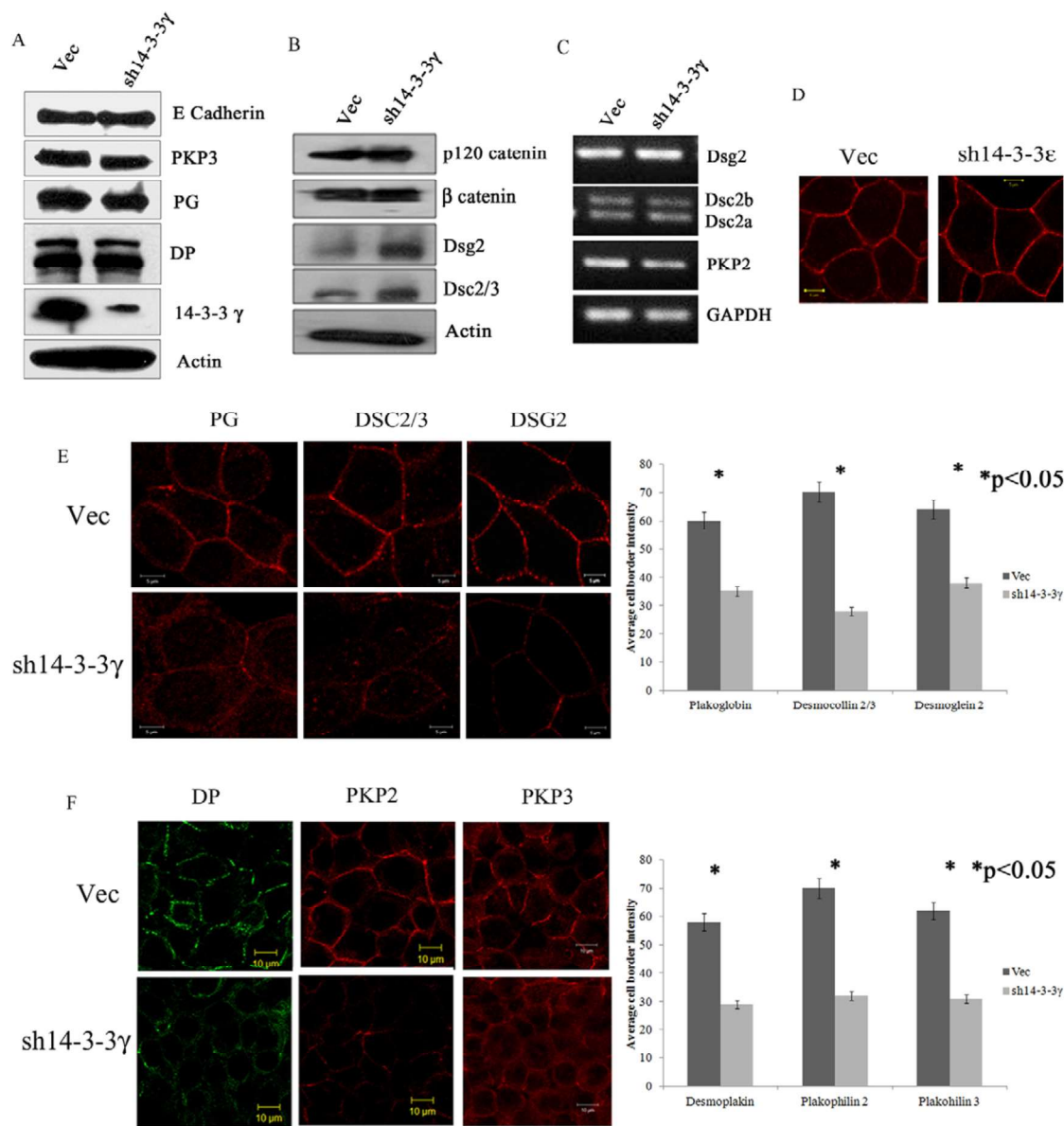


Fig. 3. Localization of plakoglobin is altered in sh14-3-3γ cells. (A,B) Protein extracts from the vector control (Vec) and 14-3-3γ-knockdown (sh14-3-3γ) cells were resolved on SDS-PAGE gels followed by western blotting with the indicated antibodies. Western blotting for actin served as a loading control. (C) mRNA was prepared from the control and sh14-3-3γ cells, and RT-PCR reactions were performed with oligonucleotide pairs specific for the indicated genes. The oligonucleotides used for DSC2 amplified both splice isoforms, DSC2a and DSC2b, as indicated. GAPDH served as a reaction control. (D) Plakoglobin (PG) levels at the cell borders were determined in the vector control and 14-3-3ε knockdown cells. Note that plakoglobin levels did not change at the cell border upon knockdown of 14-3-3ε (sh14-3-3ε). (E,F) Control and sh14-3-3γ cells were stained with the indicated antibodies, and the staining was observed by using confocal microscopy. Representative images are shown. The border intensity was measured for at least 20 cells in three different experiments. The mean±s.d. is shown for three independent experiments. Scale bars: 5 μm (D,E); 10 μm (F). DP, desmoplakin.

suggesting that the activity of PKCμ or PKCα is not required for the association of desmoplakin or PKP3 with 14-3-3γ. In agreement with these results, immunofluorescence analysis using antibodies against plakoglobin demonstrated that the treatment of cells with Go6976 decreased the localization of plakoglobin at the cell border in comparison with that of cells that had been treated with either DMSO or BisI (Fig. 5D).

Because the motif scan software identified S236 as a potential site for phosphorylation by PKCμ, we inhibited the expression of PKCμ using vector-driven RNA interference (RNAi) in HCT116 cells using a previously described sequence that inhibits PKCμ expression but not PKCα expression (Park et al.,

2009). HCT116 cells were transfected with either the vector plasmid or a plasmid that expressed shRNA sequences that target PKCμ (shPKCμ). Forty-eight hours post transfection, the cells were transferred to medium containing puromycin in order to enrich for transfected cells. Western blot analysis demonstrated that PKCμ levels were reduced, as expected; however, plakoglobin and desmoplakin protein levels were reduced in cells that had been transfected with the shRNA against PKCμ, suggesting that PKCμ might also regulate the stability of these proteins (Fig. 5E). No change in the levels of PKP3 was observed, and western blots for actin were performed as loading controls. The levels of plakoglobin, desmoplakin and

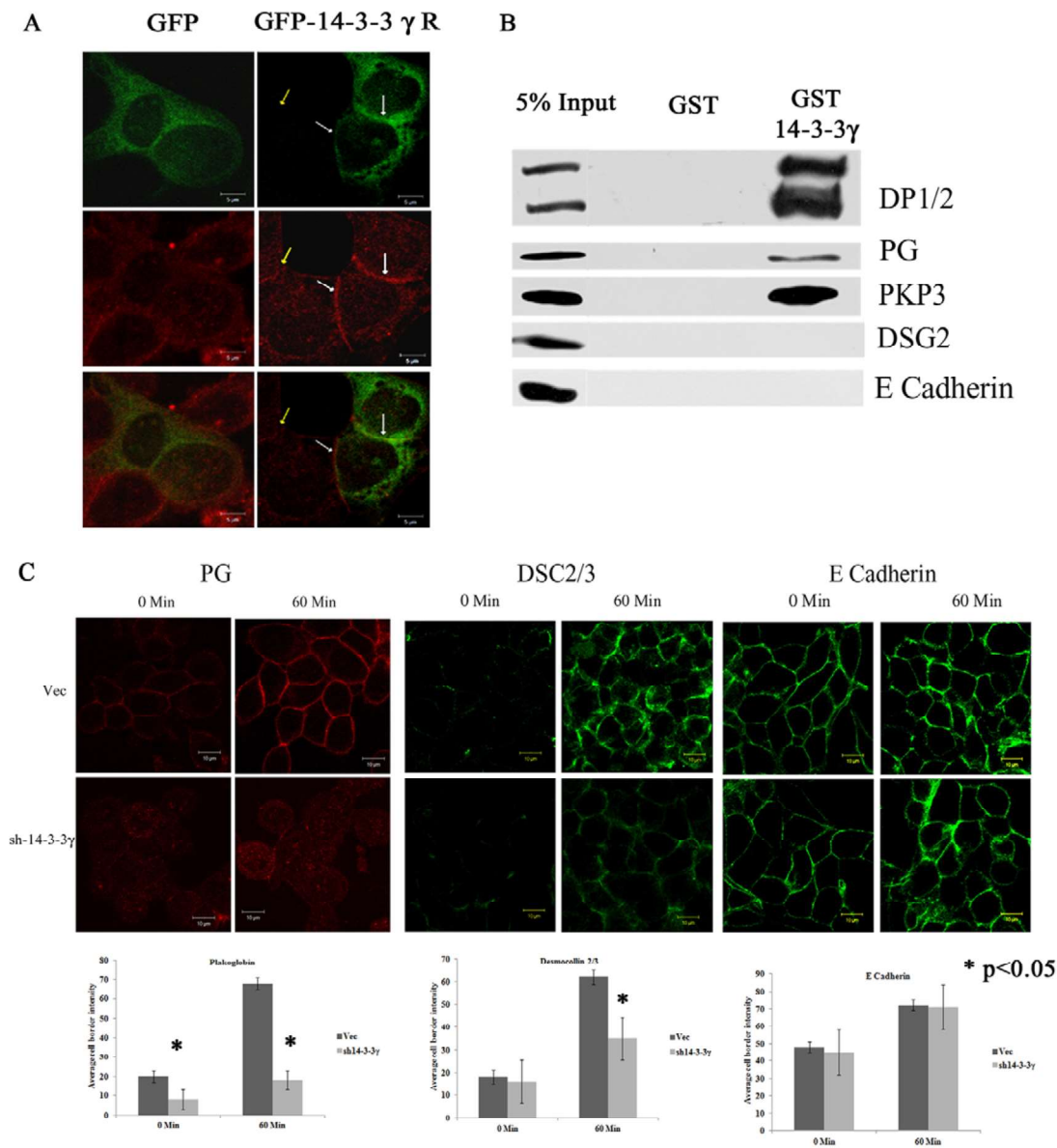


Fig. 4. 14-3-3 γ is required to initiate desmosome formation. (A) 14-3-3 γ -knockdown (sh14-3-3 γ) cells were transfected with either GFP alone or a GFP–14-3-3 γ construct that was resistant to RNAi (GFP-14-3-3 γ R). The cells were stained with antibodies to plakoglobin (PG, red) and analyzed by using confocal microscopy. (B) Protein extracts of HCT116 cells were incubated with either GST or GST–14-3-3 γ . The reactions were resolved on SDS-PAGE gels, and followed by western blotting with the indicated antibodies. (C) Vector control (Vec) and sh14-3-3 γ cells were incubated in low-calcium medium for 24 hours (0 min). After calcium addition for 60 minutes, the cells were fixed and then stained with the indicated antibodies and analyzed by using confocal microscopy. Note that the levels of the desmosomal proteins do not increase at the border in sh14-3-3 γ cells in comparison with control cells. No change in E-cadherin staining was observed. The border intensity was measured for at least 20 cells in three different experiments. The mean and standard deviation for three independent experiments is shown. Scale bars: 5 μ m (A); 10 μ m (C).

PKP3 at the cell borders were decreased in cells that had been transfected with the PKC μ shRNA in comparison with cells that had been transfected with the vector control, and the remaining protein in these cells was not localized to the border (Fig. 5F). These results suggest that, in addition to the decreased protein levels, there is a decrease in the localization of the desmosomal components to the cell borders in the absence of PKC μ . This is in contrast with the results obtained for cells that lacked 14-3-3 σ , in which a decrease in the levels of plakoglobin was observed but there was no defect in plakoglobin localization to the border (supplementary material Fig. S4C). To determine whether PKC μ phosphorylated plakoglobin directly, the first 300 amino

acids of plakoglobin, which comprise the putative 14-3-3-binding site, were purified from bacteria as a GST fusion protein and used as a substrate in an *in vitro* kinase assay using purified PKC μ . A peptide derived from CREB (catalog number C50-58, Signal Chem) was used as a positive control in these assays. As shown in Fig. 5G, the GST–PG1-300 fusion protein was phosphorylated *in vitro* by PKC μ , and the level of phosphorylation increased markedly with an increase in substrate concentration, in contrast with the results observed with GST alone. These results suggest that PKC μ regulates localization of plakoglobin to the cell border, and plakoglobin expression or stability.

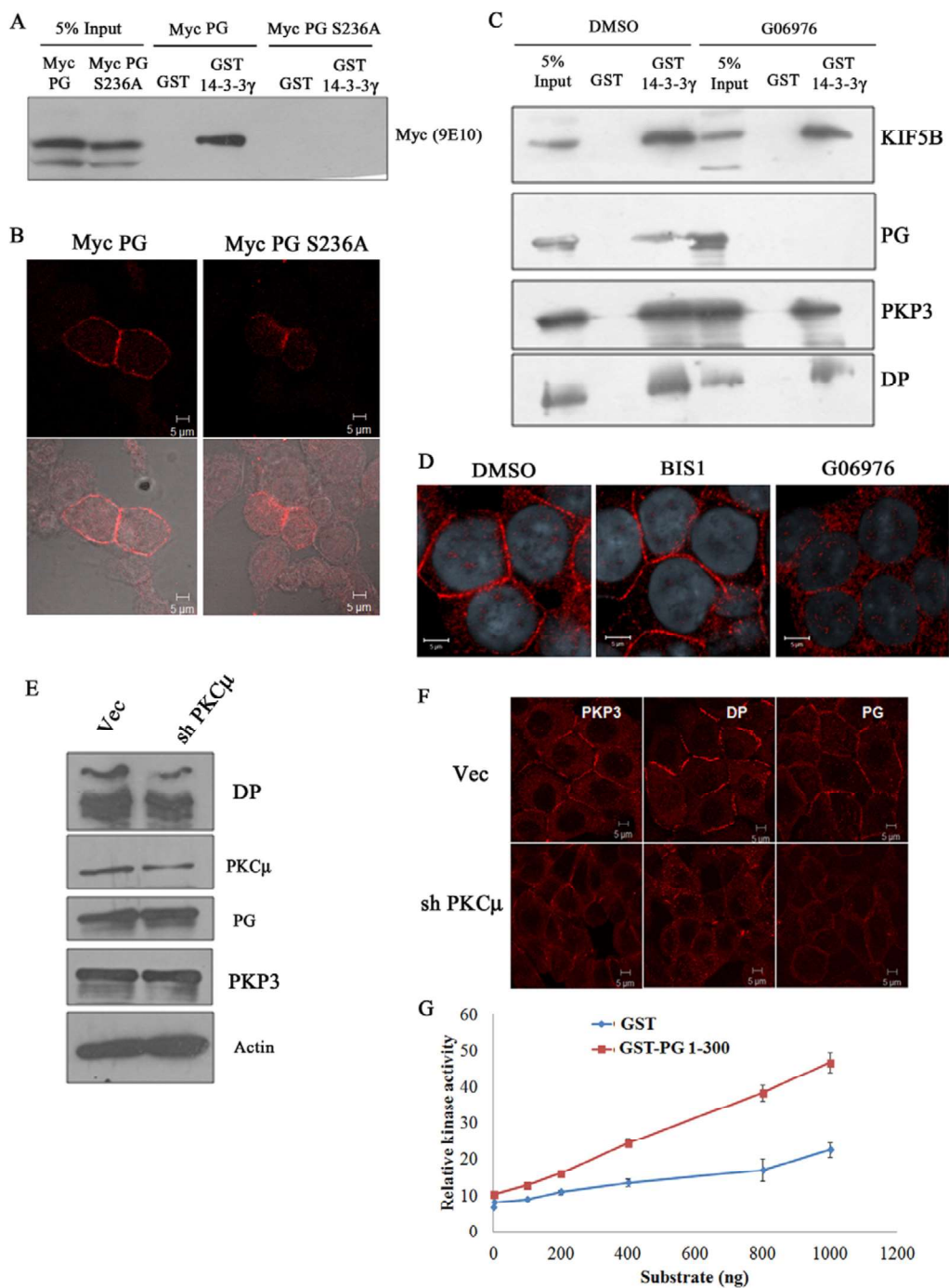


Fig. 5. The association of 14-3-3γ with plakoglobin requires PKCμ activity. (A,B) HCT116 cells were transfected with either MYC-epitope-tagged wild-type plakoglobin (PG) or the S236A mutant of plakoglobin. 48 hours post transfection, protein extracts were incubated with GST or GST–14-3-3γ followed by western blotting with antibodies against MYC (A), or the cells were stained with antibodies against the MYC-epitope (B). Differential interference contrast images for the fields are shown in the lower panels. (C,D) HCT116 cells were treated with either the vehicle control (DMSO), the pan-PKC inhibitor (BisI), or the PKCα- and PKCμ-specific inhibitor (Go6976). Protein extracts from these cells were incubated with either GST or GST–14-3-3γ, the reactions were resolved on SDS-PAGE gels, and western blots were performed with the indicated antibodies (C). The cells were also stained with antibodies against plakoglobin (D). (E,F) Protein extracts from vector control (Vec) or PKCμ-knockdown cells (shPKCμ) were resolved on SDS-PAGE gels, and western blots were performed with the indicated antibodies. Note that there is a decrease in plakoglobin and desmoplakin (DP) levels upon PKCμ knockdown, but no difference in PKP3 levels is observed. (F) Control cells and shPKCμ cells were fixed and then stained with the indicated antibodies. (G) The PG1-300 construct, comprising the first 300 amino acids of plakoglobin, was produced in bacteria as a GST fusion protein, and kinase assays were performed using recombinant PKCμ. GST alone was used as a negative control in this assay. Different concentrations of the substrate are shown on the x-axis and enzyme activity is recorded on the y-axis. The mean±s.d. is shown. Note that an increase in kinase activity is observed upon an increase in the concentration of PG1-300 but not with an increase in the concentration of GST alone. Scale bars: 10 μm (B); 5 μm (D,F).

KIF5B binds to 14-3-3 γ and is required for desmosome assembly

A proteomic screen conducted in our laboratory identified the kinesin 1 family member KIF5B (Cross and Carter, 2000) as a potential ligand for 14-3-3 γ (data not shown). As kinesin motor proteins are required for the transport of proteins to the cell border (Cross and Carter, 2000) and have been shown to be required for the transport of the desmosomal cadherins to the cell border (Nekrasova et al., 2011), we hypothesized that plakoglobin was transported to the border by KIF5B. To determine whether

14-3-3 γ forms a complex with KIF5B, HCT116 cells were transfected with either the vector control (pcDNA3) or hemagglutinin (HA)-tagged 14-3-3 γ , and immunoprecipitation reactions were performed using antibodies to the HA epitope. 14-3-3 γ formed a complex with KIF5B, suggesting that 14-3-3 γ might load plakoglobin onto KIF5B and lead to the transport of plakoglobin to the cell border (Fig. 6A). To test this hypothesis, KIF5B expression was stably downregulated using vector-driven RNAi. Five clones (K1–K5) were isolated that showed a decrease in KIF5B protein expression in comparison with the vector

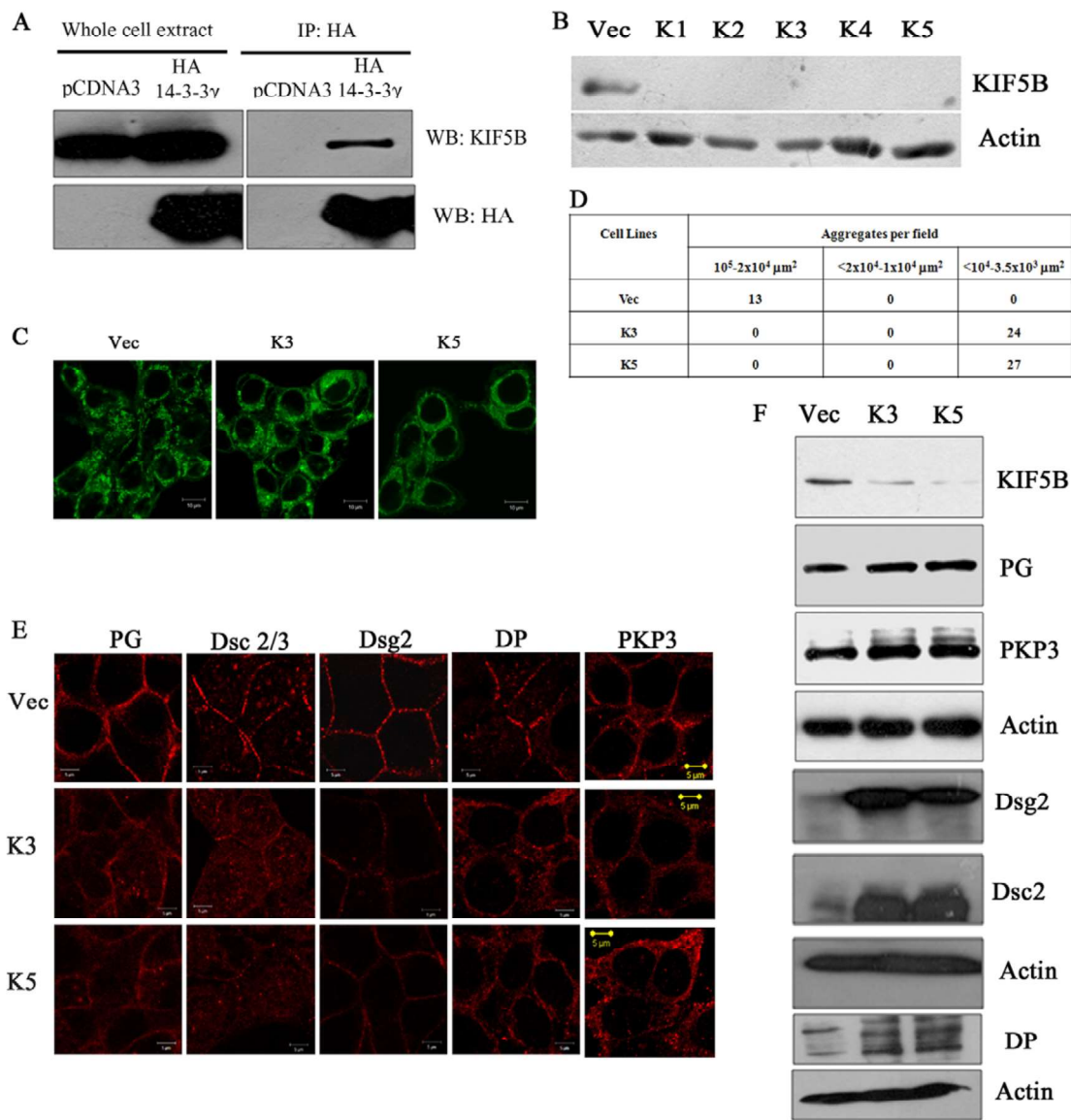


Fig. 6. KIF5B is required for the transport of plakoglobin to the cell border. (A) HCT116 cells were transfected with the vector control (pcDNA3) or HA–14-3-3 γ and immunoprecipitations (IP) were performed with antibodies against the HA epitope. The reactions were resolved on SDS-PAGE gels, and then western blots (WB) were performed with the indicated antibodies. (B) HCT116 cells were transfected with constructs expressing an shRNA targeting KIF5B. Individual cell clones were expanded, and protein extracts from these clones were resolved on SDS-PAGE gels followed by western blotting with antibodies to KIF5B. A western blot for actin served as a loading control. Note that the knockdown clones (K1–K5) have a lower level of KIF5B than the vector control (Vec). A western blot for actin served as a loading control. (C) Vector control or the KIF5B-knockdown clones K3 and K5 were incubated with Mitotracker Green FM. (D) Hanging-drop assays were performed to determine cell–cell adhesion. K3 and K5 formed fewer and smaller clumps in comparison with the control cells. (E) Control, K3 and K5 cells were stained with antibodies against plakoglobin (PG), DSC2 and DSC3, DSG2, desmoplakin (DP) and PKP3 and the intensity of the surface staining was quantified by using confocal microscopy. The total magnification was $\times 630$ with $\times 2$ optical zoom. Bars correspond to 5 μ m. (F) Protein extracts prepared from the control, K3 and K5 cells were resolved on SDS-PAGE gels and then analyzed by western blotting with the indicated antibodies. Scale bars: 10 μ m (C); 5 μ m (E).

control cells (Fig. 6B). Loss of KIF5B led to a perinuclear accumulation of mitochondria, as reported previously (Tanaka et al., 1998) (Fig. 6C). Furthermore, hanging-drop assays demonstrated that loss of KIF5B led to a decrease in cell–cell adhesion in comparison with the control cells (Fig. 6D; supplementary material Fig. S3B).

To determine whether the decrease in cell–cell adhesion that was observed upon KIF5B knockdown was accompanied by a decrease in the localization of the desmosomal proteins to the cell borders, the control cells and the KIF5B knockdown clones K3 and K5 were stained with antibodies against components of desmosomes or adherens junctions. Similar to that observed in the sh14-3-3 γ cells, the levels of plakoglobin, PKP3, desmoplakin, DSC2 and DSC3, and DSG2 substantially decreased at the border in K3 and K5 KIF5B-knockdown cells – a phenotype similar to that of the control cells (Fig. 6E,F). Intensity profiles for the staining are shown in supplementary material Fig. S2. By contrast, knockdown of KIF5B did not lead to a decrease in the levels of E-cadherin, p120 catenin, α -E-catenin and β -catenin at the cell border (supplementary material Fig. S3C,F,G). The decrease in the levels of desmosomal proteins at the border was not due to a decrease in protein expression levels, as indicated by western blot analysis. In contrast with the results that were observed for plakoglobin, PKP3 and desmoplakin, a large increase in the levels of DSC2 and DSC3, and DSG2 were observed in the kinesin-knockdown cells (Fig. 6F), although this was not observed at the mRNA level (supplementary material Fig. S3E). In cells that had been fixed with methanol, we observed low levels of DSC2 and DSC3, and DSG2, in the cytoplasm (Fig. 6E); however, fixation with paraformaldehyde revealed high levels of DSC2 and DSC3, and DSG2, in the cytoplasm (supplementary material Fig. S4E), suggesting that these proteins accumulate in the cytoplasm upon loss of KIF5B. PKP2 mRNA levels were not altered upon knockdown of kinesin (supplementary material Fig. S3E).

Because kinesin motor proteins transport their cargo on microtubules, we investigated whether disruption of the microtubule network would lead to a decrease in the concentration of plakoglobin at the cell border. Treatment with nocodazole, but not the vehicle control, did indeed lead to a decrease in the levels of plakoglobin at the border (supplementary material Fig. S3D). To then determine whether complex formation between KIF5B and plakoglobin is dependent upon PKC μ , protein extracts from Go6976- or DMSO-treated HCT116 cells were incubated with GST–14-3-3 γ . GST–14-3-3 γ formed a complex with KIF5B under both conditions but did not interact with plakoglobin in protein extracts from cells that had been treated with Go6976 (Fig. 5C), indicating a requirement for active PKC μ for the association between plakoglobin and 14-3-3 γ but not for the association between KIF5B and 14-3-3 γ .

To further confirm the role of KIF5B in transporting plakoglobin to the border, we determined whether a dominant-negative KIF5B construct could inhibit transport of plakoglobin to the cell border. The dominant-negative kinesin heavy chain constructs used here have a point mutation in the ATPase domain (see Materials and Methods), which results in an inability of the proteins to move along the microtubules but preserves the ability of kinesins to bind to cargo (Cross and Carter, 2000). Yellow fluorescent protein (YFP)-tagged versions of wild-type and dominant-negative (mutation T92N) KIF5B, or the GFP-tagged wild-type and dominant-negative (mutation T107N) kinesin 2 family member KIF3A (Cross and Carter, 2000) constructs were

transfected into HCT116 cells. After transfection, the cells were stained with antibodies against plakoglobin and visualized by using confocal microscopy. Cells that expressed wild-type YFP–KIF5B showed border staining for plakoglobin. By contrast, plakoglobin was not localized at the cell border in cells that expressed dominant-negative YFP–KIF5B (Fig. 7A). Cells that had been transfected with either of the KIF3A constructs showed border staining for plakoglobin. Cells that had been transfected with either of the dominant-negative constructs had round edges and showed a morphology that was different from that of cells that had been transfected with either of the wild-type constructs, presumably because overexpression of the dominant-negative constructs affects other cellular processes, such as microtubule organization (Silver and Harrison, 2011). However, despite the change in morphology, only the cells that had been transfected with the dominant-negative KIF5B construct, and not those transfected with the dominant-negative KIF3A construct, showed a disruption of plakoglobin localization (Fig. 7A). These results suggest that KIF5B specifically is required for transport of plakoglobin to the border.

Kinesin motor proteins are heterodimers that consist of two heavy chains and two light chains (Cross and Carter, 2000). KIF5B associates with two different kinesin light chains (KLCs) – KLC1 and KLC2 (Verhey and Hammond, 2009). To determine which of these is required for plakoglobin transport to the cell border, bacterially produced GST-tagged KLC1 and KLC2 were incubated with protein extracts that had been prepared from HCT116 cells, and the reactions were resolved on SDS-PAGE gels followed by western blotting with antibodies against plakoglobin, KIF5B and 14-3-3 γ . Both KLC1 and KLC2 formed a complex with KIF5B; however, only KLC1 could form a complex with both plakoglobin and 14-3-3 γ (Fig. 7B). KLCs contain a coiled-coiled domain, which is required for complex formation with the kinesin heavy chain, and a cargo-binding domain [which comprises tetratricopeptide repeats (TPRs)] (Verhey and Hammond, 2009) (Fig. 7C). To determine whether the coiled-coiled domain of KLC1 could form a complex with plakoglobin, protein extracts from HCT116 cells were incubated with either GST–KLC1 or the GST-tagged coiled-coiled domain of KLC1. GST–KLC1 could form a complex with KIF5B, plakoglobin and 14-3-3 γ , whereas the coiled-coiled domain bound to KIF5B but not to plakoglobin and 14-3-3 γ (Fig. 7D). Therefore, the coiled-coiled domain of KLC1 might be acting as a dominant-negative mutant because it should bind to the heavy chain but fail to form a complex with plakoglobin and 14-3-3 γ . To test this hypothesis, HCT116 cells were transfected with either GFP–KLC1 or the GFP-tagged KLC1 coiled-coiled domain only and stained with antibodies against plakoglobin. Overexpression of the KLC1 coiled-coiled domain disrupted the transport of plakoglobin to the cell border, whereas cells that expressed the wild-type protein did not show any alteration in plakoglobin localization (Fig. 7E). These results suggest that the KIF5B–KLC1 complex is required for the transport of plakoglobin to the cell border.

Loss of KIF5B leads to sterility in male mice

The results described above suggest that 14-3-3 γ and KIF5B are required for desmosome formation in epithelial cells. To determine whether loss of KIF5B leads to a decrease in cell–cell adhesion in the seminiferous epithelium, KIF5B expression was inhibited in the testis, as described previously (Sehgal et al., 2011). Loss of KIF5B in the testis led to a phenotype similar to that observed for

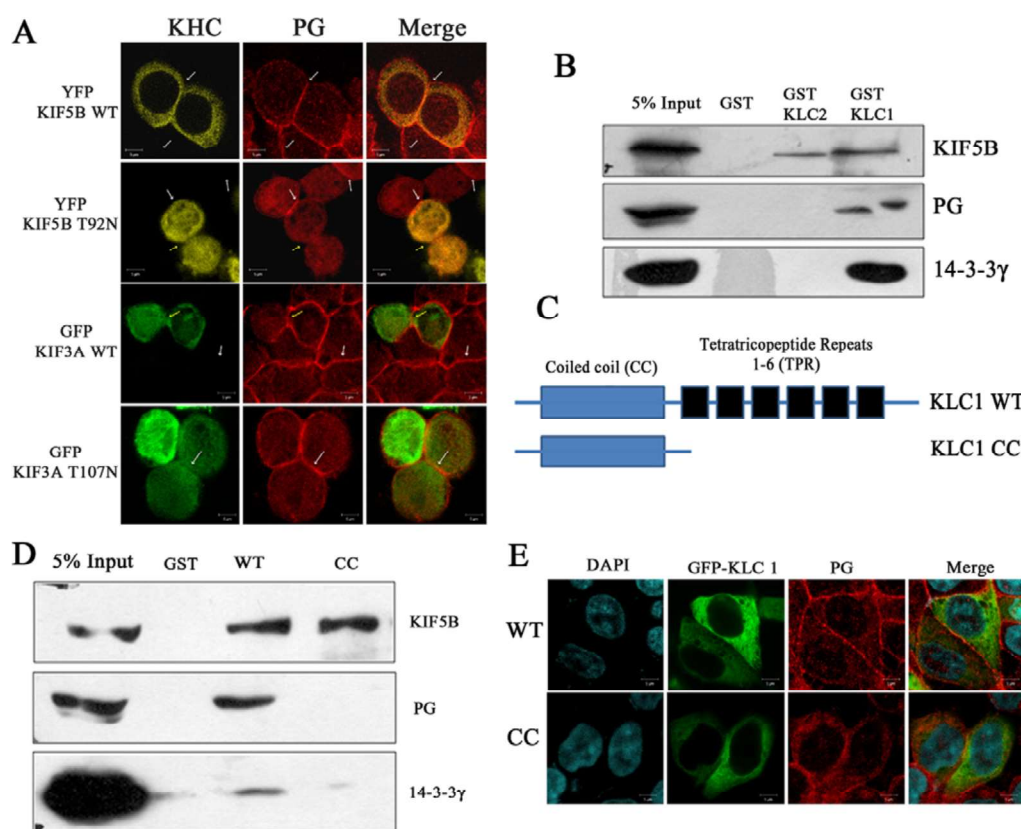


Fig. 7. Dominant-negative mutants of KIF5B and KLC1 inhibit plakoglobin transport to the border. (A) HCT116 cells were transfected with kinesin heavy chain constructs (KHC) – YFP-tagged wild-type (WT) or dominant-negative (T92N) KIF5B, or GFP-tagged wild-type or dominant-negative (T107N) KIF3A. Post transfection, the cells were fixed and stained with antibodies against plakoglobin (PG). (B) Protein extracts from HCT116 cells were incubated with GST alone or GST–KLC1 or GST–KLC2. The reactions were resolved on SDS-PAGE gels followed by western blotting with the indicated antibodies. (C) The KLC1 mutant KLC1-CC comprises only the coiled-coiled domain and not the tetratricopeptide repeat domain (TPR). (D) Protein extracts from HCT116 cells were incubated with GST alone, wild-type GST–KLC1 and GST–KLC1-CC. The reactions were resolved on SDS-PAGE gels followed by western blotting with the indicated antibodies. (E) GFP–KLC1 or GFP–KLC1-CC were transfected into HCT116 cells. Forty-eight hours post transfection, the cells were fixed and then stained with antibodies against plakoglobin. The nuclei were stained with DAPI. Total magnification is $\times 630$ with $\times 2$ optical zoom. Scale bars: 5 μ M.

the loss of 14-3-3 γ (Fig. 8A–C), suggesting that both KIF5B and 14-3-3 γ are independently required to regulate cell–cell adhesion in the testis. Importantly, an immunohistochemical analysis demonstrated that loss of either KIF5B or 14-3-3 γ did not lead to a decrease in the levels of the other protein (Fig. 8B). Loss of 14-3-3 ϵ did not lead to a decrease in cell–cell adhesion and spermatogenesis, suggesting that the effects observed upon knockdown of 14-3-3 γ are specific to 14-3-3 γ (Fig. 8A,B), a result that is consistent with those observed in HCT116 cells (Fig. 2). In addition, loss of either 14-3-3 γ or KIF5B led to a detachment of the cells from the basal lamina. To determine whether the detachment of the primary germ cells and the Sertoli cells from the basal lamina led to an increase in cell death, the testis sections were stained using a TUNEL staining kit. As shown in supplementary material Fig. S1A, treatment of the positive-control sections with DNase resulted in a strong positive signal in the TUNEL assay. Testis sections from mice that had been injected with the 14-3-3 γ -knockdown construct showed low levels of TUNEL positivity in comparison with testis sections from the control or KIF5B-knockdown mice. Given that the testis morphology of the KIF5B-knockdown mice and the 14-3-3 γ -knockdown mice was very similar, it is likely that the loss of cell–matrix adhesion does not lead to cell death, which is consistent

with our results in the cell line model. These results suggest that cell–cell adhesion in the testis requires both 14-3-3 γ and KIF5B and that loss of either protein leads to defects in cell–cell adhesion.

To determine whether desmosome organization was altered in the 14-3-3 γ - and KIF5B-knockdown testis, testis sections were stained with antibodies against plakoglobin, PKP3, DSC2 and DSC3, N-cadherin and E-cadherin. Plakoglobin, PKP3 and DSC2 and DSC3 localized to the border in testis that had been injected with the control virus; however, the levels of these proteins at the cell border were greatly diminished in the 14-3-3 γ - and KIF5B-knockdown testis (Fig. 8D). By contrast, there was no change in E-cadherin localization in the 14-3-3 γ - and KIF5B-knockdown testis in comparison with testis sections that had been injected with the vector control, a phenotype similar to that observed in HCT116 cells in culture. In contrast with the results obtained for E-cadherin, it was observed that N-cadherin localized to the border in the vector control and 14-3-3 γ -knockdown testis but not in the KIF5B-knockdown testis (Fig. 8D). These results are consistent with our observations that the KIF5B-knockdown testis showed a more severe adhesion phenotype than the 14-3-3 γ -knockdown testis and that KIF5B might be required for the transport of other cell–cell adhesion molecules to the border, in addition to desmosomal proteins. Overall, our results suggest that

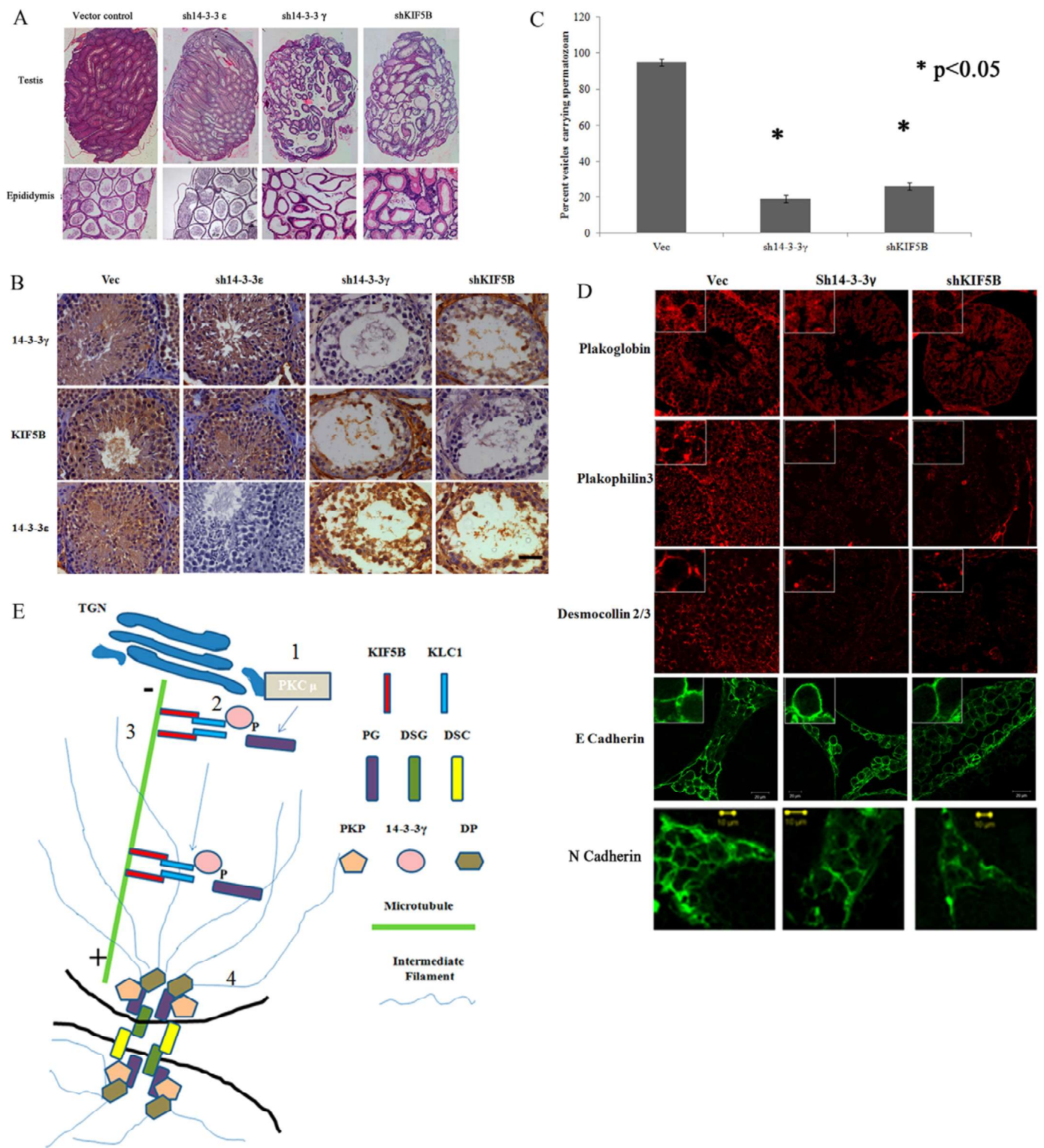


Fig. 8. See next page for legend.

14-3-3 γ and KIF5B are required for the formation of desmosomes *in vivo*.

DISCUSSION

Our results suggest that 14-3-3 γ and the KIF5B–KLC1 complex are required for the transport of plakoglobin to cell borders in

human cell lines and in the mouse testis, and disruption of this interaction with 14-3-3 γ leads to a defect in the localization of plakoglobin. In addition, loss of 14-3-3 γ leads to a disruption of cell–matrix adhesion, which might affect cell–cell adhesion *in vitro* and *in vivo*. The association of plakoglobin with 14-3-3 γ , and the transport of plakoglobin to the border is dependent on

Fig. 8. Loss of KIF5B and 14-3-3 γ in the testis leads to a disruption of desmosome formation and sterility. (A–D) Lentiviruses encoding the vector control or shRNAs targeting 14-3-3 ϵ , 14-3-3 γ or KIF5B were injected into the testes of Swiss mice (sh14-3-3 ϵ , sh14-3-3 γ and shKIF5B, respectively). 35 days post-injection the mice were killed, sections of the epididymis and testes were stained with hematoxylin and eosin and examined by using microscopy (A). Immunohistochemical analysis using antibodies against the different proteins that were knocked down demonstrated that the expression of 14-3-3 ϵ , 14-3-3 γ and KIF5B is inhibited in the testis that had been injected with the appropriate lentivirus (B). The percentage of epididymal vesicles that showed the presence of mature spermatozoa in three different animals was determined and the means \pm s.d. are shown. (C) Testis sections were stained with antibodies against plakoglobin (PG), plakophilin 3 (PKP3), desmocollins (DSC)2 and DSC3, N-cadherin and E-cadherin. (D) The total magnification was $\times 630$ with $\times 2$ optical zoom. The inset images show a higher magnification of the cells to demonstrate border localization. (E) Desmosome assembly based on the experimental findings presented here. (1) PKC μ phosphorylates plakoglobin, thereby, allowing association with 14-3-3 γ and resulting in the loading of plakoglobin onto the KIF5B–KLC1 complex. (2) The motor protein complex containing plakoglobin moves along microtubules (3) resulting in desmosome assembly at the border (4). TGN, trans-Golgi network. Scale bars: 20 μ m (B); 10 μ m (C).

PKC μ activity; thus, loss of either 14-3-3 γ or KIF5B inhibits plakoglobin transport, resulting in a decrease in desmosome formation and cell–cell adhesion in HCT116 cells and the testis, leading to male sterility. The decrease in the levels of N-cadherin at cell borders in KIF5B-knockdown testis resulted in a more drastic phenotype in these animals than in those that had been subjected to knockdown of 14-3-3 γ , suggesting that N-cadherin is required for cell–cell adhesion in the testis as previously reported (Andersson et al., 1994; Lee et al., 2003).

Previous results have shown that loss of plakoglobin leads to the depletion of desmosomal proteins from the cell border and to defects in desmosome formation (Acehan et al., 2008; Gosavi et al., 2011; Knudsen and Wheelock, 1992; Lewis et al., 1997). Although the presence of a classical cadherin seems to be required for plakoglobin recruitment to the cell border (Michels et al., 2009; Tinkle et al., 2008), the mechanisms by which plakoglobin is transported have not been identified. The results presented here suggest that phosphorylation of plakoglobin by PKC μ at residue S236 leads to the generation of a binding site for 14-3-3 γ , and that 14-3-3 γ is required for the transport of plakoglobin to the cell border in order to initiate desmosome formation, presumably in a complex with a classical cadherin (Michels et al., 2009; Tinkle et al., 2008). 14-3-3 γ might be required to load plakoglobin onto the KIF5B–KLC1 complex, which precedes the transport of plakoglobin on microtubules (Fig. 8E). This is consistent with previous observations that showed that PKC μ localizes to the Golgi complex (Hausser et al., 2002; Prestle et al., 1996) and is required for the fission of vesicles carrying cargo to the cell border (Liljedahl et al., 2001). A 14-3-3 γ dimer is required for carrier formation at the Golgi complex along with PKC μ (Valente et al., 2012), suggesting that the loss of 14-3-3 γ could disrupt desmosome formation owing to defects in plakoglobin transport.

The treatment of cells with an inhibitor that inactivates both PKC α and PKC μ led to a decrease in the localization of plakoglobin at cell borders and abolished complex formation between plakoglobin and 14-3-3 γ . However, treatment with the inhibitor does not inhibit the interaction between 14-3-3 γ and other desmosomal proteins or KIF5B. These results suggest that phosphorylation of plakoglobin by PKC μ is required for complex formation between plakoglobin and 14-3-3 γ and the loading of

plakoglobin onto KIF5B, which is essential for the transport of plakoglobin. Alternatively, it is possible that plakoglobin, desmoplakin and PKP3 are transported independently to the border and that the absence of plakoglobin at the border prevents the formation of a functional desmosome. Furthermore, it was observed that loss of plakoglobin did not affect the localization of DSC2 and DSC3, and DSG2 to cell borders, unlike the loss of 14-3-3 γ or KIF5B. This might be because 14-3-3 γ is required for the localization of PKP3, desmoplakin and plakoglobin; therefore, the defects in the localization of the desmosomal cadherins that is observed upon 14-3-3 γ loss are not observed upon plakoglobin loss. Plakoglobin is probably required to stabilize and maintain the organization of the desmosome, which is why loss of plakoglobin leads to a decrease in cell–cell adhesion in these cells as previously reported (Gosavi et al., 2011). PKC μ was also shown to directly phosphorylate a peptide comprising the first 300 amino acids in plakoglobin, which contains the S236 residue, consistent with the notion that S236 serves as site for phosphorylation by PKC μ . This does not exclude the possibility that PKC μ phosphorylates other residues in plakoglobin and might provide an explanation for the observation that plakoglobin protein levels decreased when PKC μ expression was inhibited. It is possible that PKC μ regulates other aspects of plakoglobin function that are not limited to the transport of plakoglobin to the cell border, such as the retention of plakoglobin at the border or the stability of the plakoglobin protein.

In the absence of KIF5B, or upon expression of a dominant-negative KIF5B construct, plakoglobin does not localize to the cell border, leading to a decrease in the recruitment of other components of the desmosome, as previously reported (Gosavi et al., 2011; Lewis et al., 1997). Previous experiments have suggested that inhibiting KIF5B expression does not affect the localization of plakoglobin to the border in SCC9 cells (Nekrasova et al., 2011). Our results, however, suggest that loss of KIF5B in HCT116 cells and the testis results in an inhibition of plakoglobin transport to the border. Consistent with the results reported by Nekrasova and colleagues (Nekrasova et al., 2011), we did not observe any defects in plakoglobin localization upon expression of a dominant-negative KIF3A mutant. The discrepancy in these two reports might be due to the use of different cell types; other kinesin-family members could regulate plakoglobin transport in SCC9 cells in the absence of KIF5B. Similarly, Pasdar and colleagues have reported that a microtubule network is not essential for desmosome formation (Pasdar et al., 1991); however, the results from this report and others suggest that the transport of desmosomal components to the border is dependent on an intact microtubule network (Gloushankova et al., 2003; Nekrasova et al., 2011). This is consistent with reports that suggest that desmosome organization, function and composition vary in different cell types (reviewed in Cross and Carter, 2000; Garrod and Chidgey, 2007; Getsios et al., 2004; Green and Gaudry, 2000; Hatzfeld, 2007) and with the observations that loss of the different desmosomal components in the mouse leads to a vast variety of phenotypes (Chidgey et al., 2001; Gallicano et al., 1998; Grossmann et al., 2004; Koch et al., 1997; Lechler and Fuchs, 2007; Ruiz et al., 1996; Sklyarova et al., 2008; Vasioukhin et al., 2001).

Although 14-3-3 γ seems to be required for the transport of plakoglobin, it might also be required for the transport of PKP3 and desmoplakin to the cell border in a manner that is independent of plakoglobin transport. This is consistent with our observation that inhibition of both PKC α and PKC μ did not

lead to the disruption of the interaction between 14-3-3 γ and desmoplakin or PKP3. The transport of DSG2 to the border is dependent on KIF5B, whereas the transport of DSC2 requires KIF3A and PKP2 (Nekrasova et al., 2011). Our results suggest that plakoglobin transport to the border is dependent on KIF5B, but not KIF3A, suggesting that the transport of desmosomal cadherins and plaque proteins to the border occurs through independent microtubule-dependent pathways. Alternatively, because 14-3-3 proteins bind to their ligands as dimers, with each member of the dimer forming a complex with a phosphopeptide (Brunet et al., 2002; Yaffe et al., 1997), it is possible that 14-3-3 γ bridges interactions between the different desmosomal plaque proteins, thereby allowing the formation of an intact desmosome, as previously postulated by Bonn   and colleagues (Bonn   et al., 2003). The only argument against this hypothesis is that, according to our study, 14-3-3 γ does not localize to the desmosome (Fig. 4A). In fact, the lack of any colocalization between 14-3-3 γ and plakoglobin suggests that any function that 14-3-3 γ performs, with respect to plakoglobin localization, is transient in nature; therefore, we favor the hypothesis that 14-3-3 γ is required for loading plakoglobin onto the KIF5B–KLC1 complex.

In contrast with the results reported here, previous work has suggested that 14-3-3 γ -knockout mice are viable, and no adhesion or sterility defects have been reported in these mice (Steinacker et al., 2005). Plakoglobin-knockout mice die during embryogenesis owing to cardiac defects arising as a result of decreased desmosome formation, and, as these mice die before the testis is formed, no information is available on the effects of loss of plakoglobin in the testis (Ruiz et al., 1996). Taken together, these previously published reports suggest that the functions of plakoglobin that are required for desmosome formation are not altered in the 14-3-3 γ ^{−/−} mice. Our results indicate that 14-3-3 γ regulates desmosome formation in multiple cell types, as loss of 14-3-3 γ in HCT116 cells, which are derived from the colon, and in the seminiferous epithelium leads to a decrease in cell–cell adhesion and in desmosome formation. Our results are also consistent with the previously reported role of 14-3-3 γ in the transport of proteins from the Golgi complex to the cell border (Valente et al., 2012). One reason for the differences in these results and those reported by Steinacker and colleagues (Steinacker et al., 2005) could be that another 14-3-3 family member binds to plakoglobin and stimulates desmosome formation in the 14-3-3 γ ^{−/−} mice, and that this compensation is not observed upon shRNA-mediated knockdown in the testis. Another possibility is that these are strain-specific variations that are due to differences in the genetic background of the mice used in the two studies. The generation of an inducible knockdown of 14-3-3 γ , in either the Swiss mice used in this study or in other mouse strains, could help determine whether loss of 14-3-3 γ leads to defects in desmosome formation and cell–cell adhesion in other tissues and not just in the testis.

The results described above point to the following model. 14-3-3 γ binds to plakoglobin that has been phosphorylated at residue S236 by PKC μ and loads plakoglobin onto the KIF5B–KLC1 complex for transport to the cell border (Fig. 8E). Loss of either 14-3-3 γ or KIF5B, or the dominant-negative versions of KIF5B and KLC1, inhibit the transport of plakoglobin to the border. Because 14-3-3 γ forms a complex with PKP3 and desmoplakin, loss of 14-3-3 γ might also lead to defects in transport of these proteins to the border. As loss of plakoglobin does not substantially affect the localization of the cadherins to the

border, it is possible that loss of plakoglobin leads to a defect in cadherin retention or the formation of an intact desmosome at the border in the absence of 14-3-3 γ . Furthermore, loss of KIF5B in the testis led to sterility and a decrease in desmosome formation. This is consistent with previously reported results that showed that disruption of cell–cell adhesion (Cheng and Mruk, 2002) and desmosome-like junction formation in the testis leads to an increase in sterility (Li et al., 2009; Lie et al., 2010).

To conclude, 14-3-3 γ and the KIF5B–KLC1 complex are required for regulating the transport of plakoglobin to the cell border. A decrease in 14-3-3 γ levels leads to a decrease in desmosome formation and the recruitment of other desmosomal proteins to the border. 14-3-3 γ might be required to maintain cell–cell adhesion in multiple tissues; however, this can only be confirmed by additional experiments *in vivo*.

MATERIALS AND METHODS

Animals

Swiss mice Crl:CFW(SW) were bred and maintained in the laboratory animal facility of the Advanced Centre for Treatment Research and Education in Cancer (ACTREC). Protocols for the experiments were approved by the Institutional Animal Ethics Committee of ACTREC. The animal study proposal number is 11/2008 dated August 19, 2008. The testis injections were performed as previously described (Sehgal et al., 2011).

Plasmids

Details of the oligonucleotides used in this study are available in supplementary material Table S1. The GST–14-3-3 γ , HA-epitope-tagged 14-3-3 γ and shRNA-resistant GFP–14-3-3 γ constructs have been previously described (Hosing et al., 2008). Site-directed mutagenesis (Stratagene) was used to generate the MYC–PG-S236A construct. The full-length KLC1 and KLC2 cDNA (Rahman et al., 1998), KLC-1 deletion (GST–KLC1 WT, GST–KLC1-CC and GST–KLC1-TPR) (Aoyama et al., 2009), GFP–KIF3A (Haraguchi et al., 2006), wild-type YFP–KIF5B (Gu et al., 2006), dominant-negative kinesin (GFP–KIF3A–T107N and YFP–KIF5B–T92N) (Wiesner et al., 2010), wild-type GFP–KLC1 and the GFP-tagged KLC1 coiled-coiled domain (Araki et al., 2007) constructs have been described previously. To generate the shRNA constructs against KIF5B and PKC μ , oligonucleotide pairs (supplementary material Table S1) were ligated into the pLKO.1 Puro or pLKO.1 EGFP-f Puro vectors as described previously (Sehgal et al., 2011). GST–PG1-300 was generated by amplifying the first 300 amino acids of plakoglobin (supplementary material Table S1) and cloning the fragment into the pGEX4T1 vector (Amersham).

Cell lines and transfections

The HCT116 (American Type Culture Collection) and the HCT116-derived stable cell lines were cultured as described previously (Hosing et al., 2008). To generate the KIF5B-knockdown clones in the HCT116 cell line, the cells were transfected with 1 μ g of the shRNA constructs that targeted human KIF5B. Sixty hours post transfection, the cells were transferred to medium that contained 0.5 μ g/ml of puromycin (Sigma) to generate single-cell clones. The clones K3 and K5 were used for the indicated experiments. The HCT116-derived plakoglobin-knockdown clones have been described previously (Gosavi et al., 2011).

Antibodies and western blotting

The antibodies against PKP3, both DSC2 and DSC3, DSG2, plakoglobin, desmoplakin, K8 (keratin 8), actin, E-cadherin, β -catenin and α -E-catenin were used in western blots as previously described (Gosavi et al., 2011; Khapare et al., 2012; Kundu et al., 2008). Tissue culture supernatants of the antibodies against HA (12CA5), 14-3-3 γ (CG31) and 14-3-3 σ (CS112) were used at a dilution of 1:50. The antibodies against 14-3-3 ϵ (T-16, Santa Cruz, dilution of 1:2000), p120 catenin (mouse monoclonal from BD Transductions, catalog number 610134, dilution of 1:1000) and

PKC μ (rabbit monoclonal obtained from Abcam, catalog number 3146-1, dilution of 1:500) were used for western blot analysis. The secondary antibodies against mouse and rabbit IgGs were conjugated to horseradish peroxidase and used at a dilution of 1:1000 (Invitrogen) and 1:5000 (Pierce), respectively.

Immunofluorescence and calcium-switch assays

The cells were cultured on chromic-acid-treated, poly-L-lysine-coated glass coverslips at a confluence of 70–80%. Before fixation, the cells were carefully washed twice with 1 \times PBS. HCT116-derived clones were fixed in absolute methanol for 10 minutes at -20°C to detect α -tubulin, KIF5B, PKP2, Par3, ZO1, P-cadherin, desmoplakin, plakoglobin, DSC2 and DSC3, DSG2, E-cadherin and PKP3. In some experiments, cells were fixed in 4% paraformaldehyde and permeabilized with Triton X-100 as described previously (Gosavi et al., 2011). The antibodies against PKP3, both DSC2 and DSC3, DSG2, plakoglobin, desmoplakin, K8, actin, E-cadherin, β -catenin, ZO-1 and α -E-catenin were used in immunofluorescence analysis as described previously (Gosavi et al., 2011; Khapare et al., 2012; Kundu et al., 2008). Antibodies against PKP2 (BD Clontech, dilution 1:25), KIF5B (Abcam, dilution 1:100), α -tubulin (Abcam, dilution 1:150), Par3 (Millipore, dilution 1:50), ZO-1 (Abcam, dilution 1:100), P-cadherin (BD Transduction Laboratories, dilution 1:100), HA (12CA5, supernatant), p120 catenin (BD Transductions, dilution 1:100), N-cadherin (Life Technologies, catalog number 33-3900, dilution 1:50), α -E-catenin (Santa Cruz Biotechnology, dilution 1:25) and E-cadherin (clone 36/E-cadherin, mouse monoclonal, BD Transduction Laboratories, dilution 1:100) were incubated with the cells for 1 hour at room temperature at the indicated dilutions as described previously (Gosavi et al., 2011). To stain mitochondria, Mitotracker Green FM (Invitrogen) was used at a concentration of 100 nM to stain live cells. Confocal images were obtained by using a LSM 510 Meta Carl Zeiss confocal system with argon 488-nm and HeNe 543-nm lasers. All images were obtained by using an Axio Observer Z.1 microscope (numerical aperture 1.4) at a magnification of $\times 630$ ($\times 63$ objective and $\times 10$ eyepiece) with a $\times 2$ or $\times 4$ optical zoom. The surface intensity of staining was measured for the different proteins in a minimum of 24 cells using the Axiovision software, and the mean and standard deviation were plotted.

Hanging-drop assays

Hanging-drop assays were used to measure cell adhesion as described previously (Kundu et al., 2008).

GST-pulldown and immunoprecipitation assays

These assays were performed as described previously (Dalal et al., 1999).

GST-plakoglobin production and kinase assays

GST alone or GST-PG1-300 was purified from bacteria as described previously (Dalal et al., 2004). The purified proteins were used in kinase assays with recombinant PKC μ and a peptide that had been derived from CREB as a positive control (Signal Chem). Kinase activity was determined by using the ADP glow assay kit (Promega) according to the manufacturer's instructions.

Histology and immunohistochemistry

Mouse testes were fixed in 10% formaldehyde overnight and processed for histology as described previously (Kundu et al., 2008). TUNEL assays were performed as per the manufacturer's instructions (Promega).

Electron microscopy

Wild-type and 14-3-3 γ -knockdown testes were fixed with 3% glutaraldehyde and post-fixed with 1% osmium tetroxide (Tedpella). Grids were contrasted with alcoholic uranyl acetate for 1 minute and lead citrate for 30 seconds. The grids were observed under a Carl Zeiss LIBRA120 EFTEM transmission electron microscope at an accelerating voltage of 120 kV and at $\times 325,000$ magnification. Images were captured using a Slow Scan CCD camera (TRS, Germany).

Statistical Analysis

All *P*-values were generated using a Student's *t*-test.

Acknowledgements

We thank Young-hoon Lee (Korea Advanced Institute of Science and Technology, Daejeon, Korea), Stefan Linder (Institute of Medical Microbiology, Hamburg, Germany), Tetsu Akiyama (University of Tokyo, Tokyo, Japan), Chen Gu (Ohio State University, Columbus, OH) and Lawrence Goldstein (University of California San Diego, San Diego, CA) for supplying us with constructs that were used during the course of this study. We would also like to thank the ACTREC imaging facility for help with confocal microscopy, the ACTREC animal facility, and Sharda Sawant for helping with the preparation of the grids for electron microscopy.

Competing interests

The authors declare no competing interests.

Author contributions

L.S., M.M.V., F.S., U.K. and S.N.D. designed experiments and wrote the manuscript. L.S. performed the majority of the experiments with contributions from A.R., N.K., M.S., K.B., S.A. and N.A. A.M. determined that 14-3-3 γ forms a complex with KIF5B, S.S.V. performed the PKC μ -knockdown experiments and solubility assays, L.B. performed electron microscopy, R.M. performed the PKC μ kinase assays, M.G. and S.B. performed the RT-PCR assays and helped with confocal microscopy, H.A. performed the cell-matrix adhesion assays, R.T. performed the testis injections and A.S.H. generated the 14-3-3 γ -knockdown clones.

Funding

This work was supported by grants from the Department of Biotechnology, India [grant numbers BT/PR6521/Med/14/828/2005 and BT/PR12578/MED/31/75/2009]; and the Advanced Centre for Treatment Research and Education in Cancer (to L.S. and S.N.D.). A fellowship from the University Grants Commission supported A.M.

Supplementary material

Supplementary material available online at <http://jcs.biologists.org/lookup/suppl/doi:10.1242/jcs.125807/-/DC1>

References

- Acehan, D., Petzold, C., Gumper, I., Sabatini, D. D., Müller, E. J., Cowin, P. and Stokes, D. L. (2008). Plakoglobin is required for effective intermediate filament anchorage to desmosomes. *J. Invest. Dermatol.* **128**, 2665–2675.
- Andersson, A. M., Edvardsen, K. and Skakkebaek, N. E. (1994). Expression and localization of N- and E-cadherin in the human testis and epididymis. *Int. J. Androl.* **17**, 174–180.
- Aoyama, T., Hata, S., Nakao, T., Tanigawa, Y., Oka, C. and Kawaichi, M. (2009). Cayman ataxia protein caytaxin is transported by kinesin along neurites through binding to kinesin light chains. *J. Cell Sci.* **122**, 4177–4185.
- Araki, Y., Kawano, T., Taru, H., Saito, Y., Wada, S., Miyamoto, K., Kobayashi, H., Ishikawa, H. O., Ohsugi, Y., Yamamoto, T. et al. (2007). The novel cargo Alcadein induces vesicle association of kinesin-1 motor components and activates axonal transport. *EMBO J.* **26**, 1475–1486.
- Bass-Zubek, A. E., Godsel, L. M., Delmar, M. and Green, K. J. (2009). Plakophilins: multifunctional scaffolds for adhesion and signaling. *Curr. Opin. Cell Biol.* **21**, 708–716.
- Bierkamp, C., McLaughlin, K. J., Schwarz, H., Huber, O. and Kemler, R. (1996). Embryonic heart and skin defects in mice lacking plakoglobin. *Dev. Biol.* **180**, 780–785.
- Bonné, S., Gilbert, B., Hatzfeld, M., Chen, X., Green, K. J. and van Roy, F. (2003). Defining desmosomal plakophilin-3 interactions. *J. Cell Biol.* **161**, 403–416.
- Brunet, A., Kanai, F., Stehn, J., Xu, J., Sarbassova, D., Frangioni, J. V., Dalal, S. N., DeCaprio, J. A., Greenberg, M. E. and Yaffe, M. B. (2002). 14-3-3 transits to the nucleus and participates in dynamic nucleocytoplasmic transport. *J. Cell Biol.* **156**, 817–828.
- Caldelari, R., de Bruin, A., Baumann, D., Suter, M. M., Bierkamp, C., Balmer, V. and Müller, E. (2001). A central role for the armadillo protein plakoglobin in the autoimmune disease pemphigus vulgaris. *J. Cell Biol.* **153**, 823–834.
- Chan, T. A., Hermeking, H., Lengauer, C., Kinzler, K. W. and Vogelstein, B. (1999). 14-3-3 σ is required to prevent mitotic catastrophe after DNA damage. *Nature* **401**, 616–620.
- Chen, X., Bonne, S., Hatzfeld, M., van Roy, F. and Green, K. J. (2002). Protein binding and functional characterization of plakophilin 2. Evidence for its diverse roles in desmosomes and β -catenin signaling. *J. Biol. Chem.* **277**, 10512–10522.
- Cheng, C. Y. and Mruk, D. D. (2002). Cell junction dynamics in the testis: Sertoli-germ cell interactions and male contraceptive development. *Physiol. Rev.* **82**, 825–874.

- Chidgey, M., Brakebusch, C., Gustafsson, E., Cruchley, A., Hail, C., Kirk, S., Merritt, A., North, A., Tselepis, C., Hewitt, J. et al. (2001). Mice lacking desmocollin 1 show epidermal fragility accompanied by barrier defects and abnormal differentiation. *J. Cell Biol.* **155**, 821–832.
- Cross, R. A. and Carter, N. J. (2000). Molecular motors. *Curr. Biol.* **10**, R177–R179.
- Dalal, S. N., Schweitzer, C. M., Gan, J. and DeCaprio, J. A. (1999). Cytoplasmic localization of human cdc25C during interphase requires an intact 14-3-3 binding site. *Mol. Cell. Biol.* **19**, 4465–4479.
- Dalal, S. N., Yaffe, M. B. and DeCaprio, J. A. (2004). 14-3-3 family members act coordinately to regulate mitotic progression. *Cell Cycle* **3**, 670–675.
- Dusek, R. L., Godsel, L. M. and Green, K. J. (2007). Discriminating roles of desmosomal cadherins: beyond desmosomal adhesion. *J. Dermatol. Sci.* **45**, 7–21.
- Gallicano, G. I., Kouklis, P., Bauer, C., Yin, M., Vasioukhin, V., Degenstein, L. and Fuchs, E. (1998). Desmoplakin is required early in development for assembly of desmosomes and cytoskeletal linkage. *J. Cell Biol.* **143**, 2009–2022.
- Garrod, D. and Chidgey, M. (2007). Desmosome structure, composition and function. *Biochim. Biophys. Acta* **1778**, 572–587.
- Getsios, S., Huen, A. C. and Green, K. J. (2004). Working out the strength and flexibility of desmosomes. *Nat. Rev. Mol. Cell Biol.* **5**, 271–281.
- Gloushankova, N. A., Wakatsuki, T., Troyanovsky, R. B., Elson, E. and Troyanovsky, S. M. (2003). Continual assembly of desmosomes within stable intercellular contacts of epithelial A-431 cells. *Cell Tissue Res.* **314**, 399–410.
- Gosavi, P., Kundu, S. T., Khapare, N., Sehgal, L., Karkhanis, M. S. and Dalal, S. N. (2011). E-cadherin and plakoglobin recruit plakophilin3 to the cell border to initiate desmosome assembly. *Cell. Mol. Life Sci.* **68**, 1439–1454.
- Green, K. J. and Gaudry, C. A. (2000). Are desmosomes more than tethers for intermediate filaments? *Nat. Rev. Mol. Cell Biol.* **1**, 208–216.
- Grossmann, K. S., Grund, C., Huelsen, J., Behrend, M., Erdmann, B., Franke, W. W. and Birchmeier, W. (2004). Requirement of plakophilin 2 for heart morphogenesis and cardiac junction formation. *J. Cell Biol.* **167**, 149–160.
- Gu, C., Zhou, W., Puthenveedu, M. A., Xu, M., Jan, Y. N. and Jan, L. Y. (2006). The microtubule plus-end tracking protein EB1 is required for Kv1 voltage-gated K⁺ channel axonal targeting. *Neuron* **52**, 803–816.
- Haraguchi, K., Hayashi, T., Jimbo, T., Yamamoto, T. and Akiyama, T. (2006). Role of the kinesin-2 family protein, KIF3, during mitosis. *J. Biol. Chem.* **281**, 4094–4099.
- Hatzfeld, M. (2007). Plakophilins: Multifunctional proteins or just regulators of desmosomal adhesion? *Biochim. Biophys. Acta* **1773**, 69–77.
- Hausser, A., Link, G., Bamberg, L., Burzlaff, A., Lutz, S., Pfizenmaier, K. and Johannes, F. J. (2002). Structural requirements for localization and activation of protein kinase C μ (PKC μ) at the Golgi compartment. *J. Cell Biol.* **156**, 65–74.
- Hosing, A. S., Kundu, S. T. and Dalal, S. N. (2008). 14-3-3 Gamma is required to enforce both the incomplete S phase and G2 DNA damage checkpoints. *Cell Cycle* **7**, 3171–3179.
- Khapare, N., Kundu, S. T., Sehgal, L., Sawant, M., Priya, R., Gosavi, P., Gupta, N., Alam, H., Karkhanis, M., Naik, N. et al. (2012). Plakophilin3 loss leads to an increase in PRL3 levels promoting K8 dephosphorylation, which is required for transformation and metastasis. *PLoS ONE* **7**, e38561.
- Knudsen, K. A. and Wheelock, M. J. (1992). Plakoglobin, or an 83-kD homologue distinct from beta-catenin, interacts with E-cadherin and N-cadherin. *J. Cell Biol.* **118**, 671–679.
- Koch, P. J., Mahoney, M. G., Ishikawa, H., Pulkkinen, L., Uitto, J., Shultz, L., Murphy, G. F., Whitaker-Menezes, D. and Stanley, J. R. (1997). Targeted disruption of the pemphigus vulgaris antigen (desmoglein 3) gene in mice causes loss of keratinocyte cell adhesion with a phenotype similar to pemphigus vulgaris. *J. Cell Biol.* **137**, 1091–1102.
- Kundu, S. T., Gosavi, P., Khapare, N., Patel, R., Hosing, A. S., Maru, G. B., Ingle, A., Decaprio, J. A. and Dalal, S. N. (2008). Plakophilin3 downregulation leads to a decrease in cell adhesion and promotes metastasis. *Int. J. Cancer* **123**, 2303–2314.
- Lechler, T. and Fuchs, E. (2007). Desmoplakin: an unexpected regulator of microtubule organization in the epidermis. *J. Cell Biol.* **176**, 147–154.
- Lee, N. P., Mruk, D., Lee, W. M. and Cheng, C. Y. (2003). Is the cadherin/catenin complex a functional unit of cell-cell actin-based adherens junctions in the rat testis? *Biol. Reprod.* **68**, 489–508.
- Lewis, J. E., Wahl, J. K., 3rd, Sass, K. M., Jensen, P. J., Johnson, K. R. and Wheelock, M. J. (1997). Cross-talk between adherens junctions and desmosomes depends on plakoglobin. *J. Cell Biol.* **136**, 919–934.
- Li, M. W., Mruk, D. D., Lee, W. M. and Cheng, C. Y. (2009). Connexin 43 and plakophilin-2 as a protein complex that regulates blood-testis barrier dynamics. *Proc. Natl. Acad. Sci. USA* **106**, 10213–10218.
- Lie, P. P., Cheng, C. Y. and Mruk, D. D. (2010). Crosstalk between desmoglein-2/desmocollin-2/Src kinase and coxsackie and adenovirus receptor/ZO-1 protein complexes, regulates blood-testis barrier dynamics. *Int. J. Biochem. Cell Biol.* **42**, 975–986.
- Lie, P. P., Cheng, C. Y. and Mruk, D. D. (2011). The biology of the desmosome-like junction a versatile anchoring junction and signal transducer in the seminiferous epithelium. *Int. Rev. Cell Mol. Biol.* **286**, 223–269.
- Liljedahl, M., Maeda, Y., Colanzi, A., Ayala, I., Van Lint, J. and Malhotra, V. (2001). Protein kinase D regulates the fission of cell surface destined transport carriers from the trans-Golgi network. *Cell* **104**, 409–420.
- Marcozzi, C., Burdett, I. D., Buxton, R. S. and Magee, A. I. (1998). Coexpression of both types of desmosomal cadherin and plakoglobin confers strong intercellular adhesion. *J. Cell Sci.* **111**, 495–509.
- Michels, C., Buchta, T., Bloch, W., Krieg, T. and Niessen, C. M. (2009). Classical cadherins regulate desmosome formation. *J. Invest. Dermatol.* **129**, 2072–2075.
- Muslin, A. J., Tanner, J. W., Allen, P. M. and Shaw, A. S. (1996). Interaction of 14-3-3 with signaling proteins is mediated by the recognition of phosphoserine. *Cell* **84**, 889–897.
- Nekrasova, O. E., Amargo, E. V., Smith, W. O., Chen, J., Kreitzer, G. E. and Green, K. J. (2011). Desmosomal cadherins utilize distinct kinesins for assembly into desmosomes. *J. Cell Biol.* **195**, 1185–1203.
- Obenauer, J. C., Cantley, L. C. and Yaffe, M. B. (2003). Scansite 2.0: Proteome-wide prediction of cell signaling interactions using short sequence motifs. *Nucleic Acids Res.* **31**, 3635–3641.
- Palka, H. L. and Green, K. J. (1997). Roles of plakoglobin end domains in desmosome assembly. *J. Cell Sci.* **110**, 2359–2371.
- Park, J. E., Kim, Y. I. and Yi, A. K. (2009). Protein kinase D1 is essential for MyD88-dependent TLR signaling pathway. *J. Immunol.* **182**, 6316–6327.
- Pasdar, M., Krzeminski, K. A. and Nelson, W. J. (1991). Regulation of desmosome assembly in MDCK epithelial cells: coordination of membrane core and cytoplasmic plaque domain assembly at the plasma membrane. *J. Cell Biol.* **113**, 645–655.
- Prestle, J., Pfizenmaier, K., Brenner, J. and Johannes, F. J. (1996). Protein kinase C μ is located at the Golgi compartment. *J. Cell Biol.* **134**, 1401–1410.
- Rahman, A., Friedman, D. S. and Goldstein, L. S. (1998). Two kinesin light chain genes in mice. Identification and characterization of the encoded proteins. *J. Biol. Chem.* **273**, 15395–15403.
- Ruiz, P., Brinkmann, V., Ledermann, B., Behrend, M., Grund, C., Thälhammer, C., Vogel, F., Birchmeier, C., Günther, U., Franke, W. W. et al. (1996). Targeted mutation of plakoglobin in mice reveals essential functions of desmosomes in the embryonic heart. *J. Cell Biol.* **135**, 215–225.
- Russell, L. D., Ettlin, R., Sinha Hikim, A. P. and Clegg, E. D. (1990). *Histological and Histopathological Evaluation of the Testis*. Clearwater, FL: Cache River.
- Sehgal, L., Thorat, R., Khapare, N., Mukhopadhyaya, A., Sawant, M. and Dalal, S. N. (2011). Lentiviral mediated transgenesis by in vivo manipulation of spermatogonial stem cells. *PLoS ONE* **6**, e21975.
- Silver, K. E. and Harrison, R. E. (2011). Kinesin 5B is necessary for delivery of membrane and receptors during Fc γ R-mediated phagocytosis. *J. Immunol.* **186**, 816–825.
- Skiyaro, T., Bonné, S., D'Hooge, P., Denecker, G., Goossens, S., De Rycke, R., Borgonie, G., Bösl, M., van Roy, F. and van Hengel, J. (2008). Plakophilin-3-deficient mice develop hair coat abnormalities and are prone to cutaneous inflammation. *J. Invest. Dermatol.* **128**, 1375–1385.
- Steinacker, P., Schwarz, P., Reim, K., Brechlin, P., Jahn, O., Kratzin, H., Aitken, A., Wiltfang, J., Aguzzi, A., Bahn, E. et al. (2005). Unchanged survival rates of 14-3-3gamma knockout mice after inoculation with pathological prion protein. *Mol. Cell. Biol.* **25**, 1339–1346.
- Tanaka, Y., Kanai, Y., Okada, Y., Nonaka, S., Takeda, S., Harada, A. and Hirokawa, N. (1998). Targeted disruption of mouse conventional kinesin heavy chain, kif5B, results in abnormal perinuclear clustering of mitochondria. *Cell* **93**, 1147–1158.
- Telles, E., Hosing, A. S., Kundu, S. T., Venkatraman, P. and Dalal, S. N. (2009). A novel pocket in 14-3-3 ϵ is required to mediate specific complex formation with cdc25C and to inhibit cell cycle progression upon activation of checkpoint pathways. *Exp. Cell Res.* **315**, 1448–1457.
- Tinkle, C. L., Pasolli, H. A., Stokes, N. and Fuchs, E. (2008). New insights into cadherin function in epidermal sheet formation and maintenance of tissue integrity. *Proc. Natl. Acad. Sci. USA* **105**, 15405–15410.
- Valente, C., Turacchio, G., Mariggio, S., Pagliuso, A., Gaibisso, R., Di Tullio, G., Santoro, M., Formigini, F., Spanò, S., Piccini, D. et al. (2012). A 14-3-3 γ dimer-based scaffold bridges CIBP1-S/BARS to PI(4)KIII β to regulate post-Golgi carrier formation. *Nat. Cell Biol.* **14**, 343–354.
- Vasioukhin, V., Bowers, E., Bauer, C., Degenstein, L. and Fuchs, E. (2001). Desmoplakin is essential in epidermal sheet formation. *Nat. Cell Biol.* **3**, 1076–1085.
- Verhey, K. J. and Hammond, J. W. (2009). Traffic control: regulation of kinesin motors. *Nat. Rev. Mol. Cell Biol.* **10**, 765–777.
- Wiesner, C., Faix, J., Himmel, M., Bentzien, F. and Linder, S. (2010). KIF5B and KIF3A/KIF3B kinesins drive MT1-MMP surface exposure, CD44 shedding, and extracellular matrix degradation in primary macrophages. *Blood* **116**, 1559–1569.
- Wong, C. H., Mruk, D. D., Lui, W. Y. and Cheng, C. Y. (2004). Regulation of blood-testis barrier dynamics: an in vivo study. *J. Cell Sci.* **117**, 783–798.
- Yaffe, M. B. (2002). How do 14-3-3 proteins work? – Gatekeeper phosphorylation and the molecular anvil hypothesis. *FEBS Lett.* **513**, 53–57.
- Yaffe, M. B., Rittinger, K., Volinia, S., Caron, P. R., Aitken, A., Leffers, H., Gambini, S. J., Smerdon, S. J. and Cantley, L. C. (1997). The structural basis for 14-3-3:phosphopeptide binding specificity. *Cell* **91**, 961–971.

Supplementary Figure 1. 14-3-3 γ loss leads to decreased cell-cell adhesion and no changes in other junctional components. **A.** Vector control (Vec), 14-3-3 γ knockdown (sh 14-3-3 γ) and KIF5B knockdown (sh KIF5B) testis sections were assayed for cell death by performing terminal deoxynucleotidyl transferase dUTP nick end labeling (TUNEL) assays. Note that although some TUNEL-positive cells were observed in the sh14-3-3 γ testis, no staining was observed in the Vec or the shKIF5B sections. **B.** The Vec or sh 14-3-3 γ cells were incubated with extra cellular matrix (ECM) substrates and a cell-ECM adhesion assay was performed. The mean and standard deviation were plotted on the y-axis. Note that adhesion was decreased on all substrates. The p value was calculated using a students t-test and was <0.05 suggesting that cell ECM adhesion was significantly reduced in sh14-3-3 γ cells as compared to the vector control. **C.** Vec and plakoglobin (PG) knockdown cells (sh PG) were stained with antibodies to DSC2/3 and DSG2 followed by confocal microscopy. The border staining of these proteins was not altered in the shPG cells as compared with the Vec cells. **D.** Vec and sh14-3-3 γ cells were stained with antibodies to E-cadherin, P-cadherin, β -catenin, ZO-1 α -E-catenin, p120 catenin and Par-3 followed by confocal microscopy. The border staining of these proteins was not altered in the sh14-3-3 γ cells as compared to the vector control. **E.** The border intensity was measured for at least 20 cells in three different experiments. The mean and standard deviation are plotted. Total magnification is 630X with 2X optical zoom. *P*-values obtained using Student's t test. A p value of <0.05 was considered significant.

Supplementary Figure 2. Intensity profiles for desmosome proteins in the 14-3-3 γ and KIF5B knockdown cells. The vector control (Vec), 14-3-3 γ knockdown cells (sh

14-3-3 γ) and KIF5B knockdown cells (K3 and K5) were stained with the indicated antibodies and the intensity profiles were determined. Note that the desmosomal proteins show higher intensity at the cell border in the 14-3-3 γ and KIF5B knockdown cells than do the Vec cells. No change was observed in the intensity of adherens junction proteins at the cell border.

Supplementary Figure 3. Plakoglobin (PG) border localization is dependent on 14-3-

3 γ and KIF5B. **A.** Identification of a 14-3-3 binding site and potential PKC μ site in PG using motif scan. **B.** Hanging drop assays were performed to determine cell-cell adhesion. The K3 and K5 KIF5B KD cells formed fewer and smaller clumps as compared to the Vec cells. **C.** Vec, K3 and K5 cells were stained with antibodies to PG and β -catenin. Note that although PG is not localized to the border in K3 and K5, β -catenin localization to the border is not altered in K3 and K5 cells suggesting that KIF5B is required for transport of PG to the cell border. **D.** HCT116 cells were cultured in low calcium medium and then incubated in the presence or absence of Nocodazole (NOC). The cells were stained with antibodies to PG and visualized by confocal microscopy. Staining was quantified and mean and standard deviation for border staining were calculated in three independent experiments and plotted as shown. The p value was calculated using a students t-test and was <0.05 suggesting that PG border staining was significantly reduced upon treatment with nocodazole. Total magnification is 630X with 2X optical zoom. **E.** mRNA was prepared from the Vec and KIF5B knockdown cells (K3 and K5) and converted to cDNA; PCR reactions were performed with oligonucleotide pairs specific for the indicated genes. Glyceraldehyde 3-phosphate dehydrogenase (GAPDH) served as a loading control. **F.** Vec, K3 and K5 cells were stained with the

indicated antibodies followed by confocal microscopy. Note that the localization of the adherens junction proteins is not altered upon KIF5B knockdown. **G.** Protein extracts were prepared from Vec, K3 and K5 cells and were resolved on SDS-PAGE gels followed by Western blotting with the indicated antibodies. A Western blot for actin was performed as a loading control. Note that the levels of these proteins are not altered upon KIF5B knockdown.

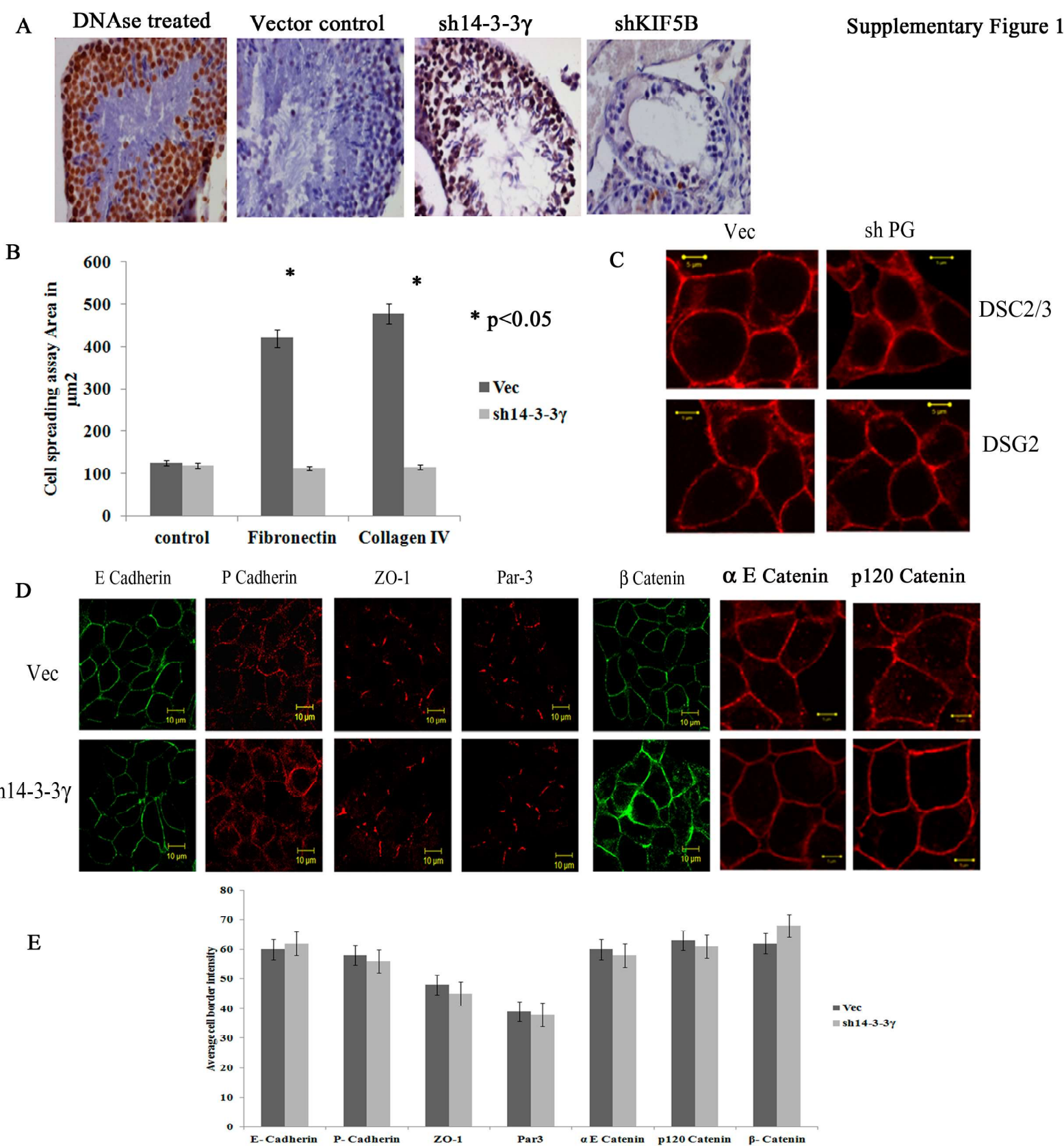
Supplementary Figure 4. Localization of desmosomal proteins in cells lacking 14-3-3 σ or upon KIF5B or 14-3-3 γ knockdown. **A.** Protein lysates were prepared from HCT116 cells either with both copies (14-3-3 σ +/+) or without both copies (14-3-3 σ -/-) of the 14-3-3 σ gene. The lysates were resolved on SDS-PAGE gels and Western blot analysis performed with the indicated antibodies. Note the decrease in PG levels observed in the 14-3-3 σ -/- cells. Actin was used as a loading control. **B.** Hanging drop assays were performed to measure cell-cell adhesion. **C.** The 14-3-3 σ +/+ and 14-3-3 σ -/- cells were stained with antibodies to PG followed by confocal microscopy. Bars correspond to 5 μ M. **D.** NP40 soluble (S) and insoluble (I) extracts prepared from Vec or sh 14-3-3 γ cells were resolved on SDS-PAGE gels and Western blots performed with the indicated antibodies. Please note that the increase in cytoplasmic localization of the desmosomal cadherins is not associated with an increase in solubility. Western blots for keratin and actin were performed as controls. **E.** Cells were fixed with paraformaldehyde and stained with the indicated antibodies. Please note that DSG2 and DSC2/3 localize to the cytoplasm in cells lacking 14-3-3 γ or KIF5B as compared with the negative control. Bars correspond to 5 μ m.

Name	Targeting sequence
14-3-3 γ ShRNA a	CCGGACTATTACCGTTACCTGGCAGTTCTCGCCAGGTA ACGGTAATAGTCCTTTTTTG
14-3-3 γ ShRNA b	AATTCAAAAAAGGACTATTACCGTTACCTGGCGAGAAC TGCCAGGTAACGGTAATAGT
KIF5B shRNA a	CCGGAACTTCATGATCCAGAAGGCTCGAGCCTTCTGGA TCATGAAGTTTTTTTG
KIF5B shRNA a	AATTCAAAAAAACTTCATGATCCAGAAGGCTCGAGCCT TCTGGATCATGAAGTT
14-3-3 γ Fwd (Mus musculus)	GGGATCCATGGTGGACCGCGAGCAAC
14-3-3 γ Rev (Mus musculus)	GCTCGAGTTAGTTGTTGCCTTCACCG
PG S236A F	GTCCGCATGCTCGCCTCCCCTGTGGAG
PG S236A R	CTCCACAGGGGAGGCGAGCATGCGGAC
PG F	GGATCCATGGAGGTGATGAACC
PG R	CTCGAGCTAGGCCAGCATGTGGTC
PKC μ shRNA a	CCGGCCATTGATCTTATCAATAACTCGAGTTATTGATA AGATCAATGGTTTTTG
PKC μ shRNA b	AATTCAAAAACCATTGATCTTATCAATAACTCGAGTTA TTGATAAGATCAATGG
GAPDH RT 5'	TGCACCACCAACTGCTTAGC
GAPDH RT 3'	GGCATGGACTGTGGTCATGAG
Desmoglein 2 RT 5'	TACGCCCTGCTGCTTCTCC
Desmoglein 2 RT 3'	TCTCCCTCCCGAAGAGCCACG
Desmocollin 2 RT 5'	GTTTTACTCAGCCCCGTCTTG
Desmocollin 2 RT 3'	GCCCATCTTCTTCTTGTCGT
PKP2 RT 5'	AGGTTTGCTGTGGAATTTGTC
PKP2 RT 3'	CGCCAGCAGAACTCATGTTT
PG 5' 1-300	aaGGATCCATGGAGGTGATGAACCTGATGGAG
PG 3' 1-300	aaCTCGAGCTGGTTGCCGTAGGCCAG

Supplementary Table 1. List of oligonucleotides used for cloning and Reverse

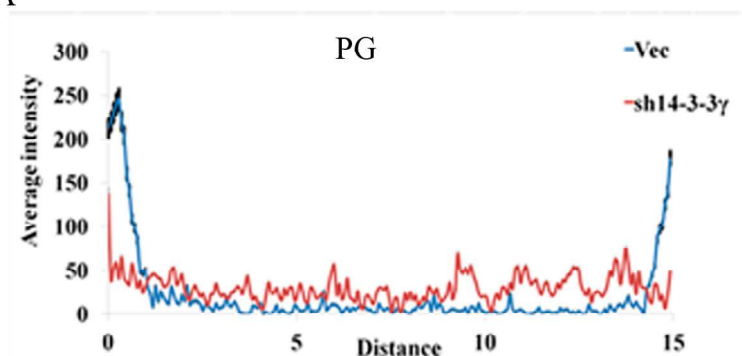
Transcriptase PCR reactions.

Supplementary Figure 1

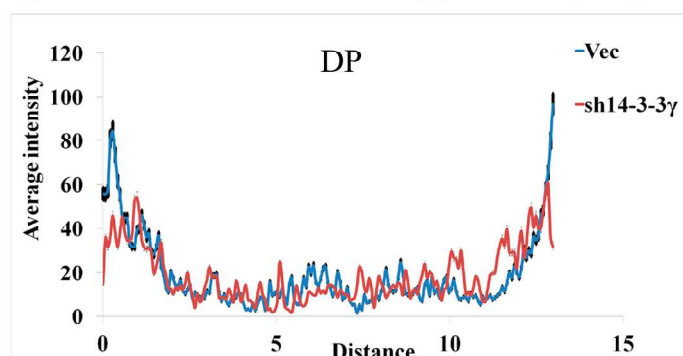


Supplementary Figure 2

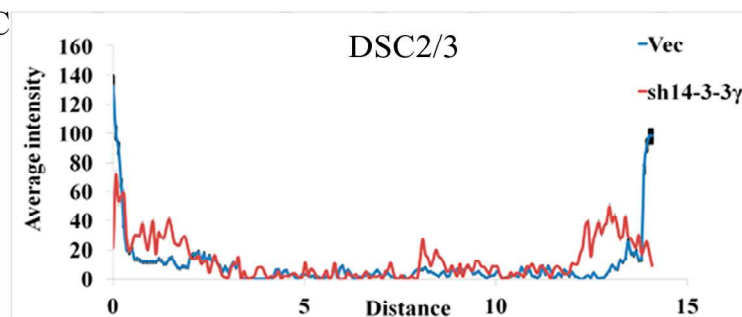
A



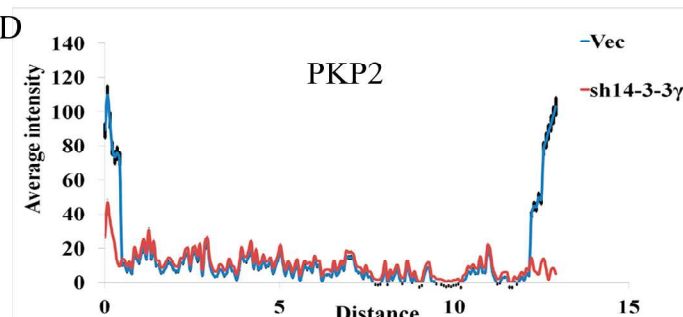
B



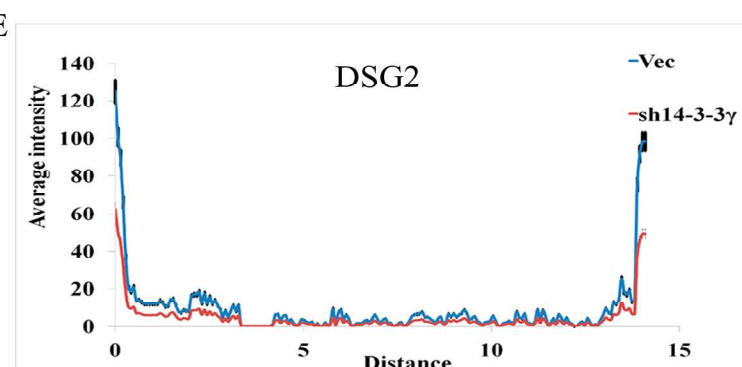
C



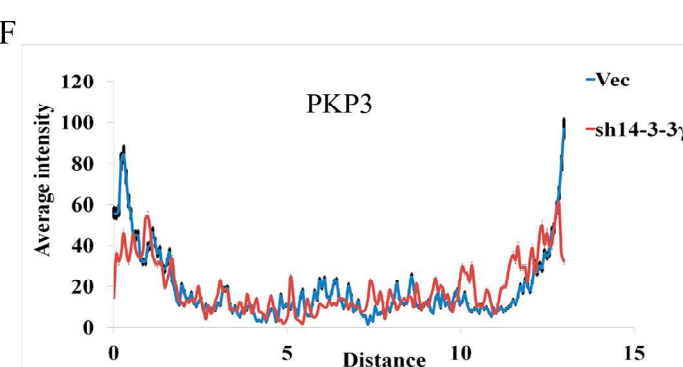
D



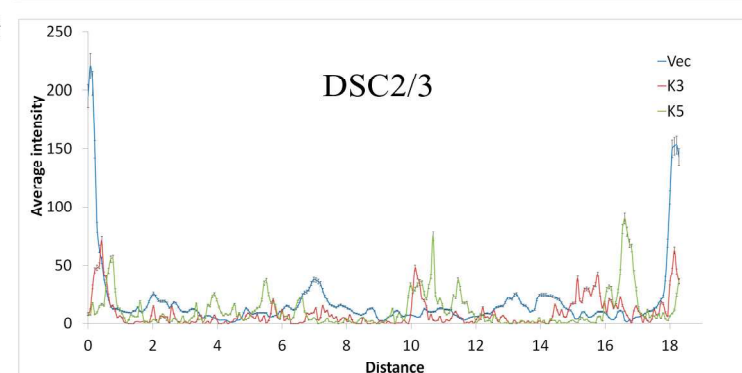
E



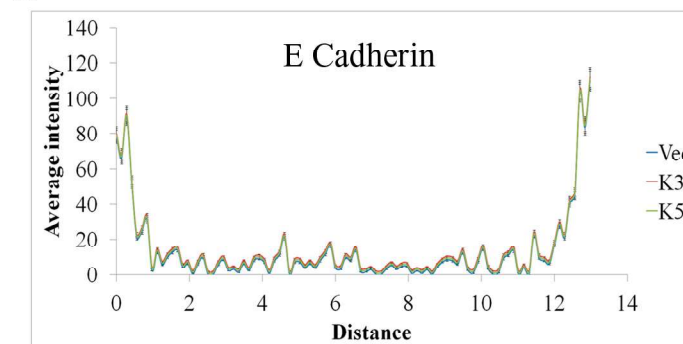
F



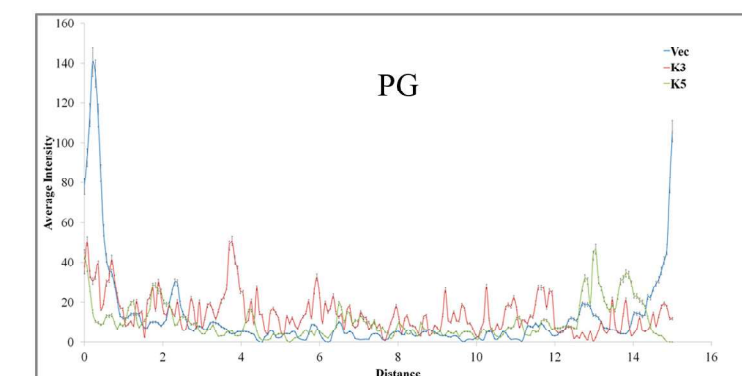
G



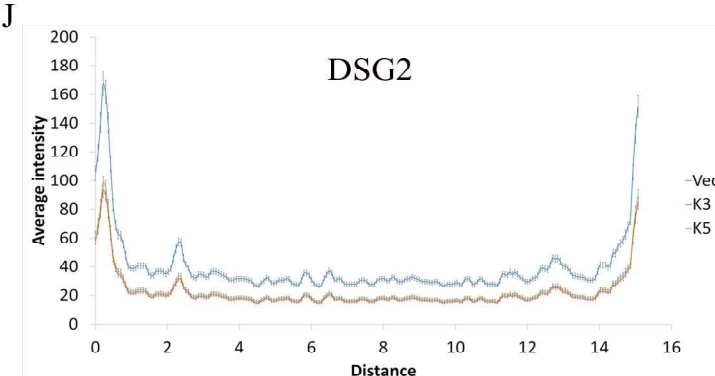
H



I



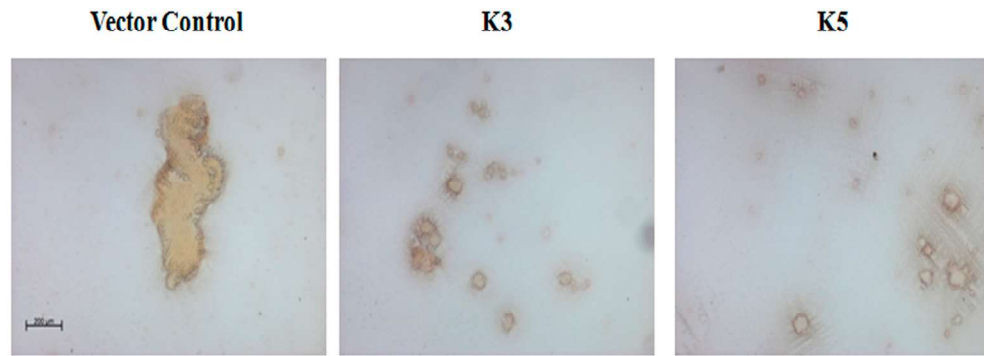
J



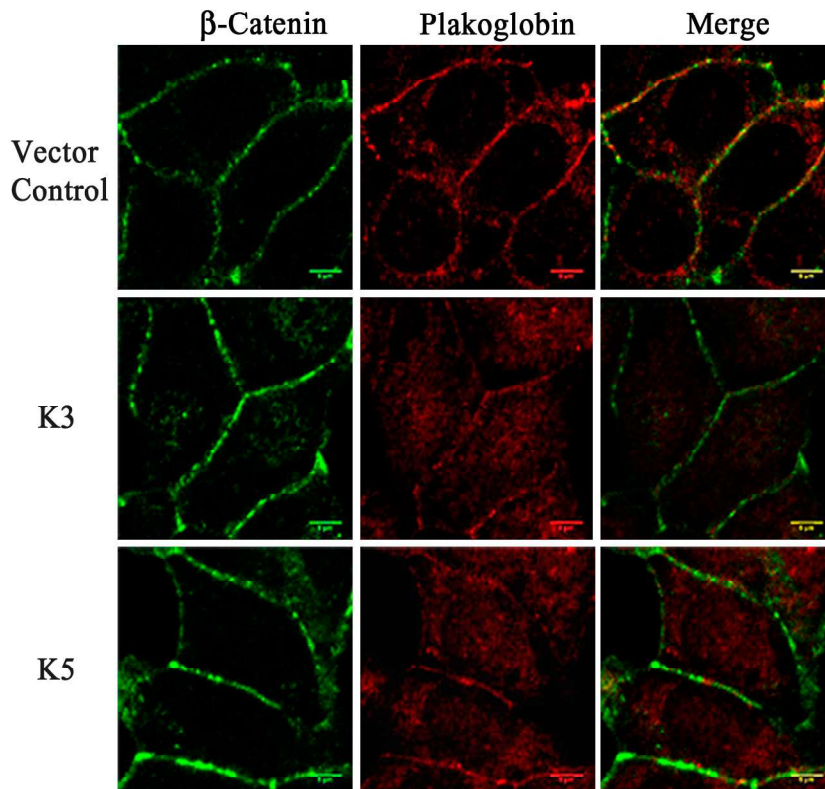
A

Phosphoserine/threonine binding group (pST bind)					
14-3-3 Mode 1			Gene Card YWHAZ		
Site	Score	Percentile	Sequence	SA	
S236	0.4336	0.606 %	PALVRMLSSPVESVL	0.385	
Basophilic serine/threonine kinase group (Baso ST kin)					
PKC mu			Gene Card PRKCM		
Site	Score	Percentile	Sequence	SA	
S236	0.4873	0.924 %	PALVRMLSSPVESVL	0.385	

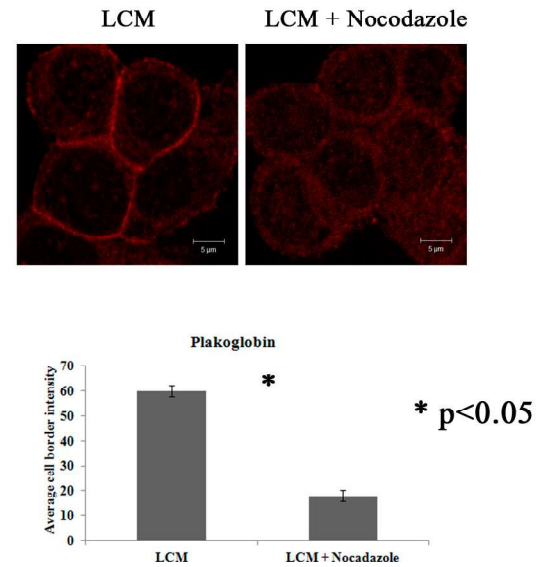
B



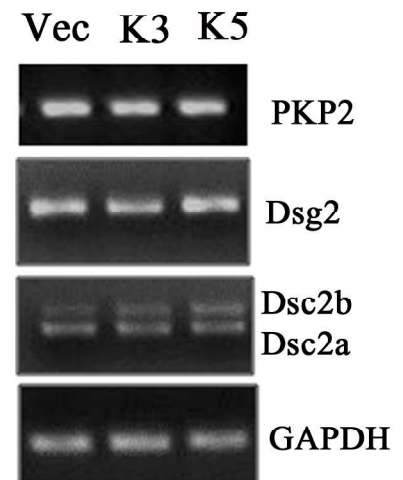
C



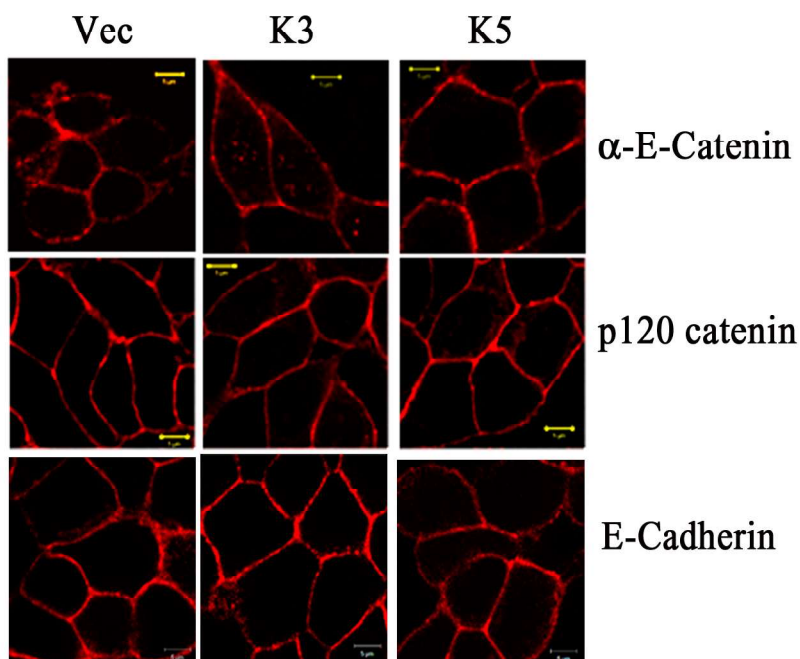
D



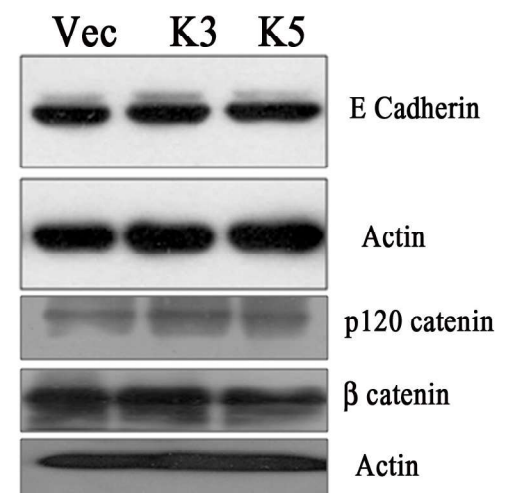
E



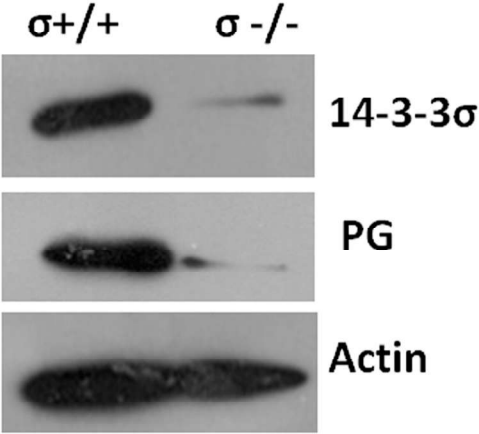
F



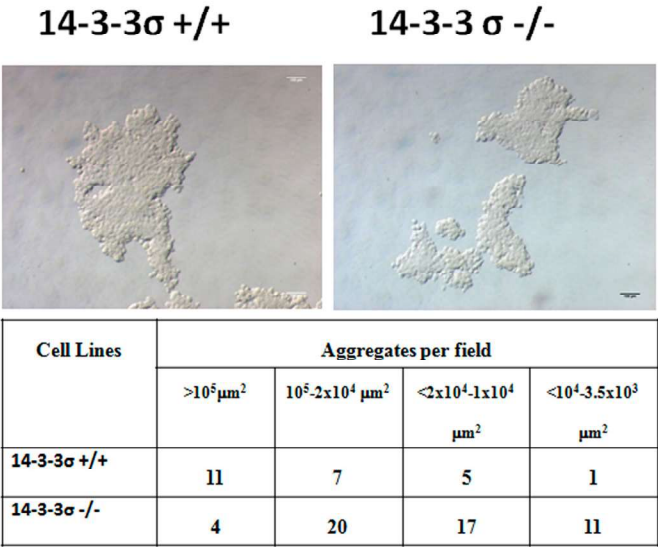
G



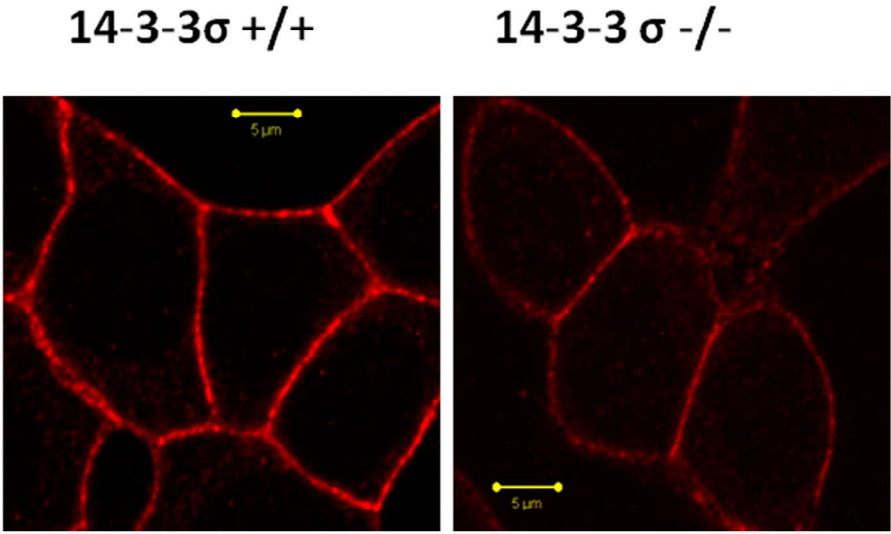
A



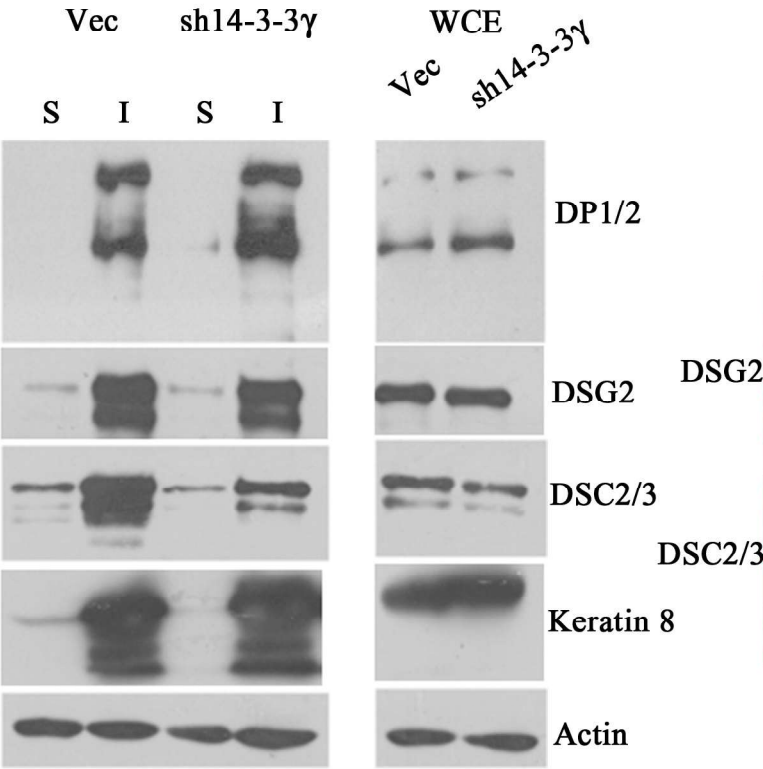
B



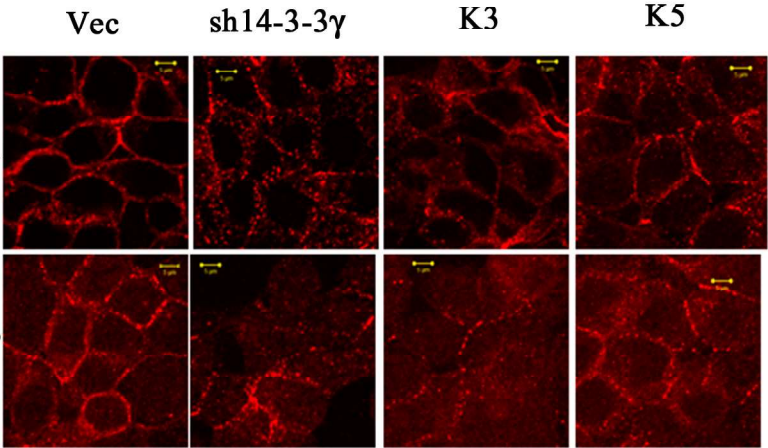
C



D



E





Plakoglobin localization to the cell border restores desmosome function in cells lacking 14-3-3 γ

Sonali S. Vishal ^{a, b}, Sarika Tilwani ^{a, b}, Sorab N. Dalal ^{a, b, *}

^a KS215, Advanced Centre for Treatment Research and Education in Cancer (ACTREC), Tata Memorial Centre, Kharghar Node, Navi Mumbai 410210, India

^b Homi Bhabha National Institute, Training School Complex, Anushakti Nagar, Mumbai 400085, India

ARTICLE INFO

Article history:

Received 1 December 2017

Accepted 14 December 2017

Available online 15 December 2017

Keywords:

Desmosome

Plakoglobin

Cell-cell adhesion

14-3-3 γ

ABSTRACT

Desmosomes are cell-cell adhesion junctions that anchor intermediate filaments. Loss of 14-3-3 γ in HCT116 cells led to defects in desmosome assembly due to a decrease in the transport of Plakoglobin (PG) to the cell border thus disrupting desmosome formation. Desmosome formation in cells lacking 14-3-3 γ was restored by artificially localizing PG to the cell border by fusing it to EGFP-f (PG-EGFP-f). These results suggest that a major role of 14-3-3 γ in desmosome assembly is to transport PG to the cell border leading to the initiation of desmosome formation.

© 2017 Elsevier Inc. All rights reserved.

1. Introduction

The 14-3-3 proteins are highly conserved in all eukaryotes (reviewed in Ref. [1]) and regulate multiple cellular pathways in eukaryotic cells [1–3]. 14-3-3 proteins bind to ligands containing a phospho-serine or threonine residue in one of two consensus motifs and bind to their ligands as either homo or heterodimers, with each monomer binding to one phospho-peptide [4,5] or through the phosphorylation independent mode III motif [6].

Desmosomes are adherens like cell-cell adhesion junctions present in all epithelial tissues [7] and are composed of three protein families, the desmosomal cadherins, desmogleins (DSGs) and desmocollins (DSCs), the armadillo repeat containing proteins, plakoglobin (PG) and plakophilins (PKPs) and plakin family proteins such as desmoplakin (DP) [8]. Defects in desmosome function lead to skin and heart disorders such as epidermolysis bullosa, ectodermal dysplasia, keratosis, keratoderma, woolly hair, and arrhythmogenic right ventricular cardiomyopathy [9–14]. Auto-antibodies to desmosomal proteins disrupt desmosome structure leading to autoimmune disorders such as pemphigus vulgaris and pemphigus foliaceus [15–17]. Disruption of desmosome function due to loss of desmosomal proteins is associated with tumor

progression and metastasis [18–23].

The localization of PG to the cell border is a prerequisite for desmosome formation partially due to a decrease in the levels of PKPs and DP at the cell border [24,25]. PG knockout mice die at embryonic day 10.5 due to the defects in the development of heart, associated with thin heart wall and defects in epidermal desmosome organization [26]. These results suggest that the recruitment of PKP3 to the border by PG is an important step in the initiation of desmosome formation. Previous results from this laboratory have demonstrated that loss of 14-3-3 γ led to a decrease in the levels of PG at the cell border leading to defects in desmosome assembly in cell lines in culture and in the seminiferous epithelium in mice [27]. To demonstrate that the only role of 14-3-3 γ in desmosome formation is the transport of PG to the border, PG was artificially localized to the cell border by fusing it to farnesylated GFP (PG-EGFP-f). Cells expressing PG-EGFP-f showed an increased localization of DP, DSG2 and PKP3 at the cell border which was accompanied by an increase in cell-cell adhesion. These results suggest that the defects in desmosome formation observed upon 14-3-3 γ loss are due to defects in PG transport.

2. Materials and methods

2.1. Plasmids and constructs

All plasmids used in this report are described in [Supplementary materials and methods](#).

* Corresponding author. KS215, Advanced Centre for Treatment Research and Education in Cancer (ACTREC), Tata Memorial Centre, Kharghar Node, Navi Mumbai 410210, India.

E-mail address: sdalal@actrec.gov.in (S.N. Dalal).

2.2. Cell lines and transfections

HCT116 is an epithelial cell line isolated from human colorectal carcinoma. The HCT116 derived knockdown cell lines were cultured as described previously [22,25,27,28]. 2.5 µg of the EGFP-f or PG-EGFP-f or EGFP or PG-EGFP cDNA was transfected into either the 14-3-3γ or PG or PKP3 knockdown cells using Polyethyleneimine (Polysciences, Inc.). 48 h post transfection cells were harvested for Western blotting or fixed for immunofluorescence assays as described below.

2.3. Antibodies and western blotting

Protein extracts were prepared in SDS sample buffer and protein estimations were performed as described previously [22,25,27]. Details of the antibodies used in this study are in [supplementary materials and methods](#).

2.4. Immunofluorescence and confocal microscopy

Transfected cells were fixed with 4% paraformaldehyde. The protocol for staining has been previously described [27]. The secondary antibodies used in immunofluorescence assay were conjugated with Alexa Fluor 633 or Alexa Fluor 568, to avoid spectral overlap with GFP. All images were captured using Zeiss LSM 780 confocal microscope. The cell border intensity of staining was measured for the different proteins for at least 33 transfected cells using Image J software, and the mean and standard error were plotted. *p* values were obtained using a student's *t*-test.

2.5. Calcium switch experiments

The HCT116 derived 14-3-3γ knockdown cell line was transfected with EGFP-f or PG-EGFP-f cDNA, 24 h post transfection cells were incubated in low calcium medium. After 24 h, the cells were fed with medium with normal calcium levels for 15 min and the cells fixed and processed for immunofluorescence and confocal microscopy as described [25,27,29].

2.6. Hanging drop assays

Cells were transfected with either pCDNA3.1 Puromycin EGFP-f or pCDNA3.1 Puromycin PG-EGFP-f. 24 h post transfection, the cells were transferred to medium containing 0.5 µg/ml of puromycin for four days to kill the un-transfected cells. The remaining cells were processed for hanging drop assays as previously described [22].

3. Results and discussion

3.1. Localization of PG to the cell border results in increased border localization of other desmosomal proteins

Our previous studies had demonstrated that 14-3-3γ was required for PG transport to the border and hence desmosome formation [27]. PG staining in the HCT116 vector control and 14-3-3γ knockdown clones confirmed that PG localized to the border in the vector control cells but not in the 14-3-3γ knockdown clones (Fig. 1A). The levels of 14-3-3γ were greatly reduced in the 14-3-3γ knockdown cells as compared to the vector control (Fig. 1B [27]). A Western blot for β-actin, served as a loading control. To determine if artificially localizing PG to the cell border stimulated desmosome formation, HCT116 derived 14-3-3γ knockdown cells were transfected with PG-EGFP-f or EGFP-f cDNA and the localization of the different desmosomal proteins was determined. The expression of PG-EGFP-f resulted in a significant increase in the cell border

localization of DPI/II and DSG2 as compared to un-transfected or EGFP-f transfected cells (Fig. 1C and E). The levels of PKP3 at the border did increase, though the increase was not statistically significant (Fig. 1C and E). A Western blot analysis demonstrated that this was not due to a change in protein levels or changes in protein solubility (Sup Fig. 1A–B). Importantly, expression of a PG-EGFP construct that does not localize to the cell border did not result in an increase in the localization of DP I/II at the cell border (Fig. 1D and F) suggesting that PG over-expression is not sufficient for the localization of DP I/II to the cell border. PG-EGFP shows a pan-cellular localization (Fig. 1D), which is consistent with data indicating that 14-3-3γ is required for transporting PG to the cell border [27].

To determine if the restoration of desmosome formation by PGEGFP-f is dependent on endogenous PG, HCT116 derived PG knockdown cells were transfected with shRNA resistant versions of either PG-EGFP-f or PG-EGFP cDNA and stained with antibodies to DSG2. Unlike the results observed in the 14-3-3γ knockdown cells, both PG-EGFP and PG-EGFP-f localized to the border suggesting that the transport of PG to the cell border was intact in cells expressing 14-3-3γ (Fig. 2A). The expression of either PG-EGFP or PG-EGFP-f led to a restoration of DSG2 localization to the cell border in the absence of endogenous PG in contrast to the controls (EGFP-f or EGFP) (Fig. 2A). The levels of over-expressed and endogenous PG were determined using Western blot analysis (Fig. 2B). These results suggest that in cells expressing 14-3-3γ, PG is transported to the cell border and is capable of restoring DSG2 localization to the cell border.

In the absence of PKP3, DP, DSG2 and DSC2/3 do not localize to the cell border but PG is present at the border [25]. To study if the PG-EGFP-f can rescue transport and localization of DP and DSG2 in the absence of another ARM protein, PKP3 knockdown cells were transfected with PG-EGFP-f and localization of DP determined. Expression of PG-EGFP-f or EGFP-f does not restore DP border localization in cells lacking PKP3 (Fig. 2C–D). These results are consistent with a model in which PG is required to recruit PKP3 to the cell border to initiate desmosome formation [25].

The results described above suggest that the localization of PG at the cell border allows recruitment of DPI/II, DSG2 and PKP3 to the cell border and are consistent with a previously published report which suggests that PG localization at the cell border is required for DP and DSG2 recruitment to the cell border [30]. Consistent with the observation that PG forms a strong complex with DSG2, but not DSC2 [31], the results in this report demonstrate that PG localization to the cell border results in the recruitment of DSG2 but not DSC2/3. PG might form a complex with DSG2 and transport DSG2 to the cell border as PG has been shown to bind another desmoglein family member, DSG3, which results in the localization of DSG3 to the cell border [31,32]. Alternatively, DSG2 retention at the cell border may not be stable in the absence of PG. The recruitment of DSC2/3 to the cell border might be dependent on the presence of PKP3 at the cell border [25,33] and since the increase in PKP3 levels at the cell border is partially attenuated in the PG-EGFP-f expressing cells, this might be the reason why DSC2/3 does not localize to the border in these cells and are consistent with observations suggesting that the presence of DSC2 with PKP2 or PKP3 is sufficient to induce desmosome formation in epithelial cells [33]. It is possible that the recruitment of PKP3 to the cell border in cells expressing PG-EGFP-f is normal but its retention at the border is compromised in the absence of DSC2/3 at the cell border. This is consistent with our observations suggesting that the retrograde transport of PG and PKP3 occurs via vastly different mechanisms in HCT116 cells [34].

To determine whether 14-3-3γ is required for desmosome formation in other cell types, the ability of 14-3-3γ to regulate

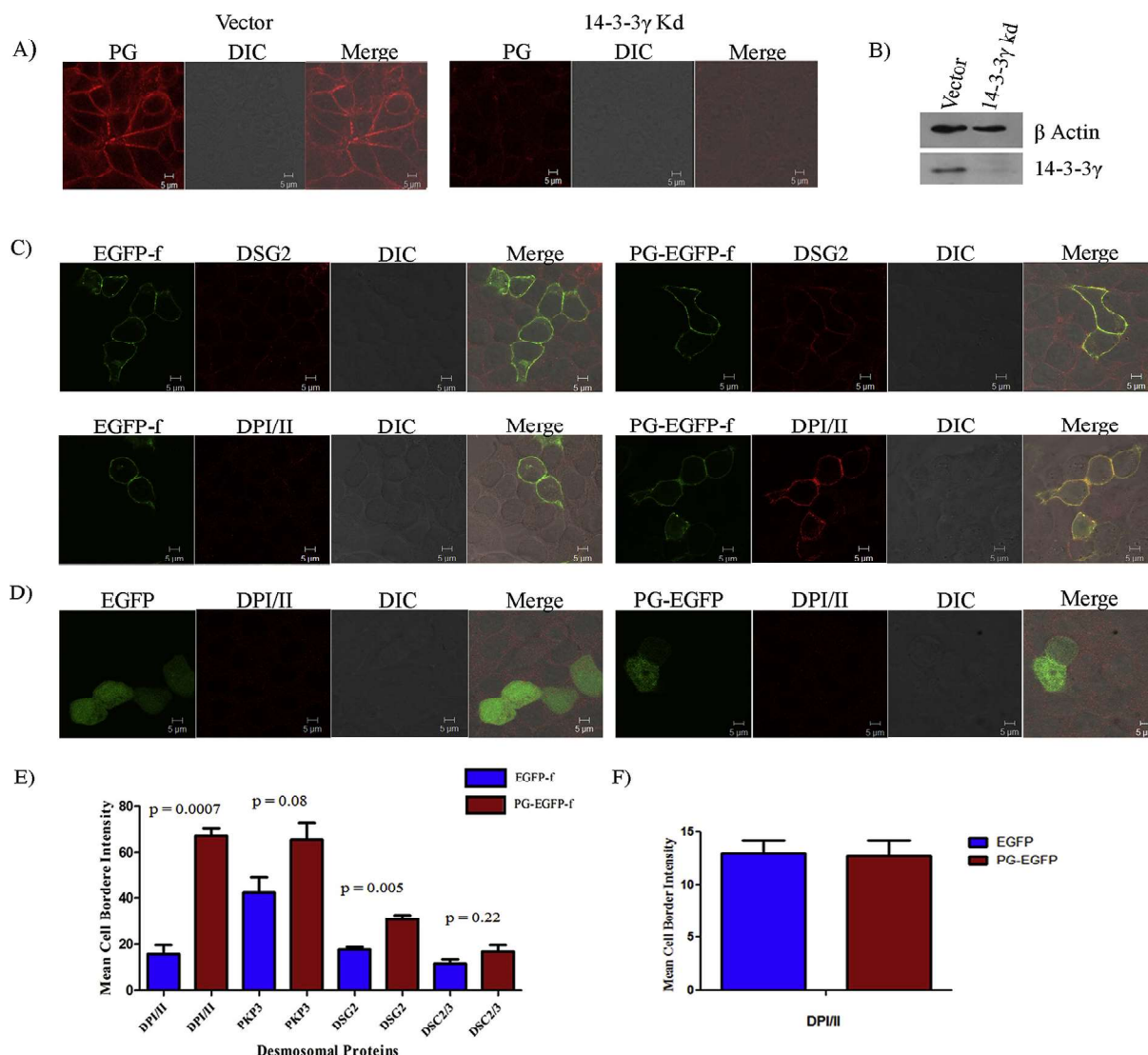


Fig. 1. Localization of PG to the cell border results in increased border localization of other desmosomal proteins. (A–B) HCT116 derived vector control and 14-3-3 γ knockdown cells were stained with antibodies to PG followed by confocal microscopy (A) or protein extracts prepared and resolved on SDS-PAGE gels followed by Western blotting with the indicated antibodies. Western blots for β Actin served as a loading control (B). (C) HCT116 derived 14-3-3 γ knockdown cells were transfected with either EGFP-f or PG-EGFP-f (green) and were stained with antibodies to the indicated proteins (red) followed by confocal microscopy. (D) The 14-3-3 γ knockdown cells were transfected with EGFP or PG-EGFP (green) and the cells fixed and stained with antibodies to DP (red). (E–F) The intensity of border staining, for the different desmosomal proteins, was measured for transfected cells in three different experiments and the mean cell border intensity and standard error from three different experiments is plotted. *p* value was calculated using student's *t*-test. (For interpretation of the references to color in this figure legend, the reader is referred to the Web version of this article.)

desmosome formation was determined in the immortal keratinocyte line, HaCaT. HaCaT derived vector control cells, 14-3-3 γ knockout cells and 14-3-3 ϵ knockout cells were generated and a Western blot analysis demonstrated that loss of 14-3-3 γ in HaCaT cells led to a decrease in the levels of PG, DP, DSG2, PKP3 and DSC2/3 when compared to the vector control and 14-3-3 ϵ knockout cells (Sup Fig. 2A), which was accompanied by a decrease in the localization of DP, DSC2/3 and PG to the cell border as compared to the 14-3-3 ϵ knockout cells and vector control cells (Sup Fig. 2B). HaCaT derived 14-3-3 γ knockout cells had decreased cell-cell adhesion (Sup Fig. 2C) and reduced desmosome size as compared to the 14-3-3 ϵ knockout cells and vector control cells (Sup Fig. 2D). These results suggest that 14-3-3 γ is required for desmosome formation in multiple cell types; however, the mechanisms by which it regulates desmosome formation are different in different cell types. These effects are specific to 14-3-3 γ as loss of 14-3-3 ϵ does not lead to alteration in desmosome protein levels and desmosome

assembly in HCT116 cells and in the mouse testis as previously reported [27].

3.2. Localization of PG to the cell border stimulates desmosome formation and cell-cell adhesion

To determine whether the expression of PG-EGFP-f resulted in an increase in cell-cell adhesion in cells lacking 14-3-3 γ , hanging drop assays were performed as described [27]. A large number of small cell clusters were observed in the 14-3-3 γ knockdown cells expressing EGFP-f whereas expression of PG-EGFP-f in the 14-3-3 γ knockdown cells led to the formation of larger, but fewer, cell clusters (Fig. 3A). Consistent with the increase in cell-cell adhesion, calcium switch assays demonstrated that the rate of localization of DSG2 to the cell border in the 14-3-3 γ knockdown cells was greatly stimulated in cells expressing PG-EGFP-f (Fig. 3B). Therefore, the expression of PG-EGFP-f in 14-3-3 γ knockdown cells results in the

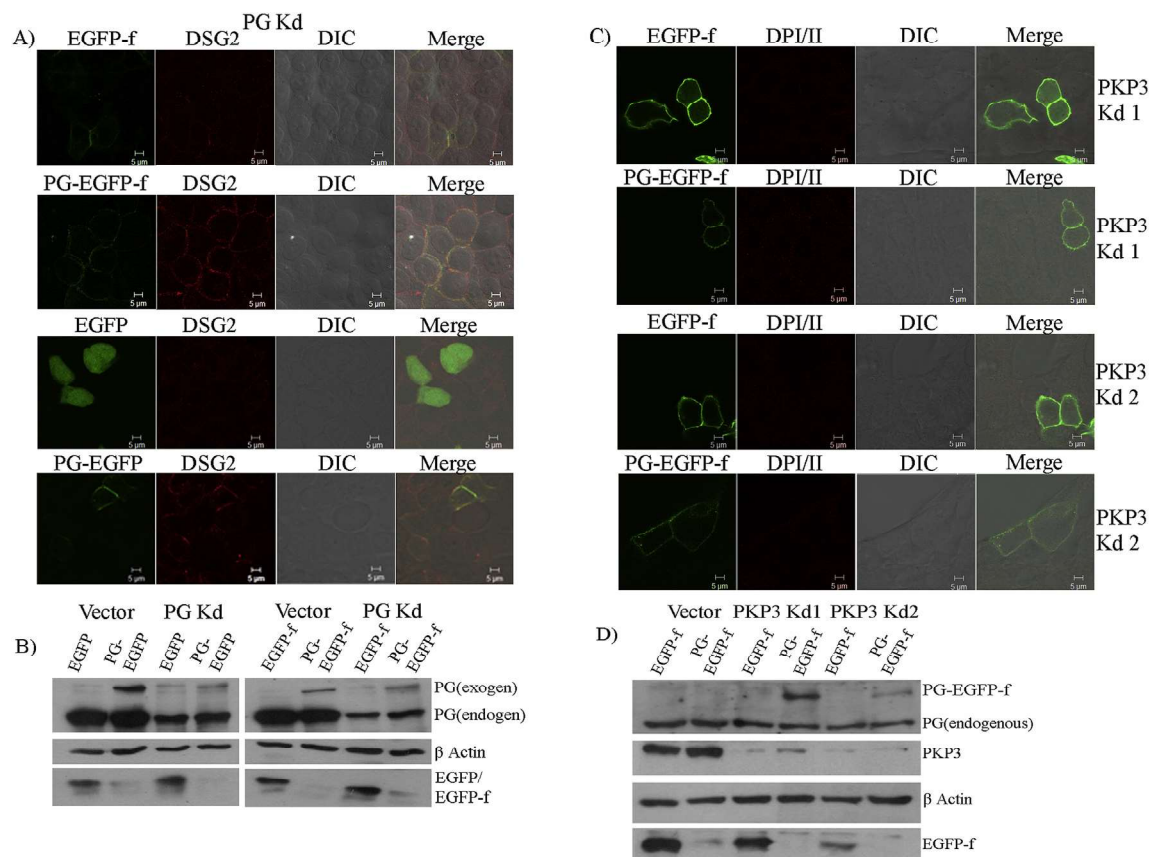


Fig. 2. PG-EGFP-f rescues desmosome formation in PG knockdown cells but requires PKP3 expression for the restoration of desmosome formation. (A–B) HCT116 derived PG knockdown clones were transfected with either EGFP-f or PG-EGFP-f or EGFP or PG-EGFP (green) and were stained with antibodies to DSG2 (red) followed by confocal microscopy. Representative images are shown and scale bars are shown in each panel (A) or protein extracts were prepared and resolved on SDS-PAGE gels followed by Western blotting with the indicated antibodies. Western blots for β Actin served as a loading control. PG (exogen) is over expressed/exogenous PG and PG (endogen) is endogenous PG (B). (C–D) HCT116 derived PKP3 knockdown clones were transfected with either EGFP-f or PG-EGFP-f (green) and were stained with antibodies to DPI/II (red) followed by confocal microscopy (C) or protein extracts were resolved on SDS-PAGE gels followed by Western blotting with the indicated antibodies. Western blots for β Actin served as a loading control (D). Representative images are shown and scale bars are shown in each panel (C). (For interpretation of the references to color in this figure legend, the reader is referred to the Web version of this article.)

formation of functional desmosomes. These results indicate that localizing PG to the cell border is sufficient to restore cell-cell adhesion in the 14-3-3 γ knockdown cells.

Given the data in this report and previous results about the role of the Armadillo proteins in desmosome assembly, we would like to propose the following model (Fig. 4). 14-3-3 γ is required for the transport of PG to the cell border [27]. As, unlike the desmosomal cadherins, PG is localized to the cell border in HCT116 cells in low calcium media [25], PG localization at the border might mark the sites of future desmosome formation. As previously reported, upon calcium addition PG localization at the cell border is increased [25], which might be indicative of PG being transported to the border as part of a pre-assembled desmosome complex [25]. Therefore, the PG in the cytoplasm in the 14-3-3 γ knockdown cells is unable to contribute to the initiation of desmosome formation because it isn't transported to the border. In the presence of 14-3-3 γ , both PG-EGFP and PG-EGFP-f restore desmosome formation in PG knockdown cells suggesting that 14-3-3 γ transport of PG to the border is required for the initiation of desmosome formation (Fig. 2A). The forced localization of PG to the cell border in cells lacking 14-3-3 γ , results in the localization of DSG2, PKP3 and DP at the cell border thus stimulating desmosome formation (Fig. 3). Previous reports have suggested a hierarchy in the accumulation of desmosome formation where PKP3 is required to recruit DP to the desmosome precursors, PKP2 is required to recruit the DP containing

desmosome precursors to the cell border and DP recruitment to cell border is further stimulated by PKP3 recruitment to the border [35]. Our previous results suggest that PG is required for the recruitment of PKP3 to the cell border [25] and in the absence of 14-3-3 γ , the levels of the desmosomal cadherins are reduced at the cell border [27] suggesting that in the absence of PG, the cadherins cannot accumulate at the site of desmosome formation. Therefore, it is possible that the transport of the cadherins to the border is not defective but that their retention at the cell border is deficient in the 14-3-3 γ knockdown cells because stable desmosomes are not being formed.

To conclude, our results suggest that one major role of the 14-3-3 γ is to mediate the transport of PG to the cell border. The presence of PG at the cell border results in the increased recruitment of DP, DSG2 and PKP3 to the cell border, however, the level of PKP3 at the cell border is attenuated in cells lacking 14-3-3 γ suggesting that these proteins play a role in the transport of PKP3 to the cell border. Thus, different ARM protein family members are required for different aspects of desmosome formation and stability in epithelial cells.

Conflicts of interest

The authors declare that there is no conflict of interest.

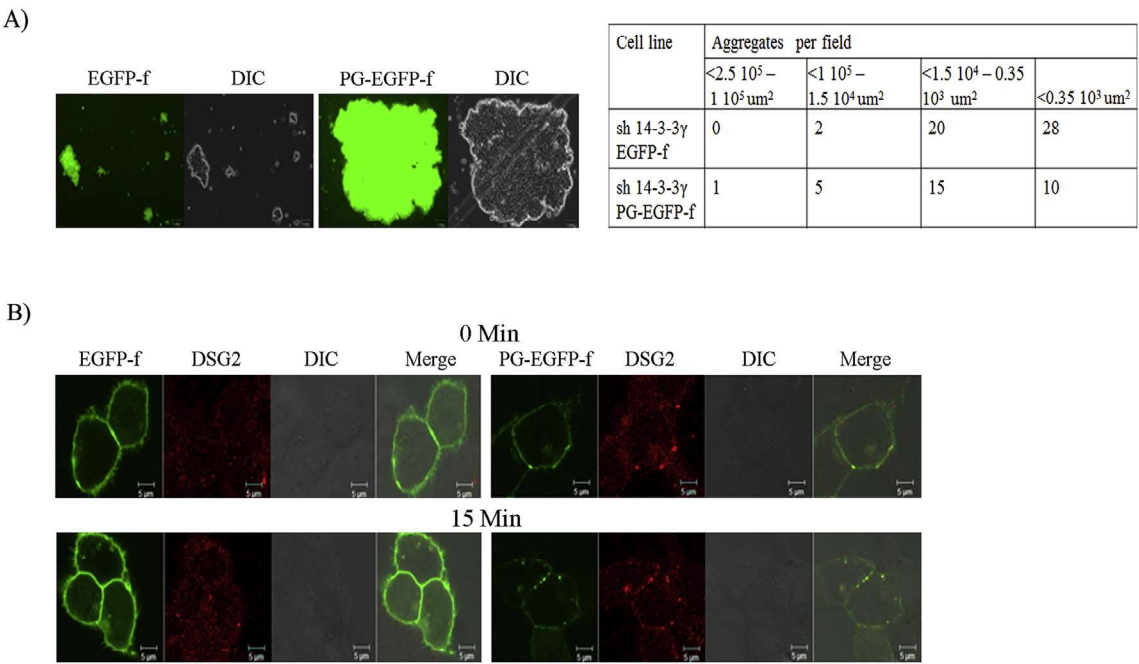


Fig. 3. Localization of PG to the cell border stimulates desmosome formation and cell-cell adhesion. (A) Hanging drop assays were performed to determine cell-cell adhesion in HCT116 derived 14-3-3γ knockdown cells expressing EGFP-f or PG-EGFP-f. Representative images are shown and scale bars are shown in each panel. The size and number of clusters is indicated in the table. (B) Calcium switch assays were performed on 14-3-3γ knockdown cells transfected with pEGFP-f or PG-EGFP-f (green) as described. Cells were fixed at the indicated time points and stained for DSG2 (red). Representative images are shown and scale bars are shown in each panel. (For interpretation of the references to color in this figure legend, the reader is referred to the Web version of this article.)

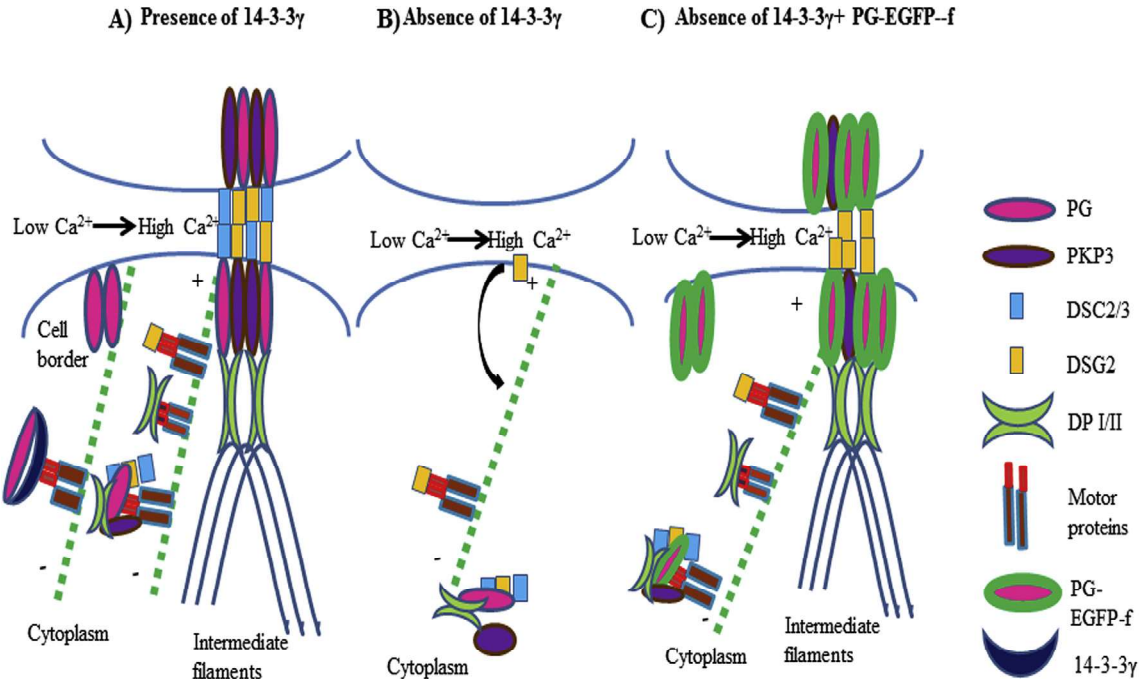


Fig. 4. Model illustrating the role of PG and 14-3-3γ in regulating desmosome assembly. In low calcium media, PG is localized to the cell border but the other desmosomal components remain in the cytoplasm. Upon calcium addition, the other components are transported to the border either in complex with one another or individually to form an intact desmosome (A). In the absence of 14-3-3γ, PG is not transported to the border, either in the presence or absence of calcium, leading to a decrease in desmosome formation (B). The desmosomal cadherins might be transported to the border but might not be retained at the border due to the absence of PG and other plaque proteins. When PG is artificially targeted to the cell border (PG-EGFP-f) in cells lacking 14-3-3γ, a restoration of desmosome function is observed with the desmosomal proteins being transported either in complex with one another or individually to the cell border (C).

Acknowledgements

We thank Dr. Neelam Shirsat (ACTREC) and her lab members for providing us with LentiCRISPR v1 plasmid. We also thank the ACTREC light microscopy facility and ACTREC electron microscopy facility for help with all the imaging experiments in this report. The work was funded by grants from the Department of Biotechnology (BT/PR5748/MED/31/166/2012) to SND.

Appendix A. Supplementary data

Supplementary data related to this article can be found at <https://doi.org/10.1016/j.bbrc.2017.12.080>.

References

- [1] A. Aitken, 14-3-3 and its possible role in co-ordinating multiple signalling pathways, *Trends Cell Biol.* 6 (1996) 341–347.
- [2] A.K. Gardino, S.J. Smerdon, M.B. Yaffe, Structural determinants of 14-3-3 binding specificities and regulation of subcellular localization of 14-3-3 ligand complexes: a comparison of the X-ray crystal structures of all human 14-3-3 isoforms, *Semin. Cell Biol.* 16 (2006) 173–182.
- [3] G. Tzivion, Y.H. Shen, J. Zhu, 14-3-3 proteins; bringing new definitions to scaffolding, *Oncogene* 20 (2001) 6331–6338.
- [4] A.J. Muslin, J.W. Tanner, P.M. Allen, A.S. Shaw, Interaction of 14-3-3 with signaling proteins is mediated by recognition of phosphoserine, *Cell* 84 (1996) 889–897.
- [5] M.B. Yaffe, K. Rittinger, S. Volinia, P.R. Caron, A. Aitken, H. Leffers, S.J. Gamblin, S.J. Smerdon, L.C. Cantley, The structural basis for 14-3-3 phosphopeptide binding specificity, *Cell* 91 (1998) 961–971.
- [6] B. Coblitz, S. Shikano, M. Wu, S.B. Gabelli, L.M. Cockrell, M. Spieker, Y. Hanyu, H. Fu, L.M. Amzel, M. Li, C-terminal recognition by 14-3-3 proteins for surface expression of membrane receptors, *J. Biol. Chem.* 280 (2005) 36263–36272.
- [7] S.M. Troyanovsky, Mechanism of cell-cell adhesion complex assembly, *Curr. Opin. Cell Biol.* 11 (1999) 561–566.
- [8] K.J. Green, C.L. Simpson, Desmosomes: new perspectives on a classic, *J. Invest. Dermatol.* 127 (2007) 2499–2515.
- [9] D.K. Armstrong, K.E. McKenna, P.E. Purkis, K.J. Green, R.A. Eady, I.M. Leigh, A.E. Hughes, Haploinsufficiency of desmoplakin causes a striate subtype of palmoplantar keratoderma, *Hum. Mol. Genet.* 8 (1999) 143–148.
- [10] D.M. Hunt, L. Rickman, N.V. Whittock, R.A. Eady, D. Simrak, P.J. Dopping-Hepenstal, H.P. Stevens, D.K. Armstrong, H.C. Hennies, W. Kuster, A.E. Hughes, J. Arnemann, I.M. Leigh, J.A. McGrath, D.P. Kelsell, R.S. Buxton, Spectrum of dominant mutations in the desmosomal cadherin desmoglein 1, causing the skin disease striate palmoplantar keratoderma, *Eur. J. Hum. Genet.* 9 (2001) 197–203.
- [11] G. McKoy, N. Protonotarios, A. Crosby, A. Tsatsopoulou, A. Anastasakis, A. Coonar, M. Norman, C. Baboonian, S. Jeffery, W.J. McKenna, Identification of a deletion in plakoglobin in arrhythmogenic right ventricular cardiomyopathy with palmoplantar keratoderma and woolly hair (Naxos disease), *Lancet* 355 (2000) 2119–2124.
- [12] E.E. Norgett, S.J. Hatsell, L. Carvajal-Huerta, J.C. Cabezas, J. Common, P.E. Purkis, N. Whittock, I.M. Leigh, H.P. Stevens, D.P. Kelsell, Recessive mutation in desmoplakin disrupts desmoplakin-intermediate filament interactions and causes dilated cardiomyopathy, woolly hair and keratoderma, *Hum. Mol. Genet.* 9 (2000) 2761–2766.
- [13] L. Rickman, D. Simrak, H.P. Stevens, D.M. Hunt, I.A. King, S.P. Bryant, R.A. Eady, I.M. Leigh, J. Arnemann, A.I. Magee, D.P. Kelsell, R.S. Buxton, N-terminal deletion in a desmosomal cadherin causes the autosomal dominant skin disease striate palmoplantar keratoderma, *Hum. Mol. Genet.* 8 (1999) 971–976.
- [14] N.V. Whittock, M. Haftek, N. Angoulvant, F. Wolf, H. Perrot, R.A. Eady, J.A. McGrath, Genomic amplification of the human plakophilin 1 gene and detection of a new mutation in ectodermal dysplasia/skin fragility syndrome, *J. Invest. Dermatol.* 115 (2000) 368–374.
- [15] R.W. Eyre, J.R. Stanley, Human autoantibodies against a desmosomal protein complex with a calcium-sensitive epitope are characteristic of pemphigus foliaceus patients, *J. Exp. Med.* 165 (1987) 1719–1724.
- [16] J.C. Jones, J. Arnn, L.A. Staehelin, R.D. Goldman, Human autoantibodies against desmosomes: possible causative factors in pemphigus, *Proc. Natl. Acad. Sci. U. S. A.* 81 (1984) 2781–2785.
- [17] S. Karpai, M. Amagai, R. Prussick, K. Cehrs, J.R. Stanley, Pemphigus vulgaris antigen, a desmoglein type of cadherin, is localized within keratinocyte desmosomes, *J. Cell Biol.* 122 (1993) 409–415.
- [18] H. Aberle, C. Bierkamp, D. Torchard, O. Serova, T. Wagner, E. Natt, J. Wirsching, C. Heidkamper, M. Montagna, H.T. Lynch, et al., The human plakoglobin gene localizes on chromosome 17q21 and is subjected to loss of heterozygosity in breast and ovarian cancers, *Proc. Natl. Acad. Sci. U. S. A.* 92 (1995) 6384–6388.
- [19] E.L. Davies, J.M. Gee, R.A. Cochrane, W.G. Jiang, A.K. Sharma, R.I. Nicholson, R.E. Mansel, The immunohistochemical expression of desmoplakin and its role in vivo in the progression and metastasis of breast cancer, *Eur. J. Canc.* 35 (1999) 902–907.
- [20] I. Holen, J. Whitworth, F. Nutter, A. Evans, H.K. Brown, D.V. Lefley, I. Barbaric, M. Jones, P.D. Ottewell, Loss of plakoglobin promotes decreased cell-cell contact, increased invasion, and breast cancer cell dissemination in vivo, *Breast Canc. Res.* 14 (2012) R86.
- [21] K. Kolegraff, P. Nava, M.N. Helms, C.A. Parkos, A. Nusrat, Loss of desmocollin-2 confers a tumorigenic phenotype to colonic epithelial cells through activation of Akt/beta-catenin signaling, *Mol. Biol. Cell* 22 (2011) 1121–1134.
- [22] S.T. Kundu, P. Gosavi, N. Khapare, R. Patel, A.S. Hosing, G.B. Maru, A. Ingle, J.A. Decaprio, S.N. Dalal, Plakophilin3 downregulation leads to a decrease in cell adhesion and promotes metastasis, *Int. J. Canc.* 123 (2008) 2303–2314.
- [23] W.K. Peitsch, Y. Doerflinger, R. Fischer-Colbrie, V. Huck, A.T. Bauer, J. Utikal, S. Goerd, S.W. Schneider, Desmoglein 2 depletion leads to increased migration and upregulation of the chemoattractant secretoneurin in melanoma cells, *PLoS One* 9 (2014), e89491.
- [24] D. Acehan, C. Petzold, I. Gumper, D.D. Sabatini, E.J. Muller, P. Cowin, D.L. Stokes, Plakoglobin is required for effective intermediate filament anchorage to desmosomes, *J. Invest. Dermatol.* 128 (2008) 2665–2675.
- [25] P. Gosavi, S.T. Kundu, N. Khapare, L. Sehgal, M.S. Karkhanis, S.N. Dalal, E-cadherin and plakoglobin recruit plakophilin3 to the cell border to initiate desmosome assembly, *Cell. Mol. Life Sci.* 68 (2011) 1439–1454.
- [26] C. Bierkamp, K.J. McLaughlin, H. Schwarz, O. Huber, R. Kemler, Embryonic heart and skin defects in mice lacking plakoglobin, *Dev. Biol.* 180 (1996) 780–785.
- [27] L. Sehgal, A. Mukhopadhyay, A. Rajan, N. Khapare, M. Sawant, S.S. Vishal, K. Bhatt, S. Ambatipudi, N. Antao, H. Alam, M. Gurjar, S. Basu, R. Mathur, L. Borde, A.S. Hosing, M.M. Vaidya, R. Thorat, F. Samaniego, O. Kolthur-See-tharam, S.N. Dalal, 14-3-3gamma-Mediated transport of plakoglobin to the cell border is required for the initiation of desmosome assembly in vitro and in vivo, *J. Cell Sci.* 127 (2014) 2174–2188.
- [28] A.S. Hosing, S.T. Kundu, S.N. Dalal, 14-3-3 Gamma is required to enforce both the incomplete S phase and G2 DNA damage checkpoints, *Cell Cycle* 7 (2008) 3171–3179.
- [29] M. Pasdar, W.J. Nelson, Kinetics of desmosome assembly in Madin-Darby canine kidney epithelial cells: temporal and spatial regulation of desmoplakin organization and stabilization upon cell-cell contact. II. Morphological analysis, *J. Cell Biol.* 106 (1988) 687–695.
- [30] T. Yin, S. Getsios, R. Caldelari, L.M. Godsel, A.P. Kowalczyk, E.J. Muller, K.J. Green, Mechanisms of plakoglobin-dependent adhesion: desmosome-specific functions in assembly and regulation by epidermal growth factor receptor, *J. Biol. Chem.* 280 (2005) 40355–40363.
- [31] N.A. Chitaev, R.E. Leube, R.B. Troyanovsky, L.G. Eshkind, W.W. Franke, S.M. Troyanovsky, The binding of plakoglobin to desmosomal cadherins: patterns of binding sites and topogenic potential, *J. Cell Biol.* 133 (1996) 359–369.
- [32] C.D. Andl, J.R. Stanley, Central role of the plakoglobin-binding domain for desmoglein 3 incorporation into desmosomes, *J. Invest. Dermatol.* 117 (2001) 1068–1074.
- [33] M. Fujiwara, A. Nagatomo, M. Tsuda, S. Obata, T. Sakuma, T. Yamamoto, S.T. Suzuki, Desmocollin-2 alone forms functional desmosomal plaques, with the plaque formation requiring the juxtamembrane region and plakophilins, *J. Biochem.* 158 (2015) 339–353.
- [34] K. Raychudhuri, M. Gurjar, S.N. Dalal, Plakophilin3 and Plakoglobin recycling are differentially regulated during the disassembly of desmosomes, *J. Biochem. Technol.* 6 (2015) 634–642.
- [35] V. Todorovic, J.L. Koetsier, L.M. Godsel, K.J. Green, Plakophilin 3 mediates Rap1-dependent desmosome assembly and adherens junction maturation, *Mol. Biol. Cell* 25 (2014) 3749–3764.



GENERATION OF MICE WITH TISSUE SPECIFIC TRANSGENE EXPRESSION USING SPERM MEDIATED GENE TRANSFER

SONALI S. VISHAL^{1,2}, SARIKA TILWANI^{1,2}, RAHUL THORAT¹, SORAB N. DALAL^{1,2*}

¹*KS230, Advanced Centre for Treatment Research and Education in Cancer (ACTREC), Tata Memorial Centre, Kharghar Node, Navi Mumbai 410210. India.*

²*Homi Bhabha National Institute, Training School complex, Anushakti Nagar, Mumbai, INDIA 400085.*

ABSTRACT

The production of transgenic animals has extended our knowledge of physiology and allowed the generation of animal models for human diseases. Previous work in the laboratory had reported the use of lentiviral vectors to generate transgenic animals using sperm mediated gene transfer (SMGT). To determine if lentivirus mediated SMGT could be used to generate tissue specific transgenic animals, a lentiviral vector containing the K14 promoter driving the expression of turbo RFP was used to generate transgenic animals. The pups were screened for presence of the transgene and for transgene expression for two generations. Transgenic animals were generated at a very high frequency and the transgene was stably inherited in the germline. In addition, the transgene was expressed in the hair follicle as previously reported for K14 driven transgenes suggesting that our SMGT protocol can be used to generate tissue specific transgenic animals.

KEYWORDS: *Transgenic, SMGT, K14 promoter, Turbo RFP.*



SORAB N. DALAL^{1,2*}

¹*KS230, Advanced Centre for Treatment Research and Education in Cancer (ACTREC), Tata Memorial Centre, Kharghar Node, Navi Mumbai 410210. India.*

²*Homi Bhabha National Institute, Training School complex, Anushakti Nagar, Mumbai, INDIA 400085.*

Received on: 23-01-2017

Revised and Accepted on :02-03-2017

DOI: <http://dx.doi.org/10.22376/ijpbs.2017.8.2.b324-329>

INTRODUCTION

Transgenic animals are important tools to study animal physiology and to generate animal models of human disease, which can lead to the generation of novel therapeutic strategies. Transgenic animals were earlier produced by microinjection of the transgene into two or four cell embryos or by fusion of the blastocyst with modified embryonic stem cells.¹⁻⁴ However, these techniques are expensive, require specialized training and equipment and transgene positive pups are obtained at low efficiency. To overcome these drawbacks, techniques involving the *in vivo* and/or *ex vivo* modification of male gametes at different stages of spermatogenesis were developed. These included (i) incubating sperm with circular or linearized DNA fragments,⁵ (ii) *in vitro* modification of spermatogonial stem cells using either retroviruses or cDNA constructs followed by introduction of the modified spermatogonial stem cells into the testes of chemically sterilized animals,⁶⁻⁹ (iii) injecting the transgene into the testes of animals,¹⁰ (iv) injection of the DNA construct into the testes followed by electroporation^{11, 12} and (v) retroviral or lentiviral mediated transduction of spermatogonial stem cells *in vivo*.^{13, 14} Collectively, these techniques are termed Sperm Mediated Transgenesis or Sperm Mediated Gene Transfer (SMGT). The constitutive expression of a transgene is important while studying the role of a particular gene in the development of an organism or in diseases where global expression of a particular protein is affected and this altered protein expression plays an important role in disease development. Similarly, studying the development of a particular tissue or pathological conditions arising in a specific tissue, requires tissue specific gene manipulation. This tissue specific manipulation can be achieved using tissue specific promoters as described previously.¹⁵ Therefore, transgenic animals with tissue specific expression are equally or more important than transgenic animals with constitutive transgene expression. Previous work from this laboratory has demonstrated that modifying spermatogonial stem cells *in vivo* using lentiviral particles leads to the generation of transgenic animals with constitutive transgene expression and stable transgene integration at very high efficiency.¹⁴ To determine if a similar approach can be used to generate transgenic animals with tissue specific transgene expression, lentiviral particles containing turbo RFP under the control of the K14 promoter were injected into the testes of pre-pubescent male mice. The progeny of these mice generated transgenic animals at high frequency, which showed tissue specific transgene expression.

MATERIALS AND METHODS

Plasmids

pCCLK14 GFP plasmid was a kind gift from Dr. Francesca Miselli (University of Modena and Reggio Emilia, Italy). Turbo RFP cDNA was PCR amplified from pTRIPz vector (Open Biosystems) using primers containing Age I and Sal I restriction sites (Table I). The PCR product was cloned into TA vector (Thermo Scientific) and was further sub-cloned into pCCLK14

GFP plasmid using Age I and Sal I sites to generate pCCLK14 turbo RFP.

Lentivirus Packaging

All cell lines used in this study were cultured in DMEM (Gibco) with 10% FBS (Gibco). 293T cells were co-transfected with pCCLK14 turbo RFP and virapower packaging mix (Invitrogen) according to the manufacturer's instructions to generate lentiviral particles containing the transgene. The viral particles were concentrated as described.¹⁶ Viral titer was determined by infecting HaCaT cells with 10 µl of the concentrated viral suspension. 48 hours post transduction, a single cell suspension was analyzed by flow cytometry for the presence of RFP and viral titer was determined using the formula (number of fluorescent cells x dilution factor) as described.¹⁶

Animals

Swiss mice Crl:CFW(SW) were bred and maintained in the laboratory animal facility of ACTREC. Maintenance of the animal facility is as per the national guidelines provided by the Committee for the Purpose of Control and Supervision of the Experiments on Animals (CPCSEA), Ministry of Environment and Forest, Government of India. The animals were housed in a controlled environment with the temperature and relative humidity being maintained at 23±2°C and 40-70% respectively and a day night cycle of 12 hrs each (7:00 to 19:00 light; 19:00 to 7:00 dark). The animals were received an autoclaved balanced diet prepared in-house as per the standard formula and sterile water *ad libitum*. Mice were housed in the Individually Ventilated Cage (IVC) system (M/S Citizen, India) provided with autoclaved corn cob bedding material (ATNT Laboratories, Mumbai). Protocols for the experiments were approved by the Institutional Animal Ethics Committee (IAEC) of ACTREC. The animal study proposal number is ACTREC IAEC project No. 11/2012. The viral particles (3.5 x 10⁵ TU/µl) were surgically injected into pre-pubescent male mice to generate pre-founder mice as described previously.¹⁴ Five weeks post-surgery, mice were mated with wild type female mice to obtain transgenic pups.

Genotyping of Animals

Tail biopsies (~3mm) from 3 week old pups sired by pre-founder males were lysed for 16h at 50°C in high salt digestion buffer containing 50mM Tris HCl, 1% SDS, 100mM NaCl, 100mM EDTA and 1200µg/ml Proteinase K (Jackson Laboratories). The lysate was processed for isolation of DNA using phenol-chloroform extraction followed by ethanol precipitation.¹⁶ The genomic DNA was subjected for PCR analysis using transgene-specific primers whose sequences are listed in Table I. Every PCR reaction set had three controls. The pCCLK14 turbo RFP plasmid was used as a template for a positive control, genomic DNA obtained from WT mice was used as a negative control and amplification of the endogenous patched (Ptch) gene was used as a loading control. Genomic DNA isolated from the human origin cell line, HCT116, was used as a negative control for the Ptch PCR. To validate the turbo RFP PCR results, two sets of primers were used. First set of PCR primer recognizes a part of turbo RFP sequence

whereas second set of primer recognizes the entire turbo RFP sequence taken from pTRIPz vector. To ensure that the PCR product is indeed turbo RFP sequence, PCR product was cloned into the pTZ57RT/T vector (Thermo Scientific) and was sequenced using Sanger sequencing.

Fluorescence Microscopy

To detect the turbo RFP expression, epidermis was separated from the dermis of the tail sections of

transgene positive pups, using 5mM EDTA solution¹⁷ and epidermis was then mounted on a glass slide using Vectashield (Vector) as per the manufacturer's instructions. The epidermis sections were then imaged using Zeiss LSM510 confocal microscope. As a control epidermis section from WT mouse was used.

Name of oligonucleotides	Sequence
Ptch Forward	CTGCGGCAAGTTTTTGTTG
Ptch Reverse	AGGGCTTCTCGTTGGCTACAAG
Turbo RFP I Forward	ATGAGCGAGCTGATCAAGG
Turbo RFP I Reverse	TTATCTGTGCCCCAGTTTGC
Turbo RFP II Forward (Age I)	GGACCGGTCGCCACCATGAGC
Turbo RFP II Reverse (Sal I)	GGGTCGACTGGCCGGCCGCATTAGTCT

Table 1

List of oligonucleotides used for genotyping.

RESULTS

Generation of pCCLK14 turbo RFP viruses

To generate mice that express the transgene only in the epidermis, we selected the Keratin 14 (K14) promoter because K14 and Keratin 5 (K5) are expressed in the basal layers of epidermis,¹⁸ are specific markers of the basal epithelium and the K14 promoter has been widely used to generate epidermis specific transgenic animals.¹⁹⁻²¹ Turbo RFP was cloned downstream of the K14 promoter in pCCLK14 vector and pCCLK14 turbo RFP viral particles were generated using the virapower packaging system. 5-10 µl of concentrated pCCLK14 turbo RFP viruses (3.5×10^5 TU/µl) were surgically injected into the testicles of pre-pubescent Swiss mice to generate pre-founder mice. Five weeks post-surgery these mouse were mated with wild type female to obtain transgenic pups.

Screening of pups by PCR amplification of turbo RFP

The pups were screened for the presence of the turbo RFP transgene by performing PCR reactions using the genomic DNA of pups as a template. As shown in Figure 1I, almost all the pups showed the presence of the turbo RFP transgene while genomic DNA from WT mice did not show the presence of the transgene. A PCR reaction for the mouse Patched (Ptch) gene was performed as a loading control and no signal was observed for Ptch in genomic DNA purified from the human cell line, HCT116 (Figure 1A-C). Since a very high number of the pups scored as transgene positive, we were concerned that this could be an artifact of the PCR reaction. Therefore, we used another set of oligonucleotide primers which amplifies the entire turbo RFP transgene. Similar results were obtained using this

primer set (Figure 1A-C), suggesting that these pups were indeed positive for the transgene. To further confirm these results, the PCR products were cloned into the pTZ57RT/T vector system and the PCR products sequenced. The sequencing reactions confirmed that the amplified product was indeed the turbo RFP transgene (Figure 1D). We did not perform Western blots to demonstrate the presence of the RFP protein in the epidermis due to the non-availability of a good antibody to RFP.

Epidermis specific turbo RFP expression

To determine whether RFP was expressed in these animals, tail snips were prepared by separating the epidermis from the muscle and cartilage and the epidermis was examined by confocal microscopy. As shown in figure 2, mice containing the turbo RFP transgene showed red fluorescence in the bulb region of hair follicle, the root sheath of the hair follicle and the sebaceous glands. The arrangement of hair follicles correlated with that given in literature.²² The pattern of turbo RFP expression was similar to that reported for keratin14^{17, 23} suggesting that we achieved tissue specific gene expression. Further, expression of turbo RFP was observed in first generation mice (1230) as well as second generation mice (83), suggesting that the inheritance of the transgene was stable and that expression was maintained over both the generations. The intensity of the turbo RFP fluorescence is greater in the second generation as compared to the first generation. Some auto fluorescence was observed in the hair shaft of WT mice, however, this does not overlap with the regions in which keratin 14 is expressed.^{17, 23} These results suggest that the transgenic mice expressed turbo RFP specifically in the epidermis

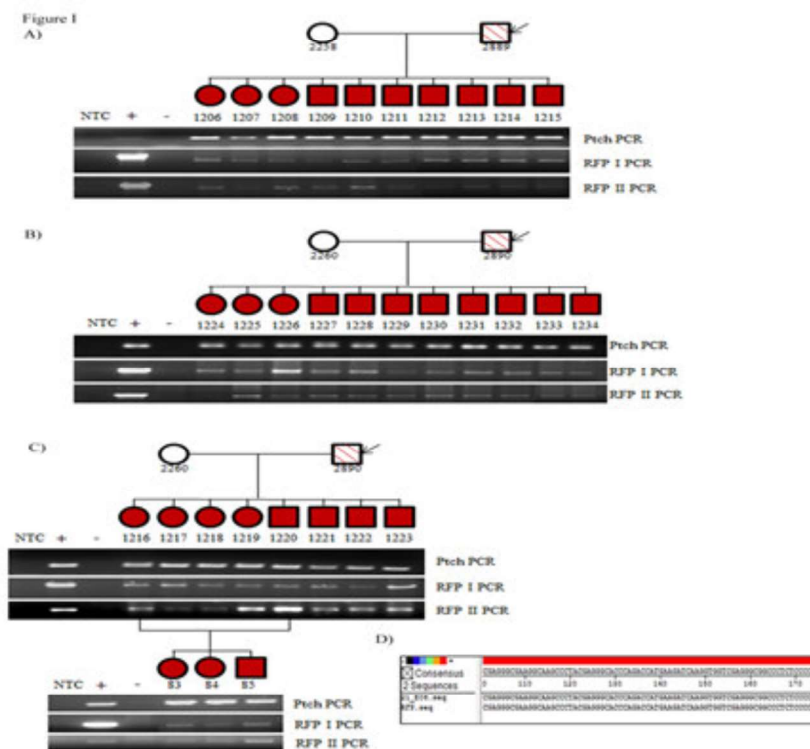


Figure 1

Stable inheritance of the RFP transgene in mice injected with the pCCLK14 turbo RFP construct. A-C. A pedigree analysis for pre-founder mice (indicated with an arrow) 2889 (A) and 2890 (B-C), showing germline transmission of the transgene. Individual mice were assigned numbers for further experiments. Genomic DNA amplification using primers for RFP (RFPI and RFPII) or Patched (Ptch) as a loading control are shown for each animal. The filled squares and circles indicate transgene positive animals. NTC is the no template control, + is a positive control where the template is the pCCLK14 plasmid and – represents the negative control, which is genomic DNA isolated from WT mice for the RFP PCR reactions and genomic DNA from HCT116 cells for the Ptch PCR reactions. D) RFP II PCR product obtained from genomic DNA of mouse 1221 was cloned into pTZ57RT/T vector and sequenced. Note that the sequence shows an exact match to the turbo RFP sequence

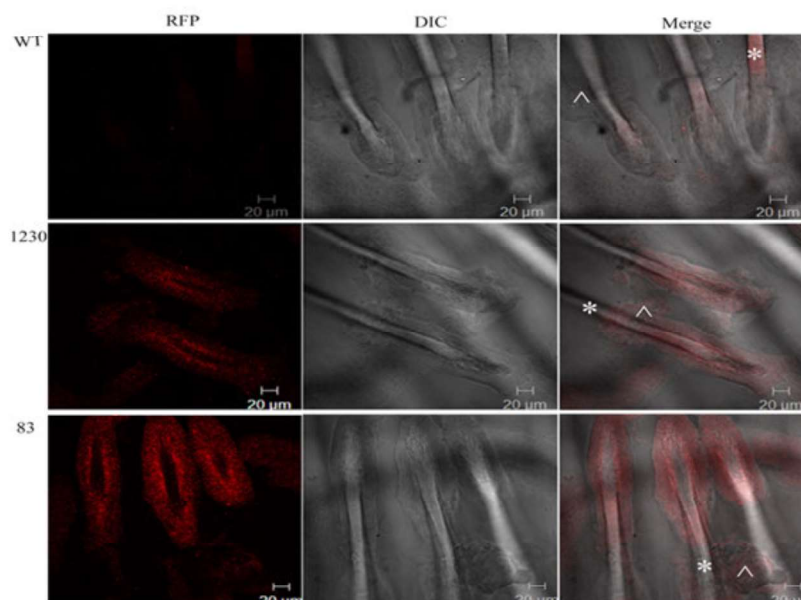


Figure 2

Turbo RFP is expressed in tissues that normally express keratin 14. Epidermis whole mounts from wild type (WT) or transgenic animals (1230 and 83) were examined by fluorescence microscopy (left panel). A DIC image (middle panel) and a merged image (right panel) are also shown. Note that the turbo RFP fluorescence is more intense in the second generation. The fluorescence in the transgenic animals is observed in the hair follicle and sebaceous glands as previously reported for keratin 14. * indicates Hair Shaft, ^ indicates Sebaceous glands.

DISCUSSION

Transgenesis revolutionized the study of mammalian biology by allowing studies on developmental biology, study of genetically inherited diseases and cancer. There are various transgenic mouse models which mimic human diseases and syndromes and hence are used for testing and developing new therapeutic strategies. The methods to achieve transgenesis have also developed considerably to make transgenesis efficient, quick and cost effective. These methods need to be validated for different types of promoter systems before generating important mouse models or before making transgenic models in larger animals. The present study wished to validate the lentiviral mediated SMGT for tissue specific transgene expression so that epidermis specific gene up-regulation or down-regulation can be achieved. The present study once again demonstrated the efficiency of viral mediated SMGT for generating transgenic animals. The vector system used in this study can be modified to induce expression of the transgene in different tissue types by using the appropriate tissue specific promoter. Alternatively, temporal induction of the transgene can be achieved by driving expression from inducible promoters, such as those containing the Tetracycline operator.¹⁵ These mice can be crossed to mice expressing the Tetracycline repressor under a constitutive promoter and expression induced by addition of Tetracycline in the drinking water. With the advent of CRISPR Cas9 technology,²⁴ already existing lentiviral systems used for SMGT can also be modified so that Cas9 expression is driven by tissue specific or inducible promoters and the guide RNA expression driven by a pol III based promoter to generate inducible or tissue specific knockout mouse. This will further simplify the generation of knockout mouse models leading to a greater understanding of mammalian

physiology and the generation of better mouse models of human disease.

CONCLUSION

The generation of transgenic animals using traditional methods is very cumbersome and all the drawbacks of traditional methods can be avoided by using SMGT. SMGT technique using lentiviral particles allows transduction of quiescent cells and stable transgene integration, which can be inherited by the progeny. The results in this report demonstrate that SMGT can be used to generate transgenic mice with tissue specific expression and this system can be modified to study the effect of over expression or down regulation of particular gene products in skin development.

ACKNOWLEDGEMENTS AND FUNDING SOURCE

We thank Drs. M. M. Vaidya and F. Miselli for the gift of the pCCLK14GFP plasmid. We thank Dr. S. Waghmare and his laboratory for helping us with preparing epidermal sections. We also thank the ACTREC animal house facility, imaging facility, flow cytometry and sequencing facility. The work was funded by the Department of Biotechnology (BT/PR5748/MED/31/166/2012).

This is the grant number from DBT (Department of Biotechnology) as listed in the acknowledgements. The grant title is "Regulation of cell-cell adhesion and spermatogenesis by 14-3-3 γ " and the grant was issued to Sorab N Dalal at ACTREC-TMC.

CONFLICT OF INTEREST

Conflict of interest declared None

REFERENCES

- Gordon JW, Scangos GA, Plotkin DJ, Barbosa JA, Ruddle FH. Genetic transformation of mouse embryos by microinjection of purified DNA. *Proc Natl Acad Sci U S A*. 1980;77(12):7380-4.
- Brinster RL, Chen HY, Trumbauer M, Senear AW, Warren R, Palmiter RD. Somatic expression of herpes thymidine kinase in mice following injection of a fusion gene into eggs. *Cell*. 1981;27(1 Pt 2):223-31.
- Jahner D, Haase K, Mulligan R, Jaenisch R. Insertion of the bacterial gpt gene into the germ line of mice by retroviral infection. *Proc Natl Acad Sci U S A*. 1985;82(20):6927-31.
- Huszar D, Balling R, Kothary R, Magli MC, Hozumi N, Rossant J, et al. Insertion of a bacterial gene into the mouse germ line using an infectious retrovirus vector. *Proc Natl Acad Sci U S A*. 1985;82(24):8587-91.
- Lavitrano M, Camaioni A, Fazio VM, Dolci S, Farace MG, Spadafora C. Sperm cells as vectors for introducing foreign DNA into eggs: genetic transformation of mice. *Cell*. 1989;57(5):717-23.
- Nagano M, Shinohara T, Avarbock MR, Brinster RL. Retrovirus-mediated gene delivery into male germ line stem cells. *FEBS Lett*. 2000;475(1):7-10.
- Nagano M, Watson DJ, Ryu BY, Wolfe JH, Brinster RL. Lentiviral vector transduction of male germ line stem cells in mice. *FEBS Lett*. 2002;524(1-3):111-5.
- Ivics Z, Izsvak Z, Chapman KM, Hamra FK. Sleeping Beauty transposon mutagenesis of the rat genome in spermatogonial stem cells. *Methods*. 2011;53(4):356-65.
- Nagano M, Brinster CJ, Orwig KE, Ryu BY, Avarbock MR, Brinster RL. Transgenic mice produced by retroviral transduction of male germ-line stem cells. *Proc Natl Acad Sci U S A*. 2001;98(23):13090-5.
- Bachiller D, Schellander K, Peli J, Ruther U. Liposome-mediated DNA uptake by sperm cells. *Mol Reprod Dev*. 1991;30(3):194-200.
- Yamazaki Y, Fujimoto H, Ando H, Ohyama T, Hirota Y, Noce T. In vivo gene transfer to mouse

- spermatogenic cells by deoxyribonucleic acid injection into seminiferous tubules and subsequent electroporation. *Biol Reprod.* 1998;59(6):1439-44.
12. Dhup S, Majumdar SS. Transgenesis via permanent integration of genes in repopulating spermatogonial cells in vivo. *Nat Methods.* 2008;5(7):601-3.
13. Kanatsu-Shinohara M, Ikawa M, Takehashi M, Ogonuki N, Miki H, Inoue K, et al. Production of knockout mice by random or targeted mutagenesis in spermatogonial stem cells. *Proc Natl Acad Sci U S A.* 2006;103(21):8018-23.
14. Sehgal L, Thorat R, Khapare N, Mukhopadhyaya A, Sawant M, Dalal SN. Lentiviral mediated transgenesis by in vivo manipulation of spermatogonial stem cells. *PLoS One.* 2011;6(7):e21975.
15. Belteki G, Haigh J, Kabacs N, Haigh K, Sison K, Costantini F, et al. Conditional and inducible transgene expression in mice through the combinatorial use of Cre-mediated recombination and tetracycline induction. *Nucleic Acids Res.* 2005;33(5):e51.
16. Sehgal L, Usmani A, Dalal SN, Majumdar SS. Generation of transgenic mice by exploiting spermatogonial stem cells in vivo. *Methods Mol Biol.* 2014;1194:327-37.
17. Braun KM, Niemann C, Jensen UB, Sundberg JP, Silva-Vargas V, Watt FM. Manipulation of stem cell proliferation and lineage commitment: visualisation of label-retaining cells in whole mounts of mouse epidermis. *Development.* 2003;130(21):5241-55.
18. Coulombe PA, Kopan R, Fuchs E. Expression of keratin K14 in the epidermis and hair follicle: insights into complex programs of differentiation. *J Cell Biol.* 1989;109(5):2295-312.
19. Christensen R, Alhonen L, Wahlfors J, Jakobsen M, Jensen TG. Characterization of transgenic mice with the expression of phenylalanine hydroxylase and GTP cyclohydrolase I in the skin. *Exp Dermatol.* 2005;14(7):535-42.
20. Arbeit JM, Munger K, Howley PM, Hanahan D. Progressive squamous epithelial neoplasia in K14-human papillomavirus type 16 transgenic mice. *J Virol.* 1994;68(7):4358-68.
21. Kopp T, Kieffer JD, Rot A, Strommer S, Stingl G, Kupper TS. Inflammatory skin disease in K14/p40 transgenic mice: evidence for interleukin-12-like activities of p40. *J Invest Dermatol.* 2001;117(3):618-26.
22. Schweizer J, Marks F. A developmental study of the distribution and frequency of Langerhans cells in relation to formation of patterning in mouse tail epidermis. *J Invest Dermatol.* 1977;69(2):198-204.
23. Nijhof JG, Braun KM, Giangreco A, van Pelt C, Kawamoto H, Boyd RL. The cell-surface marker MTS24 identifies a novel population of follicular keratinocytes with characteristics of progenitor cells. *Development.* 2006;133(15):3027-37.
24. Ablain J, Durand EM, Yang S, Zhou Y, Zon LI. A CRISPR/Cas9 vector system for tissue-specific gene disruption in zebrafish. *Dev Cell.* 2015;32(6):756-64.

Transgenesis: Embryo modification to sperm mediated gene transfer

Sonali S Vishal and Sorab N Dalal*

KS215, Advanced Centre for Treatment Research and Education in Cancer (ACTREC), Tata Memorial Centre
Kharghar Node, Navi Mumbai 410210, India

Received 1 August 2015; revised 25 January 2016; accepted 27 January 2016

The generation of transgenic animals by conventional transgenic protocols is cumbersome and not very efficient. To improve the efficiency of obtaining transgenic animals, different groups have attempted to genetically modify spermatozoa and these technologies are collectively referred to as sperm mediated gene transfer (SMGT). SMGT technologies involve the modification of either spermatozoa or spermatogonial stem cells that give rise to spermatozoa, followed by either *in vitro* fertilization or mating with a wild type female to generate transgenic progeny. In addition to the generation of transgenic mice, the use of SMGT technologies has resulted in multiple insights into male reproductive biology. SMGT has bypassed most of the problems associated with the traditional methods of transgenesis and has considerably improved the efficiency of obtaining transgenic animals. Various techniques have been developed by which SMGT can be achieved and this review provides an overview of the evolution of SMGT technology and will indicate how these might be used to further our understanding of mammalian growth and development.

Keywords: ICSI, SMGT, spermatozoa, SSC, transgenic animals, wild type

Introduction

Except for the recent past, the study of mammalian biology and its impact on disease progression was restricted to observations made on patient material and *in vitro* studies in cell lines. While much has been learnt from these efforts, the results of these studies could not be directly extended to human beings, as these studies did not address the inherent physiological complexity of mammalian systems. In order to study the contribution of various cellular pathways to human physiology, it became necessary to generate models for human disease conditions in small animals, which led to the advent of transgenic technology.

Transgenic animals are generated by introducing an expression construct (the transgene) stably into the genome of the animal. To stably modify the genome of an organism, it is necessary that the modification is performed at the early stages of embryogenesis so that most of the cells of embryo will contain the transgene. Pioneering work from the Brinster laboratory led to the technology that permitted the culture of the ovum and early stage embryos¹. Once this technical hurdle was crossed, multiple laboratories (including the Brinster laboratory) demonstrated that cultured embryos could be aggregated with teratoma cells to generate progeny,

which expressed teratoma specific genes^{2,3}. The next step in the generation of transgenic animals involves the injection of purified plasmid DNA into the male pronucleus of a 0.5 dpc mouse embryo. The microinjected embryos are then implanted into the pseudopregnant female mouse to allow the development of embryos. This technique resulted in the generation of mice, in which the plasmid DNA has integrated into the host genome⁴. This technique has been used to generate transgenic mice, which expressed high levels of Herpes Simplex Virus (HSV) thymidine kinase⁵. Other methods for generating transgenic mice, such as, retroviral infection of embryos and introduction of modified embryonic stem cells into the blastocoel cavity of embryo, have since been developed⁶⁻⁸. While this process has been used in many laboratories leading to significant advances in knowledge of mammalian biology, the technology is not used as widely as it could be because of the following issues. The pronuclei often burst post injection and integration of the transgene is often inefficient and does not improve with an increase in DNA concentration. Further, many of the embryos failed to implant or the implanted embryos fail to survive⁹. In addition, the efficiency of obtaining transgenic mice was variable, the foreign DNA is often not inherited in the germ line and these procedures took a long period of time and placed the animals

*Author for correspondence:
sdalal@actrec.gov.in

under severe physiological stress. Thus, generating transgenic animals by the standard procedures described above is a laborious, expensive and time consuming process.

Spermatogenesis

To overcome the above-mentioned problems and yet to ensure that plasmid DNA is incorporated into the genome of the embryo, different groups attempted to modify spermatozoa. The reason behind choosing spermatozoa is their ability to bind foreign DNA, whereas unfertilized ova do not bind to foreign DNA^{10,11}. A brief description of the process of spermatogenesis is required to understand the principle behind the methods that use sperm as a vehicle for transgene delivery. Spermatogenesis is the process by which spermatogonial stem cells (SSC) divide and differentiate to give rise to mature sperm (Fig. 1). The process of spermatogenesis is divided into three steps, *i.e.*, spermatogonial renewal, meiosis and spermiogenesis¹². In spermatogonial renewal, a type A spermatogonium undergoes a series of division to give rise to a type B spermatogonium (for details refer¹³). Type B spermatogonia differentiate into primary spermatocytes, which enter the meiotic programme. After meiosis I, primary spermatocytes give rise to secondary spermatocytes, which undergo meiosis II and differentiate into round spermatids with a haploid DNA content. During the process of spermiogenesis, haploid round spermatids undergo a series of changes, such as, nuclear condensation, acrosome and flagella formation and the removal of large portion of cytoplasm resulting in the formation of elongated spermatids¹². Elongated spermatids leave the seminiferous tubules and migrate to the epididymis, where they mature to give rise to spermatozoa (Fig. 1). Therefore, each SSC gives rise to multiple spermatozoa and spermatozoa are regularly produced as opposed to ova. Hence, it is easier to generate larger numbers of transgenic animals by modifying spermatozoa and using them as a vehicle for the delivery of the transgene. Multiple techniques have been used to generate transgenic mice by modifying spermatozoa or SSCs (as indicated in Fig. 1) and these have been broadly grouped under the term “Sperm Mediated Gene Transfer” (SMGT). The different techniques by which SMGT is achieved are listed below.

DNA Uptake Mediated Gene Transfer

Brackett *et al*¹¹ demonstrated that DNA bound non-specifically to spermatozoa. Lavitrano *et al*¹⁴ showed

that DNA bound to a receptor present on sperm and that this receptor could be blocked by Inhibition factor 1 (IF1), which was present in seminal fluid. Therefore, mature spermatozoa needed to be washed to remove IF1 to ensure that DNA could bind to spermatozoa. Binding of DNA to spermatozoa led to the internalization of the DNA bound receptor followed by release of DNA into sperm nuclei. In addition to the receptor, MHC II and CD4 molecules played an important role in DNA uptake and internalization by spermatozoa¹⁵. Even though MHC II was not detected in mature sperm, spermatozoa from MHC II knockout mice did not bind DNA, whereas spermatozoa from CD4 knockout mice could bind to DNA but failed to internalize the bound DNA¹⁵. Moreover, blocking CD4 receptors by treating them with neutralizing antibodies prevented DNA internalization in wild type spermatozoa¹⁵. Lavitrano *et al*¹⁰ developed a technique in which circular plasmid DNA containing a cDNA encoding bacterial chloramphenicol acetyl transferase (CAT) was incubated with a suspension of spermatozoa (washed spermatozoa). Then this

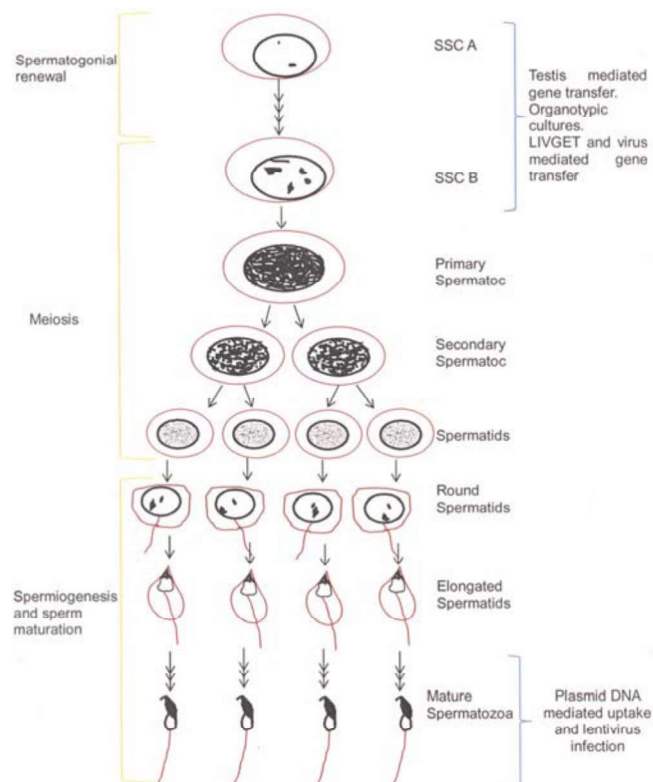


Fig. 1—The process of spermatogenesis is divided into three steps: Spermatogonial renewal, meiosis and spermiogenesis and sperm maturation. The figure also indicates which cell types are modified using the different SMGT techniques.

suspension was used in *in vitro* fertilization experiments. Progeny obtained from this method was found to be positive for the presence of plasmid DNA but did not express the CAT gene due to the rearrangement of the transgene¹⁰. Several groups have tried using this technique to obtain transgenic animals but not all of them were successful (reviewed in¹⁶). The major problems with this technique were: DNA uptake efficiency was highly variable in different species and in some species, *e.g.*, marine fish *Paralichthys olivaceus*, naked DNA damaged spermatozoa¹⁷, the transgene did not integrate into the host genome and, most important, high occurrence of rearrangement of the transgene upon integration. The efficiency of obtaining transgenic animals using this method could be improved by using Intra-Cytoplasmic Sperm Injection (ICSI), where the sperm was injected into an ovum, instead of *in vitro* fertilization¹⁸.

Lavitrano *et al*¹⁰ also performed experiments in which they used a linear DNA fragment of a plasmid expressing CAT to generate transgenic spermatozoa in a protocol similar to the one described above. They found that transgenic animals, obtained from spermatozoa pre-incubated with linearized plasmid DNA, expressed the CAT gene and that the efficiency of obtaining transgenic progeny with this protocol was much higher compared to that observed with circular plasmid DNA. Using this technology, the Lavitrano laboratory had successfully generated transgenic pigs expressing human decay accelerating factor with an efficiency of 57%¹⁹ and transgenic pigs expressing multiple transgenes, *i.e.*, enhanced blue fluorescent protein (BFP), enhanced green fluorescent protein (GFP) and DsRed²⁰. Kroll *et al*²¹ modified the above-described protocol by incubating purified *Xenopus* sperm nuclei for a short period of time (10 min) with restriction enzymes in the presence of linearized plasmid DNA containing cDNA sequence of GFP. As a result, an improvement was observed in the efficiency of integration of linearized plasmid DNA into the genome and this method was named Restriction Enzyme Mediated Insertion (REMI) SMGT. Then these modified sperm nuclei were injected into the unfertilized ovum to generate transgenic embryos²¹. Another method used to improve the efficiency of DNA uptake by spermatozoa was to disrupt the cell membrane of spermatozoa by freeze thaw cycles and inject the membrane-disrupted spermatozoa along with a plasmid DNA fragment containing a GFP expression cassette into oocytes²². This change in protocol

resulted in an increase in the efficiency of generating transgenic animals by 20%. The most critical factors associated with this method were the choice of enzyme, which is used to linearize the plasmid DNA, and the processing of sperm nuclei.

Since DNA uptake by spermatozoa have not been very efficient, some groups tried using transfection reagent lipofectamine to introduce exogenous DNA into spermatozoa²³⁻²⁶ but lipofectamine complexed with linearized DNA (lipofection combined with REMI) gave efficient transgenesis compared to lipofectamine complexed with circularized DNA^{24,26}. Some groups have also used nanoparticles, like magnetic nanoparticles, mesoporous silica nanoparticles and halloysite clay nanotubes, to deliver exogenous DNA to sperm²⁷⁻³⁰. Briefly, magnetic nanoparticles mixed with linearized DNA fragments were incubated with sperm and subjected to magnetic field for 90 min. Unbound DNA magnetic nanoparticle complex was removed and oocytes were fertilized with magnetofected sperm to obtain GFP positive embryos²⁷. The use of nanoparticles for SMGT was termed as NanoSMGT³⁰.

Transplantation of Modified Spermatogonial Stem Cells into Testis

Spermatogonial stem cells (SSCs) are progenitor cells, which undergo meiosis followed by differentiation to form spermatozoa as described above. These cells are mostly quiescent; however, they can be cultured and easily modified *in vitro*. Brinster *et al*³¹ demonstrated that transplanting SSCs from a fertile animal to an infertile animal resulted in the restoration of male fertility and suggested that modified SSCs could be used to generate transgenic animals. This technique did not involve *in vitro* fertilization or ICSI. It was also shown that SSC transplantation in a fertile mouse resulted in the generation of some pups derived from spermatozoa from the donor and some from spermatozoa derived from the recipient³². Though Brinster *et al* did not use modified SSCs one could generate transgenic animals using this method. Briefly, SSCs can be isolated, cultured and transfected with a plasmid DNA. The SSCs can then be screened for the presence of the transgene and transgene expression. These stably transfected SSCs can then be transplanted into recipient testis and the recipient male mice upon mating with wild type female mice will lead to the birth of transgenic pups. These experiments demonstrate that even a few implanted SSCs are

sufficient for the generation of transgenic progeny. The principal behind this technique formed the basis for the evolution of SMGT techniques used today. Different groups used plasmid vectors, retroviral particles, lentiviral particles and transposons for modifying SSCs *in vitro* and then transplanting them into the testis of recipient mice to generate transgenic animals³³⁻³⁵. An organotypic culture technique, for culture of testicular cells of neonatal mouse, to obtain fertile spermatozoa *in vitro* has also been developed³⁶. Using organotypic cultures from testicular cells of transgenic mice, transgene positive spermatozoa were obtained. These transgenic spermatozoa were fertile and were used for generating GFP positive transgenic mice³⁶. Even though establishing organotypic cultures is not easy but once established, spermatogenesis can be maintained over two months³⁶. It is tempting to speculate that recombinant spermatozoa generated *in vitro* in these organotypic cultures will result in the generation of compound transgenic animals carrying and expressing multiple transgenes in a single step rather than the multiple rounds of transgenesis, and mating that is the current norm.

Electroporation of Transgenic DNA into Testis

DNA can be introduced directly into target organs either in adult animals or pups and embryos using a number of procedures that are covered by the term LIVGET (localized *in vivo* gene transfer technique). LIVGET achieves the integration of plasmid DNA into the target organs by three distinct methods. The DNA is encapsulated either in a microparticle or a lipid particle that is injected into the target organ, or DNA is injected into the target organ followed by an electrical pulse across the organ. All these procedures result in the incorporation of the DNA construct into the cells of the target organ. Muramatsu *et al*³⁷ compared the efficiency of microparticle bombardment and electroporation for testis specific expression of the CAT gene. This was the first report in which cells in the testis were modified *in vivo*. They showed that, upon intratesticular DNA injection and electroporation, testicular cells showed CAT expression. Further, they also injected a plasmid expressing lacZ into the testes followed by the application of an electric current across the testis. Post 48 hours of electroporation, sections of electroporated testis were stained with X-gal, hematoxylin and eosin, and they observed lac Z expression in spermatogonium like cells, spermatocyte like cells and spermatid like cells. But they did not determine

whether the plasmid DNA had integrated into the genome of these cells³⁷. Yamazaki *et al*³⁸ demonstrated that injection of linearized plasmid DNA into seminiferous tubules, followed by the application of an electric current to the testis, resulted in long term expression of the lac-Z transgene and also in the modification of spermatogonial stem cells. In another study, by using plasmid DNA injection and electroporation of testis, transgene positive spermatozoa were obtained and used to fertilize ova using ICSI to generate transgenic progeny with high efficiency³⁹. Some groups have also tried injecting calcium phosphate bound plasmid DNA or plasmid DNA encapsulated in liposomes into the testis to obtain transgenic animals; however, these methods were not always successful^{40,41}. DNA injection into the seminiferous tubules or testis is termed as TMGT (testicular mediated gene transfer). Recently, the Majumdar laboratory has reported a method for DNA electroporation, in which linearized plasmid DNA was injected at multiple locations on mouse testis followed by electroporation. Post 35 days of injection, this pre-founder mouse was mated with wild type female mice to obtain pups and pups were screened for the presence of transgene. The results showed the efficiency of this method around 57-62%^{42,43}. However, the pulse intensity and pulse interval will have to be standardized for different species such that the testicular cells will not be affected by electroporation leading to their cell death.

Virus Mediated Transgenesis

In 2000, Nagano *et al*³³ demonstrated that spermatogonial cells could be infected with retroviruses *in vitro* and these cells upon reintroduction into the testis differentiated into transgene containing spermatozoa. Briefly, spermatogonial cells were isolated, infected with retroviral particles carrying a lacZ transgene. Then transgene positive cells were implanted in the testes of a wild type mouse. These male mice were able to sire lacZ transgenic pups when mated with wild type female mice. The transgene positive pups obtained from the recipient male mouse were inbred and it was determined that the lacZ transgene was stably integrated as the pups obtained from inbreeding of transgene positive animals were also positive for lacZ expression⁴⁴. The same group suggested that the use of lentiviruses would increase the efficiency of transgenesis due to their ability to infect quiescent germ cells³⁴. Pfeifer *et al*⁴⁵ independently

demonstrated that lentiviruses could infect embryonic stem (ES) cells. They also showed that morula stage embryos could be infected with lentiviruses *in vitro* and the infected morula could be implanted into the surrogate mother to obtain transgene positive animals. Hamra *et al*⁴⁶ demonstrated that purified SSCs isolated from rat testis could be infected with lentiviruses *in vitro*. And these modified SSC's could give rise to transgenic progeny when implanted in the rat testis. While the techniques mentioned above resulted in the generation of transgenic animals, these were cumbersome for the following reasons. SSCs need to be isolated and cultured *in vitro* without them undergoing differentiation. Further, the transduced SSCs need to be propagated in culture, which is not a trivial protocol though it has become easier over time. In addition, spermatocytes need to be depleted from the recipient male mice and often the transplantation of the recombinant SSCs into recipient mice failed, probably due to immune reactions against the modified SSCs. This protocol is also difficult to use in larger animals where spermatocyte depletion and surgery might pose unforeseen problems. In 2004, Kanatsu-Shinohara *et al*⁴⁷ suggested that all the difficulties in obtaining and culturing SSCs can be bypassed by *in vivo* retroviral transduction of SSCs. By injecting retroviruses into the testis of sexually immature mice, they obtained transgenic pups but the efficiency of obtaining transgenic pups (22%) was little less compared to the *in vitro* transduction technique (33-38%).

In 2011, Sehgal *et al*⁴⁸ reported that, upon *in vivo* lentiviral transduction of pre-pubescent male mice, the EGFP-f transgene could integrate into the DNA of the SSCs and the transgene was expressed in all the cells in the testis. More than 60% of the pups generated by mating these pre-founder mice with wild type female mice were positive for the transgene. The transgene integration sites were mapped in the transgene positive pups and demonstrated that the transgene was stably inherited to next generation and that most of the animals contained one or two integrants⁴⁸. This method is cost effective, simple and highly efficient for generation of transgenic animals as compared to the methods described above. But the site where integration is going to occur cannot be predicted and the transgene will be expressed by all the testicular cells, which are infected by lentiviruses. And if the transgene plays an important role in spermatogenesis or cell-cell adhesion then the pre-founder male mouse may become infertile⁴⁹.

However, these problems can extend to any SMGT technique that relies on the infection of SSC's. Few groups have also tried using adenoviruses for generating transgenic animals but adenoviral infection did not lead to integration of virus genome into the host cell. Hence, adenoviruses when used to generate transgenic animal by injection into seminiferous tubules did not show integration into the genome of the progenies but some of the pups expressed the transgene⁵⁰. Recently, using GFP expressing pseudotyped lentivirus infected spermatozoa, GFP positive transgenic mice were obtained⁵¹. Briefly, cauda epididymis and distal end of vas deferens were placed in a dish, punctured with needle and incubated with concentrated virus soup for 30 min to 2 h. Then the spermatozoa were washed with buffer and used for IVF to generate transgenic mouse. The efficiency of obtaining transgenic animal using this technique was found greater than 42%⁵¹. The critical factor, which affected the efficiency of fertilization in this technique, was the time interval for which viruses were incubated with spermatozoa.

Site Specific Recombination and Targeted Knockouts

Until recently, the ability to generate knockout and knockin mice was limited to technology requiring the modification of embryonic stem cells *in vitro*, followed by embryo aggregation or blastocyst injection. These methods are difficult to develop and require facilities not available in most laboratories. Kanatsu-Shinohara *et al*⁵² tried to generate knockout mice by infecting cultured SSCs with retroviruses containing neomycin resistant cassette. SSC colonies resistant to neomycin were sequenced to identify the genes flanking the retroviral genome and to find out if the neomycin resistant cassette became the part of the ORF of the flanking gene sequences, suggesting disruption of that gene. Using this random mutagenesis approach, they found that one of the disrupted genes was *occludin*. The SSC colony with a disrupted *occludin* allele was transferred to the recipient testis to generate occludin knockout mice; though the efficiency to generate knockout mice with this method was very less (1.7%)⁵². However, the advent of the SMGT technologies allows the exploitation of the nucleases like TALENs (Transcription Activator-Like Effector Nucleases) and CRISPR-Cas system (Clustered Regularly Interspaced Short Palindromic Repeats; Cas-CRISPR associated protein) to achieve targeted insertions or deletions or modifications with higher efficiency.

While using TALENs, the DNA or RNA sequences (transgene) can also be injected into the oocytes or embryos. Once inside the nucleus, TALEN binds to specific DNA sequences and introduces a double stranded break, which causes activation of the Non Homologous End Joining (NHEJ) pathway. During NHEJ, the exogenously provided template DNA or RNA is used to insert or delete a few bases at the site of strand breakage. Recently, knockin and knockout mice, and mice with a site-specific mutation were generated using TALENs⁵³⁻⁵⁵. Elimination of germline mitochondrial DNA mutations has also been achieved with the help of TALENs⁵⁶. Instead of the embryo injections, the TALENs can be encoded in a lentiviral vector and used to infect cultured SSCs. Recently, TALENs complexed with lipofectamine were used to transfect SSCs to generate or correct mutations, even electroporation of SSCs has also been done to deliver TALENs without affecting the cell viability or proliferation of SSCs^{57,58}.

In the CRISPR-Cas system, a single guide RNA (sgRNA) (20 nucleotides) directs the Cas nuclease to its target. Once activated, Cas generates double stranded breaks, activates NHEJ and NHEJ activation leads to insertion or deletion of specific nucleotides. To generate transgenic mice using CRISPR-Cas system, Cas mRNA, sgRNA and a linearized vector coding for the transgene were injected into the pronucleus or cytoplasm of a two/four cell embryo⁵⁹. Transgenic mice containing a conditional allele for *Mecp2* was also generated by injecting mouse embryos with a mixture of Cas9 mRNA, sgRNA and loxPoligos⁵⁹. These mice with conditional alleles can be mated with mice expressing tissue specific CRE recombinase to generate mice with a tissue specific knockout of *Mecp2* gene. Conditional allele can also be generated by using a pair of Cas9 nucleases and a single DNA expressing guide RNA flanked by loxP sites⁶⁰. Recently, using a single plasmid system for expressing sgRNA targeting the gene of interest and Cas9 nuclease, a tyrosinase knockout rabbit was generated⁶¹. CRISPR-Cas had been used in SSCs for genome correction with 100% efficiency, as in the case of mice carrying mutant *Crygc* gene (responsible for causing cataract), resulting into the generation of healthy progeny⁶². To make the activity of Cas highly specific and reduce off target effects, multiple sgRNA or a pair of sgRNAs can be used⁶³.

TALENs and CRISPR-Cas allowed selective modification of a genome as compared to the

conventional random mutagenesis where integration of the exogenous DNA or viral genome could not be controlled. This uncontrolled integration gave rise to different phenotypes depending upon the gene, which was disrupted due to integration of exogenous DNA. Moreover, plasmid modification used for generating transgenic mice was cumbersome in conventional methods with requirement of selective promoters, intron or exon of a gene, poly A tail and other accessory DNA elements, and was often associated with recombination problems, whereas with CRISPR-Cas systems, a mixture of DNA or RNA molecule (complementary to the targeted genomic region) and mRNA encoding for the nuclease could be directly used to achieve transgenesis in embryo or SSCs. Use of CRISPR-Cas, TALENs and other nucleases like Zinc Finger Nucleases is changing the field of transgenesis but still the questions relating to their specificity, cytotoxicity and off target effects remains to be answered.

Future Prospects

The field of sperm mediated transgenesis has evolved a great deal since the first experiments in which spermatozoa were incubated with plasmid DNA. With the development of technology, the efficiency of transgenesis has improved from approx 2-10% to above 60%. SMGT techniques also allows the development of transgenic animals in other species, *e.g.*, the development of transgenic pigs expressing human decay accelerating factor. The tissues from this transgenic pig can be used for transplantation, as the peripheral blood mononuclear cells from this animal upon incubation with fresh human serum were able to resist antibody and complement mediated cell lysis¹⁹. Isolation and culture of SSCs for *in vitro* modification of SSCs led to the standardization of process of isolation, culture, maintenance and cryopreservation of human SSCs. This has given hope to the human patients suffering from infertility or cancer (reviewed in⁶⁴). The techniques described here could be further modified, so that one day scientists will be able to generate single gene or multi gene transgenic animals with almost 100% efficiency. In addition, the transgenes will be integrated at specific sites in the genome and their expression regulated either temporally or in a tissue specific manner. These could lead to the generation of genome wide screens in small animal models. And the development of such a technology will result in the generation of animal models of

human disease that could be used to develop therapeutic strategies and to study the biology of different pathways involved in growth, development and disease pathogenesis. Finally, these technologies will allow scientists to extend their studies to larger animals, which might be better models for studying human disease.

Acknowledgement

We apologize to those authors whose work we have not cited due to space constraints. The present work was supported by grants from the Department of Biotechnology, Government of India, New Delhi and ACTREC, Kharghar, Navi Mumbai.

References

- Brinster R L, A method for *in vitro* cultivation of mouse ova from two-cell to blastocyst, *Exp Cell Res*, 32 (1963) 205-208.
- Brinster R L, The effect of cells transferred into the mouse blastocyst on subsequent development, *J Exp Med*, 140 (1974) 1049-1056.
- Mintz B & Illmensee K, Normal genetically mosaic mice produced from malignant teratocarcinoma cells, *Proc Natl Acad Sci USA*, 72 (1975) 3585-3589.
- Gordon J W, Scangos G A, Plotkin D J, Barbosa J A & Ruddle F H, Genetic transformation of mouse embryos by microinjection of purified DNA, *Proc Natl Acad Sci USA*, 77 (1980) 7380-7384.
- Brinster R L, Chen H Y, Trumbauer M, Senear A W, Warren R *et al*, Somatic expression of herpes thymidine kinase in mice following injection of a fusion gene into eggs, *Cell*, 27 (1981) 223-231.
- Jahner D, Haase K, Mulligan R & Jaenisch R, Insertion of the bacterial gpt gene into the germ line of mice by retroviral infection, *Proc Natl Acad Sci USA*, 82 (1985) 6927-6931.
- Huszar D, Balling R, Kothary R, Magli M C, Hozumi N *et al*, Insertion of a bacterial gene into the mouse germ line using an infectious retrovirus vector, *Proc Natl Acad Sci USA*, 82 (1985) 8587-8591.
- Gossler A, Doetschman T, Korn R, Serfling E & Kemler R, Transgenesis by means of blastocyst-derived embryonic stem cell lines, *Proc Natl Acad Sci USA*, 83 (1986) 9065-9069.
- Brinster R L, Chen H Y, Trumbauer M E, Yagle M K & Palmiter R D, Factors affecting the efficiency of introducing foreign DNA into mice by microinjecting eggs, *Proc Natl Acad Sci USA*, 82 (1985) 4438-4442.
- Lavitrano M, Camaioni A, Fazio V M, Dolci S, Farace M G *et al*, Sperm cells as vectors for introducing foreign DNA into eggs: Genetic transformation of mice, *Cell*, 57 (1989) 717-723.
- Brackett B G, Baranska W, Sawicki W & Koprowski H, Uptake of heterologous genome by mammalian spermatozoa and its transfer to ova through fertilization, *Proc Natl Acad Sci USA*, 68 (1971) 353-357.
- de Kretser D M, Loveland K L, Meinhardt A, Simorangkir D & Wreford N, Spermatogenesis, *Hum Reprod*, 13 (1998) 1-8.
- de Rooij D G & Russell L D, All you wanted to know about spermatogonia but were afraid to ask, *J Androl*, 21 (2000) 776-798.
- Zani M, Lavitrano M, French D, Lulli V, Maione B *et al*, The mechanism of binding of exogenous DNA to sperm cells: Factors controlling the DNA uptake, *Exp Cell Res*, 217 (1995) 57-64.
- Lavitrano M, Maione B, Forte E, Francolini M, Sperandio S *et al*, The interaction of sperm cells with exogenous DNA: A role of CD4 and major histocompatibility complex class II molecules, *Exp Cell Res*, 233 (1997) 56-62.
- Smith K R, Sperm cell mediated transgenesis: A review, *Anim Biotechnol*, 10 (1999) 1-13.
- Xin N, Liu T, Zhao H, Wang Z, Liu J *et al*, The impact of exogenous DNA on the structure of sperm of olive flounder (*Paralichthys olivaceus*), *Anim Reprod Sci*, 149 (2014) 305-310.
- Chan A W S, Luetjens C M, Dominko T, Ramalho-Santos J, Simerly C R *et al*, Foreign DNA transmission by ICSI: Injection of spermatozoa bound with exogenous DNA results in embryonic GFP expression and live rhesus monkey births, *Mol Human Reprod*, 6 (2000) 26-33.
- Lavitrano M, Bacci M L, Forni M, Lazzereschi D, Di Stefano C *et al*, Efficient production by sperm-mediated gene transfer of human decay accelerating factor (hDAF) transgenic pigs for xenotransplantation, *Proc Natl Acad Sci USA*, 99 (2002) 14230-14235.
- Webster N L, Forni M, Bacci M L, Giovannoni R, Razzini R *et al*, Multi-transgenic pigs expressing three fluorescent proteins produced with high efficiency by sperm mediated gene transfer, *Mol Reprod Dev*, 72 (2005) 68-76.
- roll K L & Amaya E, Transgenic *Xenopus* embryos from sperm nuclear transplantations reveal FGF signaling requirements during gastrulation, *Development*, 122 (1996) 3173-3183.
- Perry A C, Wakayama T, Kishikawa H, Kasai T, Okabe M *et al*, Mammalian transgenesis by intracytoplasmic sperm injection, *Science*, 284 (1999) 1180-1183.
- Ball B A, Sabeur K & Allen W R, Liposome-mediated uptake of exogenous DNA by equine spermatozoa and applications in sperm-mediated gene transfer, *Equine Vet J*, 40 (2008) 76-82.
- Harel-Markowitz E, Gurevich M, Shore L S, Katz A, Stram Y *et al*, Use of sperm plasmid DNA lipofection combined with REMI (restriction enzyme-mediated insertion) for production of transgenic chickens expressing eGFP (enhanced green fluorescent protein) or human follicle-stimulating hormone, *Biol Reprod*, 80 (2009) 1046-1052.
- Yang C C, Chang H S, Lin C J, Hsu C C, Cheung J I *et al*, Cock spermatozoa serve as the gene vector for generation of transgenic chicken (*Gallus gallus*), *Asian-Aust J Anim Sci*, 17 (2004) 885-891.
- Churchil R R, Gupta J, Singh A & Sharma D, Exogenous DNA internalisation by sperm cells is improved by combining lipofection and restriction enzyme mediated integration, *Br Poult Sci*, 52 (2011) 287-291.
- Kim T S, Lee S H, Gang G T, Lee Y S, Kim S U *et al*, Exogenous DNA uptake of boar spermatozoa by a magnetic nanoparticle vector system, *Reprod Domest Anim*, 45 (2010) e201-e206.
- Campos V F, de Leon P M, Komninou E R, Dellagostin O A, Deschamps J C *et al*, NanoSMGT: Transgene transmission into bovine embryos using halloysite clay nanotubes or nanopolymer to improve transfection efficiency, *Theriogenology*, 76 (2011) 1552-1560.

- 29 Barkalina N, Jones C, Kashir J, Coote S, Huang X *et al*, Effects of mesoporous silica nanoparticles upon the function of mammalian sperm *in vitro*, *Nanomedicine*, 10 (2014) 859-870.
- 30 Campos V F, Komninou E R, Urtiaga G, de Leon P M, Seixas F K *et al*, NanoSMGT: Transfection of exogenous DNA on sex-sorted bovine sperm using nanopolymer, *Theriogenology*, 75 (2011) 1476-1481.
- 31 Brinster R L & Zimmermann J W, Spermatogenesis following male germ-cell transplantation, *Proc Natl Acad Sci USA*, 91 (1994) 11298-11302.
- 32 Brinster R L & Avarbock M R, Germline transmission of donor haplotype following spermatogonial transplantation, *Proc Natl Acad Sci USA*, 91 (1994) 11303-11307.
- 33 Nagano M, Shinohara T, Avarbock M R & Brinster R L, Retrovirus-mediated gene delivery into male germ line stem cells, *FEBS Lett*, 475 (2000) 7-10.
- 34 Nagano M, Watson D J, Ryu B Y, Wolfe J H & Brinster R L, Lentiviral vector transduction of male germ line stem cells in mice, *FEBS Lett*, 524 (2002) 111-115.
- 35 Ivics Z, Izsvak Z, Chapman K M & Hamra F K, Sleeping beauty transposon mutagenesis of the rat genome in spermatogonial stem cells, *Methods*, 53 (2011) 356-365.
- 36 Sato T, Katagiri K, Gohbara A, Inoue K, Ogonuki N *et al*, *In vitro* production of functional sperm in cultured neonatal mouse testes, *Nature (Lond)*, 471 (2011) 504-507.
- 37 Muramatsu T, Shibata O, Ryoki S, Ohmori Y & Okumura J, Foreign gene expression in the mouse testis by localized *in vivo* gene transfer, *Biochem Biophys Res Commun*, 233 (1997) 45-49.
- 38 Yamazaki Y, Fujimoto H, Ando H, Ohyama T, Hirota Y *et al*, *In vivo* gene transfer to mouse spermatogenic cells by deoxyribonucleic acid injection into seminiferous tubules and subsequent electroporation, *Biol Reprod*, 59 (1998) 1439-1444.
- 39 Huang Z, Tamura M, Sakurai T, Chuma S, Saito T *et al*, *In vivo* transfection of testicular germ cells and transgenesis by using the mitochondrially localized jellyfish fluorescent protein gene, *FEBS Lett*, 487 (2000) 248-251.
- 40 Sato M, Iwase R, Kasai K & Tada N, Direct injection of foreign DNA into mouse testis as a possible alternative of sperm-mediated gene transfer, *Anim Biotechnol*, 5 (1994) 19-31.
- 41 Bachiller D, Schellander K, Peli J & Ruther U, Liposome-mediated DNA uptake by sperm cells, *Mol Reprod Dev*, 30 (1991) 194-200.
- 42 Usmani A, Ganguli N, Sarkar H, Dhup S, Batta S R *et al*, A non-surgical approach for male germ cell mediated gene transmission through transgenesis, *Sci Rep*, 3 (2013) 3430.
- 43 Dhup S & Majumdar S S, Transgenesis *via* permanent integration of genes in repopulating spermatogonial cells *in vivo*, *Nat Methods*, 5 (2008) 601-603.
- 44 Nagano M, Brinster C J, Orwig K E, Ryu B Y, Avarbock M R *et al*, Transgenic mice produced by retroviral transduction of male germ-line stem cells, *Proc Natl Acad Sci USA*, 98 (2001) 13090-13095.
- 45 Pfeifer A, Ikawa M, Dayn Y & Verma I M, Transgenesis by lentiviral vectors: Lack of gene silencing in mammalian embryonic stem cells and preimplantation embryos, *Proc Natl Acad Sci USA*, 99 (2002) 2140-2145.
- 46 Hamra F K, Gatlin J, Chapman K M, Grellhesl D M, Garcia J V *et al*, Production of transgenic rats by lentiviral transduction of male germ-line stem cells, *Proc Natl Acad Sci USA*, 99 (2002) 14931-14936.
- 47 Kanatsu-Shinohara M, Toyokuni S & Shinohara T, Transgenic mice produced by retroviral transduction of male germ line stem cells *in vivo*, *Biol Reprod*, 71 (2004) 1202-1207.
- 48 Sehgal L, Thorat R, Khapare N, Mukhopadhyaya A, Sawant M *et al*, Lentiviral mediated transgenesis by *in vivo* manipulation of spermatogonial stem cells, *PLoS One*, 6 (2011) e21975.
- 49 Sehgal L, Mukhopadhyay A, Rajan A, Khapare N, Sawant M *et al*, 14-3-3 γ -mediated transport of plakoglobin to the cell border is required for the initiation of desmosome assembly *in vitro* and *in vivo*, *J Cell Sci*, 127 (2014) 2174-2188.
- 50 Takehashi M, Kanatsu-Shinohara M, Inoue K, Ogonuki N, Miki H *et al*, Adenovirus-mediated gene delivery into mouse spermatogonial stem cells, *Proc Natl Acad Sci USA*, 104 (2007) 2596-2601.
- 51 Chandrashekrana A, Sarkar R, Thrasher A, Fraser S E, Dibb N *et al*, Efficient generation of transgenic mice by lentivirus-mediated modification of spermatozoa, *FASEB J*, 28 (2014) 569-576.
- 52 Kanatsu-Shinohara M, Ikawa M, Takehashi M, Ogonuki N, Miki H *et al*, Production of knockout mice by random or targeted mutagenesis in spermatogonial stem cells, *Proc Natl Acad Sci USA*, 103 (2006) 8018-8023.
- 53 Davies B, Davies G, Preece C, Puliadi R, Szumska D *et al*, Site specific mutation of the Zic2 locus by microinjection of TALEN mRNA in mouse CD1, C3H and C57BL/6J oocytes, *PLoS One*, 8 (2013) e60216.
- 54 Ponce de Leon V, Merillat A M, Tesson L, Anegon I & Hummler E, Generation of TALEN-mediated GR^{dim} knock-in rats by homologous recombination, *PLoS One*, 9 (2014) e88146.
- 55 Tesson L, Usal C, Menoret S, Leung E, Niles B J *et al*, Knockout rats generated by embryo microinjection of TALENs, *Nat Biotechnol*, 29 (2011) 695-696.
- 56 Reddy P, Ocampo A, Suzuki K, Luo J, Bacman S R *et al*, Selective elimination of mitochondrial mutations in the germline by genome editing, *Cell*, 161 (2015) 459-469.
- 57 Fanslow D A, Wirt S E, Barker J C, Connelly J P, Porteus M H *et al*, Genome editing in mouse spermatogonial stem/progenitor cells using engineered nucleases, *PLoS One*, 9 (2014) e112652.
- 58 Sato T, Sakuma T, Yokonishi T, Katagiri K, Kamimura S *et al*, Genome editing in mouse spermatogonial stem cell lines using TALEN and double-nicking CRISPR/Cas9, *Stem Cell Rep*, 5 (2015) 75-82.
- 59 Yang H, Wang H, Shivalila C S, Cheng A W, Shi L *et al*, One-step generation of mice carrying reporter and conditional alleles by CRISPR/Cas-mediated genome engineering, *Cell*, 154 (2013) 1370-1379.
- 60 Lee A Y & Lloyd K C, Conditional targeting of Ispd using paired Cas9 nickase and a single DNA template in mice, *FEBS Open Bio*, 4 (2014) 637-642.
- 61 Honda A, Hirose M, Sankai T, Yasmin L, Yuzawa K *et al*, Single-step generation of rabbits carrying a targeted allele of the tyrosinase gene using CRISPR/Cas9, *Exp Anim*, 31 (2015) 31-37.
- 62 Wu Y, Zhou H, Fan X, Zhang Y, Zhang M *et al*, Correction of a genetic disease by CRISPR-Cas9-mediated gene editing in mouse spermatogonial stem cells, *Cell Res*, 25 (2015) 67-79.
- 63 Ran F A, Hsu P D, Lin C Y, Gootenberg J S, Konermann S *et al*, Double nicking by RNA-guided CRISPR Cas9 for enhanced genome editing specificity, *Cell*, 154 (2013) 1380-1389.
- 64 Kubota H & Brinster R L, Technology insight: *In vitro* culture of spermatogonial stem cells and their potential therapeutic uses, *Nat Clin Pract Endocrinol Metab*, 2 (2006) 99-108.